A dynamic Bayesian Markov model for health economic evaluations of interventions in infectious disease

Katrin Dorothee Häußler

A dissertation submitted in partial fulfillment

of the requirements for the degree of

Doctor of Philosophy

of

University College London

Department of Statistical Science

April 2017

Meiner geliebten Oma,
die mich nicht nur das *seidene Stricken* lehrte,
in tiefer Dankbarkeit gewidmet.
Ich werde sie für immer in guter Erinnerung behalten.

This is dedicated to my beloved granny,
who did not just teach me to knit;
I will always be thankful to her
and I cherish her memory with all my love.

Declaration

I, Katrin Dorothee Häußler, confirm that the work presented in this PhD thesis is my own. Where information has been derived from other sources, I confirm that this has been indicated in this thesis with an appropriate reference.

Katrin Dorothee Häußler

Acknowledgements

First of all, I would like to thank my supervisor Dr. Gianluca Baio for his great support and patience in the development of this PhD thesis. He was always very encouraging and made time for regular meetings despite his other responsibilities. In addition, he enabled me to present my research at several international conferences and provided a job opportunity after my PhD funding expired.

I am also very much grateful to my co-supervisor Dr. Ardo van den Hout who gave me valuable advice in the preparation of a publication on the methodology of this PhD thesis.

In addition, I would like to thank Prof. Rumana Omar and Prof. Tom Fearn. Rumana made my dream of working abroad come true. Without her, I would not have been able to live in an international environment and to gain a lot of valuable experience, both professionally and in my private life. Tom and the Department of Statistical Science assigned me a departmental PhD studentship.

My special thanks go to my boyfriend Dr. Simón Lunagómez, my parents Christine and Alfons Häußler and my friends Tina Hildebrand, Ralf Wittlinger, Bernhard and Alena Kupfer, Spyros Poulimenos, Dr. Yi-Da Chiu, Rani Bal and Dr. Ah Yeon Park. I will never forget their emotional and professional support during the challenging years of PhD research.

Abstract

Background. Health economic evaluations of interventions against infectious diseases are commonly based on the predictions of compartmental models such as ordinary differential equation (ODE) systems and Markov models (MMs). In contrast to standard MMs, ODE systems of infectious diseases are commonly dynamic and account for the effects of herd immunity. This is crucial to prevent overestimation of infection prevalence.

Despite their computational effort, ODE systems including whole distributions on model parameters are considered the "gold standard" in infectious disease modelling. However, the literature mainly contains ODE-based models which only include a predefined value on each model parameter and thus do not account for parameter uncertainty. As a consequence, probabilistic sensitivity analysis, a crucial component of health economic evaluations, cannot be conducted straightforwardly.

Methodology. We present an approach to a dynamic MM under a Bayesian framework. The stochastic MM incorporates a probability distribution on each model parameter. We extend a static MM by incorporating the force of infection into the state allocation algorithm. The corresponding output is based on dynamic changes in population prevalence. In contrast to deterministic ODE-based models including a predefined value for each parameter, probabilistic sensitivity analysis can be conducted straightforwardly. The main motivation for our approach was to conduct a cost-effectiveness analysis of human papillomavirus vaccination.

Results. We introduce a case study of a fictional sexually transmitted in-

fection. By means of this example, we show that our methodology produces results which are comparable to the “gold standard” of an ODE system in a Bayesian framework.

When applied to a cost-effectiveness analysis of human papillomavirus vaccination, our method indicates that universal vaccination (including both sexes) is cost-effective. A comparison of universal to female-only vaccination and cervical screening-only results in an *Incremental Cost-Effectiveness Ratio* (ICER) of € 11,600 and € 1,500, respectively.

Conclusions. The dynamic Bayesian MM is suitable to include a high number of states and age cohorts, which are for example required in conclusive human papillomavirus modelling. In contrast to deterministic ODE systems, the setting is fully probabilistic at manageable computational effort.

Contents

List of Figures

List of Tables

List of Acronyms

AIC Akaike Information Criterion.

BCEA Bayesian Cost-Effectiveness Analysis.

BEST Bayesian modelling assessing the Effectiveness of a vaccination Strategy To prevent HPV-related diseases.

BIC Bayesian Information Criterion.

BMM Bayesian Markov Model.

BODE Bayesian ODE-based model.

CEA Cost-Effectiveness Analysis.

CEAC Cost-Effectiveness Acceptability Curve.

CI Credible Interval.

CIN Cervical Intraepithelial Neoplasiae.

CRD Centre for Review and Dissemination.

DARE Database of Abstracts of Reviews of Effects.

DDR Double Data Rate.

DNA Deoxyribonucleic Acid.

dODE deterministic ODE-based model.

EVPI Expected Value of Perfect Information.

EVPPI Expected Value of Perfect Partial Information.

GAM Generalised Additive Model.

GB Gigabyte.

GOF Goodness-Of-Fit.

GP Gaussian Process.

HDD Hard Disk Drive.

HPV Human papillomavirus.

HSIL High-grade Squamous Intraepithelial Lesions.

HTA Health Technology Assessment.

ICER Incremental Cost-Effectiveness Ratio.

ISPOR International Society for Pharmacoeconomics and Outcomes Research.

ITT Intention-To-Treat.

JAGS Just Another Gibbs Sampler.

LHS Latin Hypercube Sampling.

LSIL Low-grade Squamous Intraepithelial Lesions.

MCMC Markov Chain Monte Carlo.

MM Markov Model.

Natsal National survey of sexual attitudes and lifestyles.

NB Monetary Net Benefit.

NHS National Health Service.

NHS EED National Health Service Economic Evaluation Database.

NICE National Institute for Health and Care Excellence.

ODE Ordinary Differential Equation.

Pap test Papanicolaou test.

PDE Partial Differential Equation.

PeIN Penile Intraepithelial Neoplasm.

PISCES Psychological Impact of cervical Screening and Condylomas: an Epidemiological Study.

POMP Partially Observed Markov Process.

PSA Probabilistic Sensitivity Analysis.

PVC Present Value of Cost.

PVU Present Value of Utility.

QALY Quality-Adjusted Life Year.

QoL Quality of Life.

RAM Random Access Memory.

RRP Recurrent Respiratory Papillomatosis.

SATA Serial Advanced Technology Attachment.

SAVI Sheffield Accelerated Value of Information.

SDE Stochastic Differential Equation.

STI Sexually Transmitted Infection.

VaIN Vaginal Intraepithelial Neoplasm.

VIN Vulvar Intraepithelial Neoplasm.

WBDiff WinBUGS Differential Interface.

WinBUGS Bayesian inference Using Gibbs Sampling (for Windows).

Chapter 1

Introduction

1.1 Background of research

Vaccines against infectious diseases offer major health benefits to society [279, 386] and have been instrumental in the prevention of conditions previously causing egregious burden from the public health perspective. Examples include the worldwide eradication of smallpox [378] and the extremely low incidence of tetanus, diphteria, congenital rubella syndrome, mumps and measles in the Western world [282]. However, despite being frequently successful from a clinical point of view, vaccination programmes are often costly and complex to apply to the target population. Given that publicly funded health care systems such as the UK National Health Service face increasing budget limitations, health interventions (including vaccination programmes) are increasingly subject to cost-effectiveness analysis (CEA) [51, 281] as a pre-requisite to their implementation.

In a CEA, the impact of the interventions under investigation is evaluated through an outcome in effectiveness, such as the quality of life or life years gained, medical conditions avoided etc. The costs of the different interventions to increase the effectiveness by one unit are then compared [268].

Much of the recent research in health economics has been focussed on grounding CEA on sound statistical bases, increasingly often following a

Bayesian approach [22, 276, 329]. Unlike a standard statistical or epidemiological analysis, where the objective is to produce a form of inference (e.g. to evaluate treatment efficacy [320] or to estimate the prevalence of a disease [208]), health economic evaluations aim at identifying the best course of action, given the current evidence. Here, "best" means to exclusively focus on interventions which are effective and at the same time affordable to public health insurance systems.

Several sources of uncertainty play a role in health economic evaluations, including structural and parameter uncertainty. The first refers to the simplifications and scientific judgements made [41], e.g. with respect to the natural history of disease and the corresponding interventions. For example, not all body areas affected by a certain pathogen are necessarily considered, and not all treatments against the health condition under investigation are necessarily compared. This can considerably influence the decisions made based on health economic evaluations. A study showed that the effects of structural uncertainty are ignored often (in 78 out of 90 model-based submissions to the *National Health Service* (NHS) [40]). A second source of uncertainty, parameter uncertainty, is especially relevant in the case of infectious disease. For instance, the actual mechanisms of pathogen transmission are often not fully understood and there is substantial uncertainty on parameters such as the probability of infection per contact, which are sometimes based mostly on expert judgement. Therefore, it is essential to assess the impact of parameter uncertainty on the decision making outcome, a process typically known as *Probabilistic Sensitivity Analysis* (PSA) [22, 24, 51].

PSA is usually based on a simulation approach [22, 45, 246, 272, 288, 372]: uncertainty about the relevant parameters is described by a suitable probability distribution, from which a large sample of values is obtained, e.g. via Markov Chain Monte Carlo (MCMC) sampling under a Bayesian framework or using bootstrap in a frequentist approach. These are used to induce a distribution over the possible decisions and can be analysed

to determine the impact of parameter uncertainty on the decision-making process. If the optimal decision varies substantially across the simulations, then the decision-making process is sensitive to the uncertainty in the model parameters. As a consequence, further research needs to be conducted as recommended by the health technology assessment bodies.

The *National Institute for Health and Care Excellence* (NICE) is arguably the leading health technology assessment agency in the world. In the UK, NICE is responsible for providing guidance and advice on whether proposed interventions should be publicly funded. Over the years, NICE has developed a set of criteria and guidelines that drive the analytic process of CEA [268]. Crucially, these involve the explicit necessity of PSA.

Interestingly, however, in the UK the assessment and appraisal of vaccines falls under the remit of the *Joint Committee for Vaccines and Immunisations*, an independent expert advisory committee to the ministers and health departments. Since 2009, the Health Protection Regulation obliges the Secretary of State to ensure that recommendations for national vaccination programmes are based on an assessment demonstrating cost-effectiveness [198]. However, there are currently no vaccine-specific guidelines for developing clinical or cost-effectiveness evidence. One of the reasons for this circumstance is perhaps the intrinsic complexity of infectious disease modelling, which is typically performed through *compartmental* models [371, 376]. These are highly complicated mathematical tools capable of simulating the natural history of disease infection and progression.

1.2 Compartmental models

In pathogens transmissible among humans, compartmental models need to account for population dynamics and the effects of *herd immunity* [12]; due to lower infection prevalence, the introduction of a preventive measure such as vaccination induces a reduced risk of pathogen exposure. Only dy-

namic models are able to account for these effects and as a consequence to prevent incorrect predictions [129, 291]. Furthermore, in order to perform a full PSA, it is necessary to quantify the joint uncertainty in the model parameters, resulting in a probabilistic model output. Thus, a dynamic compartmental methodology that is able to incorporate stochastic variations in the model parameters is the most appropriate choice of model.

Several subgroups of compartmental models are presented in the literature on infectious disease transmission modelling; these are either *deterministic* or *stochastic* models. In a deterministic model, the same set of parameter values and initial conditions always results in the same model output. In contrast, a stochastic model produces different output each time the model is run, accounting for randomness. The parameters of deterministic models are commonly assigned one predefined value, e.g. a point estimate (mean, median, mode); however, assigning suitable probability distributions is also possible. Stochastic models are based on stochastic processes; therefore, the states of the model have distributions. However, as for deterministic models, a corresponding model parameter can either consist of a single value, or a whole distribution of values.

A common approach to deterministic models is given by systems of Ordinary Differential Equations (ODEs). These can be extended to account for chance variation by a so-called “error term” which is based on a stochastic process, resulting in systems of Stochastic Differential Equations (SDEs). In addition, stochastic models based on discrete- and continuous-time stochastic processes (such as Poisson processes, Bernoulli processes or Markov processes) are presented for infectious diseases; however, only models based on Markov processes are common in the health economics literature. These are often termed multi-state or Markov models (MMs).

Compartmental models differ in the ways of accounting for i) dynamic interactions between members of the population, as well as ii) parameter uncertainty and thus the eligibility to conduct PSA in a straightforward

way. From the technical point of view, dynamic compartmental models are usually fitted by solving systems of ODEs. While these automatically deal with features such as herd immunity (and thus are considered the "industry standard" in infectious disease modelling), they are almost invariably characterised by a notable computational effort. An ODE-based model in a Bayesian context would increase this effort to a level which would no longer be computationally feasible, especially if the model were highly complex (e.g. including a large number of states or age cohorts). One important consequence is that, in most cases, epidemiological and economic modelling for infectious disease performed by means of ODEs does not account for parameter uncertainty.

In the context of deterministic ODE-based models, methods such as Monte Carlo Sampling and Latin Hypercube Sampling [255] can be used to incorporate distributions on the model outcome, as shown in [35, 203, 204]. Latin Hypercube Sampling was developed to reduce the amount of simulations required by Monte Carlo Sampling, based on a technique of stratified sampling, ensuring that extreme values of the distribution are sampled with precision [255]. However, applying these sampling methods is rather complex and computationally intensive. In addition, they are prone to result in incorrect predictions on the natural history of disease since parameter uncertainty is not accounted for directly in the compartmental model, but only in retrospect.

The difficulties in accounting for parameter uncertainty in ODE systems might be one of the reasons why the *International Society for Pharmacoeconomics and Outcomes Research* (ISPOR) guideline for best modelling practice in infectious disease suggests that PSA is *not* a fundamental component of health economic assessment [291]. This recommendation is given in contrast with NICE and virtually any other disease area. As a consequence, most economic models for vaccines only consider deterministic sensitivity analysis, which is based on selecting a grid of "plausible" values for a sub-

set of model parameters in order to assess the robustness of the decision-making process. This approach is however not recommended in general, as it fails to account for potential correlation among the parameters [15, 22, 51].

An alternative compartmental specification is given by MMs. As described above, a MM is based on a Markov process which is a specific case of a stochastic process, defined by a Markov property. In a MM, the movements of individuals across the states is thus governed by this property. Typically it is assumed that the chance of leaving the current state depends only on (some of) the past state(s). However, especially in the health economic literature, the Markov property is often relaxed, and movements can additionally depend on specific covariates. MMs are used to model disease progression over time across a finite set of states. Although MMs can also be computationally intensive, it is generally feasible to incorporate distributions on the model parameters (e.g. using a Bayesian framework) or to use re-sampling methods such as the bootstrap to characterise the uncertainty in the model parameters. Perhaps for this reason, MMs are a very popular tool in health economic evaluation. Nevertheless, a major limitation in infectious disease transmission modelling and economic evaluations of the related interventions is that in their standard format, MMs are intrinsically static, i.e. they do not account for population dynamics [53] and the effects of herd immunity.

However, it is possible to indirectly account for herd immunity in static MMs as shown by [16, 82, 83, 365, 370]. Once a vaccine is introduced in a population at a specific coverage rate, these authors reduce pathogen prevalence in unvaccinated people through multiplication by adjustment factors. Another possibility is to lower transition probabilities to the state of infection proportionally on vaccine-specific parameters (such as coverage, efficacy and compliance rates). In indirect adjustment approaches, population dynamics, mixing patterns between people and dynamic changes in pathogen prevalence are not considered. Thus, these are not comparable to

a fully dynamic approach and commonly result in under- or overestimation of pathogen prevalence. The quality of the corresponding model outcome could be improved through extensive calibration to prevalence data collected after vaccine introduction; however, these prevalence data are not available for newly introduced vaccines. Thus, this approach is not recommended in general. Further details are discussed in Sections 4.4.2 and 4.6 as well as Appendices B.3 and B.4.

1.3 Contributions

With a view to simplifying the process of PSA in health economic models of interventions for infectious diseases, we introduce in this PhD thesis an extension to standard discrete-time MMs, which we term dynamic Bayesian MMs. Discrete-time MMs are frequently used in the health economics literature. Continuous-time MMs are also presented; however, due to their higher effort on implementation and computation, these are not very common. The expression “Bayesian” refers to the inference conducted. Dynamic interactions between people are considered through the force of infection of the pathogen, which is a function of the probability of infection transmission, contact patterns between people, and infection prevalence (as understood in [371]). We directly include the force of infection, which automatically accounts for the effects of herd immunity, into the state allocation algorithm of a standard MM. In other words, the movement of a susceptible individual to the state of infection is directly represented by the dynamic force of infection. Our approach does not involve ODEs. A publication introducing our methodology was submitted to the journal *Medical Decision Making*.

A direct inclusion of the force of infection into the state allocation algorithm of a MM [92, 156] or its direct consideration in a model based on a stochastic process [20, 141, 155] was presented previously by several authors; details on these models are given in Section 2.3. Three of these

models [20, 141, 156] are implemented in a Bayesian framework. However, in contrast to our dynamic Bayesian MM, these models are only suitable to include a low number of states due to computational limitations and consist of no more than four states. Our dynamic Bayesian MM is especially suitable to incorporate an extensive number of states as described below and shown in Chapter 5 for the application to human papillomavirus modelling. Another difference to our approach is that these authors do not conduct a health economic evaluation. In the health economics literature, to the best of our knowledge, no approach of a dynamic stochastic model including a high number of states is presented. Another aspect worth mentioning is that stochastic models account for chance variation in the model output but not necessarily for parameter uncertainty. However, this is essential in infectious disease (especially if sexually transmitted) for a number of reasons.

Due to ethical constraints, clinical trials on most influential parameters such as the probability of pathogen transmission between individuals cannot be conducted to resolve parameter uncertainty; however, data from observational studies are available for certain pathogens. Data on partner acquisition rates are obtained through surveys and commonly include a lot of noise as a consequence of societal expectations. Depending on the quality of the literature information, evidence synthesis can contribute to a considerable reduction in the amount of parameter uncertainty. The probabilistic output of the dynamic Bayesian MM can be processed into a PSA as an essential part of a CEA without the necessity of further simulation approaches.

Application to human papillomavirus modelling

The main motivation for the development of the dynamic Bayesian MM was to identify the most cost-effective (i. e. affordable and beneficial to society) intervention strategy against human papillomavirus (HPV). HPV is mainly sexually transmitted and can induce neoplastic malignant and benign lesions in a variety of body regions, especially in the cervix and anogenital

area [127]. The virus places a considerable clinical and economic burden on public health providers; additionally, it has high impact on quality of life and life expectancy of affected individuals [257, 260]. At present, a vaccine against HPV is recommended for teenage females in most Western countries, and males are commonly not included in HPV vaccination schedules.

The aim of research is to compare predictions of the dynamic Bayesian MM on the natural history of HPV infection and disease progression in different intervention scenarios to investigate the impact of i) the inclusion of a large number of HPV-induced diseases; ii) the effects of herd immunity; and, most importantly, iii) the extension of the HPV vaccination schedule to males.

In contrast to the vast majority of HPV models in the literature which only account for cervical cancer, the dynamic Bayesian MM structure consists of a large number of states, including anogenital warts, HPV-induced cancers and precancerous stages of the cervix, vagina, vulva, penis, anus, as well as head and neck. We observe a "virtual" population consisting of multiple age cohorts which enter the model and move between the states over a pre-specified follow-up period. The movement to the state of HPV infection is directly represented by the dynamic force of infection. Thus, in contrast to standard MMs, acquiring the HPV infection becomes dynamic and depends on the HPV transmission probability per partnership, sexual mixing behaviour as well as HPV prevalence in the mating partners. As a consequence, herd immunity is accounted for, which is especially important in context of CEAs of preventive interventions such as vaccination. We account for three different interventions: in *female-only* and *universal* vaccination (including both sexes), the youngest age cohorts have the chance to receive the vaccine at a pre-specified uptake rate; in addition, cervical screening is offered to females at age-specific rates. In contrast, in *screening-only*, cervical screening is the only preventive measure.

At the end of the follow-up, the model outcome on the number of indi-

viduals in the states over the whole observation time period is processed in terms of a CEA, comparing costs and benefits of *universal* vaccination to those of *female-only* vaccination and *screening-only*, respectively. Due to the fact that our model is implemented in a Bayesian framework, parameter uncertainty is accounted for, which increases the predictive qualities. Furthermore, PSA can be conducted straightforwardly once the model outcome is available. A paper on the HPV model describing the findings of the natural history of disease and the corresponding CEA is published in [178].

1.4 Contents of PhD thesis

This PhD thesis is structured in two parts. The first part (including Chapters 2 and 3) introduces compartmental models for health economic evaluations and the dynamic Bayesian Markov model. In the second part (including Chapters 4 - 6), the dynamic Bayesian Markov model is specified to conduct a CEA of HPV vaccination.

Chapter 2 gives an extensive overview on compartmental methodology, especially focussing on ODE-based and MMs. Most importantly, the contribution of the dynamic Bayesian MM is described in detail, including the calculation of the force of infection, its integration into the state allocation algorithm, and model implications. In addition, hybrid models which combine static and dynamic methodology are introduced.

In Chapter 3, three different methodologies (a deterministic ODE-based model, a Bayesian ODE-based model and the dynamic Bayesian MM) described in Chapter 2 are compared in practice. The term “deterministic” refers to the nature of the parameters, whereas the term “Bayesian” refers to the inference conducted. A case study on a chronic sexually transmitted infection is introduced, and the outcome of the three models on infection prevalence as well as the results of the corresponding CEAs are compared. This includes three different calibration approaches; the implications

of visual calibration, frequentist probabilistic and Bayesian calibration are shown. A selection of the corresponding programme code is presented in Appendix A.

Chapter 4 describes the literature review on the CEA models of different HPV vaccination strategies. This includes details on the databases searched, the corresponding search word combinations as well as a summary on the most important findings on model assumptions and results. The summary is arranged according to model assumptions (including vaccination strategies), methodologies, and model outcome. Summary tables including details on all publications retrieved are presented in Appendix B.

In Chapter 5, the specification of the dynamic Bayesian MM for the CEA of HPV vaccination is described in detail. This includes assumptions on interventions, the model structure, sexual mixing and a selection of transition probabilities in females. Further details on the model structure, transition probabilities in both sexes, sources of prior information and posterior results are presented in Appendices C-F.

Chapter 6 presents the results, including convergence and autocorrelation diagnostics, visual calibration of a selection of states to data, the natural history of HPV-induced diseases as well as the health economic evaluation including PSA. More extensive calibration results are displayed in Appendix G.

The thesis ends with a summary and final conclusion, describing advantages and limitations of the dynamic Bayesian methodology in comparison to ODE-based models. Furthermore, the results of the CEA of HPV vaccination strategies are summarized.

Part I

A dynamic Markov model in a Bayesian framework

Chapter 2

Compartmental models

2.1 Introduction

Statistical models are designed to make statements on the general population through random samples. The overall population of individuals affected by a certain infectious disease cannot be observed. However, it is possible to simulate the natural history of disease infection and progression through suitable statistical methodology, involving the observation of a random sample of individuals over a pre-specified follow-up period. The purpose of infectious disease modelling is to result in most reliable predictions on the implications of infectious diseases. A large variety of modelling approaches are available; yet, compartmental models are most widely used in the health economics literature.

This chapter gives a general overview on compartmental models and mainly focusses on two categories which are represented by Ordinary Differential Equation (ODE)-based models and Markov models (MMs). These two can be combined into so-called hybrid models. Stochastic modelling approaches based on Stochastic Differential Equations (SDEs) are briefly explained. Following the description of established methodology, we introduce our contribution of a dynamic Bayesian MM, including details on the calculation of the force of infection, its direct integration into the estima-

tion of the acquisition of the infectious agent, and model implications in the Bayesian framework.

2.2 Overview

Compartmental models consist of a set $\mathcal{S}$ of mutually exclusive and exhaustive states describing disease infection and progression. We indicate the elements of $\mathcal{S}$ as $s = 1, \ldots, S$. Members of a "virtual" population move across the states over a pre-specified time horizon. Compartmental models are population-based; thus, individual members of the population are indistinguishable, and only proportions of the population in the states can be evaluated.

Figure 2.1 shows an example of a compartmental model incorporating the natural disease history of a chronic sexually transmitted infection (STI) with $S = 5$ states. The assumptions encoded by this structure are that the whole population initially is in the state *Susceptible* (indexed by $s = 1$), from which a proportion can move to the state *Infected* ($s = 2$). Following this, a proportion of the population moves to an *Asymptomatic* state ($s = 3$). A progression to the state *Morbid* ($s = 4$) induces the development of disease symptoms. The state *Dead* ($s = 5$) can be reached from any state; people die due to any cause or as a consequence of being in the state *Morbid*. Compared to the average population, the latter have a higher risk of death. A transition from one state to another is defined according to suitable *transition parameters* [380]. They are indicated as $\phi_{r,s}$, where $r, s \in \mathcal{S}$ represent the original and target state, respectively. We consider an open model structure in which people which are alive are able to proliferate at a rate χ, resulting in a replenishment of the pool of susceptibles at risk of contracting the infection.

Compartmental models may differ in three important characteristics. The first is the specification of time. The most realistic option is to allow transi-

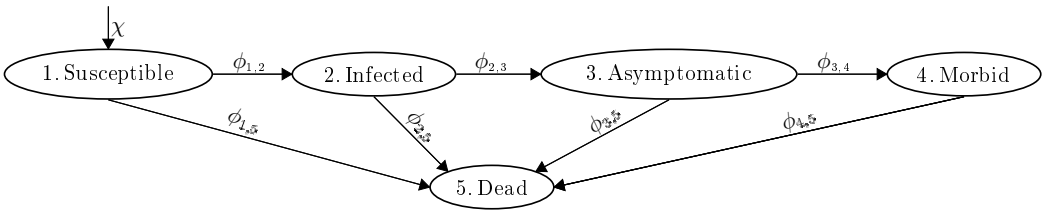

Figure 2.1: Model structure of a hypothetical chronic sexually transmitted infection consisting of five states. The arrows represent the possible transitions. These are governed by the parameters $\phi_{r,s}$ with indices $r, s \in \mathcal{S}$ representing origin and target states, respectively. The replenishment of the pool of susceptibles by newborns proceeds at a rate χ.

tions among the states to happen at any point in time $t > 0$; this is a so-called "continuous-time approach". Alternatively, it is possible to assume that transitions occur in discrete time where only one transition is possible within a pre-defined time interval $\mathcal{I}_t = [t, t + \kappa)$, where κ determines the corresponding interval width, commonly referred to as *cycle*. Depending on the medical context, κ can be specified in terms of daily, weekly, monthly or yearly cycles. The second difference concerns the way in which population dynamics are considered: models including a force of infection which accounts for population prevalence are referred to as *dynamic*, while those that include a fixed force of infection and thus ignore the effects of herd immunity are termed *static*. A third characteristic is that compartmental models are either deterministic or stochastic. In a deterministic model, the same model output is always obtained for the same values of the model parameters. In contrast, a stochastic model accounts for chance variation and results in different output even if the values of the parameters do not change.

In addition, different approaches to model parameter specification exist, which may have major impact on the outcome of health economic evaluations. Depending on the compartmental methodology used, the induced effort on implementation and computation does not necessarily allow the inclusion of probability distributions on all model parameters. In that case, model parameters are assigned fixed values. Commonly, these are inferred through a relevant summary (e.g. mean, median or mode), for example ob-

tained from available data. The point estimate is then used as a plug-in for the corresponding parameter. In contrast, if probability distributions are assigned to parameters, parameter uncertainty is propagated through the infection progression. While frequentist versions of this strategy exist (e.g. based on bootstrap), this type of modelling is most naturally handled within a Bayesian paradigm.

2.2.1 Ordinary Differential Equation models

ODE systems are deterministic by definition. The rate of change in the members of a population within a given state is modelled in continuous time; thus, the corresponding parameters are transition *rates* and we denote them as $\rho_{r,s}(t)$, with $r, s \in \mathcal{S}$ representing again the origin and target states, respectively. In principle, transition rates can depend on t, but do not necessarily have to. The number of people transitioning in each state at t is multiplied by the corresponding transition rates to obtain the inflow and outflow to and from a state. The difference between the number of people entering and leaving a state corresponds to the derivative of the number of those in the respective state.

Back to our example, we define the vector $\boldsymbol{n}(t) = (n_1(t), \ldots, n_S(t))'$, where $n_s(t)$ is the number of people in state s at time t, and χ is the proliferation rate. The corresponding ODE system is given by the set of equations

$$\begin{aligned}
\frac{dn_1(t)}{dt} &= \chi[n_1(t) + n_2(t) + n_3(t) + n_4(t)] - \rho_{1,2}(t)n_1(t) - \rho_{1,5}n_1(t) \\
\frac{dn_2(t)}{dt} &= \rho_{1,2}(t)n_1(t) - \rho_{2,3}n_2(t) - \rho_{2,5}n_2(t) \\
\frac{dn_3(t)}{dt} &= \rho_{2,3}n_2(t) - \rho_{3,4}n_3(t) - \rho_{3,5}n_3(t) \\
\frac{dn_4(t)}{dt} &= \rho_{3,4}n_3(t) - \rho_{4,5}n_4(t) \\
\frac{dn_5(t)}{dt} &= \rho_{1,5}n_1(t) + \rho_{2,5}n_2(t) + \rho_{3,5}n_3(t) + \rho_{4,5}n_4(t).
\end{aligned} \tag{2.1}$$

The rate of change in the number of people in each state at each point in

time t is subject to population dynamics and exposure to sources of infection. The transition to the state of infection is determined by the dynamic, time-specific force of infection of the pathogen, indicated by $\rho_{1,2}(t)$ in (2.1). This is a function of the probability of pathogen transmission, partner acquisition rates and population prevalence.

In a deterministic ODE system, a point estimate (e.g. mean, median or mode) is usually taken from available data to inform the model parameters. In that case, parameter uncertainty is not accounted for; as a consequence, the corresponding model output can be incorrect. An example for a point estimate is given by a summary statistic on disease incidence. The term incidence is often reported as a rate per 100,000 people at risk and refers to newly acquired disease within a pre-defined period of time. An incidence rate can thus for example be used to inform the transition rate of susceptibles to the state of infection. In addition, scenario analyses are often also performed, for example by plugging in more extreme estimates (e.g. lower or upper quantiles) for the parameters. As mentioned earlier, this is not equivalent to the application of a full PSA.

Theoretically, it is possible to assign a suitable probability distribution to each parameter of an ODE-based model, for example in a Bayesian context. The uncertainty is then propagated through the estimation procedure, which again generates a full distribution of outcomes. This type of model can be analysed using for instance Markov Chain Monte Carlo (MCMC) samplers such as `WinBUGS` [355] (via the interface `WBDiff` [247]) or `Stan` [4], a very promising tool, which in general performs extremely well with relatively complex systems. Both include ODE solvers and can be linked to the statistical programming language `R`.

However, `WBDiff` is generally computationally intensive and the ODE solvers provided by `Stan` struggled in "stiff"[1] regions of ODE systems until

[1] An ODE is termed *stiff* if the solution of the function varies slowly in the beginning, followed by a sudden rapid change [262].

the very latest releases. The underlying numerical solver became unstable unless the step-size was set to very small values. The newest release (2.14) seems to have overcome this issue and thus `Stan` looks very promising for future developments [5].

More importantly, in realistic problems including a large number of states and complex structures, ODE models including probability distributions on all model parameters may be impractical since the model needs to be run for a large number of simulations to ensure convergence of each parameter and thus the ODE system has to be solved repeatedly for each parameter combination. The increase in the computational time is mainly induced by the length of the observation time horizon, the overall amount of parameters with assigned probability distributions, the complexity of contacts, the number of differential equations in the ODE system and their nature (stiff, non-stiff, or a combination of both). Consequently, complex ODE-based models which incorporate a distribution on each model parameter are rare exceptions in the literature on infectious disease transmission modelling [33].

Accounting for parameter uncertainty does not mean that an ODE system is no longer deterministic. However, deterministic ODE systems can be extended to introduce chance variation in the model output by the inclusion of an "error term" on the coefficient (i.e. the transition rate) of the ODE. This error term is indicated by a stochastic process [286]. This results in so-called Stochastic Differential Equations (SDEs). In infectious disease, SDEs are especially used when the spread of pathogens in small populations is modelled; in that case, chance variation plays an important role since the pathogen could go extinct under certain conditions, but does not necessarily have to. If a deterministic ODE system was used in that case, the pathogen would either always or never go extinct which is not realistic [60]. A simple SDE model is for example given by

$$\frac{dS}{dt} = -(\rho + \sigma_\star G(t))S(t)$$
$$\frac{dI}{dt} = (\rho + \sigma_\star G(t))I(t),$$

where ρ is a transition rate, $S(t)$ and $I(t)$ are the number of susceptible and infectious people over time, respectively, $\sigma_\star$ is the scaling parameter of the stochastic process, and $G(t)$ represents the stochastic process.

A stochastic process is a family of random variables $\{X_{\lambda_\star}\}$ and is indexed by $\lambda_\star \in \Lambda_\star$. A stochastic process can either be specified in continuous or discrete time. In a continuous time process, $\Lambda_\star$ is defined as a time interval or the whole real line. In contrast, in a discrete time process, $\Lambda_\star$ is either defined in $\mathbb{N}$ or $\mathbb{Z}$ [343]. Specific cases of stochastic processes are given by Poisson and Markov processes. A Poisson process can for example be applied to estimate the number of people in a certain state over time, e.g. in context of a SDE. If time series data are available, these can be used to estimate the corresponding event rate, e.g. through maximum likelihood estimation or a Bayesian approach. Once the event rate is known, future predictions can be made. A Poisson process can as well be a Markov process. A Markov process is defined through the Markov assumption as described in the following.

2.2.2 Markov models

A Markov model is based on a Markov chain. A Markov chain contains a continuous or discrete set of states, the so-called state space. We focus on discrete state space, including a predefined number of mutually exclusive and exhaustive states. The main characteristic of a Markov chain is the Markov assumption which says that the conditional distribution of a future state given the present and the past states is equal to the conditional distribution of the future state given the present state and the k_* previous states,

where $k_* \in \{0, 1, 2\}$. However, the Markov assumption can be relaxed by accounting for covariates (e.g. age and sex), time-specific population prevalence, population dynamics or time spent in the current state in the transition parameters. The Markov assumption is frequently relaxed in the transition parameters of MMs in the health economic literature through the inclusion of covariates.

If the time spent in the current state influences the transition to a future state, a so-called semi-Markov model can be implemented. This is for example the case in chronic infectious diseases with periods of exacerbation; the longer the patient was in a state of remission, the higher the risk of exacerbation. The Markov assumption is then relaxed by accounting for the time spent in the current state [73]. However, semi-Markov models are beyond the scope of this PhD thesis and thus not explained in further detail.

As for ODE-based models, MMs can be implemented for continuous time; for consistency, we will briefly describe these and refer to [128] for more extensive detail. As suggested earlier, in the former, the rates of change are calculated dynamically through differentiation, while in the latter, the transitions are described by a Markov process. This continuous-time Markov process can account for population dynamics and is defined by a transition rate matrix $\boldsymbol{Q}$ and the corresponding initial state distribution. The time spent in a state is described through exponentially distributed rates. The probability distribution on the state space p is given by the Kolmogorov Forward Equation [128]

$$\frac{dp(t)}{dt} = p(t)\boldsymbol{Q}.$$

Solving this differential equation given the initial condition $p(0)$ results in the state distribution $p(t)$ of the Markov process at time point t,

$$p(t) = p(0)e^{t\boldsymbol{Q}}.$$

This solution is based on the exponential of the transition rate matrix and can thus be computationally intensive for large matrices if many states are included in the model [14]; however, a solution can also be obtained through an ODE solver, e.g. based on the Runge-Kutta method [309].

Continuous-time MMs have the advantage that transitions across the states are possible at any point in time t. However, the vast majority of MMs in the health economic literature is based on a discrete-time approach [363] and thus these are described in more detail in this section. In a discrete-time MM, members of the population move across the states according to a set of transition *probabilities* only once per time interval (commonly referred to as "Markov cycle"). These probabilities can be arranged in a matrix $\mathbf{\Pi} = (\pi_{r,s})$, whose elements represent the transition probabilities for movements from an original state r to a target state s. For the model structure of Figure 2.1, the transition probability matrix is defined as

$$\mathbf{\Pi} = \begin{pmatrix} \pi_{1,1} & \pi_{1,2} & 0 & 0 & \pi_{1,5} \\ 0 & \pi_{2,2} & \pi_{2,3} & 0 & \pi_{2,5} \\ 0 & 0 & \pi_{3,3} & \pi_{3,4} & \pi_{3,5} \\ 0 & 0 & 0 & \pi_{4,4} & \pi_{4,5} \\ 0 & 0 & 0 & 0 & 1 \end{pmatrix},$$

implying that, for example, a susceptible either acquires the infection (with probability $\pi_{1,2}$), dies (with probability $\pi_{1,5}$), or remains susceptible, which occurs with probability $\pi_{1,1} = 1 - \pi_{1,2} - \pi_{1,5}$.

If we define the vector $\boldsymbol{n}_t = (n_{1t}, \ldots, n_{St})'$, where n_{st} is the number of people in state s and at each time interval $\mathcal{I}_t$, then transitions across the states from one time interval to the next are calculated as

$$\boldsymbol{n}_{t+1} = \mathbf{\Pi}\boldsymbol{n}_t. \tag{2.2}$$

The number of people in the states are integers and are thus rounded up or off once the state allocation algorithm was run. MMs are relatively straight-

forward to implement and are commonly used to model the progression of non-communicable conditions such as cardiovascular disease and cancer. Therefore, they are established in the health economic literature and well-known to both clinicians and decision makers. However, the process of pathogen transmission is not estimated correctly by MMs presented in the literature (apart from [92, 156]). A transition of susceptibles to the state of infection is commonly represented by a static transition parameter which does not consider changes in the population prevalence over time. These especially occur after the introduction of a preventive intervention such as vaccination into a fully susceptible population.

The predictions of static MMs on population prevalence are commonly incorrect (although notable exceptions include scenarios with very low vaccine coverage or pathogens that cannot be transmitted between humans, e.g. tetanus). In the worst case, the whole model outcome on infection prevalence and the related CEA can be incorrect, e.g. because of the impact of an unrecognised shift in the age of infection of childhood diseases. Some childhood diseases are relatively harmless in young children but prone to lead to serious health issues in adults. The consequences of incorrect predictions of static MMs on population health and induced costs, e.g. through hospitalisation and treatment, can be dire [53].

As for ODE-based models, a dynamic force of infection could be incorporated into the transition probabilities to account for the effects of herd immunity. To the best of our knowledge, the health economic literature does not include any dynamic Markov models. A dynamic hidden MM is presented by Cooper and Lipsitch [92] and a dynamic Bayesian MM by Gibson and Renshaw [156]; however, these models only include a small number of states, are implemented in continuous time, and the authors do not conduct a health economic evaluation.

2.2.3 Hybrid models

An interface between static and dynamic alternatives is given by the so-called *hybrid* models. These are combinations of the two different versions of models. First a dynamic transmission model, commonly based on ODEs, is implemented to estimate infection prevalence. Then the prevalence estimate is used as input for the natural history model of disease progression, which is for example a static MM or microsimulation model. As a consequence, the disease acquisition is estimated in a dynamic way. These approaches are often used in human papillomavirus modelling. Examples in the health economics literature include [215, 339].

While useful in some circumstances, a hybrid approach has several drawbacks. First, the transmission models involved commonly include fixed values on model parameters (rather than whole distributions). Consequently, even if PSA is performed on the disease progression part of the hybrid model, it does not refer to the crucial disease transmission component. Second, hybrid models are extremely complex since they consist of two separate components based on different methodologies. These are run sequentially since an interim step is necessary to include the estimated prevalence results into the disease progression model.

2.3 Dynamic Bayesian Markov models

To overcome the limitations discussed above and with a view to extending the modelling framework for health economic evaluation of interventions in infectious disease, the main idea behind our proposed model is to add a force of infection which depends on population dynamics and prevalence into a discrete-time MM setting. As a consequence, the transition probabilities from the state *Susceptible* to the state *Infected* are directly defined by the dynamic force of infection.

Specifically, we set up our model so that the force of infection is calculated separately within each cycle of the state allocation algorithm corresponding to (2.2) as a function of

- the probability of pathogen transmission per contact, which we indicate as β;
- the rate of contacts between susceptible and infectious members of the population ω; and
- the time-dependent pathogen prevalence

$$\psi_t = \frac{I_t}{N_t},$$

where I_t represents the number of people in the state of infection and, assuming that state S indicates death,

$$N_t = \sum_{s=1}^{S-1} n_{st}$$

is the number of those alive at time interval $\mathcal{I}_t$. Depending on the medical context, prevalence might be specific to covariates such as age and sex, and cycle length is adjusted.

The force of infection is recalculated at each Markov cycle as

$$\rho_t = \beta\omega\psi_t. \tag{2.3}$$

Since ω is a rate, (2.3) also results in a transition rate. Assuming that ρ_t remains constant within each time interval, the corresponding time-dependent transition probability for the discrete-time MM is estimated as

$$\pi_{1,2,t} = 1 - e^{-\rho_t}. \tag{2.4}$$

The estimation is only approximate due to the competing risk of death and the assumption of uniformity within the intervals $\mathcal{I}_t$. This assumption is not likely to hold if the disease is characterised by very fast transmission, or when events associated with the infection are likely to occur in short periods of time. In these cases, it is perhaps advisable to reduce the length of the cycles κ and the duration of the follow up.

This probability can be multiplied by the proportion of the population in the state *Susceptible* to provide an estimation of the contingent of movements to the state *Infected*, effectively including dynamic, time-dependent changes in the population prevalence in the corresponding transitions.

The dynamic Bayesian MM can be implemented for closed as well as open populations, accounting for deaths, births (as shown in Section 3.3) and the entering of healthy individuals (as described in Section 5.2). In comparison to hybrid models, our approach does not require two separate modules for disease transmission and progression. In addition, computational time is reduced by fitting models that do not involve complex ODEs, while still allowing for mixing patterns within the population.

A third potential advantage of the dynamic MM framework is that it is fairly simple to incorporate probability distributions on all model parameters, even if the model is complex with an extremely large number of parameters and states. In contrast, the related computational effort in a comparable ODE-based model would be extremely high. As a consequence, at the current stage of research, the literature does not present any complex ODE-based models which incorporate a high number of model parameters with assigned probability distributions [33].

Accounting for parameter uncertainty is particularly relevant because, for obvious ethical and practical reasons, it is invariably difficult (if possible at all) to obtain and use experimental evidence to inform the pathogen transmission probability β and the active contact rate ω — arguably the crucial parameters. Often observational studies or expert opinions are the only

available information with the consequence that large uncertainty remains over the most likely range, let alone the "true" value of the parameters. A Bayesian approach may provide great benefit in allowing this uncertainty to be fully propagated and perhaps in integrating different sources of evidence (e.g. using evidence synthesis [380]); this indeed has been advocated for MMs in the health economics literature [22,93,380] and is described in more detail in Section 5.6.

In a Bayesian dynamic MM setting, it is possible to assign prior distributions to the parameters (β, ω) to represent the state of science — if data are available, these are updated into posterior distributions although it is possible to still propagate uncertainty in the priors even when no data on pathogen transmission or active contacts are observed. In addition, the quantity ψ_t is estimated as a function of transition probabilities, which can be modelled using suitable distributions. This modelling process induces a probability distribution on ψ_t and a fortiori also on ρ_t, which is defined as a function of the three parameters (β, ω, ψ_t). Thus, the corresponding transition probabilities $\pi_{1,2,t}$ are modelled probabilistically, meaning that uncertainty in the population dynamics is propagated through the economic model.

As suggested earlier, another crucial aspect in infectious disease modelling (and more generally in statistical analysis) is that of calibration of the model output [151, 366]. In a Bayesian framework, the transition probabilities can be calibrated directly in the process of updating the prior into the corresponding posterior distributions. For example, available data on the proportion of the population progressing to a more severe state following infection as observed in large population registries can be used to update the prior distribution of the corresponding transition probability. Furthermore, the Bayesian framework enables the calibration of the numbers of people in the states directly in the state allocation algorithm, using available time series data for a specific time frame of follow-up as described in Section 3.5.

Finally and specifically for the purpose of economic evaluation, the dy-

namic BMM has the advantage that PSA can be performed "for free", once the model output is produced. In a Bayesian framework, the MCMC simulations for all the model parameters can be combined to obtain a full characterisation of the uncertainty in the decision-making process. This can be post-processed (e.g. using the `R` package `BCEA` [3]) to produce relevant summaries such as the cost-effectiveness plane, the cost-effectiveness acceptability curve (CEAC) and the analysis of the value of information. We report these in details in the next chapter. A publication describing the methodology of the dynamic Bayesian MM is in preparation and will be submitted to the journal *Medical Decision Making*.

We present a discrete-time rather than a continuous-time MM since these are commonly used in the health economics literature and thus well-known to both clinicians and decision makers. In addition, the related effort on implementation and computation is lower, especially if the state space contains a large number of states as for the application to human papillomavirus described in Chapter 5. In a continuous-time MM, the model outcome on the time spent in each state can either be obtained through solving the exponential of the transition rate matrix or a numerical approximation procedure by means of an ODE solver. Both are extremely computationally and memory intensive for large state space, and the latter might require many time steps and thus is prone to approximation error [14].

Our approach is comparable to Cooper and Lipsitch's dynamic version of a hidden Markov model on hospital infections in continuous time [92]. Hidden Markov models are for example used if infection prevalence cannot be measured with precision. This is the case in hospital infections since the majority of infected people are asymptomatic carriers. In [92], observed pathogen prevalence is estimated through a Poisson model, whereas realised prevalence is estimated through two hidden states in a dynamic continuous-time Markov chain. Transmission of the pathogen is modelled through a dynamic force of infection, accounting for the rate of transmission, rate of

pathogen carriage before hospital admission, discharge rate from the ward, and pathogen prevalence. The model differs from our approach through i) the frequentist setting; ii) the continuous-time approach; iii) the hidden Markov chain and the Poisson observation model; iv) the parameters considered in the force of infection, and v) the context, which is not related to health economics. Adapting this model to a Bayesian framework would considerably increase computational effort and thus is possibly not feasible at present.

Forrester and Pettit [141] present a stochastic model on the estimation of transmission rates of methicillin-resistant staphylococcus aureus. Their compartmental model is based on stochastic processes, accounting for the force of colonization which is assumed to follow a binomial distribution. A transition between the states is defined as a stochastic event. The transition rates are estimated by fitting the model to data, both through a frequentist and a Bayesian approach.

Auranen et al. [20] present a Bayesian hierarchical model to estimate the duration of immunity to haemophilus influenzae. The force of infection is defined as the event rate of a Poisson process.

Other stochastic approaches are presented by Gibson and Austin [155] and Gibson and Renshaw [156]. In [155], the authors model the spread of a plant disease by a stochastic process, where the probability of an infectious plant to infect a susceptible plant is a function of infection rate and position of infected and susceptible plants. In [156], a continuous-time MM is fitted to partially observed data through a Bayesian approach. An example of a smallpox epidemic is presented; the force of infection is directly incorporated in the transition probabilities of the MM.

These stochastic formulations provide valuable contributions in infectious disease modelling; however, due to their computational complexity, to date, mainly small population sizes are considered [212], and an inclusion of an extensive number of states is not feasible.

2.4 Conclusion

This chapter provided an overview on infectious disease transmission modelling through compartmental models, particularly focussing on ODE-based and MMs. In order to result in correct model predictions, a dynamic methodology incorporating the effects of herd immunity is essential. At the same time, the methodology used should enable accounting for parameter uncertainty. By doing so, PSA as part of a full CEA can be performed straightforwardly. Both aspects are fulfilled by our contribution of a dynamic Bayesian MM which was introduced in this chapter. We avoid the limitation of standard MMs which by definition do not account for population dynamics and time dependent changes in prevalence. Furthermore, when compared to a Bayesian ODE-based model, the computational effort of a Bayesian MM is considerably lower; it commonly does not induce computational issues.

The next chapter compares a deterministic ODE-based model (including point estimators as parameter values), a Bayesian ODE-based model and the dynamic Bayesian MM in practice through a case study of a fictional chronic sexually transmitted infection. The terms “deterministic” and “Bayesian” refer to the nature of the parameters and inference conducted, respectively. In the next chapter, the prevalence outputs as well as the results of a CEA of the three models are evaluated, and PSA is conducted for the two Bayesian models.

Chapter 3

Case study for comparison of compartmental models

3.1 Introduction

3.1.1 Parameter, methodological and structural uncertainty

The impact of uncertainty on the predictions of models of infectious diseases can be considerably high. Uncertainty originates from different sources and is mainly explained through parameter, methodological and structural uncertainty. In the literature, structural uncertainty is also referred to as model uncertainty [52]. Parameter uncertainty (i.e. uncertainty on the realised value of a parameter) is usually adressed in the vast majority of health economics literature – either in a univariate or in a multivariate setting through deterministic or, more properly, probabilistic sensitivity analysis. Another form of uncertainty is given by methodological uncertainty. According to [239, 332], methodological uncertainty refers to the nature of the model assumptions and methodology used, for example i) the time horizon of the follow-up, ii) the discount rate, iii) the methodological approach of measuring quality of life (e.g. time trade-off [18] or standard gamble [146] method), and most importantly v) the choice of the mathematical modelling approach. Structural

uncertainty commonly includes i) how many relevant health states are considered and thus ii) whether all possible implications of the infectious agents are incorporated into the model, iii) the number of interventions compared (omitting relevant interventions could result in falsified CEA results), iv) incorporation of time dependency and risk factors into continuous- or discrete time transition parameters [8, 41, 332], and v) whether dynamic changes in prevalence are considered.

In contrast to parameter uncertainty, structural uncertainty is only accounted for in rare cases by implementing several models in parallel with different structure [54] or by accounting for model discrepancy. This is possibly a consequence of the instructions given in the relevant ISPOR guideline [52]. This ISPOR guideline states that fully accounting for structural uncertainty might not be feasible due to time constraints and thus recommends summarizing sources of structural uncertainty with respect to future research. In contrast, the NICE guideline [268] recommends to conduct deterministic sensitivity analysis and scenario analysis to compare cost-effectiveness outcomes of models with different structure; however, a more systematic approach as described in the following is not recommended.

Four systematic approaches to investigate structural uncertainty are given by i) model averaging, ii) model selection, iii) parameterization and iv) investigating model discrepancy. In model averaging, a variety of models with different structure or assumptions are implemented and the overall costs and QALYs are calculated for each model. Afterwards, the corresponding measures of cost-effectiveness are calculated through the (weighted) average of costs and QALYs of all implemented models. Model selection includes the calculation of maximum likelihood information criteria (Akaike Information Criteria, AIC) or Bayesian Information Criteria (BIC); the model with the best fit to the data results in lowest AIC or BIC, respectively, and is thus selected. Parameterization refers to the inclusion of one or several additional model parameters with suitable distributions to account for uncer-

tainty in the selection of a specific methodology. For example, if it is not known whether transition probabilities of survival are best estimated by a Weibull or a Gamma distribution, this uncertainty could be incorporated as an additional model parameter. A discrepancy approach estimates the deviation of a set of possible models from "reality" by an error term. Sets of models can either be closed, implying that one of the models reflects the truth, or open, implying that no model in the set is perfect [8, 41, 332].

Ignoring structural uncertainty can result in an over- or underestimation of the cost-effectiveness of the interventions under investigation; under certain circumstances, these differences can be so high that a decision in favour of the intervention has to be reversed [41]. However, this is not necessarily the case and the literature shows several examples were accounting for structural uncertainty did not change the decision since the corresponding measures of cost-effectiveness were still well below [41] or clearly above [239] the threshold of cost-effectiveness for model scenarios compared.

In this chapter, we describe methodological uncertainty in several ways: through a case study, we firstly investigate the impact of the choice of methodology on model predictions and secondly, we evaluate the shortcomings of models including fixed values rather than whole distributions on parameters. We consider again the fictional chronic STI described in Chapter 2 and compare our methodology of a dynamic Bayesian MM to both an ODE system with fixed parameter values and a Bayesian ODE-based model. Deterministic and probabilistic methodologies are defined in Section 2.2.1. The literature shows that model parameters can also be classified into deterministic and stochastic, as shown for fixed and random effects models in [227]. A deterministic model parameter is then defined as a fixed value, whereas a stochastic parameter is assigned a suitable distribution. Thus, we refer to the ODE system including fixed parameter values as a deterministic ODE system. In the following, we denote the Bayesian Markov model as BMM,

the Bayesian ODE system as BODE, and the deterministic ODE system as dODE. The main aim of model comparison is to evaluate whether our BMM produces results that are in line with the BODE. We consider BODEs as the "gold standard" in infectious disease modelling with respect to CEA; this is a consequence of their continuous-time approach, dynamic nature and suitability to incorporate parameter uncertainty. Structural uncertainty is not investigated in a systematic way; however, we describe possible sources and implications.

3.1.2 Inclusion of data

First we consider the case in which we do not have access to individual-level, prevalence and time series data on the natural history of the STI. If models in health economics include a large number of parameters, individual-level data to inform each parameter are rarely available. Therefore, we conduct the analysis including exclusively informative prior distributions informed through aggregate data and expert opinion. The main purpose of this analysis is to evaluate whether the outputs of the dODE, BODE and BMM are comparable. The outputs of the three models are not calibrated to prevalence or time series data; model calibration would reduce potential differences in results. We focus on differences in outputs of the three models and approaches to explain and minimise these. In addition, we evaluate whether the BMM is able to reproduce the output of the "gold standard" of the BODE.

In Section 3.4, we assume to have access to individual-level, time series and prevalence data; since the case study is a fictional example, we simulate these data. The time series data are simulated by running the dODE for a follow-up period of five years as described in Section 3.5.2. Simulation of the prevalence data is conducted through a slightly modified version of the dODE termed `prevSim` as described in Section 3.5.1. The prevalence data

are used to conduct visual calibration approaches in the dODE, BODE and BMM. The time series data are used to conduct systematic calibration approaches - a frequentist probabilistic calibration approach in the dODE and Bayesian calibration approaches in the BODE and BMM. The time series data are not produced from the Bayesian models themselves and do thus not necessarily fit to the corresponding outcome well.

The main purpose of using different calibration approaches is to evaluate their advantages, disadvantages and accuracy with respect to outcome of natural history of disease and health economic evaluations. In Section 3.5.1, we conduct the visual calibration approach for the dODE, BODE and BMM. The three models are calibrated visually to the simulated prevalence data. As a next step, systematic calibration approaches are applied in Section 3.5.2. The systematic calibration approaches vary between the three models; the dODE is calibrated through a frequentist probabilistic calibration approach, whereas the two Bayesian models are calibrated through what we term a Bayesian calibration approach; this is equivalent to Bayesian inference.

In a Bayesian framework, data can be considered in several ways. We include simulated data on a selection of parameters to update the priors into the corresponding posteriors. However, this only ensures that the corresponding parameters are informed by available evidence. Despite posterior sampling, it could still be possible that the predicted outcome implied by the Bayesian models was not comparable to high-quality data obtained from large data registries. Therefore, in addition to posterior sampling of the model parameters, we use the simulated time series data to update the posteriors on the number of people in the states. In fact, this is an additional process of Bayesian inference, updating the model outcome through additional data.

3.1.3 Sampling techniques

The statistical sampling technique of Markov Chain Monte Carlo (MCMC) simulation is used in different ways in the case study. Therefore, this chapter includes a brief summary on this methodology. Furthermore, essential diagnostic techniques to assess convergence and autocorrelation are described.

3.2 Markov Chain Monte Carlo simulation

Bayesian inference requires the computation of posterior distributions. A simulation method to obtain samples from these is given by Markov Chain Monte Carlo (MCMC) simulation. MCMC simulation was developed to simulate from distributions which are not analytically tractable, or if an analytic solution requires extensive calculation. One example is given by posterior distributions, which involve the solution of rather complex integrals [151].

The core idea behind MCMC methods is to construct a Markov chain which has the posterior distribution as its stationary distribution [269]. In MCMC methods, the transition kernels are built so that the limit distribution coincides with the stationary distribution. This is achieved by proposing kernels that ensure that the chain is irreducible[1], aperiodic[2] and positive-recurrent[3] [175, 301].

A Markov chain is a particular case of a Markov model as explained in Section 2.2.2. In a Markov chain, the conditional distribution of the future state of the process given the current and past states depends only on its current state. In a Markov chain of order k_*, this additionally depends on

[1] Irreducible implies that any set S can be reached from any other set T with nonzero probability, where S and T have nonzero probability themselves.

[2] Aperiodic implies that the greatest common denominator of the set of times for which the chain starting at a given state can return to that same state is equal to 1.

[3] Positive-recurrent implies that the chain can return to a set S, where S has nonzero probability in an infinite number of steps.

the $k_* - 1$ past states. A Markov chain of first order can thus be expressed mathematically as [22]

$$P(X_{t+1}|X_0, X_1, ..., X_t) = P(X_{t+1}|X_t),$$

where $X_0, X_1, ..., X_t$ represent a sequence of random variables, and t is the time point of the simulation.

The *Fundamental Theorem of Markov Chains* states that for any irreducible, aperiodic, positive-recurrent Markov chain there exists a unique stationary (also called equilibrium or target) distribution which is related to the expected returned value of the Markov chain at its possible states [48, 292]. This theorem guarantees that the limit distribution of a MCMC sample will be the stationary distribution. The MCMC simulations are run until convergence to the stationary distribution p_* is achieved. The distribution p_* is stationary with respect to the Markov chain, and thus [48]

$$X_t \sim p_*$$
$$X_{t+1} \sim p_*.$$

The most widely used MCMC method is the Metropolis-Hastings algorithm. It is based on successively sampling from a proposal distribution $q(x|x^*)$ and imposing a random rejection step at each transition. The proposal distribution is in principle an arbitrary distribution from which we can sample efficiently [154, 181].

When implementing an MCMC method, the first simulations (the so-called “burn-in period”) are omitted to ensure that the distribution of the current state is close enough to the stationary distribution. Suitable convergence checks have to be performed to see whether the chain has converged. Convergence can be for example checked visually through trace plots. Usually, two or more chains with different inital values are run in par-

allel. If convergence is reached, a trace plot shows that the different chains have mixed properly, and thus the corresponding plot looks like a “big caterpillar”. Another more formal method to investigate proper convergence is the Gelman and Rubin statistic as described in Section 3.2.2. In addition to improper convergence, MCMC simulation can induce issues with autocorrelation (see Section 3.2.3). Since the future state of the process only depends on its current state, two random variables X_t and X_{t+1} which are only one time step t apart are often highly correlated. Thus, thinning is required which implies that consecutive samples are no longer considered.

Once the stationary distribution was found, it can be sampled from; this process is called posterior sampling. After successful diagnostics to ensure that there are no issues with convergence and autocorrelation, inference can be conducted on the resulting posterior distribution, e.g. to estimate the corresponding mean, quantiles, or credible intervals. For example, the mean $E(\theta|data)$ of a posterior distribution can be estimated as [22]

$$E(\theta|data) = \frac{1}{S_*} \sum_{s_*=1}^{S_*} \theta^{(s_*)},$$

where $\theta^{(1)}, \theta^{(2)}, ..., \theta^{(S_*)}$ represent samples of the posterior distribution of the parameter θ.

In this PhD thesis, exclusively the Gibbs sampler [152] in the software `JAGS` [293] and `WinBUGS` [355] is used to conduct MCMC estimation. The Gibbs sampler is a special case of the Metropolis-Hastings [181] algorithm. Samples are obtained from the full conditional distributions of the model parameters. A generic example of a Gibbs sampling algorithm is defined through the following steps, given a vector of model parameters $\boldsymbol{\theta}$ [22]:

1) Initial values are assigned to the components of the parameter vector $\theta_1^{(0)}, \theta_2^{(0)}, ..., \theta_{K_*}$.

2) Samples are drawn repeatedly from the full conditional distribution $\theta_1^{(1)}$ is drawn from $P(\theta_1|\theta_2^{(0)}, \theta_3^{(0)}, ..., \theta_{K_*}^{(0)}, data)$

$\theta_2^{(1)}$ is drawn from $P(\theta_2|\theta_1^{(1)}, \theta_3^{(0)}, ..., \theta_{K_*}^{(0)}, data)$

...

$\theta_{K_*}^{(1)}$ is drawn from $P(\theta_{K_*}|\theta_1^{(1)}, \theta_2^{(1)}, ..., \theta_{K_*-1}^{(1)}, data)$.

3) Sampling according to 2) is conducted until the Markov chain converges to the stationary distribution which corresponds to the posterior distribution.

4) A sample is then taken from the posterior distribution $P(\theta|data)$.

3.2.1 Forward sampling and updating priors through data

Bayesian tools can be used in several ways to propagate parameter uncertainty through models. One approach is to exclusively conduct "forward sampling" by means of a random number generator. An alternative is to conduct Bayesian inference by updating prior distributions by means of data. Information available in the literature or expert opinion can be included directly into the prior distributions (so-called prior elicitation). In that case, these are termed "informative" priors and can (but do not necessarily have to) be updated by available data. If a model includes exclusively informative prior distributions which are not updated by any data, the prior and posterior distributions are basically identical; the calculation of convergence statistics and an assessment of autocorrelation is thus not necessary. This approach is termed "forward sampling" and conducted in Section 3.3.2 of this PhD thesis. The Gibbs samplers in `JAGS` and `WinBUGS` as well as the software `Stan` [4] (running the "fixed parameter" algorithm) can be used to conduct forward sampling.

In contrast, in Section 3.5, individual-level and aggregate data are used to update informative and minimally-informative prior distributions into the corresponding posteriors. If a model includes at least one prior distribution which is updated by data, the remaining priors which are not updated by data can result in posterior distributions considerably differing from the

corresponding priors. This might occur in model parameters which are not independent, for example i) if a transition parameter of moving to a certain state is calculated as a function of a combination of model parameters (as for the force of infection), or ii) if transition parameters are based on hierarchical models. Thus, the assessment of convergence (through the Gelman and Rubin statistic) and autocorrelation is essential in this respect.

3.2.2 The Gelman and Rubin statistic

The Gelman and Rubin statistic (also referred to as GR statistic or Potential Scale Reduction) compares the between-chains to the within-chain variation of two or more chains which are run in parallel [151]. We use a similar notation as in [22]. For each $\theta^{(s_*)}$ of the parameter vector $\boldsymbol{\theta} = (\theta^{(1)}, ..., \theta^{(S_*)})$, the posterior variance is calculated as [22]

$$\widehat{Var}(\theta^{(s_*)}|data) = \frac{n_{sims} - 1}{n_{sims}} W(\theta^{(s_*)}) + \frac{1}{n_{sims}} B(\theta^{(s_*)}).$$

The within-chain and between-chains variance are represented by $W(\theta^{(s_*)})$ and $B(\theta^{(s_*)})$, respectively, and n_{sims} represents the overall number of simulations conducted. As a next step, the Gelman and Rubin statistic can be calculated as

$$\hat{R} = \sqrt{\frac{\widehat{Var}(\theta^{(s_*)}|data)}{W(\theta^{(s_*)})}}.$$

The Gelman and Rubin statistic $\hat{R}$ is an estimate of the reduction factor of the scale of the posterior distribution of $\theta^{(s_*)}$. If $\hat{R} \leq 1.1$, the corresponding posterior distribution is assumed to have converged properly. Larger values of $\hat{R}$ require additional measures to improve convergence, e.g. through changes in the corresponding statistical model, or a higher number of simulations [22].

3.2.3 Autocorrelation

Due to the Markov assumption described in Sections 2.2.2 and 3.2, consecutive iterations are by definition correlated. As a consequence, the sample of the posterior distribution obtained is not comparable to collected data of the same sample size, and thinning often is required [22]. Thinning implies that consecutive iterations are not considered in the sample of the posterior distribution, and only every xth iteration is included, where x is a predefined number. The higher the amount of autocorrelation, the larger the value of x needs to be defined. We adopt the notation from [22]. The term *effective sample size* n_{eff} refers to the number of simulations out of the overall number of simulations conducted which are comparable to a sample of iid observations and is estimated as

$$n_{eff} = \frac{n_{sims}}{1 + 2\sum_{l=1}^{\infty} corr_t}.$$

The correlation between two iterations is indicated by $corr_t$, where t represents the time step of the simulation. If the effective sample size n_{eff} is not considerably smaller than the overall number of iterations n_{sims}, this indicates that there are no issues with autocorrelation. The posterior can still converge properly even in case of high autocorrelation. However, if n_{eff} is considerably small, this could induce an issue in the estimation of the extreme quantiles of the corresponding posterior [196].

3.3 Model assumptions

In the three approaches compared, we distinguish between sexes as well as high- and low-risk sexual behaviour. The duration of the follow up is set at 100 years. We consider an arbitrary population size of 1,000,000 and initially assume that 600 people are infected, whereas the remainder are susceptible. Males amount to 50% and the high-risk group to 20% of the

population; the sex ratio in the two risk groups is equal. The proportion of infecteds in both sexes and risk groups is identical; this is to ensure equal conditions in the beginning of follow-up. We account for sex-specific differences in sexual behaviour, assuming higher partner acquisition rates in males. The population size changes due to births and deaths.

We conduct our analysis for two fictional competing health-care interventions. We assume that in the *status-quo*, screening takes place at intervals of five years at a pre-defined rate to enable an early detection of the STI. For simplicity, we assume that under the *vaccination* scenario no screening takes place. However, in real life, screening and vaccination are often combined; screening has commonly already been conducted before the introduction of vaccination, and the combination of both interventions results in maximal protection. We assume that the vaccine is only effective before initial STI infection occurs; thus, susceptibles are vaccinated at a specified vaccine uptake rate. The vaccine is given at intervals of five years, based on the assumption that vaccine-induced immunity lasts for five years. Following STI diagnosis, treatment is provided in both interventions.

All rates of change in the ODE systems differ according to the two characteristics considered. We refer to these using the indices $v, v' = (M\text{ale}, F\text{emale})$ to indicate the respective sex and its opposite. For example, a male is represented through the index M; the index of his female mixing partner is F. The sexual behaviour group is indicated through the index $b = (L\text{ow}, H\text{igh})$. In the ODE model, the transition rate $\rho_{v,b,1,2}(t)$ from the state *Susceptible* to the state *Infected* is calculated similarly to Equation 2.3; however, it additionally depends on the covariates sex and behaviour as described in the next section. In the BMM, the sex- and behavioural specific transition probability $\pi_{v,b,1,2,t}$ is estimated by transforming $\rho_{v,b,1,2}(t)$ according to Equation 2.4. As a consequence of the definition of the transition probabilities for movements from a certain state which must sum up to 1, the estimation of $\pi_{v,b,1,2,t}$ affects the transition probability $\pi_{1,1}$ of remaining in the

state *Susceptible*.

Since disease progression in the chronic STI is a very slow process, we assume a yearly Markov cycle length to be sufficient. To reduce the shortcomings induced by the discrete-time approach, we conduct a half-cyle correction which is based on the assumption of uniformity within a Markov cycle [51,264,327]. The correction is calculated by averaging the number of people who are in the same state at two consecutive cycles and assigning the result to the latter cycle.

3.3.1 The force of infection

For simplicity, we exclusively account for random mixing and heterosexual relationships; members of the population of sex v randomly select sexual partners of the opposite sex v'. The advantage of random mixing is that it is a realistic assumption in sexual partnership formation. Effects of saturation (infectious people mix with infectious people and thus do no longer spread the infection) are less likely. In contrast, in assortative mixing (where people are more likely to mix with members of their own risk group), the effects of saturation would affect members of the high-risk group. In addition, those in the low-risk group would preferably mix with low-risk people and thus reduce their risk of infection. Overall, STI prevalence would thus decrease, possibly resulting in lower cost-effectiveness of the STI vaccine.

Because of the impact of the covariates, the estimation of the overall prevalence in the sexual partners of sex v' is a weighted average of the prevalence in both behaviour groups of sex v'. We show the corresponding equations for the continuous-time approach as functions of t; for a discrete-time approach, these are similar. The time-specific probability of selecting a partner from the high-risk group, which we indicate as $g_{v'H}(t)$, depends on the partner acquisition rates $\omega_{v'H}$ and $\omega_{v'L}$ as well as on the population sizes $N_{v'H}(t)$ and $N_{v'L}(t)$. The probability of selecting a partner from the low-risk

group is represented by $g_{v'L}(t)$. The corresponding equations adapted from [371] only account for two sexual behaviour groups and are thus extended for heterosexual mixing, to give

$$\begin{aligned} g_{v'H}(t) &= \frac{\omega_{v'H} N_{v'H}(t)}{\omega_{v'H} N_{v'H}(t) + \omega_{v'L} N_{v'L}(t)} \\ g_{v'L}(t) &= 1 - g_{v'H}(t). \end{aligned}$$

We estimate the sex-, behavioural- and time-specific force of infection as

$$\rho_{v,b,1,2}(t) = \beta \omega_{vb} \overline{\psi}_{v'}(t), \tag{3.1}$$

where

$$\overline{\psi}_{v'}(t) = \left(g_{v'H}(t) \frac{I_{v'H}(t)}{N_{v'H}(t)} + g_{v'L}(t) \frac{I_{v'L}(t)}{N_{v'L}(t)} \right)$$

is the weighted average of the STI population prevalence. This in turn is estimated as a function of the probabilities $g_{v'b}(t)$ of selecting a partner of the opposite sex from one of the two sexual behaviour groups and the time-, sex- and behavioural-specific population prevalence $\frac{I_{v'b}(t)}{N_{v'b}(t)}$. The number of infectious people $I_{v'b}(t)$ is estimated as those in the state *Infected* of the respective sex and behaviour group.

In line with (2.3), the force of infection $\rho_{v,b,1,2}(t)$ is a function of the STI transmission probability per partnership β, the partner acquisition rates ω_{vb}, and the population prevalence $\overline{\psi}_{v'}(t)$.

3.3.2 Model parameters and prior elicitation

In addition to the probability of STI transmission β and the partner acquisition rates ω_{vb}, the model contains a variety of parameters such as those determining the screening and vaccine coverage, the unit costs of STI diagnostics and treatment and the health utilities, which are relevant in context

of the cost-effectiveness analysis.

To conduct the first analysis, we assume not to have access to individual-level, prevalence and time series data on the natural history of the STI. We thus specify the distributional assumptions of the informative priors so that both the outputs of the prevalence estimation and the health economic evaluation are within realistic ranges. In contrast, the second analysis in Section 3.5 includes simulated data.

Table 3.1 shows an overview of the assumptions about the model parameters $\boldsymbol{\theta}_* = \{\omega_{vb}, \chi, \beta, \pi_{r,s}, \eta, \sigma, \alpha, \gamma, \boldsymbol{c}, u_s\}$. The means and 95% credible intervals are rounded to two decimal places. However, the 95% CI of the parameter χ is in fact defined as [0.009420;0.010596]. The 95% credible intervals of several parameters are considerably narrow; however, the case study is fictional and despite these assumptions, the amount of uncertainty in the model outcome is realistic as shown in Figures 3.1, 3.2 and 3.3.

The distributional assumptions differ between the two models as follows. Since the BMM is based on a discrete-time approach, the corresponding transition probabilities are modelled using Beta distributions (constrained between 0 and 1). In contrast, the transition rates of the continuous-time BODE are modelled using Gamma distributions (defined on $\mathbb{R}^+$). The transition rate $\rho_{\text{v,b,1,2}}$ is estimated according to Equation 3.1 and transformed into the transition probability $\pi_{\text{v,b,1,2}}$ according to Equation 2.4. The transition probabilities for movements between the other states are estimated through informative priors, and those for movements from the states *Susceptible*, *Infected* and *Asymptomatic* to *Dead* are assumed as identical; thus, only $\pi_{1,5}$ is shown. Competing risks (i.e. the fact that people in a state can move to more than one target state to account for deaths) are accounted for through the transition probability matrix shown in Equation 2.2.2. Apart from the force of infection and the transition probability of remaining susceptible, we assume for simplicity that transition parameters in the three models do not differ between the sexes and behaviour groups.

Table 3.1: Overview of the distributional assumptions for the high variability scenario. The values are fictional and were chosen so as to produce most realistic prevalence outcome and cost-effectiveness results.

Parameter	Description	Distribution BMM	Distribution BODE	Mean	95% interval
ω_{MH}	Partner acquisition rate (high-risk males)	Gamma(2070.25, 227.5)	equivalent to BMM	9.10	[8.70;9.50]
ω_{ML}	Partner acquisition rate (low-risk males)	Gamma(8100, 4500)	equivalent to BMM	1.80	[1.76;1.84]
ω_{FH}	Partner acquisition rate (high-risk females)	Gamma(1406.25, 187.5)	equivalent to BMM	7.50	[7.11;7.90]
ω_{FL}	Partner acquisition rate (low-risk females)	Gamma(3025, 2750)	equivalent to BMM	1.10	[1.06;1.14]
χ	Proliferation parameter	Beta(1099.99, 108899)	Gamma(1111.1,111111.1)	0.01	[0.01;0.01]
β	STI transmission probability per partnership	Beta(764.85, 4334.15)	equivalent to BMM	0.15	[0.14;0.16]
$\pi_{2,3}$	Transition parameter from state 2 to state 3	Beta(5119.2, 1279.8)	Gamma(25600,32000)	0.80	[0.79;0.81]
$\pi_{3,4}$	Transition parameter from state 3 to state 4	Beta(1842.66, 18631.34)	Gamma(2025,22500)	0.09	[0.09;0.09]
$\pi_{4,5}$	Transition parameter from state 4 to state 5	Beta(1535.96, 36863.04)	Gamma(1600,40000)	0.04	[0.04;0.04]
$\pi_{1,5}$	Transition parameter from state 1 to state 5	Beta(156.171, 312186.6)	Gamma(156.25,312500)	<0.01	[<0.01;<0.01]
η	Probability of STI diagnosis	Uniform(0.8, 1)	equivalent to BMM	0.90	[0.81;0.99]
σ	Screening probability	Uniform(0.8, 1)	equivalent to BMM	0.90	[0.80;1]
α	Vaccine coverage parameter	Beta(809.1, 89.9)	Gamma(8100,9000)	0.90	[0.88;0.92]
γ	Vaccine efficacy parameter	Beta(809.1, 89.9)	Gamma(8100,9000)	0.90	[0.88;0.92]
c_{screen}	Unit cost of screening in £	Lognormal(2.996, 0.693)	equivalent to BMM	25.39	[5.19;77.53]
c_{vac}	Unit cost of vaccination in £	Lognormal(5.011, 0.01)	equivalent to BMM	150.02	[147.14;152.98]
c_{test}	Unit cost of STI test in £	Lognormal(2.996, 0.03)	equivalent to BMM	20.01	[18.83;21.19]
c_{blood}	Unit cost of blood test in £	Lognormal(3.401, 0.03)	equivalent to BMM	30	[28.26;31.79]
c_{treat}	Unit cost of treatment in £	Lognormal(8.517, 0.015)	equivalent to BMM	4999.78	[4853.56;5149.24]
c_{dis}	Unit cost of disease treatment in £	Lognormal(9.210, 0.01)	equivalent to BMM	9999.95	[9802.97;10198.10]
c_{gp}	Unit cost of visit to general practitioner in £	Lognormal(3.912, 0.02)	equivalent to BMM	50.01	[48.08;52.01]
u_2	Health utility of infected (min=0, max=1)	Beta(1469.3, 629.7)	equivalent to BMM	0.70	[0.68;0.72]
u_3	Health utility of asymptomatic (min=0, max=1)	Beta(1439.4, 959.6)	equivalent to BMM	0.60	[0.58;0.62]
u_4	Health utility of morbid (min=0, max=1)	Beta(629.7, 1469.3)	equivalent to BMM	0.30	[0.28;0.32]

We do not implement a set of different model structures and only consider in theory which effects of structural uncertainty could have an impact on the results of the case study. For example, the asymptomatic state could be removed and joined with the infectious state; however, this would complicate considering the lower quality of life and higher costs in those with changes in the blood count as a consequence of STI infection. The corresponding parameters could be estimated as (weighted) average parameters of the two states, resulting in a loss of information. This could have a high impact on the health economic outcomes. In addition, it would be possible to account for the intervention of regular condom use, possibly reducing the cost-effectiveness of STI vaccination due to lower STI prevalence. Possible adverse events of vaccination and indirect costs induced by absence from work in those in the state morbid could also be included in the model. The first would decrease the cost-effectiveness of vaccination, whereas the latter would increase it.

Parameters of deterministic models are commonly informed through maximum likelihood estimates or summary statistics, e.g. mean, median or mode. For a deterministic ODE system, the parameter on the probability of screening (σ) could for example be estimated as follows. If data on the sample size N_σ and the number of screened people R_σ were available, σ could be informed through a maximum likelihood approach with a binomial likelihood, obtaining an estimator of the mean as $\bar{\sigma} = \frac{R_\sigma}{N_\sigma}$.

As a consequence of ignoring the impact of parameter uncertainty, models including fixed values (e.g. point estimates) for parameters are prone to result in incorrect outcome. Therefore, if computationally feasible, including suitable probability distributions for each model parameter is preferable. In theory, these can be included both into deterministic (e.g. ODE systems) and stochastic (e.g. SDE or Markov) models.

According to simulation studies conducted in [176] and a review published in [302], outputs of deterministic models are comparable to the mean

outputs of stochastic models if the following criteria are fulfilled: i) the models are linear, ii) the number of people in a state cannot become negative, iii) the follow-up period is predefined, and iv) the initial number of infecteds and the basic reproduction number R_0 (the number of new infections induced by one infectious person) are high enough to prevent the disease from going extinct during follow-up [302]. In the case study, criteria ii)-iv) are fulfilled. However, the models are not linear as a consequence of multiplying the force of infection $\rho_{1,2}$ (or $\pi_{1,2}$ in the BMM) with the number of susceptibles n_1 as shown in Equations 2.1 and 2.2. The function of the force of infection includes the number of infecteds n_2; the term $n_1 n_2$ introduces nonlinearity into the ODE systems and the BMM [191].

An incorrect output of models including fixed parameter values can be avoided if Bayesian estimators obtained through loss functions are used to inform the corresponding parameter values. Loss functions quantify the loss induced through the difference between realised and estimated parameter values. In health economic evaluations, the loss corresponds to an incorrect model outcome, resulting in an overestimation of costs or underestimation of benefits of interventions. In the literature, the loss is often considered to be symmetric. A symmetric loss implies that the consequences of over- and underestimation of specific model output are identical. In that case, the point estimate to inform the parameter values of deterministic models is commonly the mean. However, in the case study, this is an unsuitable estimator for two reasons: i) the distributions of specific parameters are highly skewed (e.g. Gamma distributed partner acquisition rates), and ii) the consequences of an under- or overestimation of infection prevalence are not comparable, resulting in a non-symmetric loss.

An underestimation of STI prevalence influences the results of the corresponding cost-effectiveness analysis. The higher the prevalence, the higher the probability that preventive interventions and treatments are considered cost-effective; this is induced by the higher proportion of the population

in need of the intervention. The worst consequence of prevalence underestimation could be that highly effective and affordable interventions were withheld from the population since these were considered not to be cost-effective. In that case, people were subject to unnecessary suffering and possibly death. In contrast, an overestimation of prevalence could result in wasting scarce resources for possibly ineffective and highly costly treatments. These resoures were no longer available to fund other (possibly life-saving) treatments, causing suffering in patients affected by other health conditions.

Due to the reasons listed above, withholding highly effective treatments from the population is considered slightly worse than wasting scarce resources. Thus, the loss is not symmetric. A piecewise linear loss function can be used to inform the parameter values of the dODE through specific quantiles of the parameters of the BODE, obtained through Bayesian estimators. The piecewise linear loss is given by [301]

$$L_{k_1,k_2}(\psi,\hat{\psi}) \begin{cases} k_2(\psi-\hat{\psi}) & \text{if } \psi > \hat{\psi} \\ k_1(\hat{\psi}-\psi) & \text{otherwise}, \end{cases}$$

where k_2 is the impact of a decision depending on underestimated prevalence $\hat{\psi}$ in comparison to the realised prevalence ψ, and k_1 is the impact of prevalence overestimation. These parameters represent the slopes of the loss function; the higher the slope, the higher the corresponding loss induced. A Bayesian estimator for the quantiles of the parameters of the BODE to inform the parameters of the dODE is then given by [301]

$$P(\psi < \hat{\psi} \mid \text{data}) = \frac{k_2}{k_1+k_2} = \frac{1.2}{0.8+1.2} = 0.6. \tag{3.2}$$

The values of k_2 and k_1 are determined by comparing the prevalence output of the dODE to the prevalence output of the gold standard of the BODE. If the parameters of the dODE are informed by the 60% quantiles of the

parameters of the BODE, the two prevalence outputs are almost identical. Since underestimating prevalence is considered slightly worse than an overestimation, k_2 should be slightly higher than k_1. To obtain a result of 0.6 in (3.2), we define $k_2 = 1.2$ and $k_1 = 0.8$. To result in correct prevalence outcome of the dODE, the parameters of the dODE are thus informed by the 60% quantiles of the parameters of the BODE.

Scenarios evaluated and software used

To investigate the impact of different levels of parameter uncertainty on the model outcome, we evaluate three scenarios. In a *perfect knowledge* scenario, we assume no variability in any of the parameters of the three models compared. However, this scenario is not relevant, as we never have perfect knowledge in reality. In a scenario with *low variability*, each model parameter in the BMM and BODE is assigned a prior distribution that is tightly centered around its mean. In a scenario with *high variability*, we increase the amount of parameter uncertainty in the BMM and the BODE. This scenario is the most realistic since infectious disease modelling is commonly associated with a large amount of parameter (and possibly structural) uncertainty; this is likely to have a major impact on the economic analysis.

The dODE is estimated using the `R` package `EpiModel` [199] which uses ODE solvers provided by the `R` package `deSolve` [326]. For the BMM and BODE, we estimate the parameters using forward sampling as described in Section 3.2.1, running two chains with a total of 10,000 simulations and discarding the first 500. We run the simpler BMM in `JAGS` [293], while the BODE is fitted in `Stan` to deal more efficiently with the ODE system.

In the *perfect knowledge* scenario, running the dODE for a follow-up period of 100 years on a Dell Latitude E6320 (Intel Core i5-2520M, 2x4GB DDR3 RAM, 500GB SATA HDD (2.5", 7200rpm)) takes 0.22 seconds, whereas the BODE and the BMM take 0.64 seconds and 0.09 seconds, respectively. In the scenarios including variability the BMM runs in 95.96 seconds,

whereas the BODE runs in 188.50 seconds.

3.3.3 Prevalence estimation

We first estimate the prevalence outcome of the three models as follows. In the ODE-based models, we estimate the proportion of the population which are infectious by dividing the overall number of those in the state of infection $I_{vb}(t)$ by the corresponding population size $N_{vb}(t)$, resulting in the time-specific STI prevalence. Although in the BMM time is represented by intervals, the prevalence estimation is comparable to the ODE-based models. As described in the beginning of Section 3.3, a half-cycle correction is commonly conducted in discrete-time models to adjust for incorrect results induced by a cycle length which might be too large. In our case study, assumptions on discrete time in the BMM do not seem to have an impact on the results since we found the STI prevalence outcome with and without half-cycle correction to be identical in all scenarios evaluated.

In all three scenarios, we estimate STI prevalence for the overall population. Obviously, prevalence is higher in males than in females as a consequence of differences in partner acquisition rates; on average, females tend to have lower partner acquisition rates than males, whereas a very small number of females have an extremely high number of partners. Thus, the distributions on partner acquisition rates considerably differ between the sexes. Furthermore, due to a higher number of partners, the high-risk sexual behaviour group results in a considerably higher STI prevalence. However, the main focus of our analysis is to compare the three models rather than accounting for differences in prevalence outcomes in the subgroups of the population. Thus, we only present the overall prevalence outcomes and display these graphically for the two scenarios including parameter uncertainty.

In addition to the mean prevalence output, we show 95% confidence bands for the BMM and BODE. As for the dODE, we display the range of

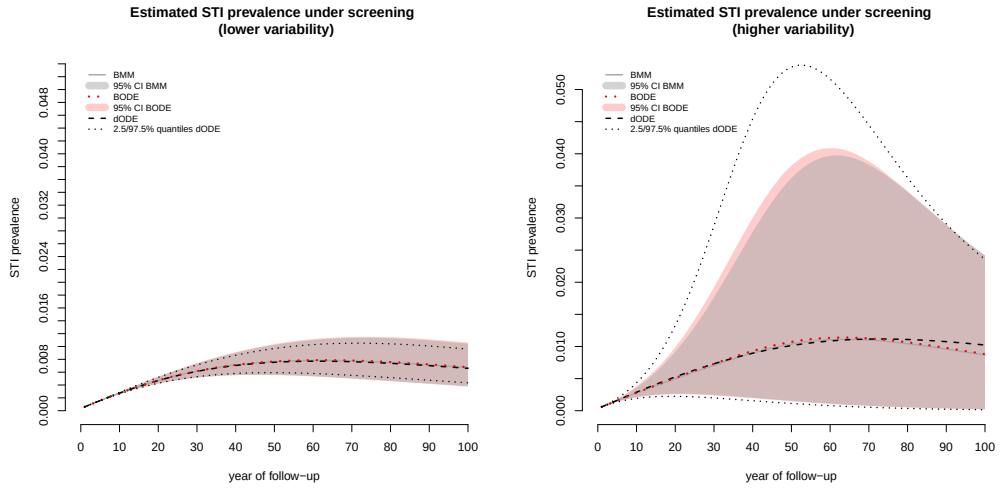

Figure 3.1: Deterministic ODE-based model, mean Bayesian ODE-based model and mean Bayesian Markov model output comparison of the chronic STI prevalence. The left panel shows the scenario with lower variability, whereas the scenario with higher variability is displayed on the right panel. The results of the deterministic ODE-based model are displayed by black dashed lines, whereas the mean prevalence output of the Bayesian Markov and ODE-based models are drawn by grey solid and red dotted lines, respectively. Scenario analysis of the deterministic ODE-based model is shown by black dotted lines for the 2.5% and 97.5% quantiles, respectively. Uncertainty in the probabilistic Bayesian Markov and ODE-based models is displayed by grey and red 95% confidence bands, which mainly overlap.

values at the extremes through a scenario analysis. In a scenario analysis, predefined quantiles are estimated from the parameter distributions. These quantiles are summary statistics and do therefore not account for the whole amount of parameter uncertainty characterised in the distributions. By contrast, in a Bayesian setting, the whole distributions and potential correlation across the parameters is considered. To conduct the analysis for the 2.5% quantile, we use the lower limits of the 95% CIs of the BMM parameters as input to inform the parameters of the dODE. The scenario analysis for the 97.5% quantile is performed accordingly, using the upper limits of the 95% CIs.

Unsurprisingly, in the *perfect knowledge* scenario, the outcome of the dODE, BMM and BODE is virtually identical and thus the corresponding re-

sults are not presented. Figure 3.1 shows the mean prevalence outcome for the scenarios incorporating a lower and higher amount of parameter uncertainty in the panels on the left and right, respectively. In the scenario with a low amount of parameter uncertainty, the mean prevalence of the three models is very similar, although the ranges of the confidence bands for the probabilistic models are slightly wider than those of the deterministic sensitivity analyses. The confidence bands for the probabilistic models are approximately identical.

In the scenario with higher variability, the outcomes of the BMM, BODE and dODE are comparable; however, the dODE slightly overestimates STI prevalence from year 80 of follow-up. The comparable outcomes are a consequence of estimating the parameters of the dODE through the 60% quantiles of the parameters of the BODE as described in the previous section. The scenario analysis of the dODE shows the wider range of the parameters. The bounds of the confidence bands of the BMM and BODE are lower than the extremes of the scenario analysis. The model outputs of the mean STI prevalence and the lower bound of the 95% CIs in the BMM and the BODE are approximately identical. In contrast, the upper bound of the 95% CI of the BODE is slightly wider in the beginning of the follow-up, and from year 60, the situation is reversed. Nevertheless, these differences are minor. Our results clearly show that the BMM approximates the BODE very closely.

3.3.4 Cost-effectiveness analysis

In cost-effectiveness analysis, costs generated by the interventions are compared to their induced benefits, e.g. an improvement in the quality of life. The quality of life of members of the population in certain states is described by so-called utilities, typically ranging between 0 and 1, representing death and perfect health, respectively. These are used to compute the Quality-

Adjusted Life Years (QALYs). We denote the unit costs and utilities as c_{sti} and u_s, with indices s, t and i representing states $s \in \{1, ..., S\}$, observation time points t and interventions $i = 1$ (status quo) and $i = 2$ (vaccination). We assume decreasing utility values for more severe states. Costs are induced by screening, vaccination, a visit at the general practitioner and diagnostic tests. Following a positive STI diagnosis, further diagnostic tests and treatment are necessary. For all these quantities, the distributional assumptions are presented in Table 3.1.

The overall costs per intervention are calculated as

$$C_i = \sum_{t=1}^{T} \sum_{s=1}^{S} \frac{c_{sti} n_{sti}}{(1+z)^{t-1}},$$

where n_{sti} is the number of people in state s at time t when intervention i is applied and z is the yearly discount rate. In both the continuous- and discrete-time approaches, the model output on the natural history of disease infection and progression is evaluated at pre-specified time points $t \in \{1, ..., T\}$, where T represents the end of follow-up. Costs and benefits induced in the distant future have a lower impact on the results since they include a higher amount of uncertainty due to unknown future events; furthermore, patients gain most from an instant improvement of their health condition. Therefore, we discount both costs and benefits at a fixed yearly rate $z = 0.03$, following ISPOR recommendations [192]. Similarly, the overall utilities are computed as

$$U_i = \sum_{t=1}^{T} \sum_{s=1}^{S} \frac{u_s n_{sti}}{(1+z)^{t-1}}.$$

The overall costs and benefits can be re-scaled to compute the population averages

$$\mu_{ci}^{\bigstar} = \frac{C_i}{N_i} \qquad \text{and} \qquad \mu_{ei}^{\bigstar} = \frac{U_i}{N_i},$$

where $N_i = \sum_t \sum_s n_{sti}$ is the total number of people in the virtual cohort.

These can be used to define the monetary net benefit $\mathsf{NB}_i(\boldsymbol{\theta}_\bigstar) = k_\bigstar \mu^\bigstar_{ei} - \mu^\bigstar_{ci}$. This quantifies the utility of intervention i as a function of a parameter of *willingness to pay* $k_\bigstar$, which determines the amount of money that the decision-maker is willing to invest to increase the benefits by one QALY. The economic evaluation is performed by calculating suitable summaries such as the increment in mean cost $\Delta_c = \mu^\bigstar_{c2} - \mu^\bigstar_{c1}$ and the increment in mean effectiveness $\Delta_e = \mu^\bigstar_{e2} - \mu^\bigstar_{e1}$ between vaccination and the status-quo, or the incremental cost-effectiveness ratio

$$\mathsf{ICER} = \frac{\mathsf{E}[\Delta_c]}{\mathsf{E}[\Delta_e]}.$$

In the BMM and BODE, these quantities are estimated directly as functions of the parameters, while in the dODE, we conduct a scenario analysis including the 2.5% and 97.5% quantiles of the ICER to evaluate the range of "plausible" results. A cut-off point of a *willingness-to-pay* $k_\bigstar$ of approximately £20,000 – £30,000 per QALY gained, adopted by NICE [298], is used as the benchmark of value for money.

As for PSA, it is usually based on: (*i*) the analysis of the cost-effectiveness plane, depicting the joint probability distribution of (Δ_e, Δ_c); (*ii*) the cost-effectiveness acceptability curve $\mathsf{CEAC} = \Pr(k_\bigstar \Delta_e - \Delta_c > 0 \mid \mathsf{data})$, which shows the probability that the reference intervention is cost-effective as a function of the willingness to pay $k_\bigstar$; and (*iii*) the expected value of "perfect" information

$$\mathsf{EVPI} = \mathsf{E}_{\boldsymbol{\theta}_*}\left[\max_i \mathsf{NB}_i\left(\boldsymbol{\theta}_*\right)\right] - \max_i \mathsf{E}_{\boldsymbol{\theta}_*}\left[\mathsf{NB}_i\left(\boldsymbol{\theta}_*\right)\right],$$

which quantifies the maximum amount of money that the decision-maker should be willing to invest (*e.g.* in a new study) in order to resolve parameter uncertainty and thus make a "better" decision. The probabilistic models can perform these analyses in a straightforward way, since these quantities are all functions of the model parameters and thus a full posterior distribution

can be directly obtained.

The BODE and dODE result in identical ICERs of £13,774, whereas the ICER of the BMM is slightly higher at £13,854. These differences do not have a significant impact on the decision-making process. Accounting for a higher amount of parameter uncertainty in the BMM and the BODE, the ICERs of the three models are considerably lower, resulting in £6,702 in the dODE, £6,800 in the BODE and £7,084 in the BMM. In comparison to the "perfect knowledge" scenario, population prevalence results in higher values. The higher the estimated prevalence, the lower the ICER; if an intervention such as vaccination can prevent more disease cases in a population and therefore show its full potential, it will result in a more cost-effective outcome.

For the dODE, we conduct a scenario analysis to estimate the 2.5% and 97.5% quantiles of the ICER, resulting in £$-$13,660 and £133,620, respectively. The ICER is defined in $\mathbb{R}$, where negative values indicate that the new intervention dominates the status quo or vice versa. Uncertainty in cost- and effectiveness differentials Δ_e and Δ_c is displayed in the cost-effectiveness plane through the joint distribution $P(\Delta_e, \Delta_c)$. However, when calculating the ICER as a ratio of expectations of the posteriors of Δ_c and Δ_e, uncertainty is averaged out. In contrast to Δ_c and Δ_e, the ICER does not have a probability distribution. In terms of a scenario analysis, ranges for ICERs can be presented; however, it would not be possible to estimate credible intervals of an ICER. Furthermore, we point out that results at the extremes commonly only occur with low probability. This is a consequence of the corresponding distributions which often have long tails. An exception would be a Uniform distribution which is not used in our models. If these aspects are ignored, the interpretation of results at the extremes could be falsified.

To estimate the 2.5% quantile of the ICER, the 97.5% quantile of the prevalence outcome is used since a high prevalence results in a low ICER. This effect is reinforced by using the 97.5% quantiles of screening cover-

age, 2.5% quantiles of vaccine coverage, 2.5% quantiles of costs induced by vaccination, 97.5% quantiles of costs induced by screening and the STI, and 2.5% quantiles of the utilities of the states. The scenario analysis of the 2.5% quantile of the ICER is conducted accordingly; however, the assumptions on the prevalence calculation, coverage rates, costs and utilities are reversed.

This analysis clearly shows that the three models result in comparable outcome. However, the quantiles to inform the parameters values of the dODE have to be estimated following careful considerations. If the mean or median is used due to simplicity, infection prevalence might be underestimated, and thus the cost-effectiveness potential of certain interventions might not be recognised. As a consequence, effective and affordable interventions might be withheld from the population, resulting in a significant deterioration of overall population health.

Figure 3.2 displays the cost-effectiveness plane for the BMM and BODE in grey and black, respectively, showing the effectiveness-differential in QALY on the $x-$axis and the cost-differential in £on the $y-$axis. The vast majority of points in both models lie within the sustainability area or close to its border, indicating that vaccination is cost-effective at a threshold of £25,000 when compared to screening.

Figure 3.3 shows the outputs of the CEACs and the EVPI analyses. The CEACs reach values of only around 30% cost-effectiveness at the break-even points of £7,084 and £6,800, respectively, and a value of 80% is reached at a willingness-to-pay of around £40,000 in both models. The EVPI analyses result in values of around £ 23 per individual in the BMM and BODE, which is considerably low. The results indicate that the amount of uncertainty in the BMM and the BODE is basically identical which is in accordance with the confidence bands shown in Figure 3.1.

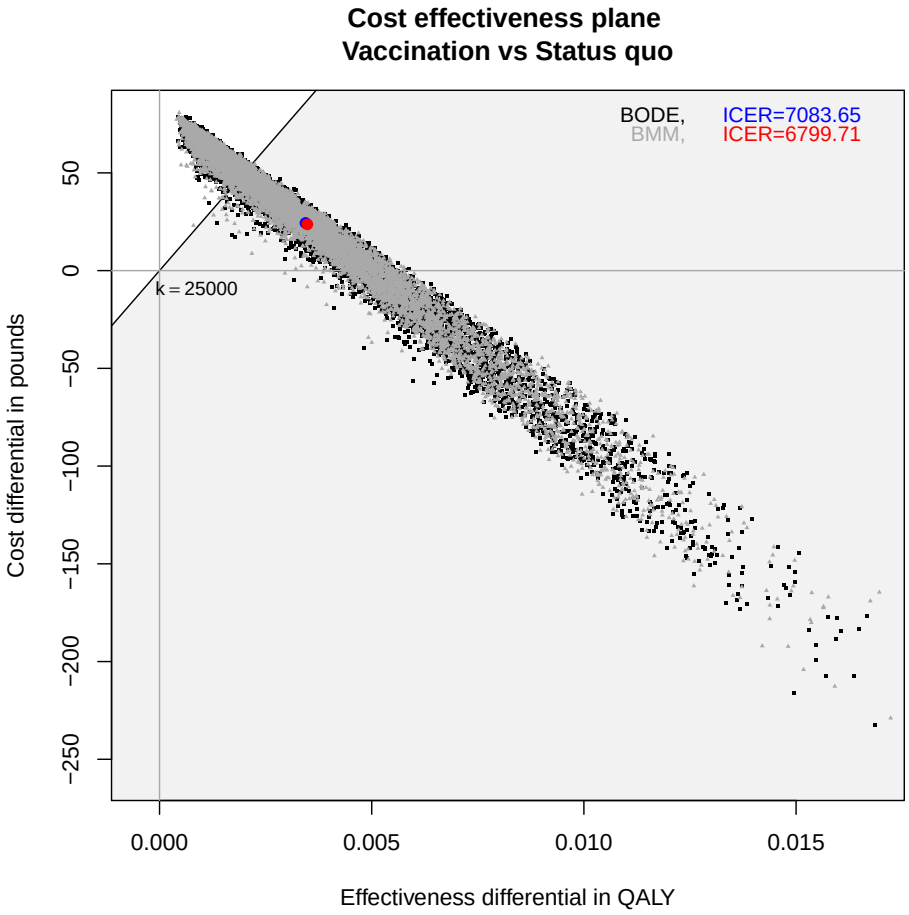

Figure 3.2: The cost-effectiveness plane indicates that vaccination is less expensive and more effective than the status-quo of STI screening. Most points are within the sustainability area, showing that vaccination is cost-effective. The results of the Bayesian Markov model are displayed in grey, whereas those of the Bayesian ODE-based model are shown in black. Additionally, the Incremental Cost-Effectiveness Ratios are displayed as a red and blue dot for the Bayesian Markov model and the Bayesian ODE-based model, respectively. The joint distributions of cost- and effectiveness differentials of both models are comparable.

Figure 3.3: In line with the previous figure, the results of the Bayesian Markov model are displayed in grey, whereas those of the Bayesian ODE-based model are shown in black. The Cost-Effectiveness Acceptability Curves only reach values of around 30% at the break-even points of around £ 7,000, and 80% cost-effectiveness is attained at a willingness-to-pay of around £ 40,000 in both models. The Expected Values of Information are considerably low at around £ 23, indicating that the value for additional research is limited.

3.4 Modelling observed data

In the analysis described in the previous sections, we assumed to have no access to individual-level data. Therefore, the prior distributions were informed through aggregate data and expert opinion as shown in Table 3.1. However, available individual-level (and aggregate) data are commonly used to update the priors in a Bayesian framework. In models including a high number of parameters, data to infer each individual parameter are rarely available. We therefore include simulated individual-level and aggregate data on a selection of parameters; these are partner acquisition rates, STI transmission probability per partnership, vaccine coverage, vaccine efficacy, probability of diagnosis and probability of screening. Minimally-informative and informative priors are specified; in case of minimally-informative priors, the data speak for themselves and the prior does not influence the result of the posterior. In the informative priors, prior knowledge is incorporated and then updated through individual-level data.

We assume to have access to individual-level data Y_{vb} obtained through a survey on the yearly number of sexual partners of altogether 2,000 individuals. This corresponds to 500 individuals in each of the two sexes and risk groups. The data Y_{vb} are simulated through random number generators; the parameters of the corresponding Gamma distributions are estimated through means and standard deviations which are comparable to those reported in the literature on sexual mixing [206, 360]. To infer the partner acquisition rates ω_{vb}, we assume to have observed Y_{vb} and use these data to update informative Gamma priors into the corresponding posteriors through Poisson-Gamma models as

$$Y_{vb} \sim \text{Poisson}(\omega_{vb})$$
$$\omega_{vb} \sim \text{Gamma}(0.1, 0.1).$$

Table 3.2: Overview of the posterior means and 95% credible intervals of the parameters of the BMM which are updated by simulated data. The posterior results of the BODE are comparable.

Parameter	Description	Model	Mean	95% interval
ω_{MH}	Partner acquisition rate (high-risk males)	Poisson-Gamma	9.10	[8.77;9.29]
ω_{ML}	Partner acquisition rate (low-risk males)	Poisson-Gamma	2.98	[2.82;3.12]
ω_{FH}	Partner acquisition rate (high-risk females)	Poisson-Gamma	9.00	[8.71;9.26]
ω_{FL}	Partner acquisition rate (low-risk females)	Poisson-Gamma	1.96	[1.86;2.09]
β	STI transmission probability per partnership	Beta-Binomial	0.16	[0.15;0.16]
η	Probability of STI diagnosis	Beta-Binomial	0.90	[0.88;0.92]
σ	Screening probability	Beta-Binomial	0.90	[0.87;0.92]
α	Vaccine coverage parameter	Beta-Binomial	0.90	[0.87;0.92]
γ	Vaccine efficacy parameter	Beta-Binomial	0.90	[0.87;0.92]

The approaches for the other parameters are similar; however, since these parameters are probabilities, the corresponding models are Beta-Binomial. As an illustrative example, we show the model for the STI transmission probability β which is specified as

$$R_\beta \sim \text{Binomial}(\beta, N_\beta)$$
$$\beta \sim \text{Beta}(0.5, 0.5).$$

The data are given by R_β and N_β which represent the number of people who become infected by the STI and the overall number of people observed, respectively. The corresponding prior is the reference prior. The reference prior ensures that the information given by the data has a maximal impact on the result of the posterior [389].

The means and 95% credible intervals of the resulting posteriors of the BMM are shown in Table 3.2. The remaining parameters are not updated by data and thus identical to those displayed in Table 3.1. The posterior results of the BODE are similar to the BMM and therefore not reported.

As described in Section 3.3.2, the BMM is run in `JAGS`. In `R`, Bayesian ODE-based models can be run through `Stan` or `WinBUGS` [355], using the interface `WBDiff` [247]. We intended to compare the two alternatives. In the previous analysis, the BODE was run in `Stan`; therefore, in the second analysis, we switch to `WinBUGS`. In most applications, however, `Stan` is more computationally efficient. An ODE solver for stiff regions of ODEs is provided in the newest release (2.14).

Both models are run for 1,000 simulations to achieve good convergence of each parameter and the output. Furthermore, issues with autocorrelation are avoided. Compared to the analysis described in Section 3.3.2, the number of simulations is reduced by around factor ten. The computation times are 146.23 seconds and 81.34 seconds for the BMM and BODE, respectively. In comparison to the first analysis, the computation time of the BMM is longer as a consequence of data inclusion, whereas the BODE runs faster in `WinBUGS` when compared to `Stan`. This is most likely a consequence of the lower number of simulations. We assess convergence and potential issues with autocorrelation using standard tools such as the Potential Scale Reduction $\hat{R}$ and the effective sample size [151]. Further details on $\hat{R}$ and autocorrelation are described in Sections 3.2.2 and 3.2.3. Convergence is sufficiently achieved with $\hat{R} < 1.1$ in all model parameters. We can conclude that there are no issues with autocorrelation since the effective sample size is almost as high as the overall number of simulations in all model parameters. The relevant model code is presented in Appendix A.

3.5 Model calibration

Model calibration is an essential part of infectious disease modelling for two reasons. The first is that not all model parameters can always be informed directly; sometimes, reliable data cannot be collected (e.g. due to ethical reasons as for the probability of infection transmission described in Sec-

tion 1.3). In this case, a common approach is to calibrate the corresponding model outcome to high quality data, e.g. obtained from a large registry. The parameter values resulting in outcome which is most comparable to these registry data are then assumed to be most realistic and used to inform the model [366]. The second reason to calibrate model outcome is to ensure that the results are in line with high quality data, even if the model parameters can be informed by data directly. If the model outcome is not comparable to the high quality data, the corresponding model parameters have to be adjusted, either through direct or indirect calibration approaches.

In the second analysis of the case study, simulated data are thus included as follows. In the Bayesian models, individual-level and aggregate data are included to update the priors into the corresponding posteriors as described in the previous section. In addition to posterior sampling, simulated data are included to calibrate the model outcome to time series data on the number of people in each state. In the dODE, simulated data are included to determine the parameter values which result in most realistic model outcome. Since the literature on infectious disease modelling includes a large variety of calibration approaches (which are often not presented in sufficient detail), we conduct the three approaches which are most commonly applied. These are visual calibration as well as frequentist probabilistic and Bayesian calibration. A visual calibration approach is also conducted for the HPV model in Section 6.3. Further details on the three approaches are described in the following.

In a visual calibration approach, the model output and data are displayed graphically and compared visually. Key model parameters are adjusted repeatedly until the model output shows reasonable fit to the data. However, this approach is quite crude and prone to induce incorrect results; thus, the application of more systematic calibration approaches (e.g. probabilistic calibration in a frequentist or Bayesian setting) is often advisable.

In a frequentist probabilistic calibration approach, large numbers of sets

of input parameter combinations are created through random sampling, e.g. forward sampling (as described in Section 3.2.1) or Latin Hypercube Sampling. A range of model outputs corresponding to each input parameter set is then compared to data [209]. The procedure involves the calculation of goodness-of-fit (GOF) statistics. Depending on the GOF statistic, lowest (sum of mean squared errors, χ^2 statistics, log-likelihood) or highest (maximum likelihood) values indicate best model fit [366].

In the Bayesian calibration approach, model parameters are inferred by fitting the model to data directly (in one step). The updating of the model output takes place by assigning suitable distributions to the data. For example, if the model output corresponds to count data (e.g. on the number of people in certain states at a specific period of follow-up), a Poisson distribution could be assigned. The event rate λ_* is then directly represented by the expectation on the model output.

In addition to Bayesian calibraton approaches, direct frequentist likelihood-based approaches exist; however, these are less flexible since parameter uncertainty cannot be propagated through the model. For example, Bretó et al. [50] fit models based on stochastic processes to time series data through frequentist likelihood-based approaches. The authors present so-called “plug and play” models, meaning that simulations of sample paths are made by repeatedly plugging random input parameters into a “black box” of “equation-free” models. Thus, transition probabilities do not have to be available in closed form, and sample paths are not predefined but simulated. Likelihood-based inference is then conducted to inform the corresponding model parameters. A variety of both frequentist and Bayesian likelihood-based methods of inference for “plug and play” models is implemented in the `R`-package `POMP` (Partially observed Markov process) [224]. The procedures in this package are very extensive and account for specific data, e.g. including measurement error, unobserved variables, covariates, irregular sampling intervals, as well as properties such as non-stationarity

and nonlinearity [77, 190, 223]. An important limitation of the package is the related computational effort which increases considerably the more states and parameters are included into a model. Thus, at present, `POMP` is not suitable to fit more complex models to data [182].

Another direct frequentist calibration approach based on the Ramsay method is presented by Koulis et al. [230]; this is applied to an experiment in psychoacoustics, where participants' reaction to specific sound is measured. Observations vary between as well as within participants. Thus, hierarchical data are obtained, with observations nested within participants. In mixed-effects models, calibration takes place through centering of the regressors towards the origin. This is conducted to break the correlation between the intercept and the slope in the regression models.

3.5.1 Visual comparison of model output to data

Before we conduct systematic calibration approaches, we describe the process of parameter adjustment through visual calibration due to the following reasons. In the health economic literature on interventions against infectious diseases, the outcome of the corresponding models is often compared visually to data. In addition, we conduct a visual calibration approach for the HPV model in Section 6.3 since time series data on HPV-induced diseases are not available; for consistency, we show this approach for the case study as well.

To conduct a visual calibration approach, we simulate data on the prevalence of the chronic STI for an observation time period of 100 years. Data simulation is conducted by running the dODE for different inital and parameter values; this dODE is termed `prevSim`. We initialize `prevSim` with a very large virtual population of 100,000,000 people, comparable to the size of a data registry. As described in Section 3.3, we assume 20% of the population to be in the high-risk group and 50% to be male. Initially, 20,000

people in each of the four subgroups (high- and low-risk female and male, respectively) are assumed to be infected. The output of `prevSim` on STI prevalence (including an average dataset of the proportion of the population in the states infected, asymptomatic and morbid) is then used to calibrate the dODE, BODE and BMM.

The key parameters which need to be adjusted in the visual calibration process are the STI transmission probability β and the transition rate and probability of moving from the state morbid to the state death ($\rho_{4,5}$ and $\pi_{4,5}$, respectively). In the Bayesian models, β, $\rho_{4,5}$ and $\pi_{4,5}$ are modified by shifting the corresponding distributions so that the means of the distributions before calibration correspond to the 97.5% quantiles of the distributions after calibration. In the dODE, the vast majority of parameter values corresponds to the mean values of the BODE; however, β and $\rho_{4,5}$ are informed by the 15% quantile and the minimum of the corresponding parameter distributions of the BODE, respectively.

Figure 3.4 shows the model outcome on STI prevalence after calibration. The two Bayesian models fit the simulated data well, with a slight STI prevalence overestimation in the BMM between years 30 and 40 of the observation time period, and a slight underestimation in the BODE between years 60 and 100. The fit of the dODE is not as good, including an underestimation before year 50, and an overestimation afterwards. These differences might be a consequence of including a much larger population into *prevsim* than into the dODE and of informing the corresponding parameters by slightly different values when compared to the dODE. These results show that visual comparison as a single calibration method is insufficient to further improve model fit to data, and the application of a more systematic calibration approach is necessary. The amount of uncertainty in the two Bayesian models is comparable. The ranges of the scenario analysis of the dODE are considerably smaller than the bounds of the 95% credible intervals of the BMM and BODE.

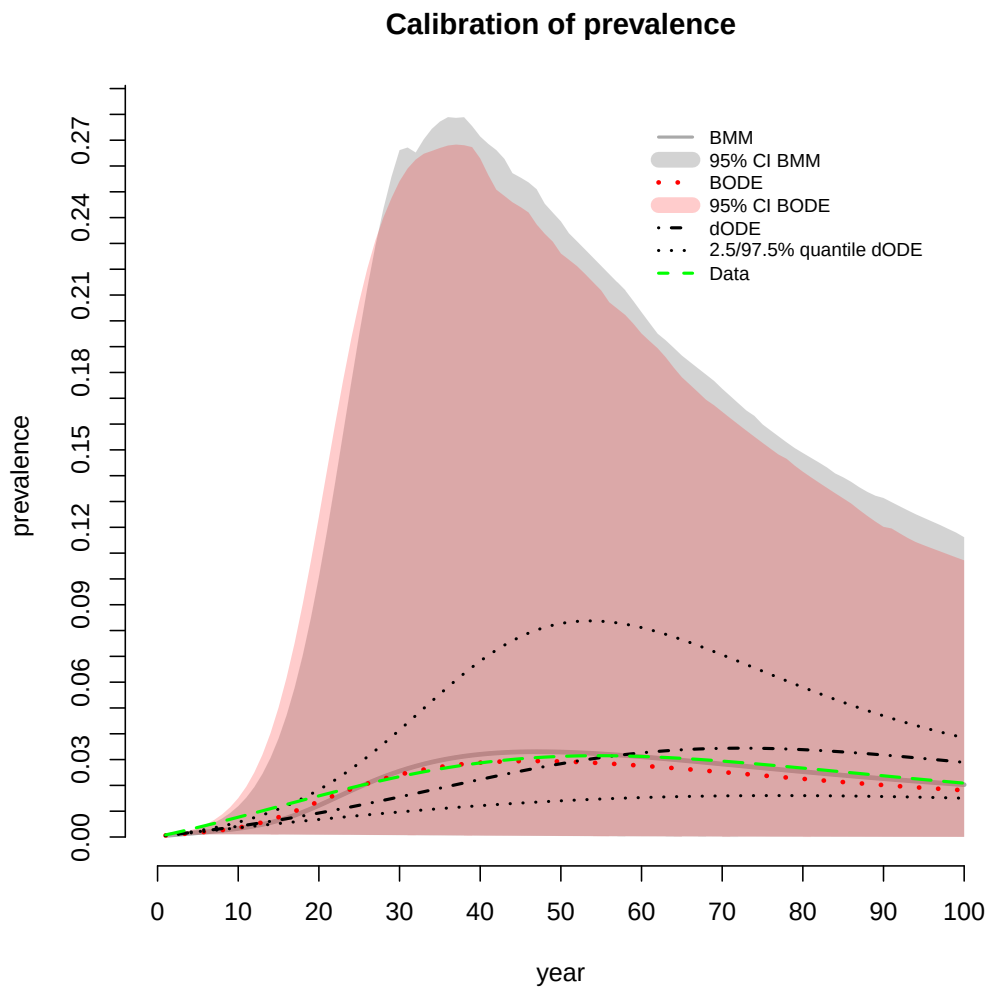

Figure 3.4: The prevalence outcome of the three models following a visual calibration approach. Prevalence of the calibrated BODE and BMM is comparable to the simulated data, whereas the calibrated dODE underestimates STI prevalence during the first 50 years of the observation time period, and overestimates it afterwards.

Following visual calibration, we conduct a cost-effectiveness analysis as described in Section 3.3.4. The ICER of the dODE results in £8,095.48 (ranging from £1,953.48 to £18,374.71 in the scenario analysis), whereas the ICERs of the BODE and BMM are considerably higher at £12,343.95 and £11,691.11, respectively. The ICERs of the three models are well below the threshold of cost-effectiveness of £25,000.

PSA on the outcome of the two Bayesian models is conducted as part

of the health economic evaluation. The CEACs and EVPIs of the two models are comparable. The joint distribution of cost- and effectiveness differentials is right-skewed. Thus, the values of the CEACs are considerably low and never reach values above 40% for a willingness-to-pay ranging between £0 and £50,000. Further details on skewed distributions of cost- and effectiveness differentials and their impact on the values of the CEAC are described in Section 6.6.1. The population EVPIs result in values of around £ 4,000,000,000.

As described, the ICER estimated through the dODE differs from those of the BODE and BMM despite visual calibration to simulated data on population prevalence. These differences are a consequence of the considerably high amount of uncertainty in the simulated prevalence data; prevalence is a summary statistic and does not include details on the number of people in each of the states over follow-up. Thus, following calibration, the model outputs on the number of people in the states can still be substantially different. Furthermore, despite repeated parameter adjustment, the model fit of the dODE to the simulated data is not ideal. To result in comparable outcome of the cost-effectiveness analysis, more systematic calibration approaches are conducted in the following.

3.5.2 Probabilistic calibration approaches

In addition to visual calibration, the literature includes probabilistic calibration approaches which can be conducted in a frequentist or Bayesian setting. The dODE is calibrated through a frequentist probabilistic calibration approach, whereas the BODE and the BMM are calibrated through Bayesian calibration approaches. Simulated time series data on the number of high-risk people in the states *Susceptible*, *Infected*, *Asymptomatic* and *Morbid* in the first five years of follow-up are used for calibration. A short observation time horizon of only a couple of years (five years in this

case) is common in available time series data. These data are simulated by running the dODE for a follow-up period of five years; the input parameter values are informed through the means of the parameters of the BODE.

The computation times are 149.81 seconds and 6,587.67 seconds (around 1 hour 50 minutes) for the BMM and BODE, respectively. When compared to the previous analysis, the number of simulations is reduced from 10,000 to 1,000. The computation time of the BMM is only 3 seconds longer. The considerably increased computation time of the BODE is a consequence of the Bayesian calibration approach which is conducted in the `WinBUGS` interface `WBDiff`. In addition, the computation time of the dODE considerably increases from 0.22 seconds to 4,480.19 seconds (around 1 hour 15 minutes) since the model is run for a high number of parameter sets in context of frequentist probabilistic calibration.

The comparison of computation times clearly shows that the BMM is highly efficient when time series data are included to calibrate the model outcome. In the BMM, model calibration almost makes no difference in computation time if the BMM is run for a reduced number of simulations. At the same time, the BMM results in model outcome comparable to the gold standard of the BODE. In contrast to the BMM, computation time increases by factor 35 and 20,365 in the BODE and dODE, respectively, when the models are calibrated. However, it is questionable to compare the computation times of the BODE with and without calibration to data since software and number of simulations differ.

Frequentist calibration of the deterministic ODE-based model

We calibrate the dODE through a frequentist probabilistic calibration approach as shown in [205, 358, 366]. Suitable probability distributions are assigned to the model parameters which play a role in natural history of disease. The parameters of the distributions are estimated through means and standard deviations obtained through expert opinion. For the STI transmis-

sion probability, transition rates and reproduction rate, these are identical to the means and standard deviations used to inform the corresponding informative priors shown in Table 3.1. For the partner acquisition rates, we calculate means and standard deviations of the simulated individual-level data which are used to update the non-informative priors as described in Section 3.4.

As a next step, sets of 50,000 parameter combinations are sampled from the predefined parameter distributions through Monte Carlo sampling. We calculate the sum of squared errors between the outputs of the 50,000 model runs (for each parameter set combination) and simulated data (which are described in Section 3.5.2) on number of high-risk people for the first five years of follow-up in four states as

$$\mathcal{Q}(\theta_*) = \sum_{t=1}^{5} \sum_{s=1}^{4} \left(y_s(t) - f_s(t \mid \theta_*)\right)^2 .$$

The dODE is based on a continuous-time approach; however, in order to result in outcome which is comparable to the BMM in discrete time, the corresponding output is evaluated at yearly time points $t \in \{1, ..., 5\}$. This cycle length is deemed appropriate since the natural history of disease of the chronic STI is considerably slow; a progression to a disease state following infection often takes several years to decades. The simulated data on the number of high-risk people in state s at time point t are indicated by $y_s(t)$, and $f_s(t \mid \theta_*)$ is the model output on high-risk people in state s at time t given the input parameter set θ_*. As a final step of the calibration, the set θ_* corresponding to the model output which results in the least sum of squares is selected; it is displayed in Table 3.3. The fit of the calibrated model output to the simulated data is assessed visually as shown in Figure 3.5.

The natural history of the disease is evaluated through the calibrated model outcome, and cost-effectiveness analysis is also conducted. Due to the fact that the model outcome of the dODE does not include distributions,

Table 3.3: Point estimates of the parameters of the deterministic ODE-based model obtained through a frequentist probabilistic calibration approach. The parameter set θ_* with the best fit to simulated data minimises the sum of squared errors.

Parameter	Description	Point estimate
ω_{MH}	Partner acquisition rate (high-risk males)	8.3515
ω_{ML}	Partner acquisition rate (low-risk males)	2.4526
ω_{FH}	Partner acquisition rate (high-risk females)	8.3836
ω_{FL}	Partner acquisition rate (low-risk females)	1.6085
χ	Proliferation parameter	0.0100
β	STI transmission probability per partnership	0.1639
$\pi_{2,3}$	Transition parameter from state 2 to state 3	0.7957
$\pi_{3,4}$	Transition parameter from state 3 to state 4	0.0891
$\pi_{4,5}$	Transition parameter from state 4 to state 5	0.0232
$\pi_{1,5}$	Transition parameter from state 1 to state 5	0.0005

PSA is not performed; yet, scenario analysis of the ICER is conducted. The results are shown in the following sections.

Bayesian calibration of the BODE and BMM

We calibrate the Bayesian models through a Bayesian calibration approach as conducted in [106, 170, 377, 379]. Both Bayesian and frequentist probabilistic model calibration are systematic approaches. Therefore, in comparison to visual calibration, we expect the differences in results of the BODE, BMM and dODE to decrease.

In the BODE, the model output on the number of people in the states over the follow-up period corresponds to the solutions of the ODEs (see Equation 2.1). In the BMM, the model output corresponds to the solutions of the state allocation algorithm; in the state allocation algorithm, members of the population are allocated to the states in each year of follow-up (see Equation 2.2). Both the solutions of the ODEs and the state allocation algorithm are constantly updated through simulated time series data on high-risk people. The procedure of data simulation and nature of data is described at the beginning of this section. The updating takes place by assigning Poisson distributions to the simulated data; the event rate λ_* is then represented

by the solutions of the ODEs and the state allocation algorithm, respectively. As a consequence, the resulting model outcome is already calibrated, and no further steps such as the calculation of GOF statistics are necessary. The evaluation of the natural history of disease and the cost-effectiveness analysis including PSA can be conducted straightforwardly.

Natural history of disease

Figure 3.5 shows the outcome on the natural history of disease of the fictional chronic STI following calibration. In contrast to Sections 3.3.3 and 3.5.1, the number of people in four of the states rather than prevalence are shown. Only the results on high-risk females are displayed; those on high-risk males are comparable.

The results of the two Bayesian models are similar. The model outcome on the states *Susceptible* and *Morbid* is basically identical, whereas the outcome of the BODE shows higher estimates on the number of infected and asymptomatic females. The outcome on the number of susceptible and morbid females is higher in the dODE; in contrast, the outcome on those in the states *Infected* and *Asymptomatic* is lower when compared to the two Bayesian models. This is a consequence of the differences in model parameter estimation (whole distributions of values in the BMM and BODE and fixed parameter values in the dODE) as well as differences in calibration approaches (Bayesian calibration in the BMM and BODE and frequentist probabilistic calibration in the dODE).

The ranges of the 95% credible intervals of the BODE and BMM are similar, showing wider ranges in the BMM. The 97.5% quantiles of the scenario analysis of the dODE are lower than the upper bounds of the 95% CIs in the states *Infected* and *Asymptomatic* and higher in the states *Susceptible* and *Morbid*, whereas the 2.5% quantiles are considerably lower than the lower bounds of the CIs (apart from the state *Susceptible*).

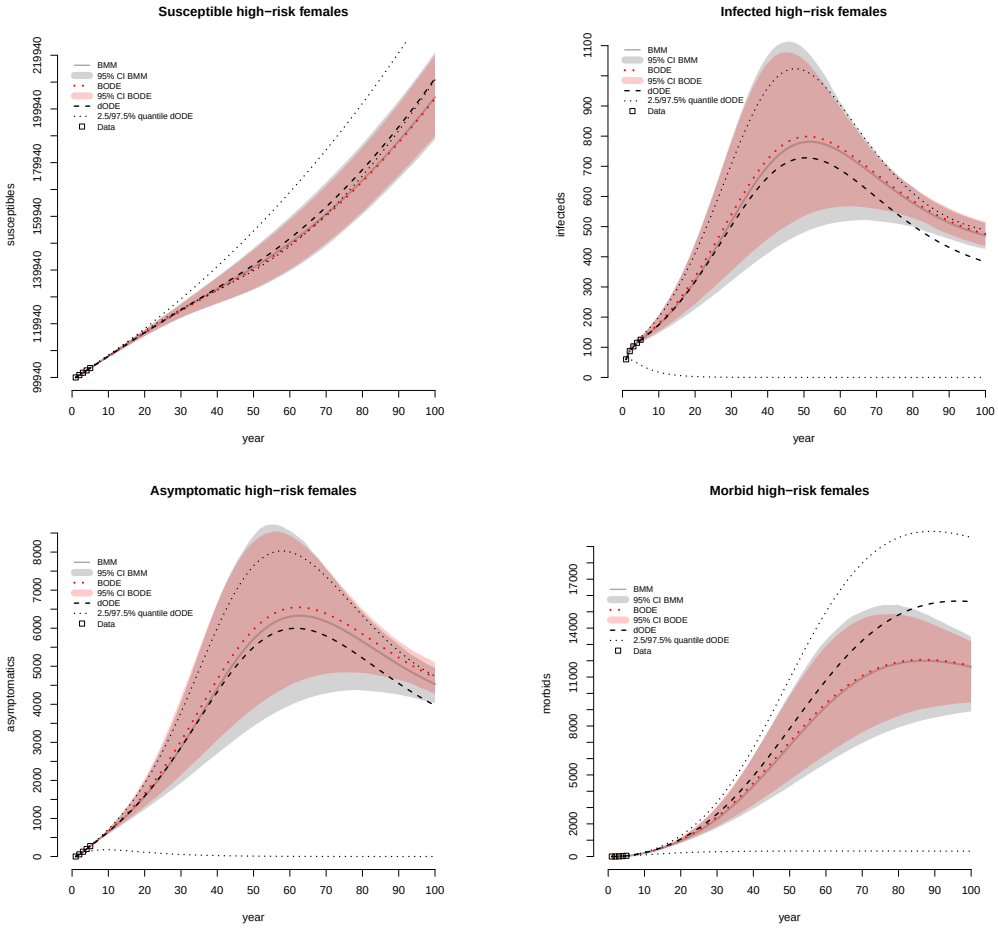

Figure 3.5: Calibration results on the number of high-risk females in the states *Susceptible*, *Infected*, *Asymptomatic* and *Morbid*. The results of the Bayesian models are similar, with a higher number of high-risk females in the states *Infected* and *Asymptomatic* estimated by the Bayesian ODE-based model. In contrast, the deterministic ODE-based model results in a lower estimate on the number of high-risk females in the states *Infected* and *Asymptomatic*; however, the outcome on the states *Susceptible* and *Morbid* is reversed.

Cost-effectiveness analysis

Details on common measures of cost-effectiveness analysis are explained in Section 3.3.4. The CEA results of the visual calibration approach are reported in Section 3.5.1. Following a frequentist probabilistic calibration approach, the ICER of the dODE results in £7,203.416, ranging between £2,592.44 and £469,906 in the scenario analysis at the 2.5% and 97.5% quantiles. The ICERs of the probabilistic models are comparable to the

dODE, resulting in £6,054.82 and £6,287.62 in the BODE and BMM, respectively.

In contrast to a visual calibration approach, systematic probabilistic calibration results in comparable outcome of cost-effectiveness analysis of deterministic and Bayesian models. In comparison to the cost-effectiveness analysis based on the visual calibration approach, the ICERs of the Bayesian models are considerably reduced, whereas the ICER of the dODE only shows a slight decrease.

PSA is conducted on the outcome of the BMM and the BODE. Figure 3.6 displays the cost-effectiveness plane which is not comparable to the one shown in Figure 3.2 since the corresponding models are informed through additional information obtained from simulated data. The joint distributions of cost and effectiveness differentials of the BODE and the BMM are symmetrical. Each point of the MCMC simulation lies within the grey sustainability area, indicating that STI vaccination is cost-effective at a threshold of £25,000 when compared to STI screening. STI vaccination is deemed to be both more expensive and more effective than STI screening since all points are located in the upper right quadrant of the graph. The ICERs of the BMM and BODE are displayed as red and blue dots, respectively.

Figure 3.7 shows the results of the CEACs and the population EVPIs of the two Bayesian models. The amount of uncertainty in the BMM is slightly larger than in the BODE; however, 80% cost-effectiveness is clearly reached at the break-even points of the ICERs of both models. The population EVPI of the BMM at around £500,000,000 is higher than in the BODE, where it reaches a value of around £400,000,000. The higher EVPI value of the BMM is a consequence of the slightly larger amount of uncertainty. Thus, the value of additional research is higher in the BMM.

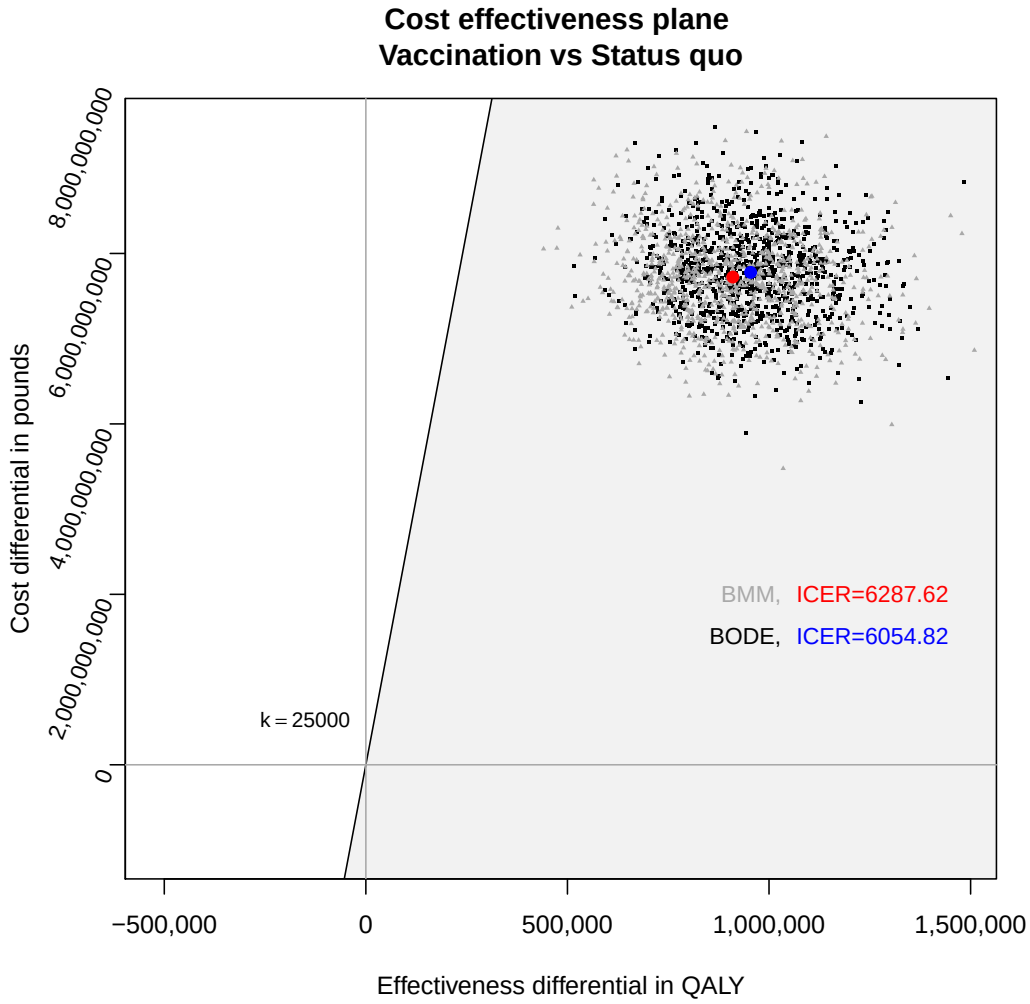

Figure 3.6: In comparison to the cost-effectiveness analysis based on visual calibration, the joint distribution of cost- and effectiveness differentials is no longer skewed. The ICERs of £6,054.82 (blue dot, BODE) and £6,287.62 (red dot, BMM) indicate cost-effectiveness of STI vaccination in comparison to STI screening at a threshold of £25,000. All points lie within the sustainability area of cost-effectiveness.

Figure 3.7: The results of the BMM are displayed in grey, whereas those of the BODE are shown in black. The amount of parameter uncertainty is higher in the BMM. The CEACs in the left panel reach values of 80% at a willingness-to-pay corresponding to the ICERs. The EVPIs for the whole population at around £500,000,000 and £400,000,000 in the BMM and BODE, respectively, are shown in the right panel. These are around ten times lower than in the CEA based on visual calibration.

3.6 Conclusions

In this chapter, the dynamic Bayesian MM was compared to a deterministic and a Bayesian ODE-based model. The terms “deterministic” and “Bayesian” refer to the nature of the parameters and the inference conducted, respectively. The main purpose of this comparison was to evaluate whether the approach of the dynamic BMM produced similar outcome as the “gold standard” of the BODE. In addition, methodological uncertainty was investigated, especially focussing on the implications of models including parameters with fixed values and thus ignoring the effects of parameter uncertainty. The comparison was made through the case study of the hypothetical chronic sexually transmitted infection (STI) which was introduced in Chapter 2; the study was described in further detail in this chapter. For the three approaches compared, STI prevalence predictions were conducted. Furthermore, the outcome of the cost-effectiveness analyis of a hypothetical vaccine against the chronic STI was evaluated, including PSA on the outcomes of the Bayesian models.

In the first part of the analysis, exclusively informative priors were included, and no data were used to update the priors. Thus, prior elicitation and forward sampling were conducted. When compared to the BODE, we could clearly show that the dynamic BMM resulted in similar prevalence and outcome of the CEA while at the same time considerably reducing the computational effort. The parameter values of the dODE were estimated by comparing the corresponding outcome to the outcome of the gold-standard of the BODE. The loss induced by prevalence under- and overestimation was non-symmetric, and thus 60% quantiles of the parameters of the BODE (instead of the mean or median) were used to inform the parameters of the dODE. If the proportion of the population under risk of infection was underestimated, this would result in the false assumption of limited vaccine requirement. As a consequence, the benefits of vaccination were under-

estimated, and the cost-effective vaccine was withheld from the population. This induced unnecessary suffering and possibly death. The non-symmetric loss could be accounted for by informing the parameter values of the dODE through the 60% quantiles of the BODE. As a consequence, the corresponding results of prevalence and the CEA were comparable to the two Bayesian models. However, a non-symmetric loss is usually not considered in deterministic models in the literature. Therefore, it is essential to calibrate model outcome to empirical data to avoid incorrect results.

In the second part of the analysis, we included simulated data into the models for two reasons. First of all, Bayesian inference was conducted by updating minimally-informative and informative priors through data into the corresponding posteriors. Furthermore, data were used to calibrate the outputs of the two Bayesian models and the dODE. A systematic calibration approach resulted in comparable outcome of natural history of disease and cost-effectiveness analysis. The differences in ICER results were considerably reduced, and benefits of vaccination were no longer underestimated by the dODE. The computational effort of the BMM was around 44 times lower when compared to the BODE and is thus still manageable even in highly complex BMMs.

Therefore, we can conclude that the dynamic BMM is especially suitable in CEAs of interventions against infectious diseases which require a high number of states and separate compartments for covariates such as age, sex and behaviour. The corresponding outcome is comparable to the “gold standard” of a BODE at reduced computation time; this is even the case if the model output is not calibrated to simulated data. One example of a complex infectious disease is human papillomavirus (HPV). A literature review on CEAs of HPV vaccination as well as the specification of the BMM to an HPV context including the corresponding results are described in the second part of this PhD thesis.

Part II

Cost-effectiveness analysis of human papillomavirus vaccination

Chapter 4

Literature review

4.1 Introduction

This chapter includes an extensive literature review on methodology and results of health economic evaluations of female-only and universal (including both sexes) human papillomavirus (HPV) vaccination strategies.

Since the early 2000s, several teams of researchers have considered the inclusion of males to existing HPV vaccination programmes. HPV is sexually transmitted; the virus can also cause diseases in males, and males are possible vectors in the virus transmission to females. As a consequence, both sexes would experience a health benefit from non-sex-specific vaccine recommendations. However, the question is whether universal HPV vaccination is cost-effective.

The main purposes of the literature review are i) to ensure that our contribution of the dynamic Bayesian MM is innovative in the context of HPV transmission modelling; ii) to investigate the differences in methodologies applied to compare universal to female-only vaccination; and iii) to evaluate the reasons for contradictory results of the cost-effectiveness of universal HPV vaccination.

First of all, we describe the databases searched and search word combinations applied. As a next step, we introduce the checklist on essential

aspects of methodology, model assumptions and research outcome we use to evaluate the retrieved publications. This checklist is especially helpful to identify reasons for varying results of cost-effectiveness analysis (CEA). Research outcomes in terms of ICERs per QALY (see Section 3.3.4) below a willingness-to-pay value of €25,000 - €40,000 per QALY gained [135, 256] are deemed to be cost-effective. This benchmark of value for money roughly corresponds to the value of £20,000 - £30,000 adopted by NICE [298].

In the end of the chapter, we discuss the results of the health economic evaluations, structured separately for publications including universal and female-only vaccination, respectively. Furthermore, we discuss the differences in methodology and model assumptions which explain contradictory cost-effectiveness outcome. Finally, we compare the approaches presented to our contribution of a dynamic Bayesian MM.

4.2 Databases and search word combinations

We perform the literature review through the databases *Scopus*, *Pubmed*, *The Cochrane Library*, *Web of Science* and the *Centre for Review and Dissemination (CRD)* of the National Institute for Health Research. The CRD combines the databases DARE (Database of Abstracts of Reviews of Effects), NHS EED (NHS Economic Evaluation Database) and HTA (Health Technology Assessment).

The following search word combinations are used to identify literature on the cost-effectiveness of HPV vaccination strategies:

```
((cost-effectiveness) OR (cost-utility) OR (cost-benefit))
AND ((HPV vaccine) OR (human papillomavirus vaccine)
OR HPV OR (human papillomavirus))
```

To focus specifically on male HPV vaccination, the search term is extended by

`AND (boys OR male).`

Possible synonyms are considered and combined with the search word `OR`, whereas obligatory search word combinations are linked with the search word `AND`.

The above search identifies 110 studies including female-only vaccination and 34 studies including universal vaccination, focussing on CEA and/or changes in natural history of HPV, such as reductions in HPV prevalence and incidence or lifetime risk of cervical cancer.

4.3 Checklist for methodology and model assumptions

Each publication retrieved is evaluated thoroughly according to a checklist in order to provide a systematized overview on methodology, model assumptions and aim of research. The checklist includes the following criteria:

- **methodology:** static vs. dynamic, deterministic vs. probabilistic;
  - **population-based:** ordinary or partial differential equation (ODE/PDE)-based vs. Markov vs. hybrid model;
  - **individual-based:** microsimulation vs. network vs. hybrid model;
- **model assumptions:** country-specific context, HPV types considered, HPV-induced diseases included, vaccine coverage rate, vaccine efficacy, vaccination age, male vaccination, duration of vaccine-induced immunity, booster application, levels of sexual activity, sexual mixing strategy, cervical screening conducted, duration of follow-up, vaccine price, discount rate;
- **aim of research:** CEA, prevalence/incidence reduction of HPV or HPV-induced diseases following vaccination.

All publications are summarized in Tables B.1 and B.2 in Appendix B.1, which are structured separately for universal and female-only vaccination strategies. The most important findings are discussed in the following. Publications on HPV prevalence predictions are only reported in Appendix B.1.

4.4 Methodology

We investigate six approaches presented in the literature on HPV transmission and HPV-induced disease progression modelling, including i) differential equation models, ii) Markov models (MMs), iii) microsimulation models, iv) network models and v) hybrid models. Differential equation models and MMs are population-based, implying that the population as a whole is observed. As a consequence, proportions of the population in each state at each time point or time interval of follow-up are evaluated. In contrast, in individual-based models such as microsimulation or network models, each individual is observed separately; thus, patient disease history is accounted for.

A variety of dynamic transmission models based on differential equations are evaluated; these primarily predict the impact of universal vaccination strategies. In context of female-only vaccination, the vast majority of authors present static MMs; however, a static methodology commonly results in falsified prevalence and CEA outcome since effects of herd immunity cannot be considered. Individual-based models are presented in dynamic or static settings. Both static individual- and population-based models can be linked to dynamic transmission models, resulting in so-called hybrid models. All methodologies are summarized in the following; additional details are presented in Appendices B.2 – B.5.

4.4.1 Differential equation models

In the literature on HPV vaccination, differential equation models are usually stratified according to age, sex and sexual behaviour. Apart from [240], all differential equation models reviewed estimate HPV transmission dynamically through the force of infection, incorporating age-, sex- and behavioural-specific sexual mixing matrices. Ten are based on ordinary differential equations (ODEs) [63, 131–133, 187, 204, 229, 240, 349, 392], whereas three incorporate partial differential equations (PDEs) [26, 38, 368]. In contrast to ODEs which are functions of time of follow-up, PDEs are functions of both age and time. The vast majority of the ODE- and PDE-based models presented inform their parameters through fixed values, e.g. point estimates [26, 131–133, 187, 204, 240, 349, 392]. Bayesian approaches are introduced for three models including a smaller number of states; however, not every model parameter is assigned a distribution, and fixed values are incorporated for certain model parameters [38, 229, 368]. Ten authors [26, 63, 131–133, 187, 204, 229, 368, 392] include universal vaccination strategies; yet, only five [131–133, 204, 392] conduct CEAs, whereof only Elbasha et al. [131] come to the conclusion that universal vaccination is cost-effective. In addition, two models [38, 349] exclusively account for female-only vaccination, with [349] conducting a CEA and resulting in cost-effective outcome. The most interesting models are described in Appendix B.2.

4.4.2 Markov models

Altogether, 30 newly developed Markov models [17, 34, 79, 83, 96, 99, 109, 111, 153, 162, 173, 225, 241, 245, 248, 263, 270, 274, 294, 311, 321, 328, 330, 342, 344, 345, 358, 365, 370, 388] are presented, including eleven which assign distributions to model parameters [34, 81, 96, 136, 153, 225, 241, 245, 294, 328, 358], whereof three [81, 136, 358] are based on a Bayesian framework. Nine of the newly developed Markov models [34, 79, 83, 109, 162, 263, 294,

358, 365] are modified as follows: Five publications [57, 82, 232, 289, 364] extend the original aim of research (e.g. including CEA), whereas 26 [9, 16, 30, 87, 113–116, 130, 164, 169, 172, 183, 226, 228, 231, 257, 273, 300, 303, 304, 333, 337, 373, 382, 383] are adjusted to settings in different countries. Three authors [83, 274, 365] use the term "Markov model" exclusively if only one cohort of individuals is incorporated; however, in the health economic literature, multi-cohort models are alternatively referred to as MMs.

Five authors [16, 82, 83, 365, 370] indirectly account for herd immunity in static methodology. This approach is not comparable to a dynamic methodology since dynamic changes in population prevalence cannot be considered. The corresponding implications and disadvantages are discussed in Section 1.2. Anonychuk et al. [16] follow an approach introduced by Bauch et al. [27] to reduce HPV prevalence in unvaccinated individuals through herd immunity. Chesson et al. [82, 83] multiply prevalence of HPV-induced diseases by adjustment factors to estimate indirect protection of unvaccinated individuals. Vanagas et al. [365] consider a reduced risk of exposure to HPV due to decreasing HPV prevalence in females after vaccine introduction. Voko et al. [370] lower the transition probability to the state of HPV infection, proportionally on vaccine coverage and vaccine efficacy.

Apart from [82, 173, 289, 330], all MMs exclusively account for female-only vaccination. Stratton et al., Chesson et al. and Pearson et al. [82, 289, 330] compare universal vaccination to screening-only and female-only vaccination, respectively, whereas Graham et al. [173] investigate the impact of male HPV vaccination on oropharyngeal cancer incidence. All Markov models result in cost-effective outcome for female-only vaccination, and apart from [289], universal vaccination is deemed to be cost-effective. We summarize specific characteristics of the Markov models in Appendix B.3.

4.4.3 Individual-based models

Two versions of individual-based models are given by network and microsimulation models. In network models, each individual is represented by a node, and interactions between individuals are enabled through links. Network models are especially useful if the sources of infection or the impact of quarantine measures are investigated. In contrast, in microsimulation models, each individual is assigned an own function. Transitions between the states are defined as events, and the probability of event occurrence depends on individual-specific covariates, estimated through the functions assigned.

Microsimulation models are an appropriate methodology if i) disease history of individuals has to be accounted for, or ii) multimorbidities are common [237]. If disease history is not considered, and the inclusion of multimorbidities is not allowed in a microsimulation model, a comparable MM can be seen as a limit of the respective microsimulation model.

In chronic health conditions such as diabetes, the history of blood glucose levels in each individual has an important impact on the risk of developing long-term health effects such as kidney failure. A Markov model on disease progression of diabetes would assume that the risk to move to a state of diabetes related complication was independent of the individual history of blood glucose level; this would result in falsified outcome. In contrast to diabetes, in context of HPV, individual disease history does not necessarily have to be accounted for; HPV-induced cancer can develop both a couple of years after first HPV infection and decades later.

Another aspect is that a microsimulation model enables the occurrence of several health conditions simultaneously, whereas in a Markov model, states are mutually exlusive and exhaustive. In subgroups of the population such as the elderly, multimorbidities are common. These are often not independent; if one condition worsens, this could have an effect on the other con-

dition(s). This mechanism is thus considered appropriately by a microsimulation model. However, as for HPV-induced diseases, a combination of conditions is rather rare and therefore not relevant. Due to these two aspects and the increased effort on implementation, microsimulation models are quite rare in the literature on the cost-effectiveness of HPV vaccination; only six authors [7, 108, 159, 220, 360, 367] present this approach. Out of these, four models [7, 108, 159, 220] are static as a consequence of exclusively incorporating a female model population, two are deterministic [7, 108], four are stochastic [159, 220, 360, 367], and five are linked to dynamic transmission models, resulting in hybrid models [161, 167, 168, 217, 219]. A selection of newly developed models is modified to different country-specific context or to extend the aim of research, resulting in 15 additional publications [55, 59, 70, 119, 122, 125, 160, 163, 166, 214, 221, 236, 243, 316, 359]. Four models [55, 59, 122, 236] investigate the impact of universal vaccination, presenting cost-effective [55, 59] and not cost-effective results [236], whereas 18 models [7, 54, 56, 57, 70, 108, 119, 125, 159, 160, 163, 166, 214, 221, 243, 316, 359, 367] exclusively account for female-only vaccination. All models apart from [108] result in cost-effective female-only vaccination. Further details on the models are described in Appendix B.4.

4.4.4 Hybrid models

In a hybrid approach, the output of dynamic disease transmission models is incorporated into static disease progression models. In the literature, ten hybrid models [37, 161, 167, 168, 185, 215, 217–219, 339] are presented. Two include MMs [185, 339], whereas eight [37, 161, 167, 168, 215, 217–219] estimate disease progression through a microsimulation model [160, 220]. Four models [185, 215, 218, 339] consider universal vaccination, whereas six [37, 161, 167, 168, 217, 219] exclusively account for female-only vaccination. Universal vaccination is not cost-effective (apart from [215]), whereas

female-only vaccination is cost-effective in all settings. Further details are presented in Appendix B.5.

4.5 Results of cost-effectiveness analysis

Apart from [108], all publications reviewed come to the conclusion that female-only vaccination is cost-effective, whereas CEA results of universal vaccination are contradictory. Different methodological approaches do not seem to play an important role with respect to the outcome of health economic evaluations. Dynamic models based on differential equations, microsimulation or hybrid approaches lead to both cost-effective and not cost-effective results of universal vaccination. The results of the MMs (apart from [289]) and the network models are cost-effective.

Differences in results occur mainly due to varying model assumptions. Commonly, results become more cost-effective i) the more diseases in both sexes are included, ii) the lower the vaccine coverage rate, iii) the higher the vaccine efficacy, iv) the longer the duration of vaccine-induced immunity, v) the higher the sexual activity, vi) the more disassortative the sexual mixing, vii) the less frequent the cervical screening, viii) the longer the observation time period, ix) the lower the discount rate, and x) the lower the unit cost of vaccination. In summary, all aspects which increase HPV prevalence in the population increase the necessity of vaccine protection; the more individuals are exposed to the virus and under risk of infection, the more HPV-induced diseases can be prevented by the vaccine. As a consequence, the vaccine can show its full potential, which is prone to result in cost-effective model outcome.

The model assumptions listed above can have a major impact on the outcome of CEAs. These assumptions can also vary considerably between different countries. If a pharmaceutical company would like to introduce HPV vaccination to more than one country, country-specific information has

thus to be considered. The most straightforward and least expensive way is to adapt a model which was already implemented for a specific country to one or more additional countries. This is a common approach in practice. Elbasha et al.'s ODE-based model was for example adapted to a variety of international settings [49, 100–103, 188, 211, 314, 357, 387], incorporating country-specific information.

Usually, the model parameters which differ most between countries are related to costs, including cost of the intervention, diagnostic measures, hospitalisation, treatment of disease and adverse events. In addition, utilities might vary since people from different cultures have different coping mechanisms with disease. Country-specific discount rates usually range between 1.5% to 10% for benefits and 0% to 10% for costs [381] as described in Section 6.5.2. Other crucial parameters are country-specific HPV prevalence and mixing behaviour between susceptible and infected people. Furthermore, the threshold of cost-effectiveness is country-specific and depends on the gross domestic product (GDP) [280]. Differences between countries are often minor if GDP, pricing, public health insurance systems, cultural background and disease prevalence are comparable (such as for Germany and France). However, these can also be considerably high if low-resource settings of developing countries are compared to Europe or the US.

4.5.1 Universal vaccination

Altogether, 34 publications including universal vaccination [26, 39, 49, 55, 59, 63, 67, 82, 85, 107, 122, 131–133, 140, 143, 185, 187, 188, 204, 215, 218, 236, 277, 278, 289, 311, 317, 324, 330, 339, 360, 368, 392] are evaluated. Out of those, eleven [49, 55, 63, 82, 131, 140, 215, 277, 278, 317, 330] report that universal HPV vaccination deems to be cost-effective, whereas eleven [67, 85, 132, 133, 188, 204, 218, 236, 289, 339, 392] conclude that exclusively female-

only vaccination is cost-effective. The remaining twelve publications do not evaluate the cost-effectiveness and report predictions on natural history of HPV.

The majority of methodology applied to evaluate the cost-effectiveness of universal vaccination is based on differential equations; nine publications [49,63,85,131–133,188,204,392] use this methodology. All differential equation models include fixed parameter values, inducing limitations in the interpretability of results. Elbasha et al. [131], Bresse et al. [49], and Brown et al. [63] present cost-effective outcome. A possible explanation for varying results might be that Zechmeister et al. [392] only account for cervical cancer, whereas Bresse et al. [49] and Elbasha et al. [132, 133] additionally account for CIN-stages, genital warts and in [131] for a great variety of HPV-induced diseases. Elbasha et al. can only show that universal vaccination is cost-effective if all HPV-induced diseases are considered [131]; otherwise, female-only dominates universal vaccination [132, 133]. Jit et al. [85, 204] account for genital warts, CIN-stages and non-cervical cancers as well; however, details on the dynamic transmission model are not reported in sufficient detail. Therefore, we are unable to evaluate the reasons for contradictory results to [131]. Accounting for different HPV types does not seem to influence the outcome; Elbasha et al., Bresse et al. and Jit et al. account for HPV 6, 11, 16 and 18, whereas Brown does not distinguish between HPV types. Zechmeister accounts for HPV 16 and 18, but not for HPV 6 and 11.

Only three MMs [82, 289, 330] are presented to investigate the cost-effectiveness of universal vaccination; due to their static nature, standard Markov models are not suitable to account for dynamic interactions between individuals. To reduce this shortcoming, Chesson et al. [82] indirectly account for the effects of herd immunity as described in Appendix B.3. Both Stratton et al. [330] and Chesson et al. [82] result in cost-effective outcome, whereas Pearson et al. [289] conclude that universal vaccination is not cost-

effective. Pearson et al.'s result could be induced by ignoring the effects of herd immunity and assuming a duration of vaccine-induced immunity of only 20 years, in contrast to lifelong immunity in [82, 330].

In contrast to standard Markov models, microsimulation models are often constructed in a dynamic way; van de Velde et al. [58, 360] present a dynamic microsimulation model which is modified in two publications [55, 236] to conduct a CEA on universal vaccination. Laprise et al. [236] compare universal to female-only vaccination strategies, concluding universal vaccination not to be cost-effective. In contrast, Brisson et al. [55] find nonavalent in comparison to quadrivalent universal vaccination cost-saving, and quadrivalent universal vaccination in comparison to screening-only cost-effective. Other versions of individual-based models – three network models [140, 277, 278] – come to the conclusion that universal vaccination is cost-effective.

Five authors [67, 215, 218, 317, 339] present combinations of static and dynamic methodologies, so-called hybrid models; two [215, 317] result in cost-effective outcome. A possible explanation for Taira et al.'s [339] results could be that the authors only account for cervical cancer. Kim et al. [218] and Burger et al. [67] account for a large variety of HPV-induced diseases; however, despite these assumptions, universal vaccination is not deemed to be cost-effective.

4.5.2 Female-only vaccination

The number of publications exclusively accounting for female-only vaccination is considerably higher with 110 [7, 9, 16, 17, 30, 31, 34, 36, 37, 54, 56, 57, 68, 70, 72, 75, 81, 83, 87, 96, 99–103, 108, 109, 111, 113–116, 119, 120, 125, 130, 134, 136, 153, 159–164, 166–169, 172, 180, 183, 201–203, 211, 213, 214, 216, 217, 219–222, 225, 226, 228, 229, 231, 232, 234, 241, 243, 245, 248, 257, 263, 270, 273, 274, 294, 300, 303, 304, 311, 314, 316, 321, 328, 333, 337, 342, 344,

345,348–350,356–359,364,365,367,370,373,382,383,387,388] compared to 34 focussing on universal vaccination.

All but one [108] publications come to the conclusion that female-only vaccination is cost-effective or even cost-saving; as a consequence, we do not face the challenge of inconclusive results as for universal HPV vaccination. Further details are presented in Appendix B.6.

4.6 Conclusion

Altogether, we reviewed 144 publications. To the best of our knowledge, we did not find a methodology in the health economic literature on HPV vaccination which is plainly comparable to our approach of a dynamic Bayesian MM. However, several authors present dynamic models based on stochastic processes [20, 92, 141, 155, 156]; yet, these are implemented in the context of other pathogens and do not include health economic evaluations.

As described in Section 4.4.2, the literature presents five MMs which estimate the effects of herd immunity in an indirect way. Most of these models incorporate exclusively female cohorts, and HPV prevalence is decreased following vaccine introduction by means of adjustment factors. Thus, HPV prevalence is a function of vaccine coverage, vaccine efficacy, and indirect vaccine protection. These approaches of indirect herd immunity adjustment only result in reliable model outcome when combined to extensive calibration approaches on HPV prevalence following vaccination. However, this might not be possible at the current stage of research since long-term data on HPV prevalence after the introduction of female-only vaccination do not exist yet. In context of universal vaccination, data are not available yet since the status quo in most Western countries (apart from Australia, Canada, USA, Israel, Switzerland, Austria) is female-only vaccination [295]. The six countries which recommended universal vaccination did so only recently. As a consequence, indirect adjustment for the effects of herd immunity is not

advisable at present.

In addition to indirect estimation of herd immunity, hybrid approaches are presented; these integrate the prevalence predictions of dynamic ODE-based or difference equation models into static Markov or microsimulation models as described in Section 2.2.3. In contrast to hybrid models, our approach consists of only one model; we do not estimate HPV transmission through an ODE system, and HPV prevalence is estimated dynamically directly by means of the Markov model. Thus, the related effort on implementation and computation is considerably reduced.

Chapter 5

Model specification

5.1 Introduction

In this chapter, we apply the methodology of the dynamic Markov model with Bayesian inference (BMM) described in Section 2.3 to estimate the cost-effectiveness of different HPV vaccination strategies in an Italian setting. We published the methodology and the corresponding findings in the journal *Value in Health* [178].

In contrast to the case study introduced in Chapter 3, the model incorporates a high variety of states, several age cohorts of both sexes and an age-specific structure. Both the case study and the HPV model include an open model structure; however, the difference is that the case study accounts for births of newborns, whereas the HPV model enables the entering of new cohorts of healthy individuals at puberty.

The chapter is structured as follows: The model specification is explained in a detailed way, including i) the reference population, ii) interventions conducted, iii) model parameters on transition probabilities, unit costs and utilities, iv) evidence synthesis to inform a selection of model parameters, v) the age-, sex- and behavioural-specific force of infection, and vi) a selection of transition probabilities in females. The remaining transition probabilities in females, the transition probabilities in males, the sources of prior infor-

mation and the posterior results are presented in Appendices D, E.2 and F, respectively.

5.2 Reference population

The BMM considers a "virtual" population, comprising of both males and females. We use official data on the population composition by age and sex from the Italian Office for National Statistics (`www.istat.it`) and derived from the 2011 census. These are used to define the population size. The model is implemented in discrete time, including yearly Markov cycles.

Initially, 14 cohorts aged twelve-25 years are considered. During the first ten years of observation, every year a new cohort of twelve year old individuals enters the model. This dynamic process results in 24 cohorts of individuals aged twelve-35, in the eleventh year of follow-up. The follow-up period is set to 55 years. At the end of observation, members of the youngest cohort that are still alive reach the age of 57; similarly, the eldest, still alive individuals, reach the age of 80 years.

We use official data from the Italian Office for National Statistics to estimate the number of new twelve year old individuals in the first ten years of follow up. In other words, those who enter the population at time interval $\mathcal{I}_t = 1$ are the individuals who were eleven years old at $\mathcal{I}_t = 0$ and are still alive; similarly, those who enter the population at $\mathcal{I}_t = 2$ are the individuals who were ten at $\mathcal{I}_t = 0$ and are still alive; and so on. Uncertainty is not accounted for in these demographic data; however, the observables included are based on a large sample size and thus provide realistic information.

It is essential to notice that, because of the much more complex structure of the comprehensive HPV model, it is not meaningful to assume a life-time follow up, which would imply extrapolation to population dynamics that could not be supported by empirical evidence and would inevitably rely on untestable assumptions. A life-time follow up is also not required since most

HPV-induced cancers commonly occur at earlier age. At the end of the follow-up period of 55 years, the cohorts are aged between 57 and 80 years. Peak prevalence of cervical cancer (the most frequent HPV-induced cancer) is already reached at age 40, and of head/neck and anal cancer at age 70. In older ages, prevalence does no longer increase and remains constant. Thus, the age ranges considered in the model are sufficient.

The input data for the first year of follow-up, $\mathcal{I}_t = 0$, are taken from the BEST I study[1] [136]. In BEST I, there is only one cohort of twelve year old individuals, healthy in the beginning, who is observed for ninety years. HPV incidence is initialized through data obtained by Myers et al. [263]. In contrast, we initialize the states of the model using the output of the BEST I, run for a follow-up of 14 years and accounting for the numbers of individuals in every state in every year. The results of the first year of simulation for BEST I are then used as input data for the youngest cohort of twelve year old individuals in the BEST II; the results of the second year of follow-up as input data for the cohort of 13 year olds and similarly, until we finish the initialization process with the results of the 14th year for the cohort of 25 year old individuals. No distinction between the interventions has to be made since vaccination does not take place during initialization.

5.3 Interventions

We consider the following intervention strategies:

1) screening in females, no intervention in males (which we term *"screening-only"*);

2) screening and vaccination in twelve year old females, no intervention in males (*"female-only vaccination"*);

[1] **B**ayesian modelling assessing the **E**ffectiveness of a vaccination **S**trategy **T**o prevent HPV-related diseases

3) screening and vaccination in twelve year old females, vaccination in twelve year old males (*"universal vaccination"*).

The health economic evaluation is performed comparing the cost-effectiveness of the two active strategies 2) and 3) against screening-only, as well as universal against female-only vaccination in an Italian context. Italian data are used to inform unit costs and utilities in order to provide results for Italian authorities such as public health insurances, comparable to the NHS in the UK. Details of cervical screening and vaccination strategies are reported in the following two sections.

Cervical screening

In every scenario, we assume that cervical screening is available for females. On the basis of the European Commission Guidelines on Quality Assurance in Cervical Cancer Screening, in Italy women aged between 25 and 64 years are recommended to undergo cervical cancer screening every three years. This is useful for early detection and treatment of pre-cancerous cervical lesions and to prevent the onset of invasive cervical cancer [88]. The level of access to screening is not consistent across the country. Consequently, more than 30% of the eligible female Italian population has never been screened during their lifetime [195]. Due to consistency, we do not include age-specific cervical cancer screening probabilities here; however, we refer to Table F.1 in Appendix F.

When a cervical lesion is diagnosed, a further Pap test (including a colposcopy and a biopsy) is performed twice in the first year [158]. We conservatively assume that screening is performed each year in a three-year period after the treatment of a precancerous cervical lesion.

Vaccination

For scenarios 2) and 3) in which vaccination is present we assume that individuals aged twelve are eligible to receive it. We account for the quadrivalent HPV vaccine, including genotypes 16, 18, 6 and 11. HPV 16 and 18 are high-risk types which can induce cancers, whereas HPV 6 and 11 can lead to benign lesions such as genital warts. We assume lifelong vaccine-induced immunity; therefore, we do not consider a vaccine booster.

Table 5.1 shows graphically the dynamics underlying the process by which the cohorts enter the observation and the availability of vaccination. Every row in the table represents one of the 24 cohorts eventually populating the model. For simplicity, we listed the cohorts in a descending order, i.e. with the oldest individuals in the top rows of the table. The columns of the table represent the years of follow-up, from $\mathcal{I}_t = 0$ (when the observation starts) to $\mathcal{I}_t = 55$, when it finishes. Empty cells indicate the fact that, for a given year of follow-up, a given cohort has not yet entered the observation. For example, cohorts 15-24 are not observed at $\mathcal{I}_t = 0$ (because none of them have reached twelve years of age).

At the time of follow-up coincinding with the year of their twelfth birthday, the cohorts successively enter the population. Depending on the vaccination strategy being tested, the subjects are given the opportunity to be vaccinated against HPV. The vaccine coverage rate of twelve year olds who are vaccinated in interventions 2 and 3 are as follows: for both females and males, we model the probability of actually receiving the vaccine using an informative Beta(7.2,0.8) distribution, resulting in a mean coverage of 90.48% and 95% credible interval of [65.97%;99.92%]. In the literature, vaccine coverage rates usually vary between 60% and 100%. A coverage rate of around 90% is thus considerably high. We based our probabilistic estimation on information given by [63, 82, 215, 339] and expert opinion.

These percentages represent the proportion of individuals who receive at

Table 5.1: Description of the dynamics in the model. Each row represents one of the cohorts sequentially populating the model. The columns represent the time intervals (years) of the virtual follow-up. The entries in the cells represent the age of each cohort at each time interval of follow-up. Cells typeset in italics indicate the moments in time when a vaccination strategy is made available for a given cohort. The label of the cohorts that directly benefit from vaccination are typeset in italics.

	Time interval of follow-up												
Cohort	0	1	2	3	4	5	6	7	8	9	10	**...**	55
1	25	26	27	28	29	30	31	32	33	34	35	...	80
2	24	25	26	27	28	29	30	31	32	33	34		79
3	23	24	25	26	27	28	29	30	31	32	33		78
4	22	23	24	25	26	27	28	29	30	31	32		77
5	21	22	23	24	25	26	27	28	29	30	31		76
6	20	21	22	23	24	25	26	27	28	29	30		75
7	19	20	21	22	23	24	25	26	27	28	29		74
8	18	19	20	21	22	23	24	25	26	27	28		73
9	17	18	19	20	21	22	23	24	25	26	27		72
10	16	17	18	19	20	21	22	23	24	25	26		71
11	15	16	17	18	19	20	21	22	23	24	25		70
12	14	15	16	17	18	19	20	21	22	23	24	...	69
13	13	14	15	16	17	18	19	20	21	22	23		68
14	*12*	13	14	15	16	17	18	19	20	21	22		67
15		*12*	13	14	15	16	17	18	19	20	21		66
16			*12*	13	14	15	16	17	18	19	20		65
17				*12*	13	14	15	16	17	18	19		64
18					*12*	13	14	15	16	17	18		63
19						*12*	13	14	15	16	17		62
20							*12*	13	14	15	16		61
21								*12*	13	14	15		60
22									*12*	13	14		59
23										*12*	13		58
24											*12*	...	57

least one shot. The actual number of fully protected and compliant individuals is thus lower, so that, in addition to the coverage rate, the vaccine compliance is also considered. Individuals who receive three shots of the vaccine are fully compliant. New research results indicate that two shots might already be sufficient for protection [236]; however, we acknowledge that our

model is based on the conservative estimate of three shots being necessary for full protection. According to the Istituto Superiore die Sanita [193], we assume a compliance rate of 93.79% for females and males. Similarly to BEST I, we assume that individuals who are not fully compliant reduce their vaccine efficacy by 50% on average. Vaccine efficacy is defined in a way that infection by HPV is prevented and as a consequence the development of HPV-induced diseases; we do not account for "leaky" vaccines which do not prevent infection with the pathogen yet pathogen related disease development [296, 299].

As described in Section 3.3.2 for the case study, we do not implement a set of models to account for structural uncertainty in practice; however, we consider the implications of structural uncertainty in the HPV model in theory. An important aspect of accounting for structural uncertainty is that all possible interventions and their implications are considered. We acknowledge that we do not compare all HPV vaccines which are currently available and only focus on the quadrivalent vaccine (containing HPV genotypes 6, 11, 16, 18). A comparison of the quadrivalent to the bivalent[2] and nonavalent[3] vaccines is increasingly often conducted in the literature and provides valuable information. However, due to the complexity of our model, we do not include separate states for HPV genotypes. This would be a straightforward approach in order to compare the different vaccines.

For the health economic analysis, the whole population will be considered: this includes cohorts directly benefiting from the vaccination (twelve year old females or twelve year old females and males) as well as cohorts indirectly benefiting from the effects of herd immunity.

[2]containing HPV genotypes 16 and 18
[3]containing HPV genotypes 6, 11, 16, 18, 31, 33, 45, 52, 58 as described in [80]

5.4 Model structure

Altogether, the dynamic BMM includes $S_F = 36$ states in females[4] and $S_M = 22$ in males[5]. Figure 5.1 gives an overview of the HPV-induced diseases in females and males. The model includes separate compartments for the two sexes. Both compartments include the states healthy, exposure, infection, clearance, reinfection, death, and non-sex-specific HPV-induced diseases, whereas sex-specific diseases are exclusively considered in the corresponding female or male compartment.

The female compartment expands on the BEST I structure [136], which accounts for genital warts, cervical intraepithelial neoplasia (CIN) stages I-III and cervical cancer, by additionally including anal, head/neck, vaginal and vulvar cancer as well as their associated pre-cancerous stages[6]. The male module considers the diseases which affect non-sex-specific organs, as well as penile cancer and its precancerous stage[7].

Individuals in each state can die, with an increased probability after cancer diagnosis. In both sexes, survival post cancer diagnosis is modelled through a sequence of three tunnel states; individuals surviving for four years are deemed to be cured.

Nodes drawn in an ellipse shape display a single state, whereas rectangles (so-called *boxes*) are a combination of states related to the respective organ. For example, Figure 5.2 shows the box *Cervical cancer* which includes the states CIN I-III, cervical cancer, and the states of one, two and three years post cervical cancer diagnosis. Further details on the HPV-induced disease boxes are displayed graphically in Appendix C.

[4]These are described in Table D.1 in Appendix D

[5]These are described in Table E.1 in Appendix E.1

[6]The pre-cancerous stages of anal cancer are low-grade squamous intraepithelial lesions (LSIL) and high-grade squamous intraepithelial lesions (HSIL). In head/neck cancer, it is assumed that no pre-cancerous stage can be diagnosed before cancer outbreak. In vaginal cancer, three precancerous stages similar to cervical neoplasms are considered; these are vaginal intraepithelial neoplasms stage I–III (VaIN I–III). As for vulvar cancer, we assume that there is only one pre-cancerous stage (vulvar intraepithelial neoplasm, VIN).

[7]penile intraepithelial neoplasm (PeIN)

Figure 5.1: Overview of the states included in the HPV model. Obviously, diseases of the cervix, vagina and vulva only affect females, whereas penile cancer is a male-specific disease. Ellipses represent a single state, whereas rectangles are a whole system of cancer related states, including precancerous stages, the cancer and the three tunnel states post cancer diagnosis in the respective organ. Arrows between nodes represent possible transitions in either one or both directions. Arrows with origin and end at the same node indicate that it is possible to remain in the respective state. Individuals can move to the state of death from every state. Death is a so-called absorbing state.

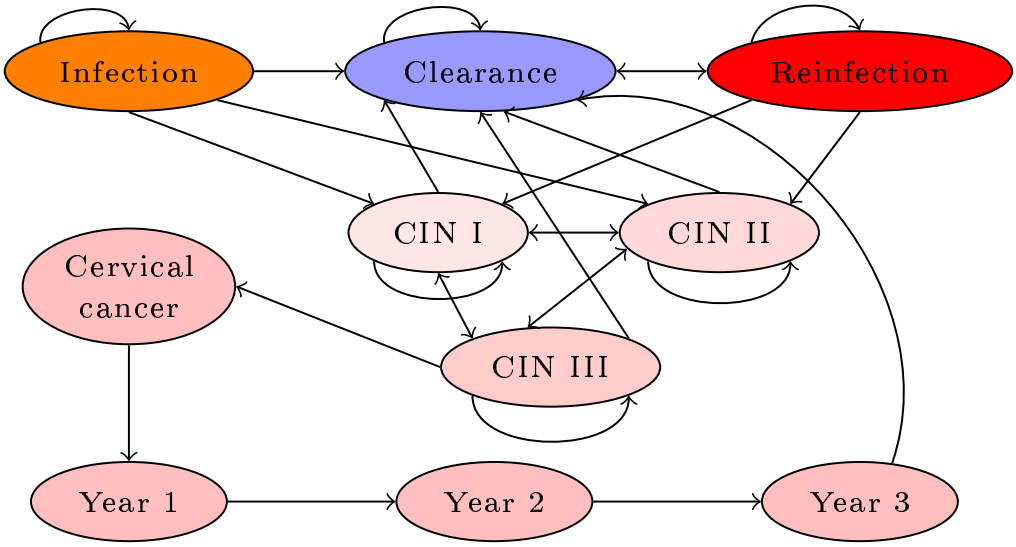

Figure 5.2: The rectangle *Cervical cancer* consists of the precancerous stages CIN I-III, cervical cancer and the three tunnel states post cancer diagnosis. After initial HPV infection, females move in between the CIN-stages and can either clear their infection or progress to cervical cancer. Having survived for four years after cancer diagnosis, we assume females to be cured. After clearance, they can be reinfected and the whole process will start from new, possibly in another organ.

All states are mutually exclusive and exhaustive. The arrows linking the states represent possible transitions from one state to another. Individuals move in between these states according to pre-specified transition probabilities, based on equations described for females in Section 5.8 and Appendix D and for males in Appendix E.2. The overview Tables D.1 and E.1 present detailed information on the states, including the corresponding numbering, which is used in the equations of the transition probabilities.

In terms of structural uncertainty, the most important point is clearly the number of HPV-induced disease states included in the model. For example, Elbasha et al. [131] could show that universal HPV vaccination only becomes cost-effective if HPV-induced diseases of the cervix, vulva, vagina, anus, head/neck as well as recurrent respiratory papillomatosis and anogenital warts are considered. Therefore, if we only included cervical cancer in our model, it was extremely unlikely that universal vaccination would be

deemed to be cost-effective.

We do not include separate states for different HPV genotypes in our model. The overall number of states is already considerably high with altogether 58 states and would double or even quadruple if we accounted for HPV 16 and 18 or HPV 6, 11, 16 and 18, respectively. As a consequence, the computational effort would no longer be manageable. In the literature, the vast majority of models account for HPV 16 and 18 (either separately or pooled), and some also for HPV 6 and 11. Models accounting for a higher number of genotypes are rare exceptions as described in Appendix B.4 for the individual-based model of Brisson et al. [58].

We acknowledge that not modelling HPV genotypes separately is a limitation since there are possible differences in the probability of HPV transmission per partnership, risk of reinfection following HPV clearance and cancer development. Bogaards et al. [38] model transmissibility and waning of natural immunity of 14 HPV genotypes. They find the yearly rate of waning resistance to reinfection to be lowest for HPV 68 (0.014, 95% CI of (0.01,0.039)) and highest for HPV 56 (0.047, 95% CI of (0.03, 0.079)). HPV 66 seems to be highly transmissible (0.94, 95% CI of (0.74, 1)), whereas HPV 68 is transmitted in fewest partnerships (0.43, 95% CI of (0.33, 0.51)). In contrast to Bogaards et al., Burchell et al. [64] report that the differences in per-partnership transmissibility among genotypes are minor as described in Section 5.7.1.

In addition, HPV-induced cancer risk differs between genotypes; around 74–77% of invasive cervical cancer in the Western world is caused by HPV 16 or 18, and mainly HPV 31, 33, 35, 45, 52 and 58 are responsible for the development of the remaining cases [325]. In our model, vaccine efficacy in the cervix is estimated in a way to consider vaccine-specific genotypes (HPV 6, 11, 16, 18) as well as a an effect of cross-protection against the remaining genotypes [136], in accordance with expert opinion. This is described for the parameter $\chi_\star$ in the next section.

5.5 Model parameters

A set of relevant model parameters are used to generate the transition probabilities and run the BMM. The vector of model parameters is

$$\boldsymbol{\theta} = (\alpha, \boldsymbol{\mu}, \boldsymbol{\gamma}, \boldsymbol{\delta}, \zeta, \boldsymbol{\eta}, \beta, \boldsymbol{\omega}, \iota, \boldsymbol{\xi^{(z)}}, \boldsymbol{\upsilon}, \boldsymbol{\rho^{\bigstar}}, \boldsymbol{\sigma}, \boldsymbol{\tau}, \boldsymbol{\phi^{\diamondsuit(z)}}, \chi_{\bigstar}, \boldsymbol{\nu}, \boldsymbol{c}, \boldsymbol{u}, \boldsymbol{\psi^{(z)}}, \boldsymbol{d}, \boldsymbol{w}),$$

which is comparable to the parameter vector of the case study shown in Section 3.3.2. The last three components are observable variables. All parameters are briefly described in the following. The corresponding posterior results (means and 95% credible intervals), distributional assumptions and sources used to inform these parameters are displayed in Appendix F.

The parameters are defined as follows:

- α is the vaccine coverage rate which expresses the proportion of individuals who take up the vaccination programme;
- $\boldsymbol{\mu_j^{(z)}}$ with $z = cerv$ (cervix), $z = an$ (anus), $z = hn$ (head and neck), $z = vag$ (vagina), $z = vulv$ (vulva), $z = pen$ (penis) (representing the location in the respective organ), and $j = 1, 2, 3, 4$ (the cancer stages), are the probabilities of being diagnosed with the respective cancer at a particular stage;
- $\boldsymbol{\gamma} = (\gamma_1, \gamma_2, \gamma_3)$ are the vaccine efficacies against cervical, anal and head/neck associated neoplasiae, respectively, expressed as the reduction in the occurrence of HPV due to vaccination. Vaccine efficacy against initial HPV infection or diseases which affect body areas other than the anus or head and neck are assumed to take the same value as against cervical diseases (γ_1). Individuals who are vaccinated fully experience a rate of occurence of HPV that is $(1 - \gamma_h)$ times that of those who are not vaccinated, with $h = 1, 2, 3$;
- $\boldsymbol{\delta} = (\delta_{0a}, \delta_1, \delta_2, \delta_3, \delta_4, \delta_5, \delta_6)$ are the probabilities for the age-specific regression from infection towards exposure, and the progression towards CIN I, CIN II, anal LSIL, anal HSIL, VaIN I/II, or PeIN, respectively. For

the transition to VIN, we assume the same value as for VaIN I/II (δ_5). The probabilities to develop anal LSIL and anal HSIL are taken from data on homosexual males or HIV positive females and therefore have to be adjusted; see the description of $\boldsymbol{\rho}^{\bigstar}$ and Appendix G.1 for further details on the adjustment parameters $\rho_2^{\bigstar}$ and $\rho_3^{\bigstar}$, respectively;

- ζ is the proportion of subjects at increased risk of reinfection, due to the presence of risk factors;

- $\boldsymbol{\eta} = (\eta_1, \eta_2, \eta_3, \eta_4, \eta_5)$ are the probabilities of being diagnosed with CIN II, CIN III (without screening), anal LSIL, anal HSIL, VaIN I/II or VIN, respectively;

- $\boldsymbol{\beta} = (\beta_1, \beta_2)$ are the HPV transmission probabilities per sexual partnership with average and high-risk sexual behaviour, respectively;

- $\boldsymbol{\omega} = (\omega_{F1}, \omega_{F2}, \omega_{M1}, \omega_{M2})$ are the partner acquisition rates in females and males with average and high-risk sexual behaviour, respectively;

- ι is the decrease in vaccine efficacy due to incomplete compliance; we assume individuals who receive three shots of the vaccine to be fully protected;

- $\boldsymbol{\xi^{(z)}} = \xi_{x,y}^{(z)}$ with $z = cerv$ (cervix), $z = an$ (anus), $z = hn$ (head and neck), $z = vag$ (vagina), $z = vulv$ (vulva) and $z = pen$ (penis), the organ involved, $x = 1, 2, 3$ (representing first, second and third degree intraepithelial neoplasiae), $y = 0, 1, 2, 3, 4$ (representing exposure, different degrees of precancerous stages and cancer) are the probabilities to acquire HPV-induced diseases. These are defined according to the possible paths described in Figures 5.1, 5.2, and C.1 – C.5. The corresponding transition probabilities are explained in Section 5.8 and Appendix D for females and Appendix E.2 for males. In case of diseases related to the cervix, the exponent is two dimensional ($\boldsymbol{z} = (z_1, z_2)$),

with the first dimension z_1 representing the organ (cervix), whereas in the second dimension, $z_2 = 1$ represents *conization* and $z_2 = 2$ *no conization*. Conization is a medical expression for the removal of abnormal cervical tissue as treatment of a CIN stage;

- $\boldsymbol{\upsilon} = (\upsilon_F, \upsilon_M)$ is the recurrence rate of genital warts in females and males, respectively;

- $\boldsymbol{\rho^\bigstar} = (\rho_1^\bigstar, \rho_2^\bigstar, \rho_3^\bigstar)$ are the changes in risk of HPV infection in individuals who present particular risk factors or are at decreased infection risk. The parameter $\rho_1^\bigstar$ represents a risk increase, e.g. induced through smoking or early first sexual intercourse. In contrast, $\rho_3^\bigstar$ is the risk decrease in developing anal LSIL or anal HSIL in heterosexual males and females when compared to homosexual males. Since heterosexual females are at a higher risk of anal cancer than heterosexual males, their risk is first decreased by factor $\rho_3^\bigstar$ and then increased by $\rho_2^\bigstar$ [8];

- $\boldsymbol{\sigma} = (\sigma_1, ..., \sigma_A)$ are the three-yearly screening probabilities, which vary by age;

- $\boldsymbol{\tau} = (\tau_1, \tau_2)$ are the probabilities in CIN I patients of undergoing an immediate or delayed conization;

- $\boldsymbol{\phi^{\diamondsuit(z)}} = \phi_{q,j}^{\diamondsuit(z)}$ are the survival probabilities of HPV-induced cancers, with $z = cerv$ (cervix), $z = an$ (anus), $z = hn$ (head and neck), $z = vag$ (vagina), $z = vulv$ (vulva) and $z = pen$ (penis) representing the body area affected, and $q = 1, ..., 4$ and $j = 1, ..., 4$ representing the years of survival and cancer stage, respectively;

[8] Technically, $\rho_3^\bigstar$ and $\rho_2^\bigstar$ are assumed to be associated with suitable Gamma distributions; for heterosexual males we consider a mean risk reduction $\rho_3^\bigstar$ of 17.1880 (95% CI [0.8714; 53.5615]) in comparison to homosexual males. For females, we assume an increased risk $\rho_2^\bigstar$ of 1.6975 (95% CI [1.5055; 1.9026]) when compared to heterosexual males.

- $\chi_\star$ is the reduction in the occurrence of HPV-related events due to the effect of *cross-protection*. This effect implies a protection against additional genotypes of the infectious agent which are not included in the vaccine. Commonly, the level of cross-protection is considerably lower than the vaccine efficacy. In the model, we account for cross-protection against HPV high-risk types different from HPV 16 and 18 only in context of diseases related to the cervix;

- $\boldsymbol{\nu} = (\nu_1, \nu_2, \nu_3)$ are the probabilities that vaccinated subjects have respectively one, two or three doses, which represent increasing levels of compliance with the vaccination programme;

- $\boldsymbol{c} = (c^{acq}, c^{adm}, c_l^{cin}, c_r^{cerv}, c^{lsil}, c^{hsil}, c_r^{an}, c_r^{hn}, c^{vain}, c_r^{vag}, c^{vin}, c_r^{vulv}, c^{gw}, c^{col}, c^{anbiop}, c^{cyt}, c^{dna}, c^{pap})$ is the vector of relevant one-year unit costs for the acquisition and administration of the vaccine, the management and treatment of HPV-induced cancers and their precancerous stages of grade x, and anogenital warts, the performance of colposcopy, anoscopy and biopsy, anal cytology, HPV DNA testing, and the Pap smear test, respectively;

- $\boldsymbol{u} = (u_v^{gw}, u^{ascus}, u_l^{cin}, u_{r_*}^{cerv}, u^{lsil}, u^{hsil}, u_{r_*,v}^{an}, u_{r_*,v}^{hn}, u_{r_*}^{vag}, u_{r_*}^{vulv}, u^{pen})$ is the vector of utilities defined in terms of qualities of life (QoL) for the states of anogenital warts, precancerous stages and HPV-induced cancers. A further description of utilities and their assessment is given in Section 3.3.4. The utilities for the states in health, exposure, infection, clearance, reinfection, as well as two and three years after diagnosis of cancer are set to 1. The utility for death is set to 0. The indices v, l and r_* represent sex, precancerous stage and cancer stage, respectively, for diseases where sex- and stage-specific utilites are available in the literature. In case we did not find any information, we used expert opinion to inform these parameters;

- $\boldsymbol{\psi^{(z)}} = (\psi_{1v}^{(z)}, ..., \psi_{Av}^{(z)})$ is the vector of age- and sex-specific prevalence of anogenital warts ($z = gw$) and head/neck cancer ($z = hn$), respectively;
- $\boldsymbol{d} = (d_{1v}, ..., d_{Av})$ is the vector of age- and sex-specific mortality rates;
- $\boldsymbol{w} = (w_1, ..., w_A)$ is the vector of age-specific probabilities of sexual activity. We assume every individual to be sexually active after having had the first sexual relationship.

When data for the model parameters are available directly, we impose minimally informative prior distributions and use the data to inform the ensuing posteriors. When data are not available directly, we encode the information obtained by literature review or assumptions based on the elicitation of opinions from clinical specialists in suitable informative prior distributions. All distributional assumptions for the priors and their corresponding sources are described in a number of tables in Appendix F, where additionally, the mean and corresponding 95% credible intervals for all parameters are displayed.

We found a medical publication to inform the age- and sex-specific incidence of anogenital warts ($\psi_{a,v}^{(gw)}$). Marra et al. [252] estimate the incidence rates of genital warts in females and males according to the respective age groups. We estimate head and neck cancer incidence $\psi_{a,v}^{(hn)}$, separately for age groups and sex, according to the data given for oral cancer on the Cancer Research UK website [352]. Since these cancers are not necessarily a consequence of a HPV infection, but can be alcohol- or tobacco-induced, we multiply the given incidence rates by 1.8, the odds ratio for developing head and neck cancer caused by HPV [322]. We will conduct our cost-effectiveness analysis specifically for Italy; therefore, whenever possible, we integrate Italian data into our model to create a most realistic situation. According to expert opinion, data from the UK are comparable to an Italian setting since public health insurance systems in both countries work in a similar way. Finally, we use official data from registry or population databases, such

as the Italian Office for National Statistics (`www.istat.it`), to obtain information on the age- and sex-specific mortality rates $(d_{a,v})$, and probability of sexual activity (w_a). Given that these are all population data, we consider them to be deterministic information, without substantial uncertainties.

5.5.1 Economic parameters

We use cost and utility information that is available from BEST I, which is updated by considering the information given by Baio et al. [23], Mennini et al. [256] and Marcellusi et al. [249]. For the extra parameters, we performed an extensive literature review and found information for the cost of anal [47, 98, 165], vaginal [179] and vulvar [179] pre-cancerous lesions, as well as for anal [340], head and neck [110, 308, 385], vaginal [149], vulvar [149] and penile [315, 362] cancer. Information from more than one source is combined through evidence synthesis as described in Section 5.6.

As for penile intraepithelial lesions, despite our attempt to identify suitable evidence from the relevant literature, we were unable to find data that could be used to inform this parameter. Thus, we consider the treatment cost for PeIN to be equivalent to the first stage of penile cancer. Additionally, according to expert opinion, we assume the cost of penile cancer stage I to be eligible to inform the corresponding cost parameters for penile cancer stages II-IV.

The utility values were found in the literature for anal LSIL and HSIL [210] and four stages of anal [341] and head/neck [110, 137, 308] cancer. Information about utilities for penile and vulvar cancer was found only for the first cancer stage [91]. For vaginal cancer, the information was given for the first and second cancer stage [91]. For the pre-cancerous lesions of rare diseases, no utility values were found. Consequently, we assume that utility values for low-grade VaIN are equal to anal LSIL utilities; similarly, we set the utilities for high-grade VaIN to the same value as those for anal

HSIL. For the pre-cancerous stage of vulvar cancer, the same utility value as for anal LSIL is assumed. Finally, we consider the same utility value as for penile cancer stage I for the pre-cancerous stage of penile cancer. For vaginal and vulvar cancer, we assume the same utility values as for cervical cancer. Part of the Italian utilities are drawn from the HPV Italian Collaborative Study group [249].

In case information from several literature sources and expert opinion is available on specific model parameters, this is combined through evidence synthesis as described in the next section.

5.6 Evidence synthesis

Before the 1960ies, the selection of medical treatments was purely based on experience of clinicians [335]. Nowadays, so-called "evidence-based medicine" becomes increasingly important in medical decision making. Evidence-based medicine relies on scientific evidence on the efficacy and safety of treatments investigated through randomised clinical trials. Outcome of different trials is often combined through evidence synthesis, resulting in a so-called meta-analysis which commonly reports a pooled estimate on a treatment effect. A meta-analysis is usually based on a larger sample size than a single clinical trial, involves thorough investigation of the quality of included studies, and thus contributes scientific evidence at highest level [380]. Frequentist [43, 90] and Bayesian [336, 380] approaches to evidence synthesis are possible.

A meta-analysis can either be conducted through a fixed or a random effects model. A fixed effects model is based on the assumption of one true treatment effect in all studies included, whereas in a random effects model, the treatment effect has a distribution and thus allows for differences between studies. Each study included is assigned a weight, either corresponding to its sample size (with larger studies contributing more information), or

to its inverse variance. However, the inverse variance is approximately proportional to the sample size. In a fixed effects model, the variance corresponds to the within-study variance. In contrast to a fixed effects model, in a random effects model, the variance is calculated as the sum of within-study and between-studies variance. Therefore, in random effects models, studies with smaller sample size are able to contribute more information than in fixed effects models [43].

Meta-analysis can also be conducted through information reweighting, which has to be distinguished from the weighting approaches to account for differences in the impact of studies discussed above. Information reweighting is conducted in a Bayesian context and a convenient approach if additional studies are included in a meta-analysis sequentially, meaning at later stages. The additional information is assigned a distribution, and the initial priors are then updated by this distribution. This process results in reweighting the posterior. The MCMC does not have to be rerun, which saves a considerable amount of time, yet could come at the cost of bias, especially if a large number of studies are included at several later stages [374].

Another technique to combine evidence from several sources is given by meta-regression. Similar to regression analysis, the impact of explanatory covariates on the dependent variable, the treatment effect, is investigated. However, in contrast to regression analysis, no individual-level data but aggregate data obtained through studies are included. Both potential categorical and continuous treatment effect modifiers can be included in a meta-regression model. In addition, so-called subgroup analyses can be conducted for categorical covariates. In a subgroup analysis, separate meta-analyses are conducted for each category of the respective covariate. In the literature, meta-regression models are often presented as an alternative to meta-analysis if a large amount of heterogeneity between the studies could be confirmed, e.g. through the I^2 statistic [90]. However, by the very nature of evidence synthesis, heterogeneity is always present since each

study included differs from the others, and statistics to detect heterogeneity have low power. Therefore, if the number of studies is high enough (more than ten), and covariates which are possible treatment effect modifiers are known, conducting meta-regression is recommended, for example to generate hypotheses for future research [283, 346].

Model parameters can be informed following a similar principle as meta-analysis and meta-regression; several literature sources from a number of clinical trials and observational studies as well as expert opinion can be combined. In a Bayesian framework, this process is commonly implemented through hierarchical models. In a hierarchical model, both within- and between-study heterogeneity is considered [336]. We use similar notation as in [22].

Figure 5.3 shows an example structure of a hierarchical model for evidence synthesis, including J studies, each including data of sample size n_j with outcome y_{hj}; h indicates an individual study participant. The parameters $\theta_1^{\diamondsuit}, \theta_2^{\diamondsuit}, ..., \theta_J^{\diamondsuit}$ are study-specific and thus represent the underlying study heterogeneity. In a hierarchical model, the parameter vector $\boldsymbol{\theta}^{\diamondsuit}$ is defined to have one common probability distribution; the parameters $\theta_1^{\diamondsuit}, \theta_2^{\diamondsuit}, ..., \theta_J^{\diamondsuit}$ are thus exchangeable. The corresponding hyperparameters of this common distribution are indicated as $\phi_{\bigstar}$ [22].

One advantage of this pooling approach is that the conclusions drawn from studies including a small sample size can be improved by other studies from the same area of research with a large sample size [22]. It is even possible to compare treatments in an indirect way as for a so-called "'network meta-analysis". For example, if treatment A and B are compared in a number of studies, and treatment B and C in several other studies, a network meta-analysis would be able to compare treatments A and C even if no study included compared those directly [117]. Several example models of Bayesian network meta-analysis are reported in the *NICE Decision Support Unit Series* [118].

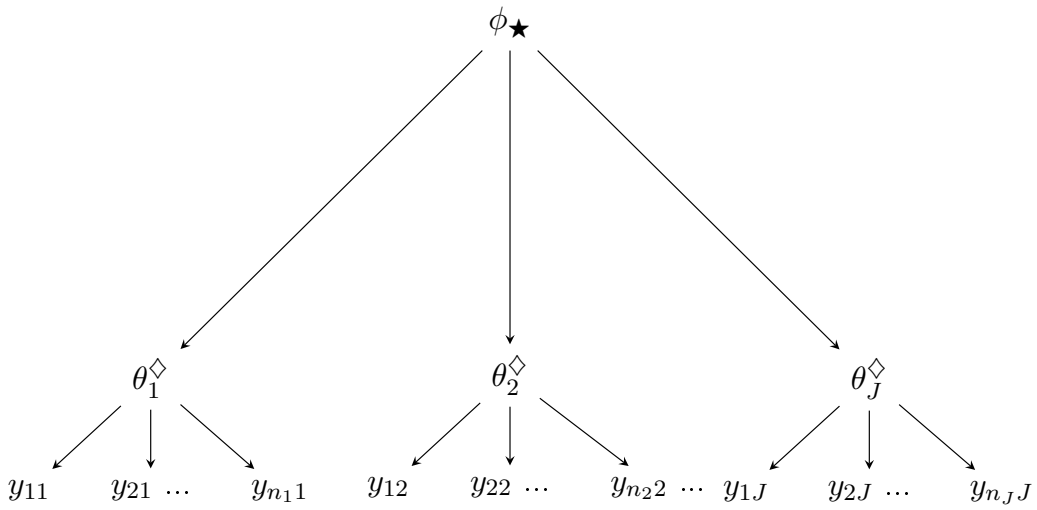

Figure 5.3: Example structure of a hierarchical model for Bayesian evidence synthesis. The data from each study of size n are indicated by y_{hj}, where h defines an individual study participant, and j the number of the study. The study-specific parameters $\theta_j^\diamondsuit$ represent within-study heterogeneity. The hyperparameter $\phi_\bigstar$ enables pooling study-specific estimates through one common distribution.

In the dynamic Bayesian HPV model, several parameters are informed through evidence synthesis; these are probabilities of stage-specific HPV-induced cancer survival, stage-specific probabilities of diagnosis, and several unit costs of diagnosis and treatment. As described above, the evidence synthesis is based on hierarchical models. As an example, we introduce the model for the pooled probability $\phi_\bigstar$ of two-year survival in head/neck cancer stage II as

$$
\begin{aligned}
R_q &\sim Binomial(\pi_q^\circ, N_q) \\
logit(\pi_q^\circ) &= \alpha_q^\bigstar \\
\alpha_q^\bigstar &\sim Normal(\mu_\circ, \tau_\bigstar) \\
\mu_\circ &\sim Normal(0, 0.0000001) \\
\sigma_\bigstar &\sim Uniform(0, 100) \\
\tau_\bigstar &= 1/\sigma_\bigstar^2.
\end{aligned}
$$

The overall number of head/neck cancer patients in stage II is represented by N_q, where the index q indicates the respective study. The number of patients who survive is given by R_q. The data are obtained by [86, 126, 310]; if R_q is not directly stated in above format, it is derived from given sample size, survival probabilities or Kaplan-Meier survival curves. The number of events regarding survival are assumed to follow a Binomial distribution.

The parameter π_q° represents the two-year head/neck cancer survival probability in stage II. To account for study heterogeneity, each π_q° is estimated to be a realisation of a Normal distribution on the logit scale. The minimally informative prior distribution for $\alpha_q^\star$ has $\mu_\circ$ and $\tau_\star$ as hyperparameters for the mean and precision, respectively. The software `JAGS` expects the precision rather than the variance as an input parameter of the Normal distribution; therefore, $\sigma_\star$ is transformed into the precision $\tau_\star$. These priors are updated by the data given by the three studies. The parameter $\mu_\circ$ is then transformed by

$$\phi_\star = \frac{e^{\mu_\circ}}{1 + e^{\mu_\circ}}$$

to result in the pooled probability of head/neck cancer survival $\phi_\star$.

5.7 The force of infection

In this section, we specify the force of infection for the HPV model. In contrast to the general case of any infectious disease described in Section 2.3, the force of infection depends on sex and sexual behaviour. This was previously explained for the case study in Section 3.3.1. Furthermore, in the HPV model, partner acquisition rates are age-specific, which is considered in Section 5.7.5 through the corresponding equation. As a consequence of the inclusion of the force of infection into the state allocation algorithm, the transitions from the state of exposure to the state of infection are dependent

on age-, sex- and behavioural-specific sexual mixing.

To specify the force of infection, first of all we make assumptions on the probability of HPV transmission per partnership. In addition, we report age-, sex- and behavioural-specific sexual mixing matrices as well as partner acquisition rates which are included in the model to simulate the process of partnership formation.

5.7.1 HPV transmission probability per partnership

This is a crucial parameter since there is very limited information and knowledge on HPV transmission in single sex acts and partnerships. In accordance to the notation of the case study, we indicate it as β. We found evidence describing HPV transmission probabilities in heterosexual couples: for example, Burchell et al. [65] estimate the probability of HPV transmission within the first four months of a partnership as 0.42 with a 95% CI of [0.36;0.47]. They consider 36 HPV genotypes (including high-risk, intermediate and low-risk types) and find that probability of transmission does not seem to differ considerably between types [64]. Furthermore, in an earlier publication including 27 HPV genotypes, Burchell et al. [66] report the median probability of transmission per sex act to be around 40% with a range of 5-100%. These findings, however, are far from definitive and suggest the likely possibility of both much lower and higher values, in different scenarios. Another challenge is that the per partnership and per sex act estimation of HPV transmission is not directly comparable. In a stable partnership, a high number of sex acts is conducted, increasing the probability of transmission when compared to a single sex act.

Korostil et al. [229] have modelled this using a Uniform distribution in the interval [0;1], which essentially amounts to allowing *any* value (between 0 and 100%) as equally possible.

Sexual behaviour

We define two different groups of sexual behaviour: individuals with two - ten lifetime partners are considered to be at "average-risk" in terms of their sexual behaviour, whereas those with eleven or more lifetime partners are at "high-risk". We assume that individuals who change their partners more frequently are generally at higher risk of sexually transmitted diseases and therefore to become infected by HPV. This seems quite reasonable, since it is likely that there is a substantial degree of correlation between high partner turn-over rates and other risk factors.

In particular, smoking, a low education level, sexual intercourse before the age of 18 and five or more lifetime partners are observed to increase the risk of acquiring an HPV infection. Marcellusi et al. [249] classify 26.3% of the population in the high-risk group. Based on these data and also accounting for van de Velde et al.'s [360] assumptions of 22% high-risk individuals and evidence based on the *National Survey of Sexual Attitudes and Lifestyles* (Natsal 2000) [206] with 34.6% of men and 19.4% of women under high risk, we assume that 20% of the population could be classified in the high-risk sexual behaviour group.

Finally, we assume the chance of being transmitted the virus to be lower in the average-risk group and modify the information given by Burchell et al. [65,66] for the two different risk groups. We assume the yearly probability of HPV acquisition to be between 17% and 35% for individuals in the average-risk group (β_1), whereas we expect β_2 to be higher and between 30% and 74% for those in the high-risk group. These assumptions are consistent with those reported by Burchell et al. [66], who assume a 40% HPV transmission probability, ranging from 5% to 100%.

The risk factors which contribute to a higher HPV transmission probability also account for a higher probability of reinfection after HPV clear-

ance. Additionally, using oral contraceptives for five or more years[9], multiparity and previous occurrence of sexually transmitted infections, especially *Chlamydia trachomatis* and Herpes simplex type 2, play a role in risk increase [44, 76, 256, 319, 323, 324].

Another source of structural uncertainty is how risk factors are incorporated into the model. We assume that those impact the probability of HPV infection and reinfection; however, another possible assumption would be to consider those in the transition probabilities of moving to infection clearance. People in the high-risk group would then require a longer amount of time to clear their infection, increasing HPV prevalence.

5.7.2 Age-dependent partnership formation probabilities

For each sex, we define the probability of a sexual partnership to vary with the age of the partner. We incorporate whole distributions of values into the model and report the mean age-, sex- and behavioural-specific probabilities in Tables 5.2–5.5.

Table 5.2: Sexual partnership probability matrix for females in the average-risk group. The entries in the table identify the mean probability that a female in the age group presented in the rows of the table chooses a male sexual partner in the age group along the columns within one Markov cycle of length one year.

Age	12-14	15-19	20-24	25-29	30-34	35-39	40-44	45-49	50-54	55-59	60-64	65-80
12-19	1	26	58	15	1	0	0	0	0	0	0	0
20-24	0	0	36	49	12	2	0	0	0	0	0	0
25-29	0	0	14	47	28	9	2	0	0	0	0	0
30-34	0	0	1	16	38	30	12	3	1	0	0	0
35-39	0	0	0	0	8	36	34	16	5	1	0	0
40-44	0	0	0	0	0	18	44	23	9	3	1	0
45-49	0	0	0	0	0	0	24	55	17	3	0	0
50-54	0	0	0	0	0	0	0	24	55	17	3	1
55-59	0	0	0	0	0	0	0	0	14	43	26	17
60-64	0	0	0	0	0	0	0	0	0	14	43	43
65-80	0	0	0	0	0	0	0	0	0	0	14	86

[9] Long-term use of oral contraceptives increases the probability of HPV persistence in the cervix [251]; in addition, females who use these are less likely to have safer sex including barrier methods such as condoms. Condoms considerably reduce the risk of HPV transmission [174].

Table 5.3: Sexual partnership probability matrix for males in the average-risk group. The entries in the table identify the mean probabilities that a male in the age group presented in the rows of the table chooses a female sexual partner in the age group along the columns within one Markov cycle of length one year

Age	12-14	15-19	20-24	25-29	30-34	35-39	40-44	45-49	50-54	55-59	60-64	65-80
12-19	58	26	15	1	1	0	0	0	0	0	0	0
20-24	0	49	36	12	2	0	0	0	0	0	0	0
25-29	0	14	47	28	9	2	0	0	0	0	0	0
30-34	0	1	16	38	30	12	3	1	0	0	0	0
35-39	0	0	0	8	36	34	16	5	1	0	0	0
40-44	0	0	0	0	18	44	23	9	3	1	0	0
45-49	0	0	0	0	0	24	55	17	3	0	0	0
50-54	0	0	0	0	0	24	55	17	3	1	0	0
55-59	0	0	0	0	0	0	14	43	26	17	0	0
60-64	0	0	0	0	0	0	0	0	0	57	38	5
65-80	0	0	0	0	0	0	0	0	0	38	57	5

As a general rule, we assume that males tend to have sexual partners who are in the same age group or younger, while females tend to have sex with partners who are in the same age group or older. However, notice that we still allow for the possibility of different behaviours (e.g. a male choosing an older female partner): these circumstances *may* happen, but with a lower chance. Also, notice that we only consider a heterosexual population.

Tables 5.2 – 5.5 are based on the data presented by van de Velde et al. [360] which were collected through PISCES (*Psychological Impact of cervical Screening and Condylomas: an Epidemiological Study*), a Canadian prospective multicentre clinical study [123, 124]. The tables show the assumptions for the partnership probabilities for females and males, for both the average- and high-risk groups. The data are self-reported, therefore, it is essential to account for parameter uncertainty by assigning suitable probability distributions to these values. Thus, the entries in the tables identify the mean probability that a random individual of a given sex v and age a (presented in the rows of the tables) mixes with a random individual of the opposite sex v' (i.e. if v indicates "female", v' indicates "male" and vice versa) and of age a' (along the columns of the tables).

As an example, consider a 20 year old female; given the estimations

Table 5.4: Sexual partnership probability matrix for females in the high-risk group. The entries in the table identify the mean probabilities that a female in the age group presented in the rows of the table chooses a male sexual partner in the age group along the columns within one Markov cycle of length one year

Age	12-14	15-19	20-24	25-29	30-34	35-39	40-44	45-49	50-54	55-59	60-64	65-80
12-19	0	37	50	11	2	0	0	0	0	0	0	0
20-24	0	0	37	50	11	2	0	0	0	0	0	0
25-29	0	0	14	47	28	9	2	0	0	0	0	0
30-34	0	0	0	28	45	18	6	2	1	0	0	0
35-39	0	0	0	0	20	39	22	11	5	2	1	1
40-44	0	0	0	0	0	20	39	22	11	5	2	2
45-49	0	0	0	0	0	0	20	39	22	11	5	4
50-54	0	0	0	0	0	0	0	20	39	22	11	9
55-59	0	0	0	0	0	0	0	0	20	39	22	19
60-64	0	0	0	0	0	0	0	0	0	20	39	41
65-80	0	0	0	0	0	0	0	0	0	0	20	80

Table 5.5: Sexual partnership probability matrix for males in the high-risk group. The entries in the table identify the mean probabilities that a male in the age group presented in the rows of the table chooses a female sexual partner in the age group along the columns within one Markov cycle of length one year

Age	12-14	15-19	20-24	25-29	30-34	35-39	40-44	45-49	50-54	55-59	60-64	65-80
12-19	50	37	11	2	0	0	0	0	0	0	0	0
20-24	0	50	37	11	2	0	0	0	0	0	0	0
25-29	0	14	47	28	9	2	0	0	0	0	0	0
30-34	0	0	28	45	18	6	2	1	0	0	0	0
35-39	0	0	0	20	39	22	11	5	2	1	1	0
40-44	0	0	0	0	20	39	22	11	5	2	2	0
45-49	0	0	0	0	0	20	39	22	11	5	4	0
50-54	0	0	0	0	0	20	39	22	11	9	0	0
55-59	0	0	0	0	0	0	20	39	22	19	0	0
60-64	0	0	0	0	0	0	0	0	41	20	34	5
65-80	0	0	0	0	0	0	0	0	10	80	5	5

produced in Table 5.2, we assume that she has on average a 36% chance of selecting a sexual partner who is a 20-24 year old male; on average a 49% chance of selecting a sexual partner who is a 25-29 year old male; on average a 12% chance of selecting a sexual partner who is a 30-34 year old male; and on average only a 2% chance of selecting a sexual partner who is a 35-39 year old male. Any other age group for potential sexual partners is ruled out under the assumptions of Table 5.2 and therefore irrelevant.

The results of the health economic evaluation are highly sensitive to the choice of these matrices; therefore, sensitivity analysis is performed to this

aspect. Model calibration as described in Section 6.3 ensures that the resulting age-dependent HPV prevalence estimates are realistic.

5.7.3 Partner acquisition rates

Van de Velde et al. [360] also present summary statistics on the rate of partner acquisition for four different levels ($\ell \in 0, 1, 2, 3$) of sexual activity: individuals who have zero - one life-time partners are defined in the $\ell = 0$ group; individuals with two - ten life-time partners are grouped in level $\ell = 1$ (notice that the combination of these two groups is what we define as the average-risk group); individuals with eleven - 39 life-time partners are grouped in level $\ell = 2$. Finally, individuals with 40 or more life-time partners are grouped in level $\ell = 3$. By combining $\ell = 2$ and $\ell = 3$, we define our high-risk group. We combine the information presented in van de Velde et al. [360] and use the matrices to model the mixing process for the individuals in our average- and high-risk groups.

Tables 5.6 and 5.7 show the annual minimum, mean and maximum partner acquisition rates for both sexes in the groups of average and high-risk sexual behaviour. The partner acquisition rates are displayed for nine different age groups, ranging from the age of twelve to the age of 60. We assign

Table 5.6: Annual minimum, mean and maximum partner acquisition rates for females and males in nine different age groups for the average-risk group, defined as two - ten life-time partners

	Females			Males		
Age	**Minimum**	**Mean**	**Maximum**	**Minimum**	**Mean**	**Maximum**
12-19	0.74	1.26	1.78	0.90	1.92	2.94
20-24	0.54	0.96	1.38	0.68	1.38	2.09
25-29	0.40	0.73	1.07	0.48	1.05	1.63
30-34	0.30	0.56	0.83	0.35	0.85	1.35
35-39	0.23	0.43	0.64	0.27	0.69	1.11
40-44	0.18	0.34	0.50	0.21	0.51	0.81
45-49	0.14	0.26	0.39	0.10	0.27	0.45
50-59	0.11	0.20	0.30	0.08	0.21	0.35
60	0.05	0.10	0.15	0.04	0.11	0.18

Table 5.7: Annual minimum, mean and maximum partner acquisition rates for females and males in nine different age groups for the high-risk group, defined as eleven or more life-time partners

	Females			Males		
Age	**Minimum**	**Mean**	**Maximum**	**Minimum**	**Mean**	**Maximum**
12-19	4.29	6.515	8.74	5.21	9.810	14.41
20-24	4.90	6.330	7.76	6.24	8.995	11.75
25-29	2.92	3.825	4.73	3.50	5.365	7.23
30-34	1.46	2.050	2.64	1.70	3.000	4.30
35-39	0.67	1.040	1.41	0.79	1.610	2.43
40-44	0.29	0.510	0.73	0.35	0.775	1.20
45-49	0.12	0.250	0.38	0.09	0.265	0.44
50-59	0.05	0.120	0.19	0.04	0.130	0.22
60-69	0.03	0.065	0.10	0.02	0.065	0.11
70-80	0.01	0.030	0.05	0.01	0.035	0.06

suitable probability distributions and incorporate probabilistic partner acquisition rates into our model. As an example, we can expect a female in the average-risk group aged 20-24 to have on average 0.96 sexual partners per year, with minimum and maximum values of 0.54 and 1.38, respectively.

As described for the case study in Section 3.3.3, on average, males tend to have a higher number of partners than females; the distributions on partner acquisition rates are thus different in the two sexes, also accounting for the fact that a small number of females have an extremely high number of male partners (e.g. prostitutes).

A correct estimation of both partner acquisition rates and the probability of HPV transmission per partnership play an extremely important role in the dynamic HPV model. Intuitively, the higher the number of partners, the higher the benefits of HPV vaccination. With low partner acquisition rates, the population is under lower risk of acquiring an HPV infection. If the HPV prevalence in the population is large, the vaccine obviously can prevent more diseases. Vaccination is still expensive because of the acquisition cost, but due to its preventive effect on many diseases, its benefits compensate for the amount of money spent.

On the other hand, if we assume that couples stay together for a long

time and remain faithful, HPV prevalence decreases and there are fewer disease cases in the population. Therefore, the vaccine cannot show its full benefits; however, it is still necessary due to other ways of disease transmission, even in faithful couples and individuals with low sexual activity. HPV can be transmitted by fomites such as public saunas or shared towels and it can remain in reservoirs within the female and male body after infection for a lifetime without causing any symptoms. Even a digital transmission is possible [242].

5.7.4 Sexual mixing matrices

We can now combine the values considered in Section 5.7.2 and Section 5.7.3 into the sexual mixing matrices, which are needed to fully describe the interaction between the two sexes. These represent the per capita annual rates at which an individual of sex v from sexual behaviour group b and of age a acquires a sexual partner of the opposite sex v' from sexual behaviour group b' and of age a'.

Following Korostil [229], we define suitable sexual mixing matrices whose elements $m_{v,b,b',a,a'}$ are given by the product of the age-dependent partnership formation probabilities and partner acquisition rates. Back to the previous example of a 20 year old female in the average-risk group (i.e. if we set $v =$ ***Female***, $b = 1$ and age group $a = 20$), we can obtain the mean values of $m_{F,1,b',20,a'}$ for all the possible age groups a' of the male partner with the following calculation:

- $m_{F,1,b',20,a'} = 36\% \times 1.38 = 0.4968$, for $a' =$ 20-24;
- $m_{F,1,b',20,a'} = 49\% \times 1.38 = 0.6762$, for $a' =$ 25-29;
- $m_{F,1,b',20,a'} = 12\% \times 1.38 = 0.1656$, for $a' =$ 30-34;
- $m_{F,1,b',20,a'} = 2\% \times 1.38 = 0.0276$, for $a' =$ 35-39;

- $m_{F,1,b',20,a'} = 0$, for any other age group a'.

Notice the differences between the sexual mixing matrix m of the HPV model and the partner acquisition rate ω in the general case described in Section 2.3; in contrast to ω, m is age-, sex-, and behavioural-specific. As for ω, the partner acquisition rates of the case study, $\omega_{v,b}$, are not age-specific either, yet depend on sex and behaviour as explained in Section 3.3.1.

5.7.5 The equation of the force of infection

Finally, we use the HPV transmission probabilities of Section 5.7.1 and the sexual mixing matrices of Section 5.7.4 to determine the force of infection, which now depends on age, sex and sexual behaviour. As described in Section 2.3, we first define the *rate* of infection $\rho^{\diamondsuit}_{v,b,a}(\mathcal{I}_t)$. This quantity measures the time-dependent overall force of HPV infection for a random member of the population of sex v, sexual behaviour b and age a and is defined as:

$$\rho^{\diamondsuit}_{v,b,a}(\mathcal{I}_t) = \beta_b \sum_{b',a'} m_{v,b,b',a,a'} \psi_{v',b',a'}(\mathcal{I}_t), \tag{5.1}$$

where, in summary:

- β_b represents the HPV transmission probability per sexual partnership, depending on sexual behaviour b and described in Section 5.7.1;

- $m_{v,b,b',a,a'}$ represents the sex-, behavioural- and age-specific sexual mixing matrix, containing yearly partner acquisition rates as described in Section 5.7.4;

- $\psi_{v',b',a'}(\mathcal{I}_t) = \left(\frac{I_{v',b',a'}(\mathcal{I}_t)}{N_{v',b',a'}(\mathcal{I}_t)}\right)$ represents the HPV prevalence in the sexual partner of sex v', sexual behaviour b' and age a' at time interval $\mathcal{I}_t$; $I_{v',b',a'}(\mathcal{I}_t)$ and $N_{v',b',a'}(\mathcal{I}_t)$ indicate the number of infected individuals and the overall population size, respectively.

In practice, Equation 5.1 implies that at each time interval of the follow up, the probability of HPV infection depends on the pool of potential partners of the opposite sex who are:

- available for mating; this depends on the age and sex of the individual being considered, as well as on their sexual behaviour;
- currently infected by HPV. As vaccination is likely to reduce the number of individuals who originally become infected, the probability of HPV infection will become smaller and will be affected by the impact of vaccination, thus mimicking the mechanism underlying herd immunity.

We can use the argument presented in Section 2.3 to obtain the corresponding *probabilities* of infection $\pi^{\bigstar}_{v,b,a}(\mathcal{I}_t)$, which represent the sex-, behavioural- and age-dependent transition probabilities to the state of HPV infection. These can be obtained by transforming the rates $\rho^{\diamondsuit}_{v,b,a}(\mathcal{I}_t)$ into probabilities, using Equation 2.4.

We assume that individuals in the states *infection*, *CIN I-III*, *LSIL/HSIL*, *VaIN I-II*, *VIN*, *PeIN*, *head/neck cancer* and *reinfection* contribute to virus spreading. Individuals in all cancer states except from head/neck cancer and those in the recovery phase of one year post cancer as well as individuals with the visible condition of genital warts are excluded from the pool of infectious subjects.

5.8 Transition probabilities in females

The transition probabilities of moving across the states are constructed using a set of clinical data, demographic statistics, expert opinion and time-dependent characteristics of HPV infection and induced diseases. They are indicated by $\pi^{F}_{i,a,r,s}$ in females and $\pi^{M}_{i,a,r,s}$ in males, where

- i indexes the intervention (see Section 5.3);

- a indexes the population member's age according to the corresponding age cohort (see Table 5.1 in Section 5.3);
- r indexes the original state;
- s indexes the target state.

In sex-specific model parameters, v indexes the individual's sex, where $v = F$ represents females and $v = M$ males. The female model compartment includes 36 states. To show the general principle of estimating transition probabilities, those for females in the states *Healthy* ($r = 1$) and *Exposure* ($r = 2$) are described in a detailed way in this section. In addition, the transition probabilities corresponding to the remaining 34 states are described in Appendix D. Table D.1 in Appendix D presents an overview to enable the reader an easy allocation of each of the 36 states to the corresponding number. The numbering of the relevant states r and s in the transition probabilities described in this section is 1=*Healthy*, 2=*Exposure*, 3=*Infection* and 9=*Dead*.

In contrast to the female model compartment, the male compartment only includes 22 states. Accordingly, the numbering is different when compared to females. A list of the states in males with the corresponding numbering as well as all male transition probabilites are displayed in Appendices E.1 and E.2.

Due to the constraint of probabilities, the sum of transition probabilities of moving from one original state to all target states has to be 1. However, due to competing risks (e.g. a high probability of dying in older ages in combination with a high probability of developing a certain HPV-induced cancer), in rare cases, this sum can be higher than 1. To ensure that the constraint of probabilities is never validated, we re-proportion the transition probabilities (we divide these by the sum of transition probabilities corresponding to the same original state).

From the state *Healthy*

Once people enter the population, they are assumed to be in the state of perfect health ($r = 1$). Within every Markov cycle, they can either have sex and move to the state of exposure ($s = 2$), with the corresponding age-dependent probability w_a, die ($s = 9$) with age- and sex-specific probability $d_{a,F}$, or remain in the state of perfect health ($s = 1$). Transitions to other states are impossible. To ensure all transition probabilities sum up to one, remaining in health is calculated as a function of the other two transitions possible. These assumptions are represented by

$$\begin{aligned}
\pi^{F}_{i,a,1,s} &= 0 \,\forall\, s \notin \{1, 2, 9\} \\
\pi^{F}_{i,a,1,2} &= w_a \\
\pi^{F}_{i,a,1,9} &= d_{a,F} \\
\pi^{F}_{i,a,1,1} &= 1 - \sum_{s \neq 1} \pi^{F}_{i,a,1,s}.
\end{aligned}$$

From the state *Exposure*

A dynamic process of sexual mixing is accounted for, represented by the force of infection $\pi^{\bigstar}_{F,b,a}(\mathcal{I}_t)$, which is described in detail in Section 5.7.5. This parameter depends on sex, sexual behaviour, age and time interval of follow-up.

The corresponding transition probability of moving from the state exposure to the state infection varies for the interventions evaluated, since we assume a protective effect of the vaccine, resulting in a lower infection probability.

For intervention $i = 1$

According to the scheme described above, individuals who were exposed to HPV can only remain in this condition ($s = 2$), progress to infection ($s = 3$), or

die ($s = 9$). Consequently, we set all transition probabilities for $s \neq 2, 3, 9$ to zero. Remaining in the state of exposure is represented by the sum-to-one constraint. In intervention $i = 1$, no vaccine is applied, therefore, there is no reduction in the probability of infection $\pi^{\bigstar}_{F,b,a}(\mathcal{I}_t)$. The transition probabilities are given as

$$\begin{aligned}
\pi^{F}_{1,a,2,s} &= 0 \,\forall\, s \notin \{2, 3, 9\} \\
\pi^{F}_{1,a,2,3} &= \pi^{\bigstar}_{F,b,a}(\mathcal{I}_t) \text{ (see Section 5.7.5)} \\
\pi^{F}_{1,a,2,9} &= d_{a,F} \\
\pi^{F}_{1,a,2,2} &= 1 - \sum_{s \neq 2} \pi^{F}_{1,a,2,s}.
\end{aligned}$$

For intervention $i = 2$ and $i = 3$

Individuals who take up the vaccination scheme (in a proportion α) experience a reduction in the chance of moving towards the state of infection (expressed by $\pi^{\bigstar}_{F,b,a}(\mathcal{I}_t)$). In contrast, the transition probability of moving to the state of death ($s = 9$) is independent of the intervention i.

The value of this reduction depends on the level of compliance with vaccination: the proportion ν_3 of patients who complete the vaccination programme by receiving the required three doses benefit from a full reduction, which is expressed by $(1 - \gamma_1)$. Conversely, individuals who take up vaccination but receive only one or two doses instead of the three doses necessary to complete the vaccination programme have a lower level of reduction, which we model using the parameter ζ. However, we acknowledge that latest research indicates that two doses of the vaccine are sufficient for protection [236].

Subjects without complete coverage miss out partially on the benefits of vaccination and thus have an intermediate risk. We assume that vaccinees who receive fewer than three doses experience approximately 50–60% of

the full expected efficacy of the quadrivalent vaccine (on the basis of the combined effect observed in an unrestricted susceptible population and an intention-to-treat population[10]). The reduction in efficacy refers to the direct protection against HPV infection. This has to be distinguished from "leaky" vaccines, which do not prevent infection with the pathogen, yet pathogen-induced disease development [296, 299].

Those people who do not take up the vaccination programme (in a population proportion of $1-\alpha$) have the same chance of being infected by HPV as in the scenario $i = 1$, where vaccination is not available. Equation 5.2 displays the indices $i = 2$; however, these are equivalent to indices of $i = 3$ and can therefore be used interchangeably.

Individuals can only move to the states $s = 2, 3, 9$, whereas all other transition probabilities are set to zero. Finally, applying the usual constraint, we define the probability to remain in the state $s = 2$, and present the transition probabilities as

$$
\begin{aligned}
&\pi^{F}_{2,a,2,s} = 0 \,\forall\, s \notin \{2,3,9\} \\
&\pi^{F}_{2,a,2,3} = \alpha[\nu_3(1-\gamma_1)\pi^{\bigstar}_{F,b,a}(\mathcal{I}_t) + (1-\nu_3)(1-\zeta\gamma_1)\pi^{\bigstar}_{F,b,a}(\mathcal{I}_t)] + (1-\alpha)\pi^{\bigstar}_{F,b,a}(\mathcal{I}_t) \\
&\pi^{F}_{2,a,2,9} = d_{a,F} \\
&\pi^{F}_{2,a,2,2} = 1 - \sum_{s\neq 2} \pi^{F}_{2,a,2,s}.
\end{aligned}
\tag{5.2}
$$

As mentioned above, the transition probabilities of moving to the remaining states are described in Appendix D.

[10] Estimated on the basis of the combined effect observed in an unrestricted susceptible population and an ITT (intention-to-treat) population. The unrestricted susceptible population is a population of young women who are initiating sexual debut; it includes all women who were seronegative and PCR-negative to HPV-16, HPV-18 or both, including those who received incomplete vaccination regimens, were exposed to HPV 16/18 before receiving three doses, or had major protocol violations. The ITT population is a population that includes all women, regardless of HPV DNA findings, serostatus, or the presence of CIN at the time of vaccination [19].

5.9 Summary

In this chapter, the dynamic BMM introduced in Section 2.3 was specified for the cost-effectiveness analysis of HPV vaccination. Model assumptions such as interventions conducted, the model structure, the process of sexual mixing and the calculation of the force of infection as well as a selection of transition probabilities in females were described in detail.

The next chapter will show the corresponding results, including diagnostic checks on convergence and autocorrelation, the model calibration to data, the natural history of HPV and induced diseases and the health economic evaluation.

Chapter 6

Results

6.1 Introduction

In this chapter, the results of the health economic evaluation on universal vaccination in comparison to screening-only and female-only vaccination are presented. Furthermore, the model output on the natural history of HPV, so-called Markov traces, is evaluated in the intervention screening-only.

To obtain the results, several steps are conducted. The Markov Chain Monte Carlo (MCMC) simulations are run to estimate the posterior distributions of all model parameters, followed by diagnostic checks on convergence and autocorrelation as described in Section 3.2. The transition probabilities are computed according to the equations specified in Section 5.8 and Appendices D and E.2; these are functions of the model parameters and as a consequence random variables. The state allocation algorithm is run, including the force of infection as described in Section 5.7.5, and all people in all age cohorts are assigned to their target states over the full observation time horizon. The Markov traces are calibrated to data obtained from cancer registries and the literature. Since time series data on the number of people in HPV-induced health states are not available, we use a visual calibration approach as described in Section 3.5.1. Following calibration, several transition probabilities are adjusted.

To conduct the health economic evaluation, first of all, overall costs and utilities are calculated. As a next step, a cost-effectiveness analysis through the Incremental Cost-Effectiveness Ratio (ICER) is performed. In addition, probabilistic sensitivity analysis is conducted through the cost-effectiveness plane, cost-effectiveness acceptability curve (CEAC), expected value of perfect information (EVPI) and the expected value of perfect partial information (EVPPI) as described in Section 3.3.4.

6.2 MCMC simulation and diagnostics

As for the BMM of the case study described in Section 3.3.2, we use the software `JAGS`, which is integrated into `R` by means of the package `R2jags`. We run two parallel chains, for which we set different starting points. To reduce the amount of autocorrelation, thinning is required. We run a very high number of simulations and just use every 360th simulation. Since results of successive iterations are not considered, the issue of autocorrelation is avoided, while at the same time the overall number of simulations is still sufficiently high. Further details on autocorrelation are described in Section 3.2.3.

We define altogether $n_{iter} = 200,000$ simulations and assume a burn-in of $n_{burn} = 20,000$, with a thinning $n_{thin} = 360$. Altogether, this finally results in a number of $n_{sims} = 1,000$ simulations, which are calculated as

$$n_{sims} = n_{chains}\frac{(n_{iter} - n_{burn})}{n_{thin}} = 2\frac{(200,000 - 20,000)}{360} = 1,000.$$

We assume 1,000 simulations to be sufficient for our analysis; essential diagnostics of MCMC sampling as described in Sections 3.2.2 and 3.2.3 confirm good convergence and no issues with autocorrelation under these assumptions. If we run the model without thinning, the effective sample size shows that the amount of autocorrelation is then higher; therefore, this

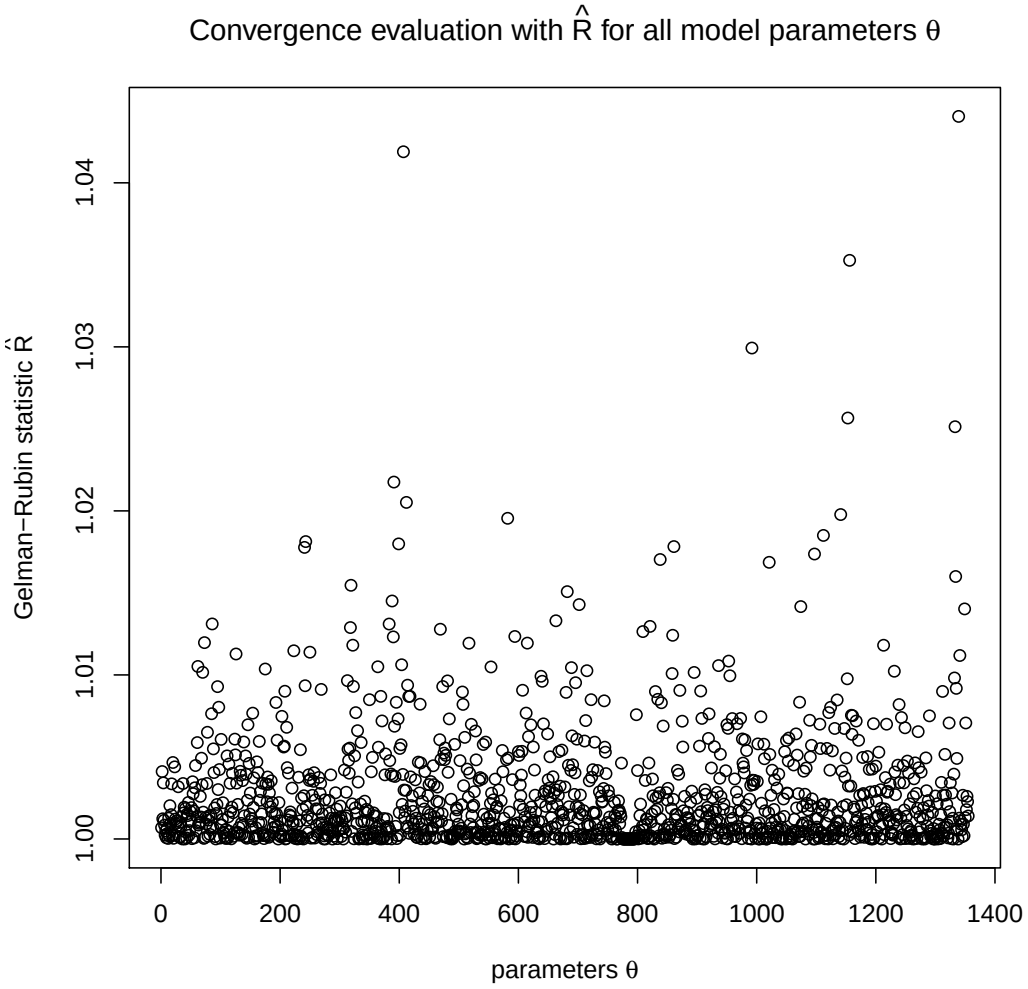

Figure 6.1: The convergence statistics $\hat{R}$ for the model parameters θ are shown graphically to give an overview of their values. No parameters show convergence problems, and $\hat{R}$ is always below 1.1.

approach is not recommended.

Figure 6.1 shows the Gelman-Rubin statistic $\hat{R}$ for all parameters included in the model. Convergence is sufficiently reached for all model parameters, resulting in values of $\hat{R}$ ranging from 1.0 to 1.045. Therefore, we can conclude that 1,000 simulations are sufficient to enable all model parameters to converge. In addition, convergence diagnostics are conducted through trace plots which confirm good convergence of all model parameters in accordance to $\hat{R}$.

6.3 Model calibration

Calibration of the model output to data is essential in order to prevent a falsified estimation of the natural history of HPV infection and imprecise results of the corresponding health economic evaluation. Data for calibration are commonly obtained from large databases such as cancer registries, or from the literature. Several calibration approaches are described in Section 3.5. Due to the complexity of the HPV model and the availability of age-specific prevalence and incidence data rather than time series data, we conduct a visual calibration approach as shown for the case study in Section 3.5.1. In the following, we describe the data used for calibration, the visual calibration approach and the results on HPV prevalence as well as cervix-related diseases in detail. The calibration results on genital warts, precancerous stages and cancers in the other body regions are reported in Appendix G.

6.3.1 Data on prevalence and incidence

We visually calibrate the model through data on prevalence and incidence of HPV infection and HPV-induced diseases. By definition, the term “prevalence” describes the number of individuals out of a specific population, e.g. a country, which are affected by a certain health condition at a specific time point (point prevalence) or a specific time interval (interval prevalence). Prevalence is also often reported as a proportion of the population at risk of disease acquisition.

In contrast, the term “incidence” describes the rate of individuals who have newly acquired a specific health condition in a predefined time interval. It is usually reported as a proportion of the population at risk, e.g. per 100,000 of the population. Incidence is often calculated for specific covariates such as sex and age. If a disease is not curable and not deadly, incidence contributes to constantly increasing prevalence; prevalence is then only reduced by cases of deaths.

We acknowledge that the data on prevalence and incidence used for calibration are only taken from one selected source per state; therefore, uncertainty in these data is not considered. However, for the calibration of HPV-induced cancer states, these are high quality data from cancer registries with large sample size. In contrast, precancerous stages are calibrated to data obtained from clinical trials with smaller sample size since there are no registries for precancerous lesions.

In the model, people affected by genital warts and precancerous intraepithelial neoplasiae can remain in the corresponding states over a considerable amount of time, and disease history is not accounted for. Therefore, prevalence data are suitable to calibrate these states. In contrast, the model outcome on HPV-induced cancers is calibrated to yearly incidence rates. Our model structure is defined in a way that individuals remain in the cancer states for one year as described in Section 5.4; this corresponds to the definition of yearly cancer incidence. Afterwards, individuals either die or move to the first post-cancer tunnel state; however, the three tunnel states following cancer diagnosis are not considered in the model calibration due to non-existing data.

We conduct an extensive literature review in order to find most suitable age- and sex-specific data on prevalence and incidence. If possible, we use Italian data on cancer incidence; however, in most organs affected by HPV-induced cancer, these are not available, and instead, we use data from the UK. We assume those to be comparable to Italian data; both countries offer related cervical screening programmes to their female population, and in both countries, the public health insurance systems are similar.

6.3.2 Visual calibration approach

The visual calibration approach conducted is similar to the one of the case study described in Section 3.5.1. We calibrate HPV prevalence and HPV-

induced diseases in the female and male model compartments through adjustments of several transition probabilities by age- and sex-specific variables $\lambda_{v,a,r,s}$, where the indices v, a, r and s indicate sex, age cohort, original and target states, respectively. The numbering of the states is described in Appendices D and E.1. We acknowledge that this approach is quite crude; however, due to unavailable time series data on the number of individuals affected by HPV-induced diseases as well as model complexity, a more systematic calibration approach is not feasible. Also, the literature shows that visual calibration approaches are quite common and generally well accepted.

As a first step, we estimate the transition probabilities through informative priors, informed by the literature. We incorporate the mean and ranges reported. Having run the model, we visually compare the results obtained to data. Therefore, we evaluate data and model outcome in graphical display. If those are not comparable, we shift the mean of the corresponding informative prior towards the upper or lower bounds of the ranges reported, including a large variance. In addition, we multiply the corresponding transition probabilities by $\lambda_{v,a,r,s}$. The final values of the variables $\lambda_{v,a,r,s}$ are estimated by rerunning the model until the results are comparable to the data. As a consequence of the adjustments, the transition probabilities become age- and sex-specific. This is reasonable since commonly, the chance of infection clearance is considerably reduced in older age cohorts, whereas the risk of progressing to more severe precancerous stages and cancer is considerably lower in younger age cohorts.

We calibrate the model output of all states in the three interventions screening-only, female-only and universal vaccination, separately for females and males. Data used for calibration are based on population prevalence and incidence of HPV-induced diseases prior to the introduction of HPV vaccination. Therefore, we assume that only the results of the intervention screening-only are comparable to the data; in the interventions including

vaccination, the model output on incidence and prevalence is considerably reduced. When compared to screening-only, the size of the reduction is approximately by factor 1.4 in female-only vaccination and 1.65 in universal vaccination.

6.3.3 HPV prevalence

The age-specific HPV prevalence data used for calibration are reported by Baussano et al. [28]. These are available for females only. At the current stage of research, no HPV tests for males are available [2]; therefore, data on male HPV prevalence are not routinely collected. As a consequence, we assume that male and female HPV population prevalence are identical.

In the Italian age-specific prevalence data, age is grouped into intervals of ten years, and reporting starts in females as young as 15 years. The oldest age group includes females aged 55 years and older. We interpolate the starting age to twelve years, assuming the same values as for 15 year olds. For the oldest age group, we consider constant prevalence results until the age of 80 years, representing the oldest people in our population. We assume people in all states apart from *Healthy*, *Exposure* and *Clearance* to be infected by HPV and as a consequence contribute to the overall HPV population prevalence. Following prevalence calibration, the HPV transmission probabilities per partnership are adjusted to on average 25.52% with a 95% credible interval of [16.7%;35.48%], and to 52.74% [29.84%;74.45%] in the average- and high-risk groups, respectively.

Figure 6.2 presents the calibration results. For screening-only, our model estimates HPV prevalence in a realistic way; the predictions show a good approximation to the data, with peak HPV prevalence in the youngest, decreasing in older people. Younger people are mainly affected by HPV due to i) commonly higher sexual activity, ii) non-existing natural immunity to HPV infection which is usually acquired following first virus exposure, and

iii) low cervical screening rates and thus infrequent intervention against pre-cancerous lesions [38]. Male HPV prevalence is higher than female as a consequence of more frequent partner change in males [360].

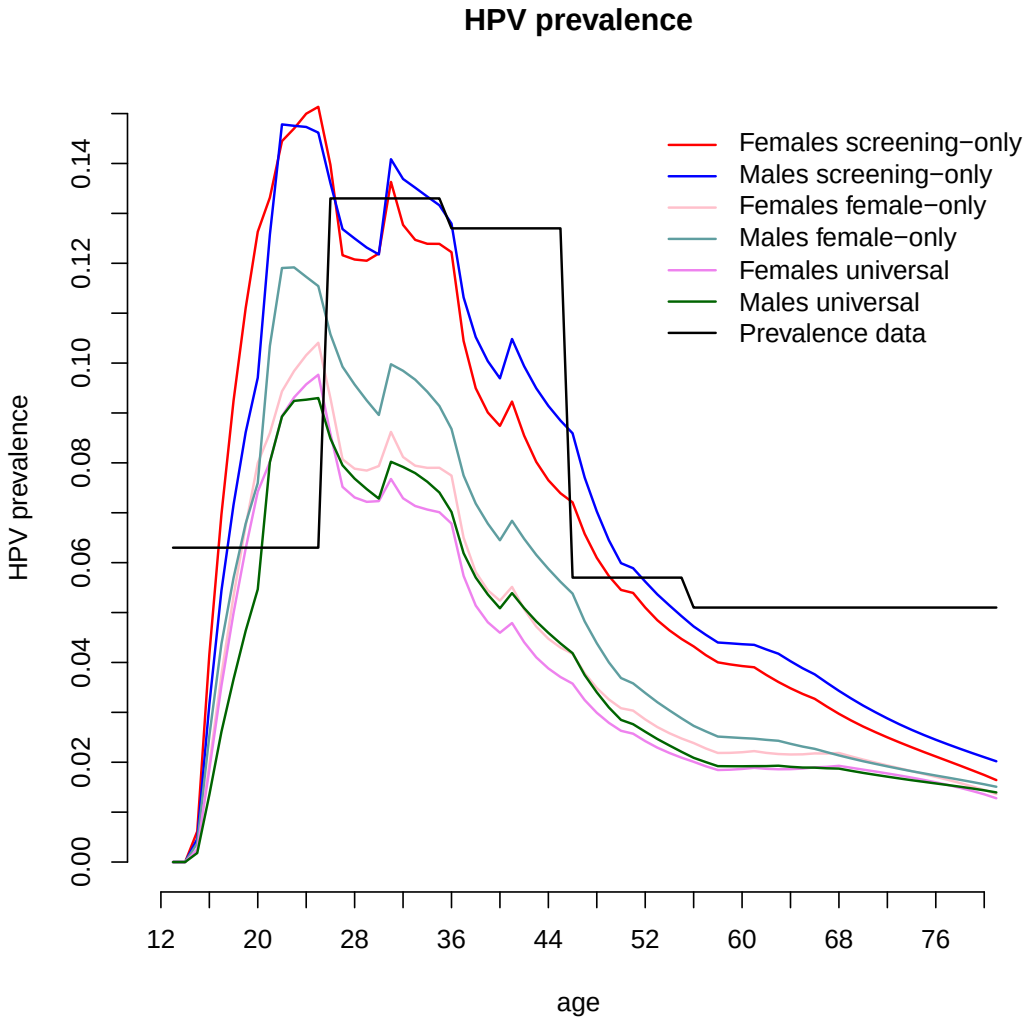

Figure 6.2: Visual calibration of the HPV prevalence model output to data taken from Baussano et al. [28]. The age- and sex- specific prevalence estimates are displayed separately for the three interventions screening-only, female-only, and universal vaccination. The figure shows that the model realistically predicts HPV prevalence, peaking in the youngest age groups.

6.3.4 Cervix-related diseases

As for the prevalence data, data on yearly cervical cancer incidence are specific to Italy, obtained from an Italian cancer registry [275]. These are used to calibrate the model output on cervical cancer. In contrast to data on cervical cancer incidence, Italian data on the age-specific prevalence of the cervical precancerous stages CIN I-III are not available. Brazilian data are available [121]; however, these differ from Italian data as described below and are thus not used for transition probability estimation through visual calibration. Instead, we only compare the model output on CIN prevalence to these data to evaluate whether the age-specific trend on CIN prevalence is estimated correctly by our model; we assume that Italian and Brazilian CIN prevalence follow similar age trends. We acknowledge that this approach is not ideal and has limitations since the real differences between CIN prevalence in the two countries are unknown and cannot be estimated straightforwardly. The actual model output on the age-specific proportion of females in the CIN-stages is thus not validated.

The corresponding transition probabilities are estimated through evidence synthesis on Italian data on CIN progression, regression, cervical screening and conization as described in Appendix D. In addition, we model the transition probability to move from CIN II to CIN III, as well as regressing from CIN III to CIN I or CIN II in an age-specific way according to [71], indicated by adjustments through $\lambda_{F,a,5,6}$, $\lambda_{F,a,6,4}$, and $\lambda_{F,a,6,5}$. Furthermore, we assume that the transition probabilities of clearing the HPV infection or developing cervical cancer for those in CIN III highly depend on age, adjusted through $\lambda_{F,a,6,13}$ and $\lambda_{F,a,6,8}$, respectively. Consequently, older individuals in CIN III have a higher risk of progressing to cervical cancer, whereas the younger are more likely to move to the state of *Clearance*. As a result, we successively increase cervical cancer incidence in older individuals since the older are both more likely to be affected by CIN III, and to progress from

CIN III to cervical cancer. This results in a shift of peak cervical cancer incidence to the oldest females, comparable to the Italian cervical cancer registry data [275].

Brazilian cervical cancer incidence is around two times higher in females up to age 29 and more than six times higher in those over 75 when compared to Italian incidence [121, 275]. Therefore, one could assume that the corresponding CIN prevalence is also increased by similar factors. However, this is not the case due to issues with Pap smears of low sensitivity in Brazil. CIN prevalence is thus considerably underestimated in Brazil as described in [94]. The positivity index (the proportion of females with a positive CIN diagnosis of all females tested) in Brazil would be expected to be considerably higher than in a developed country due to the higher cervical cancer incidence. However, the opposite is the case, resulting in a positivity index of only 2.72% in Brazil [94] when compared to developed countries which show positivity indices of 3.7% (Italy) [287], 6.5% (United Kingdom) [186] and 6.8% (USA) [104] despite considerably lower cervical cancer incidence. However, these values are only an indicator of low sensitivity of Pap smears and highly depend on tools such as laboratory equipment used for Pap smear evaluation as well as unknown true prevalence. An adjustment of Brazilian data on CIN prevalence to an Italian context by these values would thus rely on unreported or untestable assumptions and is therefore not conducted.

In Figure 6.3, we present the model outcome on the CIN stages and cervical cancer; the model outcome seems reasonable; however, conclusions have to be made with care due to the Brazilian data used. The trends of peak CIN I-II prevalence in the youngest and lower prevalence in older females seem to be estimated in a realistic way. Furthermore, the reverse trend in CIN III with a peak incidence in older females is well portrayed. Our model outcome results in peak cervical cancer incidence in middle-aged females which is a good approximation to reality. However, cervical can-

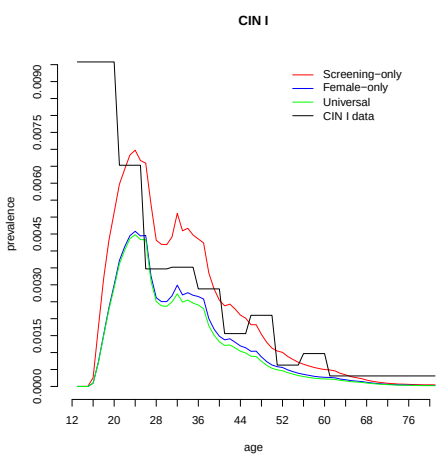

(a) The coloured curves show that the age-specific trend in CIN I with a peak prevalence in the youngest is reasonably well approximated by our model.

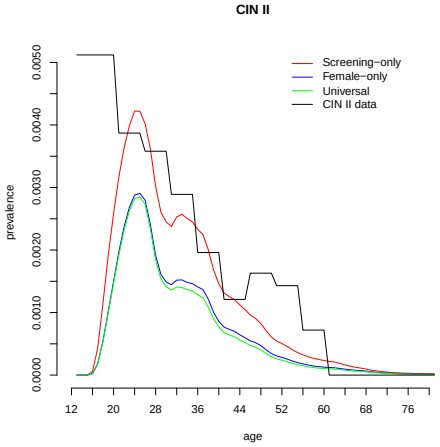

(b) As for CIN I, in CIN II, the model output shows a good approximation to the age-specific trend in prevalence.

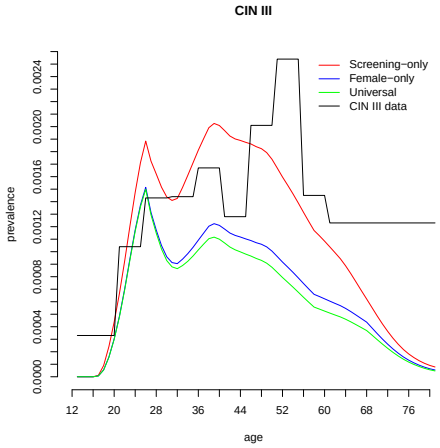

(c) The trend of a peak prevalence of CIN III in middle-aged women is reasonably represented by our model output.

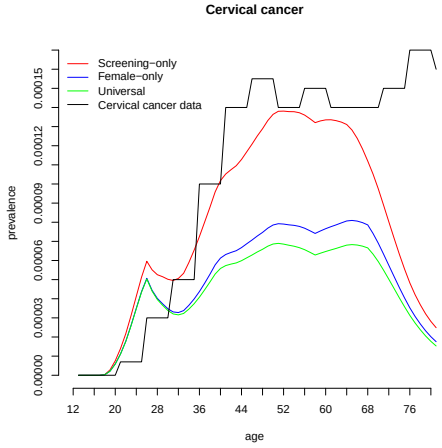

(d) The calibration result of cervical cancer clearly follows the trend of increasing incidence by age.

Figure 6.3: Visual calibration of the model outcome on cervial cancer to data on incidence. In addition, we show the age-specific trend in prevalence of the precancerous stages CIN I-III. The coloured curves display the model outcome in the three interventions screening-only, female-only and universal vaccination, whereas the black line indicates the data. We focus on the red lines representing screening-only since our data on CIN prevalence and cervical cancer incidence are based on the era pre HPV vaccine.

cer incidence in the oldest is underestimated; yet, this is not relevant since only a few age cohorts in our model reach such a high age. In addition, future events are highly discounted and have a very low impact on the results of the cost-effectiveness analysis. Therefore, the calculation of the overall

costs and QALYs is still conducted in a realistic way. As mentioned in the beginning of the section, calibration results for the other states are reported in Appendix G.

6.4 Markov traces

Following model calibration, Markov traces are evaluated to assess the model predictions on the proportions of the population in the states throughout the observation time horizon. We display the Markov traces graphically through bar charts on the natural history of HPV infection in the intervention screening-only.

Figure 6.4 shows the cumulative proportions of individuals in the states over the observation period, separately for the two sexes and diseased and unaffected people, respectively. The vast majority remains unaffected by HPV-induced diseases. However, a small proportion (up to 4% of females and 2.5% of males) acquires a disease at a particular time point of the follow-up. Anogenital warts and early precancerous stages mainly affect younger people, whereas more severe precancerous lesions and HPV-induced cancers commonly occur at a later stage in life. We do not display extremely rare cases of cancers of the anus, vulva, vagina, and penis.

6.5 Cost-effectiveness analysis

The economic evaluation is performed using the incremental cost-effectiveness ratio (ICER), accounting for the amount of money spent per quality-adjusted life-year (QALY) gained. Utilities (as described in Section 3.3.4) are used to compute the Quality-Adjusted Life Years (QALYs); therefore, the utility of a given state is multiplied with the amount of time spent within [22]. Costs averted by the implementation of vaccination as well as QALYs gained are additionally estimated. In the absence of an Italian official cost-effecti-

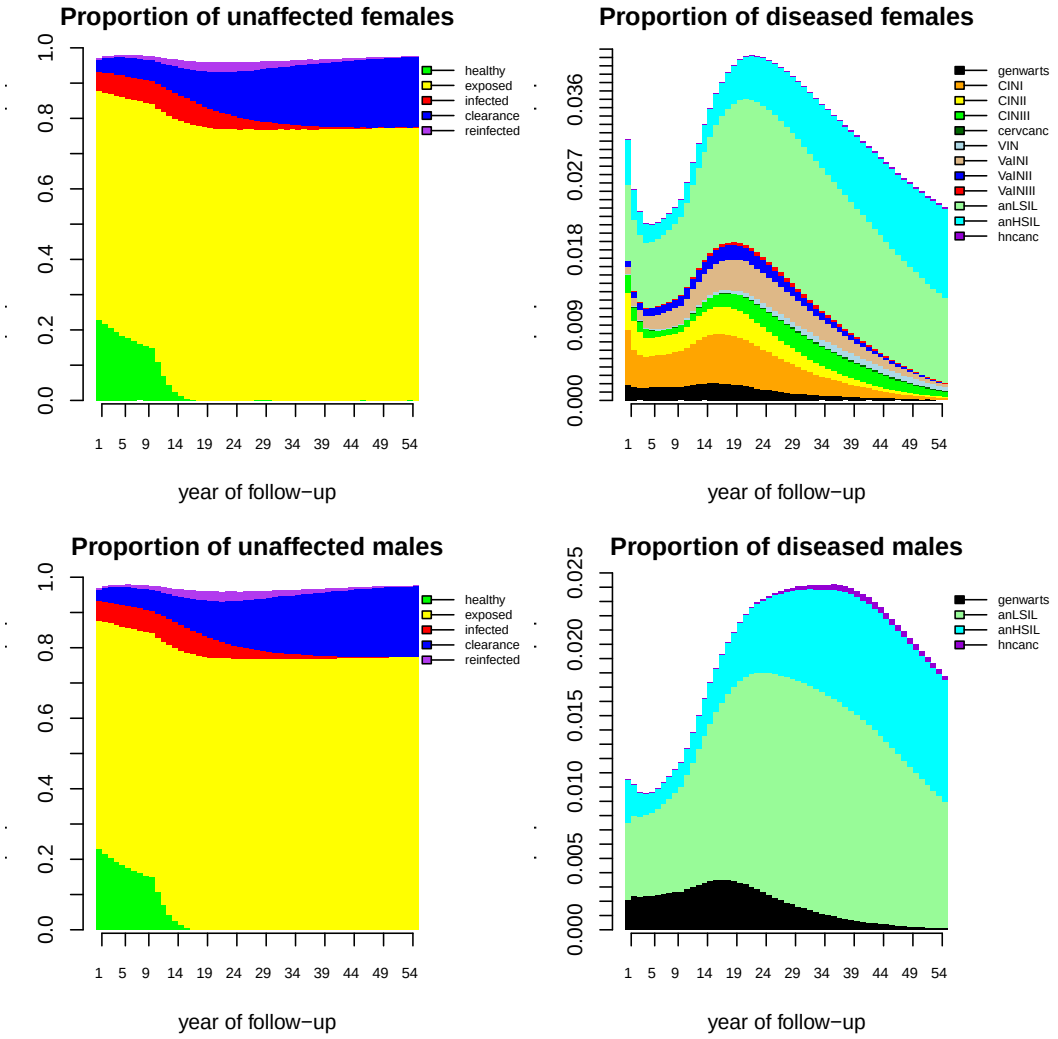

Figure 6.4: Model outcome of the natural history of HPV infection and disease progression. Cumulative proportions of unaffected and diseased people are displayed separately for the two sexes. The vast majority of people remain unaffected by the virus, whereas a small age-dependent proportion (up to 4% of females and 2.5% of males) develop an HPV-induced disease.

veness threshold, the same assumptions as described in Section 4.1 are applied to specify the willingness-to-pay of the decision maker.

6.5.1 Overall costs and utilities

Since we include 36 states in females and 22 states in males in the model, the calculations of overall costs and utilities are quite extensive. Further-

more, we consider that according to expert opinion, patients in states related to the cervix and anus do not only induce treatment expenses; additionally, the costs of diagnostic procedures have to be accounted for.

In cervical diseases, costs are induced by two Pap smears and two colposcopies in all females affected by cervical neoplasiae, and by a HPV DNA test in patients suffering from CIN III or cervical cancer. For diseases located in the anus, we assume that all patients receive an anoscopy with biopsy as well as a cytology. We assume that the information on expenses of precancerous stages and cancers of the vulva, vagina and penis as well as head/neck obtained from the literature incorporates both diagnostic and treatment costs. To result in the overall costs, we multiply the unit costs of each state with the number of people within the state, respectively. The overall costs are calculated as

$$\begin{aligned} C_{i,t} = {} & C_{i,t}^{scr} + C_{i}^{vac} + C_{i,t}^{gw} + C_{1,i,t}^{cin} + C_{2,i,t}^{cin} + C_{3,i,t}^{cin} + C_{i,t}^{cerv} + C_{i,t}^{lsil} \\ & + C_{i,t}^{hsil} + C_{i,t}^{an} + C_{i,t}^{hn} + C_{i,t}^{vin} + C_{i,t}^{vulv} + C_{1,i,t}^{vain} + C_{2,i,t}^{vain} \\ & + C_{3,i,t}^{vain} + C_{i,t}^{pein} + C_{i,t}^{pen}, \end{aligned}$$

including cervical screening as well as both diagnostic and treatment costs induced by people in all states at time t of follow-up in intervention i. For simplicity, time t indicates the time interval $\mathcal{I}_t$ of the discrete-time approach. In interventions $i = 2, 3$ where vaccination takes place, the costs of vaccine administration and the vaccine also have to be considered.

As an illustrative example, we report the calculation of the overall costs of genital warts in intervention i at time t, which is described as

$$C_{i,t}^{gw} = \mathcal{G}_{i,t} c^{gw}.$$

The number of people in intervention i at time t affected by genital warts, $\mathcal{G}_{i,t}$, is multiplied by the corresponding unit cost c^{gw}. The overall costs of the

remaining states are calculated accordingly; however, in contrast to the visible and symptomatic health condition of genital warts, precancerous lesions and cancer only result in costs after their diagnosis. Therefore, the actual costs of the respective diseases are multiplied with the corresponding probabilities of diagnosis.

The calculation of the overall utilities is straightforward; the actual number of people in each state in intervention i at time t is multiplied by the corresponding utility value, resulting in

$$\begin{aligned} U_{i,t} = & U_{i,t}^{health} + U_{i,t}^{inf} + U_{i,t}^{gw} + U_{1,i,t}^{cin} + U_{2,i,t}^{cin} + U_{3,i,t}^{cin} + U_{r,i,t}^{cerv} + U_{i,t}^{lsil} \\ & + U_{i,t}^{hsil} + U_{r,i,t}^{an} + U_{r,i,t}^{hn} + U_{i,t}^{vin} + U_{r,i,t}^{vulv} + U_{1,i,t}^{vain} + U_{2,i,t}^{vain} + U_{3,i,t}^{vain} \\ & + U_{r,i,t}^{vag} + U_{i,t}^{pein} + U_{r,i,t}^{pen}. \end{aligned}$$

For all HPV-induced precancerous stages and cancer states, the overall utilities are multiplied by the respective probabilities of diagnosis.

6.5.2 The present value of cost and the present value of utility

The overall costs and utilities $C_{i,t}$ and $U_{i,t}$ are summed up for the whole observation time period to result in the present value of cost (PVC) and the present value of utility (PVU).

Because of the model's long-term horizon, it is necessary to discount overall costs and utilities. Approaches to this differ [42]: In an Italian context, ISPOR guidelines [74] suggest discounting both costs and benefits at a 3% rate, although NICE [268] recommend a slightly higher value of 3.5%, with a 0-6% range for sensitivity analysis. Rates actually applied vary between countries, ranging from 1.5% to 10% for benefits and 0% to 10% for costs [381]. In line with [74], the annual discount rates z_c for costs and z_u for utilities are set at 3%.

The PVC and the PVU for a follow-up period of $t = 55$ years are calculated as

$$\text{PVC}_i = \sum_{t=1}^{55} \frac{C_{i,t}}{(1+z_c)^{t-1}}$$

and

$$\text{PVU}_i = \sum_{t=1}^{55} \frac{U_{i,t}}{(1+z_u)^{t-1}}.$$

6.5.3 Population sizes, overall costs and QALYs

Costs and QALYs are reported for the population as a whole. Table 6.1 shows the mean population size and mean QALYs per intervention over the whole observation time period along with the corresponding 95% credible intervals. With screening-only, population size is the lowest since more individuals die due to the higher incidence of HPV-induced cancers.

Table 6.1: Population size and overall QALYs in the three interventions over total follow-up.

	Population size	**Overall QALY**	
Intervention	**Mean**	**Mean**	**95% CI**
Screening-only	149,652,365	127,935,994	[127,884,948;127,987,040]
Female-only	149,727,525	128,409,504	[128,399,222;128,419,785]
Universal	149,736,770	128,449,826	[128,444,388;128,455,264]

The mean and median costs are shown in Table 6.2. The cost distribution in the screening-only scenario is highly right-skewed, resulting in a median that is ten times lower than the mean. In contrast, the costs in the interventions female-only and universal vaccination are symmetrically distributed; as a consequence, their mean and median are similar.

Mean overall costs differ by a factor of five between screening-only and universal vaccination, reflecting the larger population to which the vaccine

is made available in the latter case. Interestingly, QALYs are also highest under universal vaccination.

Table 6.2: Overall costs in € in the three interventions over total follow-up.

	Overall cost			
Intervention	**Mean**	**95% CI**	**Median**	**95% CI**
Screening-only	187,189,634	[169,986,589;204,392,679]	18,279,665	[13,007,644;28,495,706]
Female-only	484,357,417	[478,212,474; 490,502,360]	478,135,234	[469,493,395;487,530,520]
Universal	948,732,541	[937,699,221; 959,765,861]	941,748,716	[929,302,951;951,984,667]

6.5.4 The Incremental Cost-Effectiveness Ratio

The Incremental Cost-Effectiveness Ratio (ICER) is described in further detail in Section 3.3.4. To compare the cost-effectiveness of universal ($i = 3$) and female-only ($i = 2$) vaccination, as a first step, the cost- and effectiveness differentials $\Delta_c = \text{PVC}_3 - \text{PVC}_2$ and $\Delta_e = \text{PVU}_3 - \text{PVU}_2$ are calculated. As described in Section 5.5, all model parameters are included in the parameter vector $\boldsymbol{\theta} = (\boldsymbol{\theta}_3, \boldsymbol{\theta}_2)$, with $\boldsymbol{\theta}_3$ referring to the parameters in the reference intervention $i = 3$ and $\boldsymbol{\theta}_2$ to those of the comparator, $i = 2$. The ICER is then calculated as

$$\text{ICER} = \frac{\text{E}[\text{PVC} \mid \boldsymbol{\theta}_3] - \text{E}[\text{PVC} \mid \boldsymbol{\theta}_2]}{\text{E}[\text{PVU} \mid \boldsymbol{\theta}_3] - \text{E}[\text{PVU} \mid \boldsymbol{\theta}_2]} = \frac{\text{E}[\Delta_c]}{\text{E}[\Delta_e]}.$$

The calculation of the ICER for the comparison of universal vaccination to screening-only is conducted accordingly. When comparing universal vaccination to the other two alternatives, the ICER is about € 1,500 in comparison to screening-only and about € 11,600 in comparison to female-only vaccination.

6.6 Probabilistic sensitivity analysis

The uncertainty around the cost-effectiveness estimates is analysed by means of the cost-effectiveness plane, the cost-effectiveness acceptability curve (CEAC), the expected value of perfect information (EVPI) analysis and the expected value of perfect partial information (EVPPI) analysis. The cost-effectiveness plane, CEAC and EVPI are described in further detail in Section 3.3.4.

6.6.1 Universal versus female-only vaccination

Figure 6.5 shows a cost-effectiveness plane comparing universal to female-only vaccination, with the effectiveness differential on the x-axis and the cost-differential on the y-axis. The majority of points lie at the limit of the sustainability area, with low CEAC values as a consequence. However, mean cost- and effectiveness differentials do indicate cost-effectiveness, resulting in an ICER of around €11,600 (displayed as a red dot), well below the cost-effectiveness thresholds set in Section 4.1. This is substantially due to herd immunity. As a consequence, the higher overall cost of the universal vaccination strategy is clearly compensated by the gain in utilities.

Figure 6.6 presents a graphical summary of PSA. The left panel contains the CEAC. Typically, low values of the CEAC indicate the presence of a large amount of parameter uncertainty [22]. In Figure 6.6, the values are below 80% for the whole range of choices for the willingness-to-pay displayed. Yet, the CEAC only measures the probability of cost-effectiveness, but fails to reflect the impact of uncertainty on the consequences of a “wrong” decision.

The panel on the right shows the EVPI, again as a function of willingness-to-pay. In the present case, EVPI is at most € 320,030,305 for the overall population and € 2.1 per subject, representing the extremely low future financial investment necessary to resolve parameter uncertainty. These values indicate that the impact of parameter uncertainty on the results of the

model is extremely low, despite the low CEAC values, which are induced by a markedly skewed distribution for the underlying cost- and effectiveness-differentials. Under these circumstances, the results of the cost-effectiveness analysis are rather stable, despite the underlying parameter uncertainty.

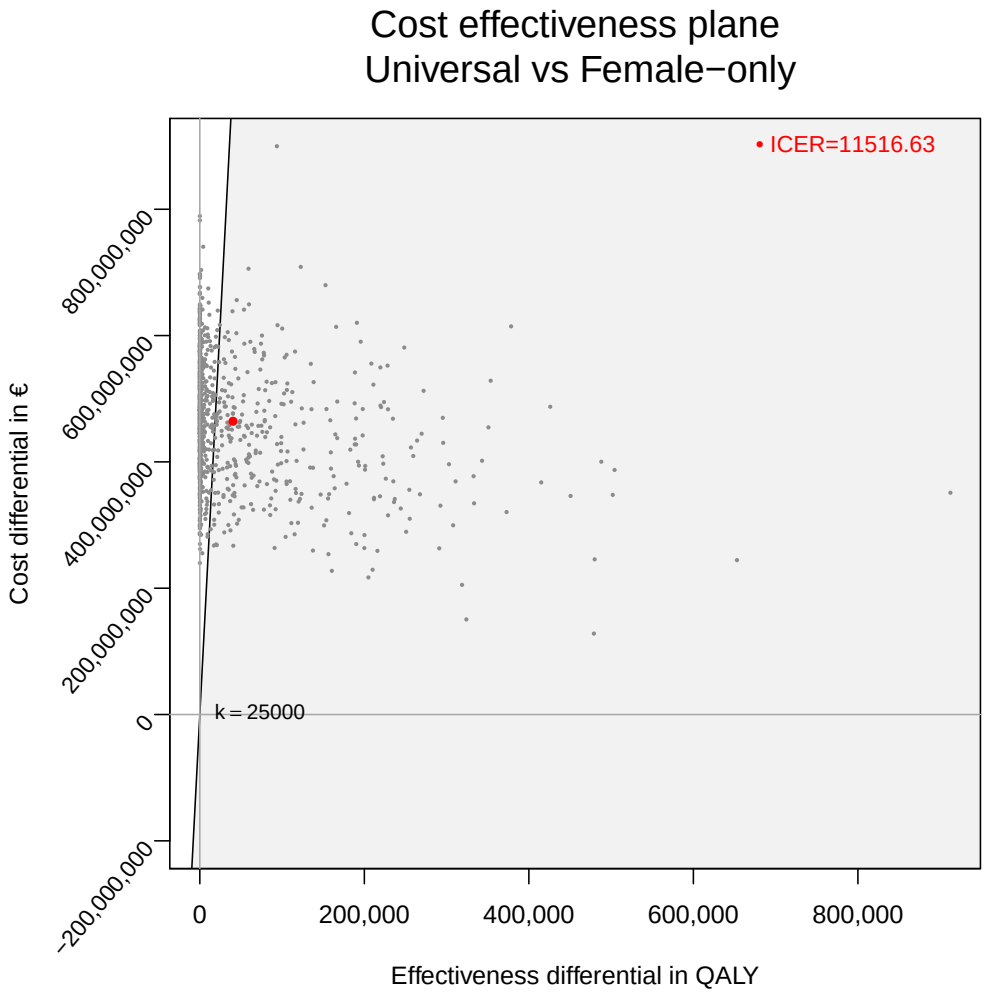

Figure 6.5: Cost-effectiveness plane comparing universal to female-only vaccination. The x-axis shows Δ_e and the y-axis Δ_c. Points lying within the grey sustainability area are cost-effective under the threshold of £ 25,000, defined by the NHS. The red dot represents the ICER; its actual value is displayed in red.

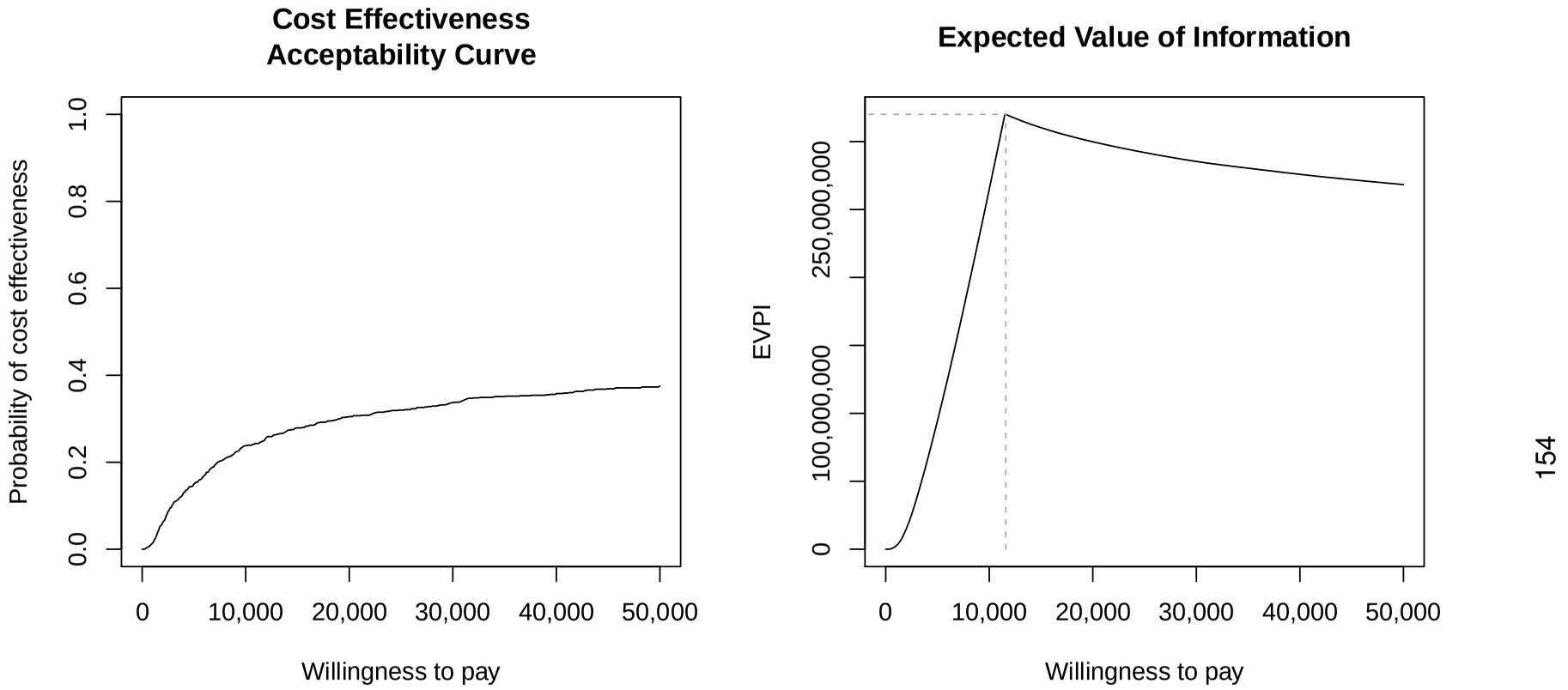

Figure 6.6: The figure presents probabilistic sensitivity analysis comparing universal to female-only vaccination by means of the cost-effectiveness acceptability curve (CEAC) on the left and the expected value of perfect information (EVPI) on the right. The CEAC shows that the probability of cost-effectiveness never reaches 80% (the value defined as reasonable cost-effectiveness [22]) as a consequence of a positively skewed joint distribution of cost and effectiveness differentials. The EVPI indicates that the value of resolving the uncertainty in the model parameters is very much limited, never exceeding €320,030,305 for the overall population.

6.6.2 Universal vaccination versus screening-only

The incremental cost of applying universal vaccination compared to screening-only is higher than in the preceding section, since fewer individuals were potentially vaccinated. However, incremental QALYs are higher, too, as a consequence of the reduced effects of herd immunity. Figure 6.7 shows the corresponding cost-effectiveness plane.

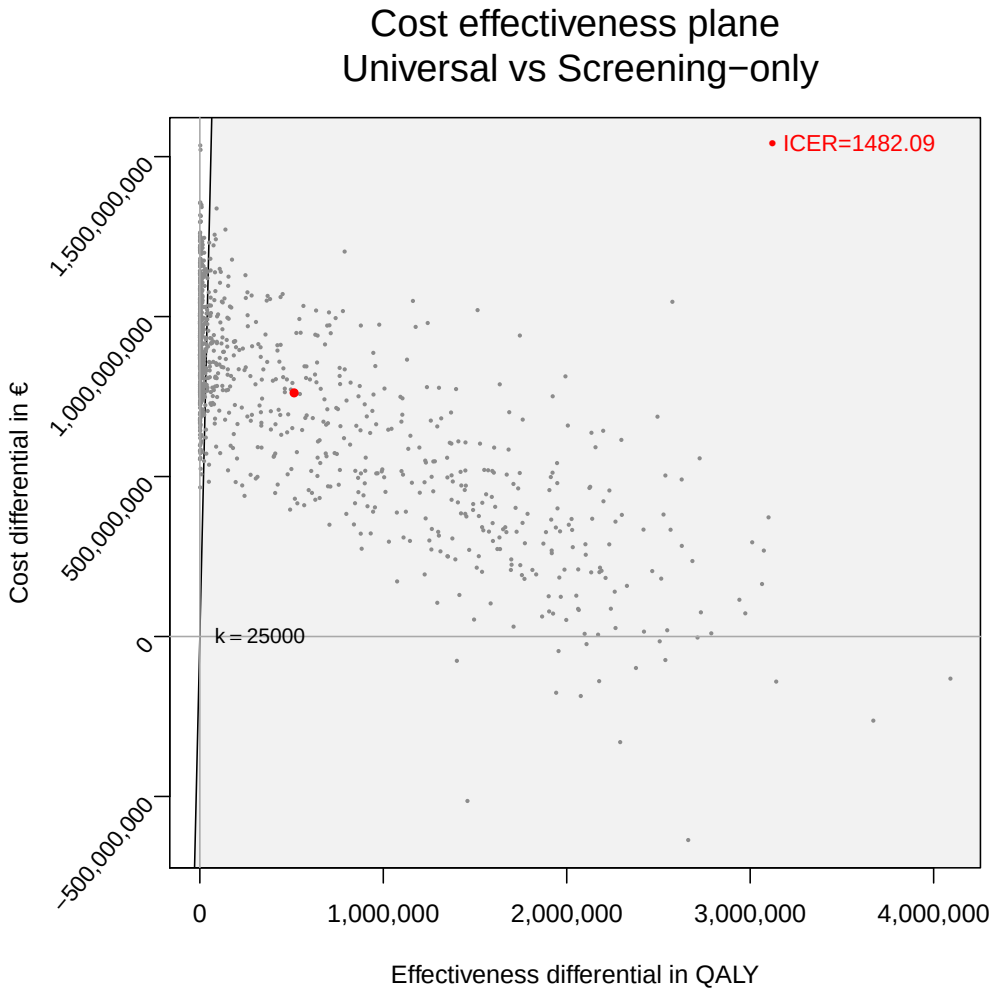

Figure 6.7: Cost-effectiveness plane for a comparison of universal vaccination to screening-only. In comparison to Figure 6.5, the joint distribution of cost and effectiveness differentials is less skewed to the right, resulting in a cost-effectiveness acceptability curve nearly reaching values of 60% cost-effectiveness.

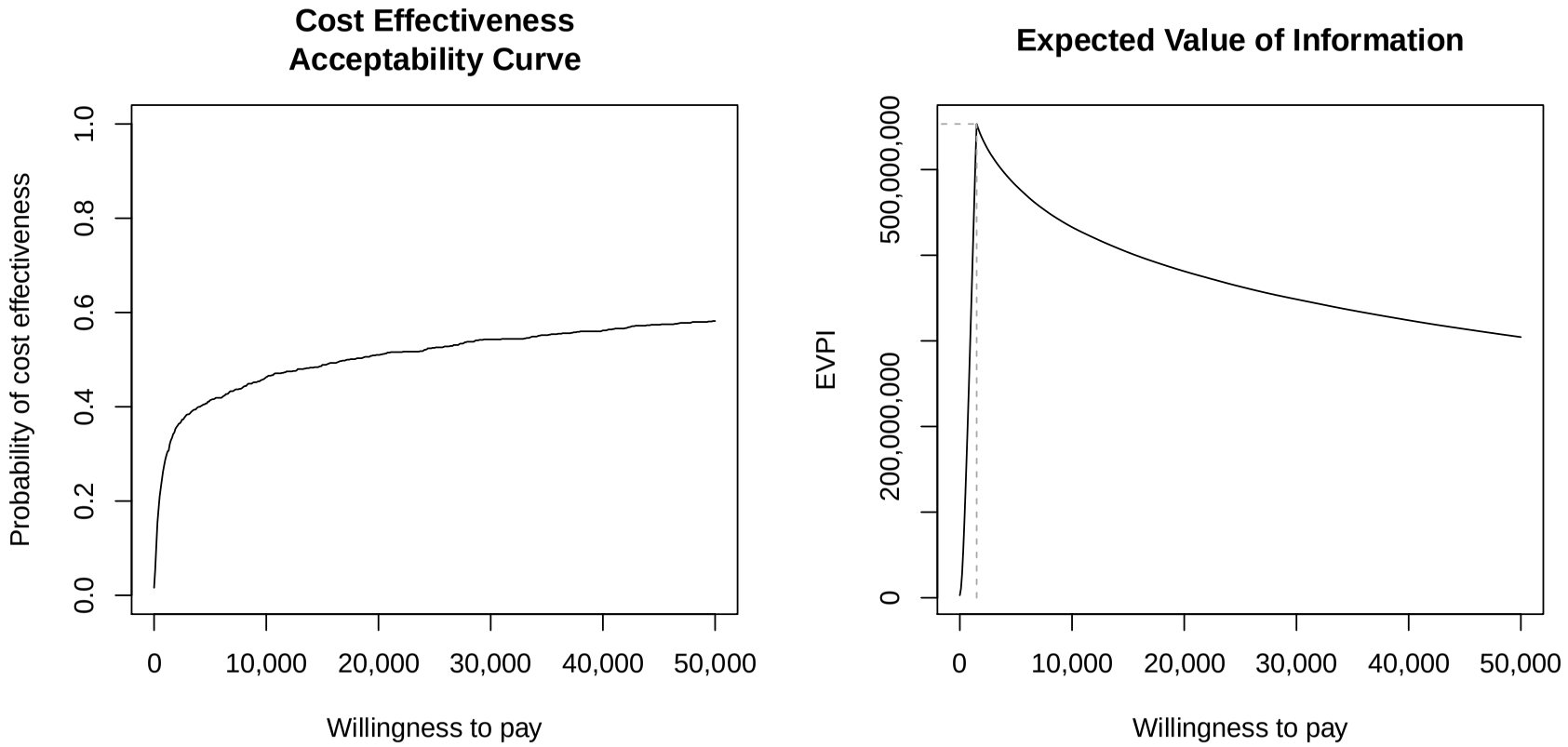

Figure 6.8: Probabilistic sensitivity analysis comparing universal vaccination to screening-only using the cost-effectiveness acceptability curve (CEAC) on the left and the expected value of perfect information (EVPI) on the right. The CEAC shows that the probability of cost-effectiveness reaches a maximum value of only around 60% at a willingness-to-pay value of €50,000. This is a consequence of the positively skewed distribution of cost and effectiveness differentials. The EVPI on the right indicates that the value of resolving parameter uncertainty in the model is very much limited, never exceeding €553,291,173 for the overall population.

In comparison to the former analysis, a higher number of points lie within the sustainability area, and the joint distribution of cost- and effectiveness differentials is less right-skewed. Thus, the CEAC exhibited in the left panel of Figure 6.8 has higher values, nearly reaching 60%. Additionally, EVPI indicates a higher value of further research amounting to up to € 3.7 per individual and € 553,291,173 for the whole population. However, this is still a comparatively low value, suggesting a low impact of parameter uncertainty. Therefore, one can conclude that despite the low CEAC, universal vaccination is a highly cost-effective alternative when compared to screening-only.

6.6.3 The Expected Value of Perfect Partial Information

The global EVPI is a measure of the overall value of future financial investment necessary to resolve uncertainty in the model parameters $\boldsymbol{\theta}$ as described in Section 3.3.4. In contrast to the global EVPI, the Expected Value of Perfect Partial Information (EVPPI) identifies the exact sources of parameter uncertainty. In an EVPPI analysis, as a first step, the EVPPI is calculated separately for each model parameter of interest. Afterwards, model parameters resulting in an EVPPI greater than zero are grouped according to the medical context in order to identify the areas with the largest value for future research.

Thus, $\boldsymbol{\theta}$ is split into $\boldsymbol{\phi_*}$ and $\boldsymbol{\psi_*}$; $\boldsymbol{\phi_*}$ represents the parameters of interest, whereas $\boldsymbol{\psi_*}$ are the remainder. A single parameter or a combination of parameters can be included in $\boldsymbol{\phi_*}$. Following parameter specification, the EVPPI is calculated as

$$\mathsf{EVPPI}(\boldsymbol{\phi_*}) = \underbrace{\mathsf{E}(\boldsymbol{\phi_*}) \left[\max_i \mathsf{E}(\boldsymbol{\psi_*}|\boldsymbol{\phi_*})\{\mathsf{NB}(i, \boldsymbol{\phi_*}, \boldsymbol{\psi_*})\} \right]}_{\text{perfect information on } \boldsymbol{\phi_*}} - \underbrace{\max_i \mathsf{E}(\boldsymbol{\theta})\{\mathsf{NB}(i, \boldsymbol{\theta})\}}_{\text{current information on } \boldsymbol{\theta}}. \tag{6.1}$$

The first term of the expression represents a scenario with perfect infor-

mation on $\boldsymbol{\phi_*}$; thus, the conditional expectation $\mathrm{E}(\boldsymbol{\psi_*}|\boldsymbol{\phi_*})$ on the net benefit $\mathrm{NB}(i, \boldsymbol{\phi_*}, \boldsymbol{\psi_*})$ is estimated per intervention i, and the maximum is calculated. The net benefit is defined in Section 3.3.4. Finally, since $\boldsymbol{\phi_*}$ is unknown, the maximum is averaged over the current information available on $\boldsymbol{\phi_*}$. The scenario with current information on $\boldsymbol{\theta}$ is represented by the maximum over the expectations of the net benefits ($\mathrm{E}(\boldsymbol{\theta})\{\mathrm{NB}(i, \boldsymbol{\theta})\}$). The larger the EVPPI, the higher the financial investment necessary to resolve uncertainty in $\boldsymbol{\phi_*}$.

As for the EVPI, the EVPPI can be estimated through Monte Carlo simulation. However, in contrast to an EVPI analysis, an EVPPI analysis induces a considerably higher computational effort, especially in more complex models: the first expression of Equation 6.1, including perfect information on $\boldsymbol{\phi_*}$, is estimated by running an inner loop to calculate the conditional expectation, followed by an outer loop to average over $\boldsymbol{\phi_*}$. To simplify computation, Strong et al. [331] introduce two innovative approaches on EVPPI analysis.

The first is a nonparametric regression approach based on a Generalised Additive Model (GAM). The conditional expectation

$$\mathrm{E}(\boldsymbol{\psi_*}|\boldsymbol{\phi_*})\{\mathrm{NB}(i, \boldsymbol{\phi_*}, \boldsymbol{\psi_*})\}$$

is a function of $\boldsymbol{\phi_*}$ since it takes a different value for each $\boldsymbol{\phi_*}$. Thus, it can be approximated by an unknown function $f(i, \boldsymbol{\phi_*})$ which consists of a set of smoothing functions, representing some form of spline.

The GAM regression is suitable for a first screening of each individual model parameter to evaluate the corresponding amount of uncertainty. However, if more than six model parameters are included in the vector of parameters of interest $\boldsymbol{\phi_*}$, GAM regression becomes unstable. As an alternative, the authors introduce a second approach of EVPPI estimation by means of Gaussian Process (GP) regression. As for the GAM regression, the conditional expectation is approximated by a function $f(i, \boldsymbol{\phi_*})$. The unknown values of the input parameters of the function are represented through a

multivariate normal distribution. The smoothness of the function $f(i, \phi_*)$ is given by a correlation matrix with respect to the parameters in ϕ_*. For further details on GAM and GP regression, see [331].

In the online appendix to [331], `R` functions for both methods are available. The function inputs consist of the distribution of the net benefits of the two interventions compared. In addition, the parameters of interest ϕ_* and the overall input parameters θ have to be specified.

We conduct the EVPPI analysis for universal vaccination in comparison to female-only vaccination and to screening-only. For a first parameter screening, we run both the GAM as well as the GP regression for every single model parameter. The results of the two approaches are approximately identical. As a next step, we group parameters with an EVPPI greater than zero according to the medical context, and apply GP regression.

Table 6.3 shows the results per individual for the comparison of universal to female-only vaccination at the break-even point of €11,600. In addition, the standard errors and the upward biases of the GP regression are displayed. The upward biases are a consequence of the maximisation step in the first term of Equation 6.1, which can be reduced through an increased number of simulations. For 500 simulations, the upward bias is considerably low and never reaches a value above 0.43. Furthermore, the standard errors are close to zero; therefore, we can conclude that all values of the EVPPI are estimated with precision.

Unsurprisingly, as for the low global EVPI, all grouped EVPPIs indicate a low future financial investment to resolve parameter uncertainty. The highest amount of uncertainty is found in some of the transition probabilities and the parameters related to age-, sex- and behavioural-specific sexual mixing and cervical screening, whereas the uncertainty in parameters related to costs and utilities seems to play a minor role. As for the transition probabilities, regressing to the state of exposure, progressing to head/neck cancer and to diseases related to the penis include the highest amount of uncertainty.

Table 6.3: Results of the EVPPI-analysis of universal in comparison to female-only vaccination. Model parameters are grouped according to the medical context, and the analysis is conducted via Gaussian Process regression.

Parameter group	EVPPI	Standard Error	Upward bias
Probabilities of screening	1.1564	0.0472	0.3107
Probabilities of diagnosis	0.4661	0.0808	0.3264
Probabilities of survival	0.6549	0.0687	0.3629
Vaccine-related parameters	0.1940	0.0699	0.0764
Transition probabilities			
Regression from HPV infection	1.0931	0.0468	0.3419
Risk of reinfection	0	0.0177	0.0075
Head/neck	1.0810	0.0525	0.3436
Genital warts	0.9564	0.0589	0.3983
Cervix	0.1971	0.0759	0.1672
Anus	0.1144	0.0644	0.0404
Vulva	0.9499	0.0605	0.4303
Vagina	0.0049	0.0148	0.0089
Penis	1.1192	0.0475	0.3233
Sexual mixing			
Average-risk female	1.0767	0.0491	0.3530
Average-risk male	1.1171	0.0486	0.3560
High-risk female	1.0262	0.0508	0.3621
High-risk male	1.0955	0.0476	0.3342
Health economic parameters			
Costs	0.4703	0.0835	0.2719
Utilities	0.0555	0.0554	0.0489

Table 6.4 shows the results of the EVPPI analysis for the comparison of universal vaccination to screening-only at the break-even point of € 1,500. Compared to the previous analysis, the overall amount of uncertainty is slightly higher; however, it is still considerably low. As for the previous analysis, the distributions of the highest amount of uncertainty are located in the parameters related to sexual mixing and in the transition probabilities of regression to the state of exposure, as well as progression to head/neck cancer and genital warts. Again, uncertainty in the distributions on costs and utilities seems to play a minor role. The standard errors and upward biases are higher when compared to Table 6.3.

Table 6.4: Results of the EVPPI-analysis of universal vaccination in comparison to screening-only. As for the previous analysis, model parameters are grouped according to the medical context, and the analysis is conducted via Gaussian Process regression.

Parameter group	EVPPI	Standard Error	Upward bias
Probabilities of screening	1.5375	0.0995	0.5566
Probabilities of diagnosis	0.4817	0.1150	0.2985
Probabilities of survival	1.9224	0.0869	0.4313
Vaccine-related parameters	0.1559	0.1082	0.0926
Transition probabilities			
Regression from HPV infection	2.0288	0.0725	0.3735
Risk of reinfection	0.0106	0.0573	0.0248
Head/neck	2.3214	0.0697	0.2657
Genital warts	2.1619	0.0743	0.3416
Cervix	0.2541	0.1176	0.1427
Anus	0.3400	0.1160	0.2273
Vulva	1.9320	0.0827	0.4198
Vagina	0.0468	0.0650	0.0708
Penis	1.6285	0.0977	0.5132
Sexual mixing			
Average-risk female	2.1550	0.0735	0.3435
Average-risk male	2.1433	0.0728	0.3539
High-risk female	2.1550	0.0735	0.3435
High-risk male	2.2223	0.0745	0.3143
Health economic parameters			
Costs	0.5374	0.1240	0.2710
Utilities	0.1705	0.1027	0.1220

6.7 Conclusion

Universal HPV vaccination is found to be a cost-effective choice when compared to either cervical cancer screening or female-only vaccination within the Italian context. These results are based on Markov traces which were calibrated to data. Extensive probabilistic sensitivity analysis was conducted in order to assess the amount of parameter uncertainty. The low values of the global EVPI and the EVPPI show that further expenses to resolve parameter uncertainty are not necessary.

Chapter 7

Summary and conclusions

7.1 Summary of the research

Standard Markov models (MMs) are static by definition of the Markov property. Thus, when applied in the context of infectious disease, changes in population prevalence over time are commonly not considered. In this PhD thesis, the standard framework of MMs is extended by directly incorporating the dynamic force of infection into the transition probabilities to the state of *Infection*, accounting for the effects of herd immunity. As a consequence, the probability of infection is modified according to the proportion of people who at any given time are infected and exposed to the infectious agent. The corresponding inference is conducted in a Bayesian context. The thesis starts with a motivation for the research in Chapter 1. Chapter 2 presents a general introduction into compartmental methodology and our approach of the dynamic Bayesian Markov model, termed as BMM.

The “gold standard” applied to perform epidemiological and economic evaluations of infectious diseases is based on systems of ordinary differential equations (ODEs) [291]. While particularly effective in modelling the dynamic transmission of infectious diseases, these are usually too complex for assigning a suitable probability distribution to each model parameter, limiting the possibility of performing extensive probabilistic sensitivity analysis

(PSA). As a consequence, PSA can only be conducted when applying additional retrospective simulation procedures such as the Latin Hypercube Sampling (LHS) [255].

However, PSA is fundamental in any health economic evaluation [22, 51, 329] and particularly so in the case of infectious disease modelling, where uncertainty surrounding the parameters and assumptions of the model may impact dramatically on cost-effectiveness results. In contrast to most ODE-based models, the BMM developed in this thesis is implemented in a Bayesian framework. Therefore, the model parameters are assigned distributions, permitting to accommodate PSA in a straightforward way. At the same time, by using discrete time rather than continuous time for modelling the Markov cycle, we are able to include the dynamics of infection and population characteristics. Regulatory bodies such as NICE may benefit from our methodology since it produces a full economic evaluation based on a tool they are familiar with; also, PSA can be directly embedded in the model. In addition to the advantages previously discussed, it considerably reduces the effort on implementation and computation when compared to standard ODE-based methodology.

The use of a Bayesian approach is particularly relevant in the case of infectious disease modelling, since it is likely that many of the fundamental parameters are informed by a combination of evidence, some of which may be based on expert opinion. Thus, it is important to fully account for the underlying uncertainty - failure to do so may result in an under- or overestimation of the economic performance of the interventions being investigated. A full Bayesian analysis also has the advantage of making the conduct of the all-important PSA relatively straightforward, as the uncertainty in the model parameters is directly accounted for in the main model computations. Using tools such as the `R` package `BCEA` [3] or the `SAVI webapp` [1], it is fairly straightforward to systematically compute the relevant summary assessments such as CEAC, EVPI and EVPPI analysis.

In Chapter 3, we apply our approach to a case study on a fictional chronic sexually transmitted infection (STI), including a small number of states. We perform two different analyses; in the first analysis, we assume not to have access to individual-level data. Thus, we include exclusively informative priors into the models. Depending on data availability of the pathogen under investigation, this could be a realistic scenario. In contrast, in the second analysis, the priors are updated by fictional aggregate and simulated individual-level data. The individual-level data are simulated through random number generators as described in Section 3.4. In addition, the model outcome is calibrated to data on STI prevalence as well as time series data on the number of people in the states. In both analyses, we compare the output of our dynamic Bayesian MM to the outputs of a deterministic (including fixed parameter values) and a Bayesian ODE-based model. Furthermore, we conduct a health economic evaluation, comparing a fictional vaccine against the STI to screening-only.

The second part of the thesis focusses on the application of our methodology to human papillomavirus (HPV) transmission and disease progression modelling, followed by a cost-effectiveness analysis of universal vaccination in comparison to female-only vaccination and screening-only. To gain insight into this area of research, an extensive literature review on health economic evaluations of different HPV vaccination strategies is presented in Chapter 4.

As shown in the literature, conclusive HPV models incorporate a high number of states; this is necessary to account for HPV-induced neoplasiae in a large number of body regions. If these are not considered, the model predictions might be falsified. Furthermore, HPV prevalence and thus the force of infection is age- and sex-specific. Therefore, in order to produce reliable results, models on HPV transmission and disease progression usually induce a considerably high level of complexity.

The specification of our BMM to an HPV context is described in Chap-

ter 5. In contrast to Bayesian ODE-based models, our methodology is especially suitable to incorporate a large number of age cohorts and states without considerably increasing the computational effort. Altogether, 24 age cohorts, 58 states and two sexual behaviour groups are included in an open model structure, enabling healthy twelve year old individuals to enter the model. The force of infection is age-, sex- and behavioural-specific. In contrast to the ODE-based models in the literature on HPV modelling, all of our model parameters are assigned distributions, and thus we are able to conduct PSA as an essential part of a full health economic evaluation in a straightforward way.

Having run the model, we investigate convergence and the amount of autocorrelation in the model parameters. We calibrate the vast majority of states to available data, taken from cancer registries and the literature. The results of MCMC diagnostics, model calibration, natural history of HPV and induced diseases as well as the health economic evaluation are presented in Chapter 6.

7.2 Summary of the results

7.2.1 Comparison of the BMM to the "gold standard" BODE

In Chapter 3, we compare the outcome of the BMM to a deterministic (including fixed parameter values) and a Bayesian ODE-based model. The prevalence outcome and the results of the cost-effectiveness analysis of the "gold standard" of the BODE and the BMM are approximately identical. Therefore, we can clearly show that population dynamics, mixing patterns between people, and time-dependent changes in population prevalence are accounted for in a realistic way by our BMM.

The loss induced by an over- or underestimation of STI prevalence is not symmetric. The lower the prevalence, the higher the ICERs of the interven-

tions under investigation. As a result, prevalence underestimation results in too high ICERs. In the worst case, the cost-effectiveness of the corresponding interventions is not recognised, and highly effective treatments are withheld from the population. In contrast, an overestimation of prevalence could result in wasting scarce resources for highly costly or inefficient interventions. In the first analysis, the model outcome is not calibrated to simulated data. To avoid falsified outcome of the dODE, the corresponding model parameters are informed through 60% quantiles of the parameters of the BODE which are estimated through a multilinear loss function. This function accounts for asymmetry in losses. As a consequence of considering the non-symmetric loss, prevalence outcome and results of the cost-effectiveness analysis of the dODE are comparable to the Bayesian models, resulting in ICERs of £ 6,702, £ 6,800 and £ 7,084 in the dODE, BODE and BMM, respectively.

In the second analysis, the outcome of the three models is calibrated to simulated data which are obtained by running the dODE for i) different initial values as well as for ii) a short observation time period of only five years. In a visual calibration approach, data on STI prevalence are used. The outcome of the BMM and BODE fit the data well. However, despite calibration, the dODE results in an underestimation of STI prevalence in the beginning of follow-up, and an overestimation at a later stage. Thus, the values of the ICERs differ, resulting in £ 8,095, £ 12,344 and £ 11,691 in the dODE, BODE and BMM.

In contrast, systematic calibration approaches result in comparable ICERs. The Bayesian models are calibrated through Bayesian calibration approaches, whereas the dODE is calibrated through a frequentist probabilistic calibration approach. When Bayesian calibration is conducted, an important advantage of the BMM is that the model runs 44 times faster than the BODE. Time series data on the number of people in the states in the first five years of follow-up are used for calibration. The corresponding outcomes

fit the data well; the ICERs result in values of £ 7,203, £ 6,055 and £ 6,288 in the dODE, BODE and BMM. The ICERs obtained through direct calibration approaches are very similar to those of the first analysis which is conducted without simulated data. The ICERs of the visual (not systematic) calibration approach differ considerably. Finally, we can conclude that the predictions of deterministic models including fixed parameter values can be considerably improved if the corresponding parameters are informed in a proper way (e.g. through multilinear loss functions), or if the model outcome is calibrated to time series data using a systematic calibration approach.

An important difference between the BMM and ODE-based models is the specification of time. If the Markov cycle length (the interval length of the follow-up) is specified properly considering the medical context, a discrete-time approach does not seem to impact the results since the model outcome with and without half-cycle correction is identical in all scenarios conducted. Furthermore, the results of the BMM and the BODE, which are based on discrete- and continous-time approaches, respectively, are basically identical.

7.2.2 Cost-effectiveness analysis of human papillomavirus vaccination

As shown in Chapter 6, our results indicate universal vaccination targeting the same age group (twelve years) to be an extremely cost-effective strategy in comparison to screening-only or to a single cohort of females vaccinated at the age of twelve years. The discounted costs per QALY gained correspond to € 1,500 (EVPI = € 3.7 per subject) and € 11,600 (EVPI = € 2.2 per subject), respectively. These values are well below the monetary threshold of sustainability for health interventions.

Moreover, recent research indicates that vaccinating individuals with only two doses of the HPV vaccine is sufficient to prevent HPV infection [236],

thus reducing vaccination expenses. The conservative vaccination schedule includes three doses for full protection; it therefore strengthens the evidence that universal vaccination can be a cost-effective intervention.

The HPV model differs from previous studies in six ways: i) incorporation of the full set of HPV-induced diseases (apart from recurrent respiratory papillomatosis (RRP)); ii) a lifelong duration of vaccine-induced immunity without booster application; iii) a comparatively low unit cost of vaccination; iv) a very high vaccine coverage rate; v) a comparatively low vaccine efficacy; and vi) a shorter follow-up of 55 years. Points i) - iii) contribute to lower ICER values, whereas points iv) - vi) tend to increase them.

The following four aspects seem to drive the results of the health economic evaluation [200, 254]:

- the dynamic force of infection, incorporating sexual mixing between females and males, thus automatically considering changes in mixing patterns and population prevalence over time. In contrast, a static force of infection in standard MMs only depends on covariates such as age;
- the inclusion of a high variety of HPV-induced diseases compared to other health economic evaluations which only account for cervical cancer [140, 339, 392];
- the assumption of lifelong immunity following initial HPV-vaccination with three doses, without the necessity of a booster application, in contrast to [140, 187, 277, 339, 392];
- the considerably low unit cost of vaccination compared to the official list price of the vaccine on the Italian market.

In the future, the benefits of HPV vaccination will be further increased since a nonavalent vaccine including genotypes 16, 18, 31, 33, 45, 52, 58, 6 and 11 is being developed. The preliminary results of the corresponding clinical

trials are promising [80]. Therefore, the cost-effectiveness of universal HPV vaccination is likely to further improve, creating added potential to optimise the control of HPV-induced diseases.

7.3 Conclusions

The BMM is a highly suitable approach for infectious disease modelling in a health economic context for a variety of reasons. Decision makers are commonly familiar with MMs. At the same time, the shortcoming of standard MMs which are static by definition is avoided; including the effects of herd immunity is essential when pathogens transmissible between humans are modelled to obtain realistic results. In the Bayesian setting, parameter uncertainty is accounted for, and PSA can be conducted straightforwardly by means of the probabilistic model output. Furthermore, in the BMM, the disadvantages of ODE-based models such as the commonly fixed parameter values (often informed through point estimates), the related difficulties in conducting PSA, the necessity of numerical approximations to solutions and the corresponding errors do not play a role. Through the case study, we clearly show that our methodology realistically accounts for population dynamics and changes in population prevalence over time; the prevalence outcome of the BODE and the BMM are basically identical.

Our methodology is especially suitable to conduct a cost-effectiveness analysis of HPV vaccination. Due to the nature of HPV, the model specification is considerably complex. In our HPV model, 58 states, 24 age cohorts, two sexual behaviour groups and the entering of new individuals are incorporated. In addition, parameter uncertainty is accounted for which is essential since several key parameters cannot be estimated with precision. For example, the probability of HPV transmission between sexual partners cannot be investigated in clinical trials due to ethical restrictions, and only observational studies can be conducted. The Bayesian framework enables

the inclusion of probability distributions. Under these conditions, the computational effort of the BMM is still manageable. In contrast to the BMM, at the current stage of research, a Bayesian ODE-based model including the same number of states and age cohorts would increase the computational effort to an extreme level. Even for programmers experienced in the language `C++` this would not be manageable [33].

In addition to the high number of advantages, our Bayesian methodology shows several limitations. The amount of parameter uncertainty is subject to the availability and quality of the literature to inform the model parameters; if no information is available, it depends on the knowledge of the medical experts consulted. A particular challenge is the estimation of measures related to quality of life, so-called utilities, especially in rare diseases. Data to inform utilities are commonly sparce or not available at all; if covariates such as sex have to be considered, expert opinion is often necessary. Another limitation is that it might be inevitable to include observable variables to estimate demographic data; these could be for example birth rates of newborns or age- and sex-specific death rates. As a consequence, no distributional assumptions on these parameters can be made, and they remain deterministic.

Appendix A

R code of the case study

In this appendix, we present the R code of the dODE, BODE and BMM for the systematic, direct calibration approaches described in Section 3.5.2. The dODE is implemented through one single R file. In contrast, the Bayesian models each consist of two files; these are R files to run the models, and text files containing the model codes in WinBUGS and JAGS, respectively. The text files are called from within R.

In the following, we present summary tables of the input parameters, data included, and outcome of the three models. Table A.1 is an extension of Table 3.1 and presents the names of the input parameters in the model code. These were chosen as self-explanatory as possible, in accordance with the notation presented in Table 3.1.

To update non-informative priors into the corresponding posteriors and to calibrate the model outcome, simulated data are included into the models. These are summarized in Table A.2 and consist of individual-level data on the yearly numbers of partners as well as the numbers of observed people and people with events. The former are included in the Poisson-Gamma models, whereas the latter are used in the Beta-Binomial models. In addition, time series data on the numbers of people in the states over follow-up are relevant for the probabilistic calibration approaches. More specific information on these data is given in Section 3.4.

Table A.1: Overview of the names of the input parameters in the programme codes of the deterministic and probabilistic ODE systems as well as the Bayesian Markov model

Parameter	Description	Name in code	Parameter	Description	Name in code
ω_{MH}	Partner acquisition rate (high-risk males)	rmalH	α	Vaccine coverage parameter	pi
ω_{ML}	Partner acquisition rate (low-risk males)	rmalL	γ	Vaccine efficacy parameter	eff
ω_{FH}	Partner acquisition rate (high-risk females)	rfemH	c_{screen}	Unit cost of screening in £	c.screen
ω_{FL}	Partner acquisition rate (low-risk females)	rfemL	c_{vac}	Unit cost of vaccination in £	c.vac
χ	Proliferation parameter	chi	c_{test}	Unit cost of STI test in £	c.test.sti
β	STI transmission probability per partnership	beta	c_{blood}	Unit cost of blood test in £	c.test.blood
$\pi_{2,3}$ and $\rho_{2,3}$	Transition parameter from state 2 to state 3	piia and rhoia	c_{treat}	Unit cost of treatment in £	c.trt
$\pi_{3,4}$ and $\rho_{3,4}$	Transition parameter from state 3 to state 4	piam and rhoam	c_{dis}	Unit cost of disease treatment in £	c.trt.dis
$\pi_{4,5}$ and $\rho_{4,5}$	Transition parameter from state 4 to state 5	pimd and rhomd	c_{gp}	Unit cost of visit to general practitioner in £	c.gp
$\pi_{1,5}$ and $\rho_{1,5}$	Transition parameter from state 1 to state 5	pisd and rhosd	u_2	Health utility of infected	u.inf
η	Probability of STI diagnosis	diag	u_3	Health utility of asymptomatic	u.asym
σ	Screening probability	screen	u_4	Health utility of morbid	u.morb

The outputs of the three models consist of the number of people in the states over follow-up, separately for the two sexes and behaviour groups. These are given in array form, including three dimensions. The corresponding numbering of the states in the dODE (shown in Table A.3) differs from the BODE and BMM (shown in Table A.4).

In the dODE, the first dimension consists of the number of parameter sets created (50,000), whereas the second dimension includes the year t of observation (100). The third dimension includes the states per sex and behaviour group, the overall sample size per sex and behaviour group as well as the respective year of follow-up, resulting in a value of 25. Thus, the

Table A.2: Overview of the data included in the models; only the time series data are included in the deterministic ODE system.

Data set	Description
datfemH	Individual-level data on yearly numbers of partners in high-risk females
datmalH	Individual-level data on yearly numbers of partners in high-risk males
datfemL	Individual-level data on yearly numbers of partners in low-risk females
datmalL	Individual-level data on yearly numbers of partners in low-risk males
popsize	Sample size in individual-level data on yearly numbers of partners
r.beta	Number of successes in STI transmission
n.beta	Number observed in terms of STI transmission
r.eff	Number of successes in vaccine efficacy
n.eff	Number observed in terms of vaccine efficacy
r.pi	Number covered by STI vaccine
n.pi	Number observed in terms of vaccine application
r.screen	Number of successes in screening
n.screen	Number observed in terms of screening
r.diag	Number of successes in diagnosis
n.diag	Number observed in terms of diagnosis
dat.sus.femH	Time series data on numbers of high-risk susceptible females
dat.inf.femH	Time series data on numbers of high-risk infected females
dat.asy.femH	Time series data on numbers of high-risk asymptomatic females
dat.mor.femH	Time series data on numbers of high-risk morbid females
dat.sus.malH	Time series data on numbers of high-risk susceptible males
dat.inf.malH	Time series data on numbers of high-risk infected males
dat.asy.malH	Time series data on numbers of high-risk asymptomatic males
dat.mor.malH	Time series data on numbers of high-risk morbid males

overall size of the array *output_dode* is $50,000 \times 100 \times 25$. The parameter set with best fit is selected through model calibration and corresponds to the least sum of squared errors. This is indicated by the index gof in the first dimension of the array. For example, the number of high-risk susceptible females per year of follow-up is given by *output_dode[gof,t,2]*. The numbering of all states (in the third dimension) is shown in Table A.3. The array *output_dode* only includes the results of the intervention screening; the results of the intervention vaccination are stored in the data frame *dode_vac* with rows representing year t and columns representing the states; the numbering of the states is identical to *output_dode*.

The arrays *solution* and *y* contain the output of the BODE and BMM, respectively. Their dimensions differ from *output_dode*; *solution* and *y* include the years of follow-up t (100) and the states per sex and behaviour group

Table A.3: Overview of the numbering of the states in the output of the deterministic ODE system

Deterministic ODE-based model			
Output	**Description**	**Output**	**Description**
output_dode[gof,t,2]	High-risk susceptible females	output_dode[gof,t,12]	Low-risk susceptible females
output_dode[gof,t,3]	High-risk infected females	output_dode[gof,t,13]	Low-risk infected females
output_dode[gof,t,4]	High-risk asympt. females	output_dode[gof,t,14]	Low-risk asympt. females
output_dode[gof,t,5]	High-risk morbid females	output_dode[gof,t,15]	Low-risk morbid females
output_dode[gof,t,6]	High-risk dead females	output_dode[gof,t,16]	Low-risk dead females
output_dode[gof,t,7]	High-risk susceptible males	output_dode[gof,t,17]	Low-risk susceptible males
output_dode[gof,t,8]	High-risk infected males	output_dode[gof,t,18]	Low-risk infected males
output_dode[gof,t,9]	High-risk asympt. males	output_dode[gof,t,19]	Low-risk asympt. males
output_dode[gof,t,10]	High-risk morbid males	output_dode[gof,t,20]	Low-risk morbid males
output_dode[gof,t,11]	High-risk dead males	output_dode[gof,t,21]	Low-risk dead males

Table A.4: Overview of the numbering of the states in the output of the probabilistic ODE system and the Bayesian Markov model

Bayesian ODE-based and Bayesian Markov model			
Output	**Description**	**Output**	**Description**
solution[t,1,i] and y[t,1,i]	Low-risk susceptible females	solution[t,11,i] and y[t,11,i]	Low-risk susceptible males
solution[t,2,i] and y[t,2,i]	Low-risk infected females	solution[t,12,i] and y[t,12,i]	Low-risk infected males
solution[t,3,i] and y[t,3,i]	Low-risk asymptomatic females	solution[t,13,i] and y[t,13,i]	Low-risk asymptomatic males
solution[t,4,i] and y[t,4,i]	Low-risk morbid females	solution[t,14,i] and y[t,14,i]	Low-risk morbid males
solution[t,5,i] and y[t,5,i]	Low-risk dead females	solution[t,15,i] and y[t,15,i]	Low-risk dead males
solution[t,6,i] and y[t,6,i]	High-risk susceptible females	solution[t,16,i] and y[t,16,i]	High-risk susceptible males
solution[t,7,i] and y[t,7,i]	High-risk infected females	solution[t,17,i] and y[t,17,i]	High-risk infected males
solution[t,8,i] and y[t,8,i]	High-risk asymptomatic females	solution[t,18,i] and y[t,18,i]	High-risk asymptomatic males
solution[t,9,i] and y[t,9,i]	High-risk morbid females	solution[t,19,i] and y[t,19,i]	High-risk morbid males
solution[t,10,i] and y[t,10,i]	High-risk dead females	solution[t,20,i] and y[t,20,i]	High-risk dead males

(20) per intervention i (2). Thus, the overall array size is $100 \times 20 \times 2$. The second dimension represents the numbering of the states. For example, the number of low-risk susceptible females in year t in intervention i (1=screening, 2=vaccination) is given by *solution[t,1,i]* and *y[t,1,i]* in the BODE and BMM, respectively. The numbering of all states is listed in Table A.4.

A.1 The deterministic ODE-based model

The dODE is implemented by means of the `R`-package `EpiModel`. In order to select a parameter set with best fit to the time series data, 50,000 parameter sets are created through forward sampling. In the intervention screening,

the model is run for each parameter set, and the parameter set corresponding to the least sum of squared errors is identified as described in Section 3.5.2. In the intervention vaccination, the model is only run once since we assume that no data are available for calibration.

```
#save start of run time
ptm <- proc.time()
#set seed
set.seed(2188)
#set working directory
setwd("C:/Users/katrin/Dropbox/TestModel/R code and CE results/
    Comparison MSM and ODE/Final code/ThesisAppendix/")
#function to estimate shape and rate parameters of the gamma
    distribution when mean and standard deviation are known
gammaPar <- function(m,s){
  a <- (m^2)/(s^2)
  b <- m/(s^2)
   list(a=a,b=b)
}
#estimating shape and rate of gamma distribution of partner
    acquisition rate in high-risk females
mean.datfemH=9
sd.datfemH=1.026698
alpha.datfemH=gammaPar(mean.datfemH,sd.datfemH)$a
beta.datfemH=gammaPar(mean.datfemH,sd.datfemH)$b
#partner acquisition rate in low-risk females
mean.datfemL=1.958
sd.datfemL=0.7857932
alpha.datfemL=gammaPar(mean.datfemL,sd.datfemL)$a
beta.datfemL=gammaPar(mean.datfemL,sd.datfemL)$b
#partner acquisition rate in high-risk males
mean.datmalH=9.058
sd.datmalH=1.075616
alpha.datmalH=gammaPar(mean.datmalH,sd.datmalH)$a
beta.datmalH=gammaPar(mean.datmalH,sd.datmalH)$b
#partner acquisition rate in low-risk males
```

```
mean.datmalL=2.976
sd.datmalL=0.7158554
alpha.datmalL=gammaPar(mean.datmalL,sd.datmalL)$a
beta.datmalL=gammaPar(mean.datmalL,sd.datmalL)$b
####creation of 50,000 parameter sets
nsets=50000
#array for results of outputs of dODE
output_dode=array(0,c(nsets,100,25))
#distributions of partner acquisition rates
rfemH.dode=rgamma(nsets,alpha.datfemH,beta.datfemH)
rfemL.dode=rgamma(nsets,alpha.datfemL,beta.datfemL)
rmalH.dode=rgamma(nsets,alpha.datmalH,beta.datmalH)
rmalL.dode=rgamma(nsets,alpha.datmalL,beta.datmalL)
#distribution of reproduction rate
chi.dode=rgamma(nsets,1111.1,111111.1)
#distributions of transition rates
rhoia.dode=rgamma(nsets,25600,32000)
rhoam.dode=rgamma(nsets,2025,22500)
rhomd.dode=rgamma(nsets,0.6944444,69.44444)
rhosd.dode=rgamma(nsets,156.25,312500)
#distribution of STI transmission probabilities
beta.dode=rbeta(nsets,16.20667,108.46)
#distribution of probabilities of diagnosis
diag.dode=rbeta(nsets,809.1,89.9)
#distribution of screening probabilities
screen.dode=rbeta(nsets,809.1,89.9)
#distribution of vaccine coverage probability
pi.dode=rbeta(nsets,809.1,89.9)
#sets of vaccine efficacy
eff.dode=rbeta(nsets,809.1,89.9)
#distributions of costs
c.screen.dode=rlnorm(nsets,2.996,0.693)
c.vac.dode=rlnorm(nsets,5.518352,0.07986607)
c.test.sti.dode=rlnorm(nsets,2.996,0.03)
c.test.blood.dode=rlnorm(nsets,3.401,0.03)
c.trt.dode=rlnorm(nsets,4.258597,0.8325546)
```

```
65 c.trt.dis.dode=rlnorm(nsets,6.194998,0.1980422)
66 c.gp.dode=rlnorm(nsets,3.912,0.02)
67 #distributions of health utilities
68 u.inf.dode=rbeta(nsets,1469.3,629.7)
69 u.asym.dode=rbeta(nsets,1439.4,959.6)
70 u.morb.dode=rbeta(nsets,629.7,1469.3)
71 ###dODE implemented through R package EpiModel
72 #loading package including ODE solver
73 library(deSolve)
74 #loading package to implement ODE system
75 library(EpiModel)
76 #Function containing the ODEs; t and t0 are defined by function
       call of control.dcm; parms are defined by params in function
       call of dcm; function is called separately for both
       interventions
77 Qmod <- function(t, t0, parms) {
78   #t0 and parms defined as list
79   with(as.list(c(t0, parms)), {
80     #Dynamic Calculations
81     #Sample size in high-risk females, high-risk males, low-risk
      females and low-risk males: those who are alive (all states
      apart from Death)
82     nfemH = sfemH+ifemH+afemH+mfemH
83     nmalH = smalH+imalH+amalH+mmalH
84     nfemL = sfemL+ifemL+afemL+mfemL
85     nmalL = smalL+imalL+amalL+mmalL
86     #probability to select a female partner from the high-risk
      group
87     gfemH = (rfemH.dode*nfemH)/((rfemH.dode*nfemH)+(rfemL.dode*
      nfemL))
88     #probability to select a female partner from the low-risk
      group
89     gfemL = 1-gfemH
90     #probability to select a male partner from the high-risk group
91     gmalH = (rmalH.dode*nmalH)/((rmalH.dode*nmalH)+(rmalL.dode*
      nmalL))
```

```
92    #probability to select a male partner from the low-risk group
93    gmalL = 1-gmalH
94    #prevalence in females: weighted average of infecteds in the
      high- and low-risk groups
95    pfem = gfemH*(ifemH/nfemH)+gfemL*(ifemL/nfemL)
96    #prevalence in males: weighted average of infected males in
      the high- and low-risk groups
97    pmal = gmalH*(imalH/nmalH)+gmalL*(imalL/nmalL)
98    # Force of infection according to sex and risk group. In
      intervention STI screening, pi.ode=1 and eff.dode=0; therefore,
       only first term of sum is considered.
99    # In intervention vaccination, force of infection is reduced
      by those who are covered (pi.dode) by (1-eff.dode).
100   lambdafemH <- (pi.dode*(1-eff.dode)*(beta.dode*rfemH.dode*pmal
      ))+((1-pi.dode)*(beta.dode*rfemH.dode*pmal))
101   lambdafemL <- (pi.dode*(1-eff.dode)*(beta.dode*rfemL.dode*pmal
      ))+((1-pi.dode)*(beta.dode*rfemL.dode*pmal))
102   lambdamalH <- (pi.dode*(1-eff.dode)*(beta.dode*rmalH.dode*pfem
      ))+((1-pi.dode)*(beta.dode*rmalH.dode*pfem))
103   lambdamalL <- (pi.dode*(1-eff.dode)*(beta.dode*rmalL.dode*pfem
      ))+((1-pi.dode)*(beta.dode*rmalL.dode*pfem))
104   #Differential Equations
105   #High-risk females
106   dSfemH = chi.dode*nfemH-lambdafemH*sfemH-rhosd.dode*sfemH
107   dIfemH = lambdafemH*sfemH-rhoia.dode*ifemH-rhosd.dode*ifemH
108   dAfemH = rhoia.dode*ifemH-rhoam.dode*afemH-rhosd.dode*afemH
109   dMfemH = rhoam.dode*afemH-rhomd.dode*mfemH-rhosd.dode*mfemH
110   dDfemH =  rhomd.dode*mfemH+rhosd.dode*nfemH
111   #Low-risk females
112   dSfemL = chi.dode*nfemL-lambdafemL*sfemL-rhosd.dode*sfemL
113   dIfemL = lambdafemL*sfemL-rhoia.dode*ifemL-rhosd.dode*ifemL
114   dAfemL = rhoia.dode*ifemL-rhoam.dode*afemL-rhosd.dode*afemL
115   dMfemL = rhoam.dode*afemL-rhomd.dode*mfemL-rhosd.dode*mfemL
116   dDfemL =  rhomd.dode*mfemL+rhosd.dode*nfemL
117   #High-risk males
118   dSmalH = chi.dode*nmalH-lambdamalH*smalH-rhosd.dode*smalH
```

```
119      dImalH = lambdamalH*smalH-rhoia.dode*imalH-rhosd.dode*imalH
120      dAmalH = rhoia.dode*imalH-rhoam.dode*amalH-rhosd.dode*amalH
121      dMmalH = rhoam.dode*amalH-rhomd.dode*mmalH-rhosd.dode*mmalH
122      dDmalH =  rhomd.dode*mmalH+rhosd.dode*nmalH
123      #Low-risk males
124      dSmalL = chi.dode*nmalL-lambdamalL*smalL-rhosd.dode*smalL
125      dImalL = lambdamalL*smalL-rhoia.dode*imalL-rhosd.dode*imalL
126      dAmalL = rhoia.dode*imalL-rhoam.dode*amalL-rhosd.dode*amalL
127      dMmalL = rhoam.dode*amalL-rhomd.dode*mmalL-rhosd.dode*mmalL
128      dDmalL =  rhomd.dode*mmalL+rhosd.dode*nmalL
129      #Output: number of individuals in the states per covariate,
         sample size per covariate, for the whole observation time
         period
130      list(c(dSfemH, dIfemH, dAfemH, dMfemH, dDfemH,
131             dSmalH, dImalH, dAmalH, dMmalH, dDmalH,
132             dSfemL, dIfemL, dAfemL, dMfemL, dDfemL,
133             dSmalL, dImalL, dAmalL, dMmalL, dDmalL),
134           nfemH = nfemH, nfemL = nfemL, nmalH = nmalH,
135           nmalL = nmalL)
136   })
137 }
138 #initialization through function call init.dcm:
139 init <- init.dcm(sfemH=100000-60, ifemH=60, afemH=0, mfemH=0,
       dfemH=0, smalH=100000-60, imalH=60, amalH=0, mmalH=0, dmalH=0,
       sfemL=400000-240, ifemL=240, afemL=0, mfemL=0, dfemL=0, smalL
       =400000-240, imalL=240, amalL=0, mmalL=0, dmalL=0)
140 #Function call of control.dcm: nsteps: number of time steps the
       model is solved for (100), new.mod: since no built-in model is
       run, function Qmod containing the model is specified
141 control <- control.dcm(nsteps = 100, new.mod = Qmod)
142 #calling function Qmod for each of the 50,000 parameter sets
143 for (s in 1:nsets){
144 param <- param.dcm(rfemH.dode = rfemH.dode[s], rfemL.dode= rfemL.
       dode[s], rmalH.dode = rmalH.dode[s], rmalL.dode = rmalL.dode[s
       ], chi.dode = chi.dode[s], beta.dode=beta.dode[s], rhoia.dode=
       rhoia.dode[s], rhoam.dode=rhoam.dode[s], rhomd.dode=rhomd.dode[
```

```
    s], rhosd.dode=rhosd.dode[s], eff.dode=0, pi.dode=1)
#parameter transfer, initialization, specification of observation
    time horizon and model through call of dcm function
mod <- dcm(param, init, control)
#output is saved in data frame dode
dode = as.data.frame(mod)
#transformation of data frame to matrix
dode2=as.matrix(dode)
#outputs of all 50,000 model runs are saved in output_dode
output_dode[s,,]=dode2
}
###GOF calculation
#sum of squared errors of model outcome in first 5 years of
    observation time and time series data dat
#dat.sus.femH[t]: number of susceptible high-risk females at time
    t
#dat.inf.femH[t]: number of infected high-risk females at time t
#dat.asy.femH[t]: number of asymptomatic high-risk females at time
     t
#dat.mor.femH[t]: number of morbid high-risk females at time t
#notation for males is equivalent
gof=((dat.sus.femH[1] - output_dode[,1,2])^2 + (dat.sus.femH[2]
- output_dode[,2,2])^2 + (dat.sus.femH[3] - output_dode[,3,2])^2
+ (dat.sus.femH[4] - output_dode[,4,2])^2 + (dat.sus.femH[5]
- output_dode[,5,2])^2 + (dat.inf.femH[1] - output_dode[,1,3])^2
+ (dat.inf.femH[2] - output_dode[,2,3])^2 + (dat.inf.femH[3]
- output_dode[,3,3])^2 + (dat.inf.femH[4] - output_dode[,4,3])^2
+ (dat.inf.femH[5] - output_dode[,5,3])^2 + (dat.asy.femH[1]
- output_dode[,1,4])^2 + (dat.asy.femH[2] - output_dode[,2,4])^2
+ (dat.asy.femH[3] - output_dode[,3,4])^2 + (dat.asy.femH[4]
- output_dode[,4,4])^2 + (dat.asy.femH[5] - output_dode[,5,4])^2
+ (dat.mor.femH[1] - output_dode[,1,5])^2 + (dat.mor.femH[2]
- output_dode[,2,5])^2 + (dat.mor.femH[3] - output_dode[,3,5])^2
+ (dat.mor.femH[4] - output_dode[,4,5])^2 + (dat.mor.femH[5]
- output_dode[,5,5])^2 + (dat.sus.malH[1] - output_dode[,1,7])^2
+ (dat.sus.malH[2] - output_dode[,2,7])^2 + (dat.sus.malH[3]
```

```
176 - output_dode[,3,7])^2 + (dat.sus.malH[4] - output_dode[,4,7])^2
177 + (dat.sus.malH[5] - output_dode[,5,7])^2 + (dat.inf.malH[1]
178 - output_dode[,1,8])^2 + (dat.inf.malH[2] - output_dode[,2,8])^2
179 + (dat.inf.malH[3] - output_dode[,3,8])^2 + (dat.inf.malH[4]
180 - output_dode[,4,8])^2 + (dat.inf.malH[5] - output_dode[,5,8])^2
181 + (dat.asy.malH[1] - output_dode[,1,9])^2 + (dat.asy.malH[2]
182 - output_dode[,2,9])^2 + (dat.asy.malH[3] - output_dode[,3,9])^2
183 + (dat.asy.malH[4] - output_dode[,4,9])^2 + (dat.asy.malH[5]
184 - output_dode[,5,9])^2 + (dat.mor.malH[1] - output_dode[,1,10])
185 ^2 + (dat.mor.malH[2] - output_dode[,2,10])^2 + (dat.mor.malH[3]
186 - output_dode[,3,10])^2 + (dat.mor.malH[4] - output_dode[,4,10])
187 ^2 + (dat.mor.malH[5] - output_dode[,5,10])^2)
188 #selecting the parameter set with the least sum of squared errors
189 index=which(gof == min(gof))
190 #save the end of model run time
191 time=proc.time()-ptm
192 #save the outputs of the 50,000 model runs, the GOF-statistics,
    and the index with the least sum of squared errors
193 save(output_dode,gof,index,file="dode.RData")
194 ####vaccination
195 #No time series data are available for the vaccination scenario;
    thus, the parameters are not selected through calibration, and
    informed by the means of the distributions.
196 param_vac <- param.dcm(rfemH.dode = mean(rfemH.dode), rfemL.dode=
    mean(rfemL.dode), rmalH.dode = mean(rmalH.dode),
197 rmalL.dode = mean(rmalL.dode), chi.dode = mean(chi.dode), beta.
    dode=mean(beta.dode), rhoia.dode = mean(rhoia.dode), rhoam.dode
    = mean(rhoam.dode), rhomd.dode=mean(rhomd.dode), rhosd.dode =
    mean(rhosd.dode), eff.dode=mean(eff.dode), pi.dode=mean(pi.dode
    ))
198 #function call of Qmod
199 mod_vac <- dcm(param_vac, init, control)
200 #saving outcome as data frame
201 dode_vac = as.data.frame(mod_vac)
```

A.2 The Bayesian ODE-based model

The Bayesian ODE-based model is implemented in the WinBUGS interface WBDiff and linked to R through the package R2WinBUGS. Bayesian calibration takes place directly in the model by assigning Poisson distributions to time series data. The event rates correspond to the model outcome on the number of high-risk people in the states as described in Section 3.5.2. The code of the BODE consists of two files; these include an R script and a text file containing the WinBUGS model which is called from inside R. The text file is called Model_BODE.txt and has to be saved in a separate file in order to run the model.

```
#save start of computation time
ptm=proc.time()
#set working directory
setwd("C:/Users/katrin/Dropbox/TestModel/R code and CE results/
    Comparison MSM and ODE/Final code/ThesisAppendix/")
#Interface connecting R to WinBUGS
library(R2WinBUGS)
#load workspace including individual-level data to update priors
load("WS.RData")
#load workspace including time series data for Bayesian model
    calibration
load("States_Data_New2.RData")
#text file including the WinBUGS code
model.file="Model_BODE.txt"
#data input, n.grid: number of time points estimated, dim: number
    of states, origin: observation start at t=1, tol= tolerance
    level, grid= observation time horizon, datfemH=individual-level
     data on yearly numbers of partners in high-risk females (
    similar for the other sex and risk group), popsize=sample size
    in data on partner acquisition rates, r.beta=number of people
    who became infected, n.beta=number of people observed (similar
    for vaccine coverage, efficacy, screening, and diagnosis), dat.
    sus.femH=time series data on number of high-risk susceptible
```

```
    females (similar for other states and high-risk males)
dataWin <- list(n.grid = 100, dim = 20, origin = 1, tol = 0.001,
    grid = seq(1,100,1), datfemH = datfemH, datmalH = datmalH,
    datfemL = datfemL, datmalL = datmalL, popsize = popsize, r.beta
     = r.beta, n.beta = n.beta, r.eff = r.eff, n.eff = n.eff, r.pi
    = r.pi, n.pi = n.pi, r.screen = r.screen, n.screen = n.screen,
    r.diag = r.diag, n.diag = n.diag, dat.sus.femH = dat.sus.femH,
    dat.inf.femH = dat.inf.femH, dat.asy.femH = dat.asy.femH, dat.
    mor.femH = dat.mor.femH, dat.sus.malH = dat.sus.malH, dat.inf.
    malH = dat.inf.malH, dat.asy.malH = dat.asy.malH, dat.mor.malH
    = dat.mor.malH)
#parameter initialization
inits <- function(){ list(rfemH=runif(1), rfemL=runif(1), rmalL=
    runif(1), chi=runif(1), beta=runif(1), eff=runif(1), pi=runif
    (1), screen=runif(1), diag=runif(1))
}
#parameters, solution: outcome on the number of people in the
    states over follow-up for both sexes and risk groups, r:
    partner acquisition rates, chi: reproduction rate, rho:
    transition rates, beta: probability of STI transmission, pi:
    vaccine coverage, eff: vaccine efficacy, screen: probability of
     screening, diag: probability of diagnosis, c: costs, u:
    utilities
parameters <- c("solution", "rfemH", "rfemL", "rmalH", "rmalL", "
    chi", "rhoia", "rhoam", "rhomd", "rhosd", "beta", "pi", "eff",
    "screen", "diag", "c.screen", "c.vac", "c.test.sti", "c.test.
    blood", "c.trt", "c.trt.dis", "c.gp", "u.inf", "u.asym", "u.
    morb")
#run the model for 2 chains, 1000 simulations, without thinning
simODE <- bugs(data=dataWin, inits=inits ,parameters.to.save=
    parameters, model.file=model.file , n.chains=2, n.iter=1000, n.
    thin=1, DIC=F, debug=F, bugs.directory="c:/Program Files/
    winbugs14/WinBUGS14/")
#attach output to R
attach.bugs(simODE)
#save end of computation time
```

```
time=proc.time()-ptm

###WinBUGS model file Model_BODE.txt --> has to be saved in
    separate text file
model{
#define ODEs in WBDiff syntax
solution[1:n.grid,1:dim,1:2]<-ode(init[1:dim,1:2],grid[1:n.grid],D
    (y[1:dim,1:2],t),origin,tol)
#for interventions i=1 (screening only) and i=2 (vaccination)
for(i in 1:2){
#ODEs for low-risk females
#Susceptible
D(y[1,i],t) <-chi*nfemL[i]-lambdafemL[i]*y[1,i]-rhosd*y[1,i]
#Infected
D(y[2,i],t) <-lambdafemL[i]*y[1,i]-rhoia*y[2,i]-rhosd*y[2,i]
#Asymptomatic
D(y[3,i],t) <-rhoia*y[2,i]-rhoam*y[3,i]-rhosd*y[3,i]
#Morbid
D(y[4,i],t) <-rhoam*y[3,i]-rhomd*y[4,i]-rhosd*y[4,i]
#Dead
D(y[5,i],t) <-rhosd*nfemL[i]+rhomd*y[4,i]
#ODEs for high-risk females
#Susceptible
D(y[6,i],t) <-chi*nfemH[i]-lambdafemH[i]*y[6,i]-rhosd*y[6,i]
#Infected
D(y[7,i],t) <-lambdafemH[i]*y[6,i]-rhoia*y[7,i]-rhosd*y[7,i]
#Asymptomatic
D(y[8,i],t) <-rhoia*y[7,i]-rhoam*y[8,i]-rhosd*y[8,i]
#Morbid
D(y[9,i],t) <-rhoam*y[8,i]-rhomd*y[9,i]-rhosd*y[9,i]
#Dead
D(y[10,i],t) <-rhosd*nfemH[i]+rhomd*y[9,i]
#ODEs for low-risk males
#Susceptible
D(y[11,i],t) <-chi*nmalL[i]-lambdamalL[i]*y[11,i]-rhosd*y[11,i]
#Infected
```

```
59 D(y[12,i],t) <-lambdamalL[i]*y[11,i]-rhoia*y[12,i]-rhosd*y[12,i]
60 #Asymptomatic
61 D(y[13,i],t) <-rhoia*y[12,i]-rhoam*y[13,i]-rhosd*y[13,i]
62 #Morbid
63 D(y[14,i],t) <-rhoam*y[13,i]-rhomd*y[14,i]-rhosd*y[14,i]
64 #Dead
65 D(y[15,i],t) <-rhosd*nmalL[i]+rhomd*y[14,i]
66 #ODEs for high-risk males
67 #Susceptible
68 D(y[16,i],t) <-chi*nmalH[i]-lambdamalH[i]*y[16,i]-rhosd*y[16,i]
69 #Infected
70 D(y[17,i],t) <-lambdamalH[i]*y[16,i]-rhoia*y[17,i]-rhosd*y[17,i]
71 #Asymptomatic
72 D(y[18,i],t) <-rhoia*y[17,i]-rhoam*y[18,i]-rhosd*y[18,i]
73 #Morbid
74 D(y[19,i],t) <-rhoam*y[18,i]-rhomd*y[19,i]-rhosd*y[19,i]
75 #Dead
76 D(y[20,i],t) <-rhosd*nmalH[i]+rhomd*y[19,i]
77 #number of low-risk females alive
78 nfemL[i] <- y[1,i]+y[2,i]+y[3,i]+y[4,i]
79 #number of high-risk females alive
80 nfemH[i] <- y[6,i]+y[7,i]+y[8,i]+y[9,i]
81 #number of low-risk males alive
82 nmalL[i]<-y[11,i]+y[12,i]+y[13,i]+y[14,i]
83 #number of high-risk males alive
84 nmalH[i]<-y[16,i]+y[17,i]+y[18,i]+y[19,i]
85 #probability of selecting a high-risk male partner
86 gmalH[i] <- (rmalH*nmalH[i])/(rmalH*nmalH[i]+rmalL*nmalL[i])
87 #probability of selecting a low-risk male partner
88 gmalL[i] <- 1-gmalH[i]
89 #probability of selecting a high-risk female partner
90 gfemH[i] <- (rfemH*nfemH[i])/(rfemH*nfemH[i]+rfemL*nfemL[i])
91 #probability of selecting a low-risk female partner
92 gfemL[i] <- 1-gfemH[i]
93 #prevalence in males
94 pmal[i] <- gmalH[i]*(y[17,i]/nmalH[i])+gmalL[i]*(y[12,i]/nmalL[i])
```

```
95 #prevalence in females
96 pfem[i] <- gfemH[i]*(y[7,i]/nfemH[i])+gfemL[i]*(y[2,i]/nfemL[i])
97 #intervention screening: vaccine coverage (pi2=1), vaccine
       efficacy (eff2=0), intervention vaccination: vaccine coverage (
       pi2=pi), vaccine efficacy (eff2=eff)
98 pi2[i]<-pi*step(i-1.1)+(1-step(i-1.1))
99 eff2[i]<-eff*step(i-1.1)
100 #force of infection in the two risk groups and sexes
101 lambdafemL[i] <-pi2[i]*(1-eff2[i])*beta*rfemL*pmal[i]+(1-pi2[i])*
       beta*rfemL*pmal[i]
102 lambdafemH[i] <-pi2[i]*(1-eff2[i])*beta*rfemH*pmal[i]+(1-pi2[i])*
       beta*rfemH*pmal[i]
103 lambdamalL[i] <-pi2[i]*(1-eff2[i])*beta*rmalL*pfem[i]+(1-pi2[i])*
       beta*rmalL*pfem[i]
104 lambdamalH[i] <-pi2[i]*(1-eff2[i])*beta*rmalH*pfem[i]+(1-pi2[i])*
       beta*rmalH*pfem[i]
105 }
106 #Initial conditions intervention screening-only:
107 init[1,1] <- 399760; init[2,1] <- 240; init[3,1] <- 0; init[4,1]
       <- 0; init[5,1] <- 0; init[6,1] <- 99940; init[7,1] <- 60; init
       [8,1] <- 0; init[9,1] <- 0; init[10,1] <- 0; init[11,1] <-
       399760; init[12,1] <- 240; init[13,1] <- 0; init[14,1] <- 0;
       init[15,1] <- 0; init[16,1] <- 99940; init[17,1] <- 60; init
       [18,1]<- 0; init[19,1] <- 0; init[20,1] <- 0
108 #initial conditions intervention vaccination are equivalent
109 init[1,2]<-init[1,1]; init[2,2]<-init[2,1]; init[3,2]<-init[3,1];
       init[4,2]<-init[4,1]; init[5,2]<-init[5,1]; init[6,2]<-init
       [6,1]; init[7,2]<-init[7,1]; init[8,2]<-init[8,1]; init[9,2]<-
       init[9,1]; init[10,2]<-init[10,1]; init[11,2]<-init[11,1]; init
       [12,2]<-init[12,1]; init[13,2]<-init[13,1]; init[14,2]<-init
       [14,1]; init[15,2]<-init[15,1]; init[16,2]<-init[16,1]; init
       [17,2]<-init[17,1]; init[18,2]<-init[18,1];
110 init[19,2]<-init[19,1]; init[20,2]<-init[20,1]
111 #Poisson-gamma model on partner acquisition rates
112 for(i in 1:popsize) {
113 datfemH[i] ~ dpois(rfemH)
```

```
datfemL[i] ~ dpois(rfemL)
datmalH[i] ~ dpois(rmalH)
datmalL[i] ~ dpois(rmalL)
}
#non-informative priors on partner acquisition rates
rfemH ~ dgamma(0.1,0.1)
rfemL ~ dgamma(0.1,0.1)
rmalH ~ dgamma(0.1,0.1)
rmalL ~ dgamma(0.1,0.1)
#informative prior on reproduction rate
chi~dgamma(1111.1,111111.1)
#informative prior on transition rate infected --> asymptomatic
rhoia~dgamma(25600,32000)
#informative prior on transition rate asymptomatic --> morbid
rhoam~dgamma(2025,22500)
#informative prior on transition rate morbid --> dead
rhomd~dgamma(1600,40000)
#informative prior on transition rate susceptible --> dead
rhosd~dgamma(156.25,312500)
#beta-binomial model on HPV transmission probability per
    partnership
r.beta ~ dbin(beta,n.beta)
beta ~ dbeta(0.5,0.5)
#beta-binomial model on vaccine coverage
r.pi ~ dbin(pi,n.pi)
pi ~ dbeta(0.5,0.5)
#beta-binomial model on vaccine efficacy
r.eff ~ dbin(eff,n.eff)
eff ~ dbeta(0.5,0.5)
#beta-binomial model on probability of diagnosis
r.diag ~ dbin(diag,n.diag)
diag ~ dbeta(0.5,0.5)
#beta-binomial model on probability of screening. r.screen: number
     of events, n.screen: sample size
r.screen ~ dbin(screen,n.screen)
screen ~ dbeta(0.5,0.5)
```

```
148 #Bayesian model calibration through data on the number of
        susceptibles, infecteds, asymptomatics, and morbids in high-
        risk females and males. These are count data and therefore
        modelled through poisson distributions. This is done for the
        first time point of follow-up.
149 dat.sus.femH[1] ~ dpois(init[6,1])
150 dat.inf.femH[1] ~ dpois(init[7,1])
151 dat.asy.femH[1] ~ dpois(init[8,1])
152 dat.mor.femH[1] ~ dpois(init[9,1])
153 dat.sus.malH[1] ~ dpois(init[16,1])
154 dat.inf.malH[1] ~ dpois(init[17,1])
155 dat.asy.malH[1] ~ dpois(init[18,1])
156 dat.mor.malH[1] ~ dpois(init[19,1])
157 #Data for time points 2-5 are also available and used to calibrate
        high-risk individuals in four of the states. The constraint (
        maximum) was included due to a computational issue, is not
        relevant and can be omitted.
158   for (n in 2:5){
159     conssusfemH[n] <- max(0.1,solution[n,6,1])
160     dat.sus.femH[n] ~ dpois(conssusfemH[n])
161     consinffemH[n] <- max(0.1,solution[n,7,1])
162     dat.inf.femH[n] ~ dpois(consinffemH[n])
163     consasyfemH[n] <- max(0.1,solution[n,8,1])
164     dat.asy.femH[n] ~ dpois(consasyfemH[n])
165     consmorfemH[n] <- max(0.1,solution[n,9,1])
166     dat.mor.femH[n] ~ dpois(consmorfemH[n])
167     conssusmalH[n] <- max(0.1,solution[n,16,1])
168     dat.sus.malH[n] ~ dpois(conssusmalH[n])
169     consinfmalH[n] <- max(0.1,solution[n,17,1])
170     dat.inf.malH[n] ~ dpois(consinfmalH[n])
171     consasymalH[n] <- max(0.1,solution[n,18,1])
172     dat.asy.malH[n] ~ dpois(consasymalH[n])
173     consmormalH[n] <- max(0.1,solution[n,19,1])
174     dat.mor.malH[n] ~ dpois(consmormalH[n])
175 }
176 ###informative priors on costs and utilities
```

```
177 tau.screen<-1/pow(0.693,2)
178 c.screen ~ dlnorm(2.996,tau.screen)
179 tau.vac<-1/pow(0.07986607,2)
180 c.vac ~ dlnorm(5.518352,tau.vac)
181 tau.test.sti<-1/pow(0.03,2)
182 c.test.sti ~ dlnorm(2.996,tau.test.sti)
183 tau.test.blood<-1/pow(0.03,2)
184 c.test.blood ~ dlnorm(3.401,tau.test.blood)
185 tau.trt<-1/pow(0.8325546,2)
186 c.trt ~ dlnorm(4.258597,tau.trt)
187 tau.trt.dis<-1/pow(0.1980422,2)
188 c.trt.dis ~ dlnorm(6.194998,tau.trt.dis)
189 tau.gp<-1/pow(0.02,2)
190 c.gp ~ dlnorm(3.912,tau.gp)
191 u.inf ~ dbeta(1469.3,629.7)
192 u.asym ~ dbeta(1439.4,959.6)
193 u.morb ~ dbeta(629.7,1469.3)
194 }
```

A.3 The Bayesian Markov model

In contrast to the BODE, the BMM is implemented `JAGS`, an alternative software to `WinBUGS`. `JAGS` is linked to `R` through the package `R2jags`. As for the BODE, Bayesian calibration takes place directly in the model by assigning Poisson distributions to time series data with event rates corresponding to the model outcome on the number of high-risk people in the states. As for the BODE, the code of the BMM consists of two files; these correspond to an `R` script and a text file containing the `JAGS` model which is called from inside `R`. The text file is called `Model_BMM.txt` and has to be saved in a separate file in order to run the model.

```
#saving the start time in ptm
ptm <- proc.time()
#set the seed for reproducable results
set.seed(2188)
#define working directory
working.dir="C:/Users/katrin/Dropbox/TestModel/R code and CE
    results/Comparison MSM and ODE/Final code/ThesisAppendix/"
#change path of working directory
setwd("C:/Users/katrin/Dropbox/TestModel/R code and CE results/
    Comparison MSM and ODE/Final code/ThesisAppendix/")
#load individual-level data on partner acquisition rates and data
    to inform the beta-binomial models
load("WS.RData")
#load workspace including time series data on number of people in
    states for calibration
load("States_Data_New2.RData")
#load library R2jags to connect R with JAGS
library(R2jags)
dataJags = list("A", "datfemH", "datfemL", "datmalH", "datmalL", "
    popsize", "r.beta", "n.beta", "r.diag", "n.diag", "r.screen", "
    n.screen", "r.pi", "n.pi", "r.eff", "n.eff", "dat.sus.femH", "
    dat.inf.femH", "dat.asy.femH", "dat.mor.femH", "dat.sus.malH",
    "dat.inf.malH", "dat.asy.malH", "dat.mor.malH")
#textfile containing the model, expected as input parameter when
    calling the function jags()
filein <- paste(working.dir,"Model_BMM.txt",sep="")
#initializing the parameters to prevent JAGS from assigning random
     values
inits <- function(){  list(rfemH=runif(1), rfemL=runif(1), rmalL=
    runif(1), chi=runif(1), piia=runif(1), piam=runif(1), pimd=
    runif(1), pisd=runif(1),beta=runif(1), diag=runif(1), screen=
    runif(1), pi=runif(1), eff=runif(1), c.screen=runif(1), c.vac=
    runif(1), c.test.sti=runif(1), c.test.blood=runif(1), c.trt=
    runif(1), c.trt.dis=runif(1), c.gp=runif(1), u.inf=runif(1), u.
    asym=runif(1), u.morb=runif(1))}
```

```
#the parameters monitored
params = c("y", "rfemH", "rfemL", "rmalH", "rmalL", "chi", "piia",
    "piam", "pimd", "pisd", "beta", "diag", "screen", "pi", "eff",
    "c.screen", "c.vac", "c.test.sti", "c.test.blood", "c.trt", "c
   .trt.dis", "c.gp", "u.inf", "u.asym", "u.morb")
#number of iterations
n.iter <- 600
#number of simulations discarded during the burn-in
n.burnin <- 100
#thinning step: no thinning is conducted
n.thin <- 1
#calling the function jags(), running 2 chains in parallel
sim <- jags(dataJags, inits, params, model.file=filein, n.chains
   =2, n.iter, n.burnin, n.thin,
  DIC=T, working.directory=working.dir, progress.bar="text", jags.
   module="dic")
#making the object sim available in R, containing the posterior
   distributions of the parameters
attach.jags(sim)
#saving the end of model run time
time=proc.time()-ptm

###JAGS model file Model_BMM.txt --> has to be saved in separate
   text file
model {
#y: array including the number of individuals per year in the
   states. The first dimension is the year of follow-up, whereas
   the second dimension is the state with 1=susceptible low-risk
   females, 2=infected low-risk females, 3=asymptomatic low-risk
   females, 4=morbid low-risk females, 5=dead low-risk females, 6=
   susceptible high-risk females, 7=infected high-risk females, 8=
   asymptomatic high-risk females, 9=morbid high-risk females, 10=
   dead high-risk females, 11=susceptible low-risk males, 12=
   infected low-risk males, 13=asymptomatic low-risk males, 14=
   morbid low-risk males, 15=dead low-risk males, 16=susceptible
   high-risk males, 17=infected high-risk males, 18=asymptomatic
```

```
    high-risk males, 19=morbid high-risk males, 20=dead high-risk
    males. The third dimension is the intervention (1=screening, 2=
    vaccination).
39 #initialization of states (5 states * 2 sexes * 2 risk groups = 20
     entries) for year 1 of follow-up (first dimension of y)
40 y[1,1,1] <- 399760; y[1,2,1] <- 240; y[1,3,1] <- 0; y[1,4,1] <- 0;
     y[1,5,1] <- 0; y[1,6,1] <- 99940; y[1,7,1] <- 60; y[1,8,1] <-
    0; y[1,9,1] <- 0; y[1,10,1] <- 0; y[1,11,1] <- 399760; y
    [1,12,1] <- 240; y[1,13,1] <- 0; y[1,14,1] <- 0; y[1,15,1] <-
    0; y[1,16,1] <- 99940; y[1,17,1] <- 60; y[1,18,1] <- 0; y
    [1,19,1] <- 0; y[1,20,1] <-0; y[1,1,2] <- y[1,1,1]; y[1,2,2] <-
     y[1,2,1]; y[1,3,2] <- y[1,3,1]; y[1,4,2] <- y[1,4,1]; y[1,5,2]
     <- y[1,5,1]; y[1,6,2] <- y[1,6,1]; y[1,7,2] <- y[1,7,1]; y
    [1,8,2] <- y[1,8,1]; y[1,9,2] <- y[1,9,1]; y[1,10,2] <- y
    [1,10,1]; y[1,11,2] <- y[1,11,1]; y[1,12,2] <- y[1,12,1]; y
    [1,13,2] <- y[1,13,1]; y[1,14,2] <- y[1,14,1]; y[1,15,2] <- y
    [1,15,1]; y[1,16,2] <- y[1,16,1]; y[1,17,2] <- y[1,17,1]; y
    [1,18,2] <- y[1,18,1]; y[1,19,2] <- y[1,19,1]; y[1,20,2] <-y
    [1,20,1];
41 #calculation of sample size according to risk-group and sex for
    year 1 of follow-up; only those alive are considered excluding
    those in the state of death with indices 5, 10, 15, 20)
42 nfemL[1,1] <- y[1,1,1]+y[1,2,1]+y[1,3,1]+y[1,4,1]
43 nfemH[1,1] <- y[1,6,1]+y[1,7,1]+y[1,8,1]+y[1,9,1]
44 nmalL[1,1] <- y[1,11,1]+y[1,12,1]+y[1,13,1]+y[1,14,1]
45 nmalH[1,1] <- y[1,16,1]+y[1,17,1]+y[1,18,1]+y[1,19,1]
46 nfemL[1,2]<-nfemL[1,1]
47 nfemH[1,2]<-nfemH[1,1]
48 nmalL[1,2]<-nmalL[1,1]
49 nmalH[1,2]<-nmalH[1,1]
50 #the probabilities of selecting a male/female partner from the
    high- or low-risk group, respectively, in year 1 of follow-up
51 gmalH[1,1] <- (rmalH*nmalH[1,1])/(rmalH*nmalH[1,1]+rmalL*nmalL
    [1,1])
52 gmalL[1,1] <- 1-gmalH[1,1]
53 gfemH[1,1] <- (rfemH*nfemH[1,1])/(rfemH*nfemH[1,1]+rfemL*nfemL
```

```
    [1,1])
gfemL[1,1] <- 1-gfemH[1,1]
gmalH[1,2]<-gmalH[1,1]
gmalL[1,2]<-gmalL[1,1]
gfemH[1,2]<-gfemH[1,1]
gfemL[1,2]<-gfemL[1,1]
#weighted average of STI prevalence in males in year 1 of follow-
    up
pmal[1,1] <- gmalH[1,1]*(y[1,17,1]/nmalH[1,1])+gmalL[1,1]*(y
    [1,12,1]/nmalL[1,1])
#weighted average of STI prevalence in females in year 1 of follow
    -up
pfem[1,1] <- gfemH[1,1]*(y[1,7,1]/nfemH[1,1])+gfemL[1,1]*(y
    [1,2,1]/nfemL[1,1])
pmal[1,2]<-pmal[1,1]
pfem[1,2]<-pfem[1,1]
#force of infection: function of STI transmission probability beta
    , partner acquisition rates in low-risk females rfemL(
    accordingly for the other sex and risk group), and sex-specific
     population prevalence pmal and pfem, in year 1 of follow-up)
lambdafemL[1,1] <-1-exp(-beta*rfemL*pmal[1,1])
lambdafemH[1,1] <-1-exp(-beta*rfemH*pmal[1,1])
lambdamalL[1,1] <-1-exp(-beta*rmalL*pfem[1,1])
lambdamalH[1,1] <-1-exp(-beta*rmalH*pfem[1,1])
lambdafemL[1,2] <-1-exp(-(pi*(1-eff)*beta*rfemL*pmal[1,2]+(1-pi)*
    beta*rfemL*pmal[1,2]))
lambdafemH[1,2] <-1-exp(-(pi*(1-eff)*beta*rfemH*pmal[1,2]+(1-pi)*
    beta*rfemH*pmal[1,2]))
lambdamalL[1,2] <-1-exp(-(pi*(1-eff)*beta*rmalL*pfem[1,2]+(1-pi)*
    beta*rmalL*pfem[1,2]))
lambdamalH[1,2] <-1-exp(-(pi*(1-eff)*beta*rmalH*pfem[1,2]+(1-pi)*
    beta*rmalH*pfem[1,2]))
#dat.sus.femH: simulated data on susceptible high-risk females,
    used for calibration in year 1. The parameter y[1,6,1] contains
     the number of susceptible high-risk females in year 1 and is
    calibrated by the data for year 1. The approach for high-risk
```

```
    females in the states infected, asymptomatic and morbid as well
     as for high-risk males in the same states is conducted
    accordingly.
dat.sus.femH[1] ~ dpois(y[1,6,1])
dat.inf.femH[1] ~ dpois(y[1,7,1])
dat.asy.femH[1] ~ dpois(y[1,8,1])
dat.mor.femH[1] ~ dpois(y[1,9,1])
dat.sus.malH[1] ~ dpois(y[1,16,1])
dat.inf.malH[1] ~ dpois(y[1,17,1])
dat.asy.malH[1] ~ dpois(y[1,18,1])
dat.mor.malH[1] ~ dpois(y[1,19,1])
#calibration in years 2-5
for(a in 2:5){
dat.sus.femH[a] ~ dpois(max(0.1,y[a,6,1]))
dat.inf.femH[a] ~ dpois(max(0.1,y[a,7,1]))
dat.asy.femH[a] ~ dpois(max(0.1,y[a,8,1]))
dat.mor.femH[a] ~ dpois(max(0.1,y[a,9,1]))
dat.sus.malH[a] ~ dpois(max(0.1,y[a,16,1]))
dat.inf.malH[a] ~ dpois(max(0.1,y[a,17,1]))
dat.asy.malH[a] ~ dpois(max(0.1,y[a,18,1]))
dat.mor.malH[a] ~ dpois(max(0.1,y[a,19,1]))
}
for (i in 1:2){
#intervention screening-only: pi2=1, else: pi2=pi
pi2[i]<-ifelse(i==1,1,pi)
#intervention screening-only: eff2=0 (no vaccine efficacy), else:
    eff2=eff
eff2[i]<-ifelse(i==1,0,eff)
###state allocation algorithm
for (a in 2:A){
#chi is the reproduction rate
#nfemL and lambdafemL were explained at an earlier stage
#pisd is the probability of death from any cause
#piia is the transition probability infection --> asymptomatic
#piam is the transition probability asymptomatic --> morbid
#pimd is the transition probability morbid --> dead
```

```
#state allocation of low-risk females in year a; y[,1]=susceptible, y[,2]=infected, y[,3]=asymptomatic, y[,4]=morbid, y[,5]=dead
y[a,1,i] <- y[a-1,1,i]+chi*nfemL[a-1,i]-lambdafemL[a-1,i]*y[a-1,1,i]-pisd*y[a-1,1,i]
y[a,2,i] <- y[a-1,2,i]+lambdafemL[a-1,i]*y[a-1,1,i]-piia*y[a-1,2,i]-pisd*y[a-1,2,i]
y[a,3,i] <- y[a-1,3,i]+piia*y[a-1,2,i]-piam*y[a-1,3,i]-pisd*y[a-1,3,i]
y[a,4,i] <- y[a-1,4,i]+piam*y[a-1,3,i]-pimd*y[a-1,4,i]-pisd*y[a-1,4,i]
y[a,5,i] <- y[a-1,5,i]+pisd*nfemL[a-1,i]+pimd*y[a-1,4,i]
#state allocation of high-risk females in year a; y[,6]=susceptible, y[,7]=infected, y[,8]=asymptomatic, y[,9]=morbid, y[,10]=dead
y[a,6,i] <- y[a-1,6,i]+chi*nfemH[a-1,i]-lambdafemH[a-1,i]*y[a-1,6,i]-pisd*y[a-1,6,i]
y[a,7,i] <- y[a-1,7,i]+lambdafemH[a-1,i]*y[a-1,6,i]-piia*y[a-1,7,i]-pisd*y[a-1,7,i]
y[a,8,i] <- y[a-1,8,i]+piia*y[a-1,7,i]-piam*y[a-1,8,i]-pisd*y[a-1,8,i]
y[a,9,i] <- y[a-1,9,i]+piam*y[a-1,8,i]-pimd*y[a-1,9,i]-pisd*y[a-1,9,i]
y[a,10,i] <- y[a-1,10,i]+pisd*nfemH[a-1,i]+pimd*y[a-1,9,i]
#state allocation of low-risk males in year a; y[,11]=susceptible, y[,12]=infected, y[,13]=asymptomatic, y[,14]=morbid, y[,15]=dead
y[a,11,i] <- y[a-1,11,i]+chi*nmalL[a-1,i]-lambdamalL[a-1,i]*y[a-1,11,i]-pisd*y[a-1,11,i]
y[a,12,i] <- y[a-1,12,i]+lambdamalL[a-1,i]*y[a-1,11,i]-piia*y[a-1,12,i]-pisd*y[a-1,12,i]
y[a,13,i] <- y[a-1,13,i]+piia*y[a-1,12,i]-piam*y[a-1,13,i]-pisd*y[a-1,13,i]
y[a,14,i] <- y[a-1,14,i]+piam*y[a-1,13,i]-pimd*y[a-1,14,i]-pisd*y[a-1,14,i]
y[a,15,i] <- y[a-1,15,i]+pisd*nmalL[a-1,i]+pimd*y[a-1,14,i]
#state allocation of high-risk males in year a; y[,16]=susceptible
```

```
    , y[,17]=infected, y[,18]=asymptomatic, y[,19]=morbid, y[,20]=
    dead
y[a,16,i] <- y[a-1,16,i]+chi*nmalH[a-1,i]-lambdamalH[a-1,i]*y[a
    -1,16,i]-pisd*y[a-1,16,i]
y[a,17,i] <- y[a-1,17,i]+lambdamalH[a-1,i]*y[a-1,16,i]-piia*y[a
    -1,17,i]-pisd*y[a-1,17,i]
y[a,18,i] <- y[a-1,18,i]+piia*y[a-1,17,i]-piam*y[a-1,18,i]-pisd*y[
    a-1,18,i]
y[a,19,i] <- y[a-1,19,i]+piam*y[a-1,18,i]-pimd*y[a-1,19,i]-pisd*y[
    a-1,19,i]
y[a,20,i] <- y[a-1,20,i]+pisd*nmalH[a-1,i]+pimd*y[a-1,20,i]
#calculation of sample size according to risk-group and sex for
    year a of follow-up; only those alive are considered excluding
    those in the state of death with indices 5, 10, 15, 20)
nfemL[a,i] <- y[a,1,i]+y[a,2,i]+y[a,3,i]+y[a,4,i]
nfemH[a,i] <- y[a,6,i]+y[a,7,i]+y[a,8,i]+y[a,9,i]
nmalL[a,i] <- y[a,11,i]+y[a,12,i]+y[a,13,i]+y[a,14,i]
nmalH[a,i] <- y[a,16,i]+y[a,17,i]+y[a,18,i]+y[a,19,i]
#the probabilities of selecting a male/female partner from the
    high- or low-risk group, respectively, in year a of follow-up
gmalH[a,i] <- (rmalH*nmalH[a,i])/(rmalH*nmalH[a,i]+rmalL*nmalL[a,i
    ])
gmalL[a,i] <- 1-gmalH[a,i]
gfemH[a,i] <- (rfemH*nfemH[a,i])/(rfemH*nfemH[a,i]+rfemL*nfemL[a,i
    ])
gfemL[a,i] <- 1-gfemH[a,i]
#weighted average of STI prevalence in males in year a of follow-
    up
pmal[a,i] <- gmalH[a,i]*(y[a,17,i]/nmalH[a,i])+gmalL[a,i]*(y[a,12,
    i]/nmalL[a,i])
#weighted average of STI prevalence in females in year a of follow
    -up
pfem[a,i] <- gfemH[a,i]*(y[a,7,i]/nfemH[a,i])+gfemL[a,i]*(y[a,2,i
    ]/nfemL[a,i])
#force of infection: function of STI transmission probability beta
    , partner acquisition rates in low-risk females rfemL (
```

```
    accordingly for the other sex and risk group), and sex-specific
     population prevalence pmal and pfem, in year a of follow-up)
146 lambdafemL[a,i] <-1-exp(-(pi2[i]*(1-eff2[i])*beta*rfemL*pmal[a,i
    ]+(1-pi2[i])*beta*rfemL*pmal[a,i]))
147 lambdafemH[a,i] <-1-exp(-(pi2[i]*(1-eff2[i])*beta*rfemH*pmal[a,i
    ]+(1-pi2[i])*beta*rfemH*pmal[a,i]))
148 lambdamalL[a,i] <-1-exp(-(pi2[i]*(1-eff2[i])*beta*rmalL*pfem[a,i
    ]+(1-pi2[i])*beta*rmalL*pfem[a,i]))
149 lambdamalH[a,i] <-1-exp(-(pi2[i]*(1-eff2[i])*beta*rmalH*pfem[a,i
    ]+(1-pi2[i])*beta*rmalH*pfem[a,i]))
150 }
151 }
152 #poisson-gamma model to update non-informative priors on partner
    acquisition rates by data
153 #datfemH: number of yearly partners in high-risk females,
    accordingly for the other sex and risk-group
154 #rfemH: partner acquisition rate in high-risk females, accordingly
     for the other sex and risk-group
155 #popsize: population size of the simulated data on yearly partners
    ; we assume that 500 individuals were interviewed on their
156 #yearly number of partners, therefore popsize=500.
157 for(i in 1:popsize) {
158 datfemH[i] ~ dpois(rfemH)
159 datfemL[i] ~ dpois(rfemL)
160 datmalH[i] ~ dpois(rmalH)
161 datmalL[i] ~ dpois(rmalL)}
162 #non-informative priors on partner acquisition rates
163 rfemH ~ dgamma(0.1,0.1)
164 rfemL ~ dgamma(0.1,0.1)
165 rmalH ~ dgamma(0.1,0.1)
166 rmalL ~ dgamma(0.1,0.1)
167 #informative prior on reproduction rate chi.
168 chi~dgamma(1111.1,111111.1)
169 #informative prior on transition probability infected -->
    asymptomatic.
170 piia~dbeta(5119.2, 1279.8)
```

```
171 #informative prior on transition probability asymptomatic -->
        morbid.
172 piam~dbeta(1842.66,18631.34)
173 #informative prior on transition probability morbid --> dead.
174 pimd~dbeta(1535.96,36863.04)
175 #informative prior on transition probability susceptible --> dead.
176 pisd~dbeta(156.1714,312186.6)
177 #beta-binomial model on probability of STI transmission. r.beta:
        number of events, n.beta: sample size
178 r.beta ~ dbin(beta,n.beta)
179 #non-informative prior on beta
180 beta ~ dbeta(0.5,0.5)
181 #beta-binomial model on probability of diagnosis. r.diag: number
        of events, n.diag: sample size
182 r.diag ~ dbin(diag,n.diag)
183 #non-informative prior on diag
184 diag ~ dbeta(0.5,0.5)
185 #beta-binomial model on probability of screening. r.screen: number
         of events, n.screen: sample size
186 r.screen ~ dbin(screen,n.screen)
187 #non-informative prior on screen
188 screen ~ dbeta(0.5,0.5)
189 #beta-binomial model on vaccine coverage. r.pi: number of events,
        n.pi: sample size
190 r.pi ~ dbin(pi,n.pi)
191 #non-informative prior on pi
192 pi ~ dbeta(0.5,0.5)
193 #beta-binomial model on vaccine efficacy. r.eff: number of events,
         n.eff: sample size
194 r.eff ~ dbin(eff,n.eff)
195 #non-informative prior on eff
196 eff ~ dbeta(0.5,0.5)
197 ### informative priors on costs and utilities
198 tau.screen<-1/pow(0.693,2)
199 c.screen ~ dlnorm(2.996,tau.screen)
200 tau.vac<-1/pow(0.07986607,2)
```

```
201 c.vac ~ dlnorm(5.518352,tau.vac)
202 tau.test.sti<-1/pow(0.03,2)
203 c.test.sti ~ dlnorm(2.996,tau.test.sti)
204 tau.test.blood<-1/pow(0.03,2)
205 c.test.blood ~ dlnorm(3.401,tau.test.blood)
206 tau.trt<-1/pow(0.8325546,2)
207 c.trt ~ dlnorm(4.258597,tau.trt)
208 tau.trt.dis<-1/pow(0.1980422,2)
209 c.trt.dis ~ dlnorm(6.194998,tau.trt.dis)
210 tau.gp<-1/pow(0.02,2)
211 c.gp ~ dlnorm(3.912,tau.gp)
212 #utility of infected
213 u.inf ~ dbeta(1469.3,629.7)
214 #utility of asymptomatic
215 u.asym ~ dbeta(1439.4,959.6)
216 #utility of morbid
217 u.morb ~ dbeta(629.7,1469.3)}
```

Appendix B

Further details on the literature review

In this appendix, the results of the literature review are reported in tabular way, separately for universal and female-only vaccination. In contrast to Chapter 4, which gives a brief summary, the methodology, model assumptions and outcomes of all publications reviewed are reported in full detail. In addition to the summary tables, most interesting publications are evaluated, separately according to the methodology used and the vaccination strategies incorporated.

B.1 Summary tables of the literature review

We present two extensive summary tables. The first one focusses on the results of the literature review on universal vaccination, whereas the second table incorporates those of female-only vaccination. Each table is structured according to the checklist of the search criteria, which is displayed in Section 4.3.

B.1.1 Universal vaccination

Table B.1 summarizes the results of the literature review on universal vaccination. For each publication found, we present the corresponding authors, the year of publication, the statistical methodology and the model assumptions. Furthermore, we describe the outcome of research in a detailed way, separately for cost-effectiveness results reported in terms of ICERs and medical parameters such as HPV prevalence or cervical cancer prevalence reduction.

Table B.1: Summary table of publications estimating the cost-effectiveness and/or HPV (or cervical cancer) prevalence reduction of universal vaccination. The most important aspects of the methodology, model assumptions and outcomes are summarized and displayed to explain possible variations in results of the research.

Authors	Year	Methodology	Model assumptions	ICER	Prevalence reduction
Institute of Medicine [330]	2000	Static Markov model	USA, 100% vaccine coverage and efficacy, € 74.11 vaccine price	€ 4,474.94 (vs. screen)	—
Hughes et al. [187]	2002	Deterministic ODE-based, 2 models, 1 adapted from Anderson and May [13]	USA, HPV 16, CIN, cervical cancer, 90% vaccine coverage, 75% vaccine efficacy, vaccination age not reported, 10 years duration of immunity, no booster, 3 levels of sexual activity, cervical screening, observation horizon not reported, vaccine price not reported, discounting not reported	—	universal vaccination 44% HPV prevalence reduction (female only 30%)
Taira et al. [339]	2004	Hybrid, population-based: dynamic deterministic HPV transmission model based on difference equations, combined with static Markov model for natural history of HPV infection [311]	USA, HPV 16 and 18, cervical cancer, 70% vaccine coverage, 90% vaccine efficacy, vaccination of infants, 12 year olds and 18 year olds, lifelong immunity, immunity of 10 years, booster, 4 levels of sexual activity, assortative mixing, cervical screening, observation horizon not reported, vaccine price € 74.11, discounting not reported	€ 10,851.25 (female vs. screen), € 329,682.85 (uni vs. female)	64% (17–46%) reduction in cervical cancer

Barnabas et al. [26]	2006	Deterministic PDE-based	Finland, HPV 16, CIN, cervical cancer, 10-90% vaccine coverage, 100% vaccine efficacy, vaccination at ages 15-30, lifelong duration of immunity, no booster, 4 levels of sexual activity, mixing strategy not reported, cervical screening, observation horizon 85 years, vaccine price not reported, discounting not reported	—	Cervical cancer reduction 32–98%
DACEHTA [140]	2007	Dynamic probabilistic individual-based network	Denmark, HPV 16, 18, CIN I, CIN II/III, cervical cancer, vaccine coverage 70% and 85%, vaccine efficacy not reported, vaccination of 12 year old individuals (catch-up to 19 years), lifelong immunity, 10 years immunity, booster, 2 sexual activity levels, age-dependent mixing, cervical screening, observation time period of 70 years, vaccine price € 156 (€ 80.44 – € 123.94), 3% (0%, 5%) discounting	€ 11,414.79 – € 18,508.60 per LYG (female vs. screen), € 31,239.36 – € 47,052.63 per LYG (uni vs. screen)	70% reduction of cervical cancer, 25% of CIN I, 60% of CIN II
Elbasha et al. [132]	2007	Deterministic ODE-based	USA, HPV 6, 11, 16, 18, CIN, cervical cancer, genital warts in both sexes, 90% vaccine coverage (0%–75% in the catch-up), 90% vaccine efficacy, vaccination of 12 year olds with catch-up in 12-24 year olds, lifelong immunity, waning immunity after 10 years, no booster, 3 levels of sexual activity, assortative and proportionate mixing, cervical screening, observation horizon 100 years, vaccine price € 88.93 (€ 74.11 – € 123.51) (incl. admin. cost), 3% discounting	€ 2,201.92 (female vs. screen), female only dominates universal, dominated –€ 39,383 (universal strategies)	genital warts 97%, CIN 2/3 91%, cervical cancer 91%
French et al. [143]	2007	see Barnabas et al. [26]	Finland, HPV 16, cervical cancer, vaccine coverage 10-90%, 100% vaccine efficacy, vaccination of 12 year olds, vaccination of 12 yo, 15 yo, 12-18 yo or 15-18 yo, lifelong immunity, no booster, 4 levels of sexual activity, mixing strategy not reported, cervical screening, observation horizon of 100 years, vaccine price not reported, discounting not reported	—	67% (females aged 15 years) – 87% (universal) reduction of cervical cancer after 60 years

Insinga et al. [188]	2007	see Elbasha et al. [132]	Mexico, 0-70% vaccine coverage, 90% vaccine efficacy, assortative mixing according to age and sexual activity level, other assumptions according to [132], vaccine price € 151.25, 3% discounting	€ 1,693.04 (female vs. screen), female dominates universal, € 1,898.27 – € 10,400.95 (different catch-up strategies)	Incidence reduction 93% in genital warts, 39% in CIN II/III and 4% in cervical cancer
Kim et al. [215]	2007	Hybrid: Deterministic ODE-based [26], probabilistic microsimulation	Brazil, low resource setting, HPV 16 and 18, CIN, cervical cancer, 0-90% vaccine coverage, high vaccine efficacy, vaccination before the age of 12, lifetime vaccine protection, no booster, 4 levels of sexual activity, proportionate and assortative mixing, no cervical screening, lifelong observation, vaccine price € 6.18 – € 98.82 (incl. admin. cost), 3% discounting	cost-saving – € 3,108.04 per LYS (female vs. screen), € 81.79 – € 101,799.43 per LYS (universal vs. female)	14-67% cervical cancer reduction
Elbasha et al. [133]	2008	Deterministic ODE-based	USA, HPV 6/11, 16/18, CIN, cervical cancer, genital warts, 0-70% vaccine coverage, 90% efficacy, vaccination before age 12 with a catch-up in 12-24 year olds, lifelong protection, waning after 10 years, no booster, 3 sexual activity groups, assortative and proportionate mixing, cervical screening, observation horizon length not reported, vaccine price € 88.94, discounting takes place, actual rates not reported	€ 2,193.77 (female vs. screen), female dominates universal, € 33,347.66 (universal vs. universal+female catch-up)	—
Jit et al. [204]	2008	Dynamic deterministic transmission model	UK, HPV types 6, 11, 16, 18 and third group of high-risk types, CIN, cervical cancer, squamous cell carcinomas, adenocarcinomas, non-cervical cancers, genital warts, 70% and 90% vaccine coverage, 100% vaccine efficacy, vaccination at the age of 12 or 13 and 14 or 12, 16, 18 and 25, vaccine protection between 10 years and lifelong, no booster, number of sexual activity levels not reported, mixing strategies not reported, cervical screening, 100 years observation time, vaccine price € 71.53 – € 95.97, 3.5% discounting	€ 18,099.17 – € 40,611.02 (female vs. screen), € 136,512.40 – € 623,836.21 (universal vs. female 12-25 yo)	—

Kim and Goldie [218]	2009	Hybrid: see Kim et al. [215]	USA, anal, oral cancers, RRP, vaccination at age 12, 75% vaccine coverage, 90-100% vaccine efficacy, vaccine price € 88.94, other assumptions identical to [215]	€ 15,535.50 – € 29,834.96 (female vs. screen), € 84,753.20 – € 214,854.66 (universal vs. female)	—
Zechmeister et al. [392]	2009	Deterministic ODE-based [150]	Austria, HPV 16 and 18, CIN, cervical cancer, 65% vaccine coverage, 90% vaccine efficacy, vaccination age 12 years, natural immunity lost at constant rate, booster after 10 years, 3 levels of sexual activity, mixing strategies not reported, cervical screening, observation time 52 years, vaccine price € 110, 5% (0–5%) discounting	€ 64,000 per LYG (female vs. screen), € 311,000 per LYG (universal vs. female)	—
Choi et al. [85]	2010	see Jit et al. [204]	UK, CIN, cervical cancer, genital warts, 88% vaccine coverage, 100% vaccine efficacy, vaccination of 12 year old or 13 and 14 or 14, 16, 18, 20 and 25 year old individuals, duration of immunity of 20 years, no booster, number of sexual activity levels not reported, mixing between completely assortative and completely proportionate, cervical screening, 60 years observation time horizon, vaccine price not reported, discounting not reported	see Jit [204]	72% (32–78%) reduction in cervical cancer incidence
Elbasha et al. [131]	2010	see Elbasha et al. [133]	USA, CIN, RRP, genital warts, cervical, vaginal, vulvar, anal, penile, head and neck cancer, vaccination ages 9-26 years, vaccine price € 98.82 (incl. admin. cost), 3% discounting, other model assumptions equivalent to [133]	€ 2,429.13 – € 16,366.67 (female vs. screen), € 18,994.90– € 144,565.23 (universal vs. female)	35% (female only) and 52% (universal) reduction in female GW, male GW reduction slightly higher
Olsen et al. [277]	2010	Dynamic probabilistic network model [140]	Denmark, HPV 6, 11, 16, 18, cervical cancer, genital warts, 70% and 85% vaccine coverage, 100% vaccine efficacy (93.5%, 99.8%), vaccination of 12 or 12 and 15 or 12-26 year olds, waning immunity after 15 years, booster after 15 and 25 years, cervical screening, 62 years observation time, vaccine price € 138.33 (incl. admin. cost), 3% discounting	€1,917 – € 8,727 (female interventions), € 18,677 (universal vs. female)	complete elimination of HPV 6/11/16/18 after 50 years

van de Velde et al. [360]	2010	Dynamic probabilistic microsimulation	Canada, 18 HPV types, no consideration of HPV-induced diseases, 100% vaccine coverage, 95% vaccine efficacy, vaccination age of 12 years with a possible catch-up until 18, waning immunity following normal distribution with mean of 20 years, no booster, 4 levels of sexual activity, assortative mixing, cervical screening, observation time of 120 years, vaccine price not reported, discounting not reported	—	60% (female only) and 95% (universal) reduction in HPV 16/18 prevalence, 100% reduction in HPV 6/11 prevalence
Bogaards et al. [39]	2011	Deterministic ODE-based	Netherlands, HPV 16, no HPV-induced diseases, 5%-95% coverage, 100% vaccine efficacy, vaccination age of 12 years, lifelong immunity, no booster, 3 levels of sexual activity, proportionate and assortative mixing, no cervical screening, observation time period of 100 years, vaccine price not reported, discounting not reported	—	single-sex vaccination leads to a faster HPV prevalence reduction than universal vaccination
Brisson et al. [59]	2011	see van de Velde et al. [360]	Canada, vaccination age 12 years, 70% vaccine coverage, time horizon of 70 years, vaccine price not reported, discounting not reported, other assumptions consistent with [360]	—	prevalence reduction of HPV 16/18 62% (female only) and 85% (universal) in both sexes
Brown et al. [63]	2011	Deterministic ODE-based to evaluate best HPV vaccination strategy	UK, no distinction between HPV types, no consideration of HPV-induced diseases, 90% coverage, efficacy not reported, vaccination age not reported, duration of immunity between 5 and 100 years, no booster, no sexual activity levels, assortative mixing, cervical screening, observation time period of 20 years, vaccine price not reported, discounting not reported	Male vaccination is cost-effective, no ICERs calculated	—
Chesson et al. [82]	2011	see Chesson et al. [83]	USA, HPV 6, 11, 16, 18, CIN, genital warts, RRP, cervical, vaginal, vulvar, anal, oropharyngeal, penile cancer, 20%, 30% and 75% vaccine coverage, 100% efficacy and 75% versus 60% in females and males respectively, vaccination age of 12 years, lifelong immunity, no booster, 1 level of sexual activity, assortative mixing, cervical screening, observation time of 100 years, vaccine price € 74.11 – € 88.94 (incl. admin. cost), discounting not reported	€ 4,218.79 – € 21,019.92 (female vs. screen), € 17,467.26 – € 548,664.30 (universal vs. female)	—

de Kok et al. [107]	2011	Mathematical formula, no model	Netherlands, HPV 16, 18, cervical, penile, vulvar, vaginal, anal, oral, oropharyngeal cancer, 100% vaccine coverage, vaccine efficacy not reported, vaccination age of 12 years, lifelong duration of immunity, no booster, sexual activity and mixing do not play a role, observation time period not reported, vaccine price € 133.33 (€ 33.33 – € 166.67), 3% discounting (no discounting)	—	—
Smith et al. [324]	2011	see Barnabas et al. [26]	Australia, HPV 16, cervical, anal, penile, mouth, tongue, tonsils, oropharynx, hypopharynx and larynx cancers, age-specific coverage ranging from 40% to 78% in females and 35.5% to 78% in males, 90-100% and 80-100% vaccine efficacy in females and males respectively, female vaccination age of 12-26 years, male vaccination age of 12 with catch-up in 13-15 year olds, duration of immunity from 10 years to lifelong, no booster, sexual activity levels and mixing strategies see [26], no cervical screening, lifelong observation, vaccine price and discounting not reported	—	73–99% (males) and 89–99% (females) reduction in HPV 16 prevalence
Drolet et al. [122]	2013	see van de Velde et al. [360]	Canada, genital warts, cervical, vulvar, vaginal, penile, anal and oral cancers, 70% vaccine coverage (<50% and > 70%), 100% vaccine efficacy against vaccine-specific HPV types, lower cross-protection levels, vaccination of 12 year olds, lifelong immunity, waning immunity after 20 years and waning cross-protection after 10 years, no booster, 4 levels of sexual activity, mixing not reported, cervical screening, observation time horizon of 80 years, vaccine price and discounting not reported	—	60–75% cervical cancer reduction depending on vaccination strategy

Horn et al. [185]	2013	Hybrid: deterministic ODE-based [85, 132, 392], Markov [313]	Germany, HPV 16, 18, CIN I-III, cervical cancer, genital warts, 50% vaccine coverage (20%, 80%), 98% efficacy, vaccination at the age of 12, waning immunity at a yearly rate of 10%, no booster, 3 sexual activity levels, assortative and proportionate mixing, cervical screening, observation time period 100 years, vaccine price and discounting not reported	—	36.8%, 43.8% (bivalent without and with cross-protection) and 41.5% (quadrivalent) cervical cancer reduction
Vänskä et al. [368]	2013	Bayesian PDE-based	Finland, 14 high-risk HPV types, no HPV-induced diseases, 80% vaccine coverage (40%-90%), type-dependent efficacy from 0% to 95%, vaccination age of 12 years, waning immunity, no booster, no sexual activity levels, proportionate mixing, cervical screening, observation time of 60 years, vaccine price and discounting not reported	—	HPV prevalence reduction of 54.6%
Bresse et al. [49]	2014	see Elbasha et al. [131]	Austria, genital warts, RRP, CIN, VIN, VaIN, cervical, anal, head/-neck, penile, vaginal, vulvar cancer, 65% vaccine coverage, 49-100% vaccine efficacy, vaccination age of 9 years, lifetime (20 years) duration of protection, no booster, 3 sexual activity groups, sexual mixing not reported, cervical screening, follow-up of 100 years, vaccine price € 110, 3% (0-5%) discounting	€ 10,033 – € 26,701 (universal vs. screen-only)	55–87% prevalence reduction
Burger et al. [67]	2014	see Kim et al. [217, 218]	Norway, HPV 6, 11, 16, 18, genital warts, RRP, anal, cervical, oropharyngeal, penile, vaginal, vulvar cancer, 71% (90%) coverage, 100% and 90% efficacy in females and males, 80% efficacy in sensitivity analysis, vaccination age of 12 years, lifetime duration of protection, no booster, 4 sexual activity levels, sexual mixing not reported, cervical screening, lifelong follow-up, vaccine price € 44.68 – € 134.05, 4% (0-3%) discounting	female-only: € 4468.47–€ 18410.12, universal: € 53711.07 – € 130032.62	41% (female-only) and 51% (universal) reduction in cervical cancer cases

Laprise et al. [236]	2015	see van de Velde et al. [360] and HPV-Advise [58]	Canada, 2- and 3-dose vaccination regimens, 18 HPV types, genital warts, cervical, vulvar, vaginal, anal, penile, oropharyngeal cancer, 80% (40-80%) coverage, 95% (90%) efficacy, vaccination age 9 years, lifelong (10 years - lifelong) immunity, no booster, sexual activity, mixing and follow-up as in [58], cervical screening, vaccine price € 54.70 per dose, 3% discounting	2-dose universal vs. 2-dose female-only: € 55,476.23, 3-dose universal vs. best strategy: € 643,502.50	2-dose female-only: 34.5% cervical cancer reduction, 2-dose universal: additional 1.6%
Pearson et al. [289]	2014	see Blakely et al. [34]	New Zealand, HPV 6/11, 16/18, genital warts, CIN, cervical, anal, oropharyngeal and vulvar cancer, 45-73% coverage, 99% efficacy, vaccination at age 12, duration of protection 20 years, no booster, sexual activity and mixing as in [360], cervical screening, lifetime follow-up, vaccine price not reported, 3% (0-6%) discounting	female-only vs. screening: € 11,234,45, universal vs. female-only: € 70,242.28	—
Graham et al. [173]	2015	Deterministic Markov	Canada, oropharyngeal cancer in males, no distinction between HPV types, oropharyngeal cancer, 50% (30-70%) coverage, 83.8% (50-99.7%) efficacy, vaccination age of 12 years, lifelong protection, no booster, sexual activity and mixing not reported, no cervical screening, lifetime duration of follow-up, time-step of follow-up 3 months, vaccine price € 260.17, 5% discounting	cost-saving ICER: - € 4975.09	—
Olsen et al. [278]	2015	see Olsen et al. [277] and DACEHTA [140]	Denmark, HPV 6, 11, 16, 18, genital warts, CIN, cervical, anal, penile, vaginal, vulvar, head/neck cancer, 85% coverage, 100% efficacy, vaccination age 12 years, lifelong immunity, booster, sexual activity and mixing not reported, cervical screening, follow-up of 62 years, vaccine price € 417, 3% (0-5%) discounting	€ 3,581 (female-only), € 41,636 (universal vs. female-only), € 27,343 (uni. vs. f-o., 2-dose regime)	—
Sharma et al. [317]	2015	see Kim et al. [215]	Southern Vietnam, HPV 16/18, genital warts, cervical cancer, 25-90% coverage, 100% efficacy, vaccination at age 12, lifelong duration of immunity, no booster, sexual activity and mixing as [26], cervical screening in sensitivity analysis, lifetime follow-up, vaccine price € 8.98 - € 179.67, 3% discounting	female-only: cost-saving - € 1686.4, universal: € 114.10 - € 7025.06	cervical cancer reduction: 20% (female-only) and 22.7% (universal)

Brisson et al. [55]	2016	see van de Velde et al. [360]	US, comparison of 4- to 9-valent vaccine, 18 HPV types, genital warts, CIN, cervical, anal, oropharyngeal, penile, vaginal, vulvar cancer, 46% and 25% coverage in females and males, 95% efficacy, vaccination at 13-17 years, lifelong (20 years) protection, no booster, 4 levels of sexual activity, assortative and disassortative mixing, cervical screening, follow-up of 70 (30) years	9-valent universal: cost-saving when compared to 4-valent universal; 4-valent universal: € 6518.8 when compared to screening-only	70% and 80% decrease in cervical cancer incidence through 4- and 9-valent universal vaccination

B.1.2 Female-only vaccination

In contrast to Table B.1 which includes publications on universal vaccination, Table B.2 summarizes the results of the literature review for female-only vaccination. The structure of the tables is identical and based on the list of search criteria presented in Section 4.3. Similarly to Table B.1, Table B.2 presents the authors, the year of publication, the statistical methodology, model assumptions and details about research outcomes. Research outcomes are reported separately in terms of ICERs, the results of cost-effectiveness analyses, and clinical parameters such as reductions in HPV prevalence and/or cervical cancer.

Table B.2: Summary table of publications estimating the cost-effectiveness and/or HPV (or cervical cancer) prevalence reduction of female-only vaccination. The most important aspects of the methodology, model assumptions and outcomes are summarized to explain possible variations in results.

Authors	Year	Methodology	Model assumptions	ICER	Prevalence reduction
Myers et al. [263]	2000	Probabilistic Markov	USA, no distinction of HPV types, CIN, cervical cancer, no HPV vaccination, only natural history model, cervical screening, observation horizon of 70 years, no vaccine price, no discounting	—	—
Goldie et al. [162]	2003	Probabilistic Markov	Cost Rica, HPV 16/18, low-risk, CIN, cervical cancer, 25-100% vaccine coverage, 50-98% vaccine efficacy, vaccination before age 13, 25-100% waning immunity after 10 years, no booster, cervical screening, duration of follow-up, vaccine price and discounting not reported	—	25–65% incidence reduction of cervical cancer
Kulasingam et al. [232]	2003	see Myers et al. [263]	USA, 50-100% vaccine coverage, 25-100% vaccine efficacy, vaccination of 12 year olds (12-19 yo), 10 years duration of protection (2-30 years), booster at 17 or 22 years, cervical screening, observation time period of 73 years, vaccine price € 49.41 (€ 24.70 – € 148.23), 3% discounting	€ 335.84 (screen vs. female) per LYG – not cost-effective (vaccination only or older vaccination ages)	Incidence reduction in cervical cancer 16.8% – 93.2%
Sanders et al. [311]	2003	Probabilistic Markov	USA, 13 high-risk HPV-types, low-risk types, CIN, cervical cancer, vaccine coverage 70% (30-100%), vaccine efficay 75% (0-100%), vaccination age 12 (15) years, duration of immunity 10 years, booster application every 10 years, no cervical screening, lifetime observation period, vaccine price € 74.11 (€24.7 – €123.52) (incl. admin. costs)	€ 17,000.37	19.87% reduction in cervical cancer cases
Goldie et al. [164]	2004	see Goldie et al. [162]	USA, 90% (50-100%) vaccine efficacy, vaccination age 12 years (12-15), lifelong immunity (5, 10, 15, 20 years), boosters, cervical screening, observation time horizon 100 years, vaccine price € 93.13 (€ 46.44 – € 139.58), 3% discounting	€ 15,246.84 – € 24,942.65 (female vs. screen)	86.9 – 99.2% cervical cancer reduction

Brisson et al. [57]	2007	see van de Velde et al. [358], comparison of bivalent and quadrivalent vaccine	Canada, vaccination of 12 (15, 20, 25) year olds, vaccine price € 94.61 (incl. admin. costs), 3% discounting	€ 21,765.33 – € 80,478.45 (bivalent) and € 14,373.80 – € 45,257.30 (quadrivalent)	—
Goldhaber-Fiebert et al. [159]	2007	Static probabilistic microsimulation model	USA, HPV 16, 18, other high-risk, low-risk, CIN I, CIN II/III, cervical cancer, 100% coverage, 100% efficacy, vaccination before the age of 12, lifelong duration of immunity, no booster, cervical screening, lifetime observation, time step 1 month, vaccine price and discounting not reported	—	Cervical cancer incidence reduction 55% (screening every 5 years) – 95% (screening every 3 years+vaccination)
Goldie et al. [163]	2007	see Kim et al. [215, 220]	Brazil, 70% vaccine coverage (10-100%), 100% vaccine efficacy (70%), vaccination before the age of 12, lifelong immunity, booster after 10 years, sexual activity levels and mixing not reported, cervical screening, lifelong observation time period, monthly time steps, vaccine price € 18.52 – € 111.09, 3% discounting	—	22% (screening) – 62% (screening+HPV DNA test+vaccine) cervical cancer reduction
Kim et al. [220]	2007	Probabilistic microsimulation model	Brazil, HPV 16, 18, other high-risk, low-risk, CIN I, CIN II/III, cervical cancer, no vaccination, cervical screening, lifetime observation period with monthly time steps, vaccination cost and discounting do not play a role	—	—
Kohli et al. [225]	2007	Probabilistic Markov	UK, HPV 16, 18, 31, 45, 52, other high-risk, low-risk, CIN I-III, cervical cancer, 80% and 100% coverage, 90% and 100% efficacy, vaccination of 12 (10, 18) year olds, lifelong immunity, waning of cross-protection after 10 years, booster application, cervical screening, lifetime observation period, vaccine price and discounting not reported	—	Cervical cancer reduction by 76% (60.8% – 79.6%)
van de Velde et al. [358]	2007	Bayesian Markov	Canada, HPV 16, 18, other high-risk, low-risk, CIN I, CIN II/III, 100% vaccine coverage, 95% vaccine efficacy (85%), vaccination age of 12 (15, 20, 30) years, lifelong (30 years) immunity, booster application, cervical screening, observation time period 90 years, vaccine price and discounting not reported	—	decrease in lifetime cervical cancer risk by 60% (45–70%)

Chesson et al. [83]	2008	Deterministic multi- and single-cohort model. Indirect consideration of herd immunity.	USA, bivalent vs. quadrivalent, HPV 16/18, 6/11, CIN I-III, cervical, anal, vaginal, vulvar and oropharyngeal cancer, genital warts, 70% coverage, 100% (95%, 99%) efficacy, vaccination of 12 year olds, lifelong immunity, booster, cervical screening, observation time period of 100 years, vaccine price € 88.88 (€ 222.02 – € 362.64), discounting at 3%	Quadrivalent: € 2,914.06 (herd immunity, all HPV-induced diseases), € 7,679.80 (no herd immunity, only CIN, cervical cancer, genital warts), bivalent: € 5,808.17, € 10,896.24	—
Dasbach et al. [101]	2008	see Elbasha et al. [132]	UK, vaccination of 12 year olds with catch-up in 12-14, 12-17 or 12-24 yo, 80% coverage, catch-up coverage in first year: 40% in 12 - 14 yo, 30% in 15-17 yo, 25% in 19-24 yo, afterwards twice as high, cervical screening, 100 years observation, vaccine price € 89.30, discounting at 3.5%	12 year old vaccination dominates screening only, € 13,674.65 when 12–24 yo vaccination is compared to 12–17 yo vaccination	86% reduction in cervical cancer incidence
Dasbach et al. [102]	2008	see Elbasha et al. [132] and Dasbach et al. [101]	Norway, catch-up in 12-24 year olds, vaccine price € 122.35 (incl. admin cost), discounting at 3.5%	€ 6,400 (female vs. screen), € 7,662.56 (catch-up vs. female)	92% cervical cancer reduction
Dasbach et al. [100]	2008	see Elbasha et al. [132] and Dasbach et al. [101]	Taiwan, catch-up in 12-24 year olds, vaccine price € 98.99 (incl. admin cost), 3% discounting	vaccination dominates screening, € 10,254.17 (catch-up vs. female) (€ 10,254.17 – € 61,640.81)	cervical cancer reduction 91%
Debicki et al. [109]	2008	Two probabilistic Markov	UK, Canada, Taiwan, Italy, model 1: HPV 16, 18 (95% efficacy), 31 (53% efficacy), 45 (88% efficacy), 52, other high-risk, low-risk, CIN I-III, cervical cancer. Model 2: no distinction between HPV types (correction factors in efficacy according to HPV type distribution), CIN I, CIN II/III, cervical cancer. 100% coverage, vaccination of 12 year olds, lifelong duration of protection, no booster, cervical screening, lifelong observation time period, vaccine price € 100.39 (UK), € 95.70 (Canada), € 99.92 (Taiwan), € 120.91 (Italy), 3.5% (UK) and 3% (Canada, Taiwan, Italy) discounting	UK: model 1: € 21,608.13, model 2: € 28,440.26, Canada: model 1: € 15,795.72, model 2: € 19,643.00, Taiwan: model 1: € 15,802.02, model 2: € 13,920.67, Italy: model 1: € 31,791, model 2: € 31,223	Cervical cancer reduction, UK: model 1: 76.1%, model 2: 76.9%, Canada: model 1: 70.5%, model 2: 71.5%, Taiwan: model 1 and 2: 71.5%, Italy: model 1: 76.2%, model 2: 75.0%

Diaz et al. [120]	2008	see Goldie et al. [163]	India, HPV 16, 18, other high-risk, low-risk, CIN I, CIN II/III, cervical cancer, 10-90% coverage, 50-100% efficacy, vaccination before age 12, waning immunity, lifelong observation, vaccine price € 1.23 – € 88.82 (incl. admin cost), 3% discounting	When compared to screening only, vaccination is cost-saving at the lowest price. Otherwise, it is dominated. € 44.40 – € 61,081.91 (different screening strategies and vaccination)	13–63% cervical cancer reduction
Goldhaber-Fiebert et al. [160]	2008	see Goldhaber et al. [159]	USA, HPV 16, 18, other high-risk, low-risk, CIN I, CIN II/III, cervical cancer, 100% vaccine coverage (25%, 75%), 100% vaccine efficacy (75%), vaccination of 12 year olds, lifelong immunity (15 years), no booster, cervical screening, lifelong observation, vaccine price € 99.19 (€ 74.02 – €222.06), 3% discounting	€ 4,458.98 when compared to no intervention, € 5,180.20 – € 12,749,000 for different screening and intervention strategies	—
Goldie et al. [168]	2008	Hybrid: ODE-based [163], microsimulation [220]	USA, 4 HPV types, CIN, cervical cancer, 70% vaccine coverage, efficacy not reported, vaccination age before 12 years, lifelong immunity, sexual activity levels and mixing according to [163], no cervical screening, lifelong observation, vaccine price € 1.48 – € 3.70, 3% discounting	€ 186.16 - € 2,211.63	40-55% lifetime cervical cancer risk reduction
Goldie et al. [167]	2008	Hybrid [163, 220]	72 developing countries, 70% coverage, high efficacy, vaccination before the age of 12, lifelong immunity, sexual activity and mixing according to [163], cervical screening according to the respective country, lifelong observation period, vaccine price € 7.40 – € 37 (incl. admin. cost), discounting not reported	cost-saving – € 2,197.88 per DALY	20.4–60.1% cervical cancer reduction
Goldie et al. [161]	2008	Hybrid [163, 220]	Carribean, Latin America, 70% coverage, 100% efficacy, vaccination of 12 year olds, lifelong immunity, sexual activity and mixing according to [163], cervical screening, lifelong observation, vaccine price € 0.41 – € 88.82 (incl. admin. cost), 3% (6%) discounting	cost-saving – € 5,232.00	14.2–68.6% cervical cancer reduction

Kim et al. [219]	2008	Hybrid [159, 163, 220]	Vietnam, 70% coverage (0-100%), 100% efficacy (50-100%), vaccination before the age of 12, lifelong immunity, sexual activity and mixing according to [163], cervical screening, observation time horizon 5 years, vaccine price € 1.48 – € 93.84, 3% discounting	cost-saving – € 49,382.07	cervical cancer reduction 20.4% – 76.1%
Kim et al. [217]	2008	Hybrid [218, 220]	USA, genital warts, cervical, vulvar, vaginal, anal, oral, oropharyngeal cancers, RRP, vaccination of 12 year olds with catch-up in 18, 21 or 26 years, 25% coverage rate within the first 5 years after vaccine introduction, followed by 75% coverage rate, 100% vaccine efficacy, lifelong (10 years) immunity, booster application, sexual activity levels and mixing strategies according to [163], cervical screening, lifelong observation, vaccine price € 88.67, 3% discounting	€ 32,265.22 (€ 25,826.98 – € 113,002.28)	—
Kulasingam et al. [231]	2008	see Myers et al. [263]	UK, HPV 6, 11, 16, 18, genital warts, CIN I, CIN II/III, cervical cancer, 100% vaccine coverage (50%, 85%), 100% vaccine efficacy (85%), vaccination of 12 year olds, vaccine-induced immunity for 20 (10) years, booster application, cervical screening, observation time horizon 73 years, vaccine price € 89.39 (€ 83.43 – € 95.35, 3% (1.5%) discounting	€ 25,199.83 (€ 3,737.08 – € 101,623.80)	58.46% cervical cancer reduction
Rogoza et al. [303]	2008	see Debicki et al. [109] and Kohli et al. [225]	Canada, The Netherlands, Taiwan, UK, USA, HPV 16, 18, 31, 45, 52, other high-risk, low-risk, CIN I–III, cervical cancer, 100% vaccine coverage, 95% efficacy against HPV 16/18 (53% against HPV 31, 88% against HPV 45), vaccination at the age of 12, lifelong duration of protection, no booster, cervical screening, lifelong observation, vaccine price € 95.45 (Canada) – € 116.72 (USA), discounting 4% costs, 1.5% benefits (Netherlands), 3% (Canada, Taiwan, USA), 3.5% (UK)	€ 5,792.94 (USA) – € 21,573.69 (UK)	cervical cancer reduction 70.5% (Canada) – 76.1% (UK)

Suárez et al. [333]	2008	see Debicki et al. [109]	Chile, Finland, Ireland, Poland and Taiwan, HPV 16, 18, CIN I, CIN II/III, cervical cancer, 100% (80%) vaccine coverage, 95% vaccine efficacy, vaccination at the age of 11, 10 (25) years duration of immunity, booster application, cervical screening, lifelong observation, vaccine price € 70 (Chile) – € 150 (Finland), discounting 3% (Chile), 3.5% (Ireland, Poland), 3% costs, 1.5% benefits (Finland, Taiwan)	€ 6,879.10 (Chile) – € 24,799 (Ireland)	20% reduction of cervical cancer cases
Szucs et al. [337]	2008	see Myers et al. [263] and Kulasingam et al. [232]	Switzerland, HPV 6, 11, 16, 18, CIN I-III, cervical cancer, genital warts, 80% coverage, 95% (90-100%) efficacy, vaccination of 11 year olds, lifelong immunity, waning immunity after 10 years, booster application, cervical screening, lifelong observation, vaccine price € 192.21, discounting 3% (costs) and 1.5% (benefits)	€ 21,044.31 (€ 18,195.56 – € 85,409.49)	62% cervical cancer reduction
Usher et al. [356]	2008	see DACEHTA et al. [140]	Ireland, female-only vaccination, HPV 16, 18, CIN I, CIN II/III, cervical cancer, 80% (30%) vaccine coverage, 95.2% (85-99%) vaccine efficacy, vaccination of 12 year olds with catch-up in 12-15, 12-17, 12-19 or 12-26 yo, lifelong immunity, waning after 10 years, booster application, sexual activity and mixing according to [140], cervical screening, observation time of 70 years, vaccine price € 100 (€ 80 – € 120), 3.5% (0–6%) discounting	€ 17,383 (€ 18,893 – € 24,534) per LYG	—
Anonychuk et al. [16]	2009	see Debicki et al. [109] with indirect consideration of herd immunity [27]	Canada, HPV 16, 18, other oncogenic, CIN I, CIN II/III, cervical cancer, 75% vaccine coverage, 98% vaccine efficacy against HPV 16/18, 37% against other oncogenic types, vaccination of 12 year olds (12-25 yo), duration of immunity for 10 or 30 years, cervical screening, lifelong observation, vaccine price € 99.84, 3% (0–5%) discounting	€ 13,829.06 – € 23,468.37	9–77% reduction in cervical cancer cases

Colantonio et al. [87]	2009	see Debicki et al. [109]	Latin America (Argentina, Brazil, Chile, Mexico, Peru), HPV 16, 18, 31, 45, CIN I, CIN II/III, cervical cancer, vaccine coverage not reported, vaccine efficacy 66.1% – 76.3%, vaccination of 12 year olds (12-18), 20 years duration of immunity, booster application, cervical screening, lifelong observation, vaccine price € 51.77 (incl. admin cost), 3% discounting	€ 3,314.74 (Peru) – € 12,796.81 (Chile)	62.73% (Brazil) – 70.09% (Argentina)cervical cancer case reduction
Coupé et al. [96]	2009	Probabilistic Markov	The Netherlands, HPV 16, 18, 31, 33, 35, 39, 45, 51, 52, 56, 58, 59, 66, 68, CIN I-III, cervical cancer, 85% coverage, 95% efficacy, vaccination of 12 year olds, lifelong immunity (10, 30 years), 3 sexual activity levels, cervical screening, observation time horizon of 88 years, vaccine price € 125 (€ 75), discounting 4% (cost) and 1.5% (benefit) (0%)	€ 19,429 (€ 17,467 – € 35,325)	86.66% reduction of cervical cancer (60.51% – 65.75%)
Dee et al. [111]	2009	Markov with fixed parameter values	Ireland, comparison of 2- and 4-valent vaccine, no distinction between HPV types, cervical cancer, genital warts, 90% (60-100%) coverage, 90% efficacy against cervical cancer, 95% efficacy against genital warts, vaccination age of 12 years, lifelong protection, no booster, cervical screening, observation time period of 88 years, vaccine price € 90, 4% (0–5%) discounting	€ 30,460 (€ 3,399 – € 45,237, bivalent), € 25,349 (€ 2,877 – € 36,548, quadrivalent)	51.28% cervical cancer reduction
de Kok et al. [108]	2009	Static deterministic microsimulation model [177]	The Netherlands, no distinction between HPV types, CIN I-III, cervical cancer, 85% vaccine coverage, 70% vaccine efficacy against cervical cancer, 35% vaccine efficacy against CIN, vaccination of 12 year olds, lifelong immunity, booster application, cervical screening, lifelong observation, vaccine price € 118 (€ 0 – € 120), 3% (0%) discounting	€ 53,500 (€ 4,100 – € 105,600)	61% reduction of cervical cancer

Elbasha et al. [134]	2009	see Elbasha et al. [132]	USA, investigate proper age of HPV vaccination, HPV 6, 11, 16, 18, CIN, cervical cancer, genital warts, 70% (50%, 90%)coverage, 90% efficacy, vaccination of 12 year olds (12-14, 12-17, 12-19, 12-24), lifelong (10 years) immunity, no booster, three sexual activity levels, age- and behavioural dependent sexual mixing, cervical screening, observation time period of 100 years, vaccine price € 88.74 (incl. admin. costs), discounting 3%	Vaccination is dominated by screening only (€ 2,307.07 – € 8,136.57 for catch-up)	6.9% (20.5%) reduction in cervical cancer cases
Hillemanns et al. [183]	2009	see Myers et al. [263]	Germany, no distinction between HPV types, CIN I-III, cervical cancer, genital warts, 80% (100%) vaccine coverage, 100% (90%) vaccine efficacy, vaccination at age 12, lifelong (10 years) protection, booster application, cervical screening, lifelong observation, vaccine price € 143.8, discounting 4% (costs) and 1.5% (benefits) (0–5%)	€ 10,530 (€ 3,049 – € 42,493)	59.27% cervical cancer reduction
Kim et al. [221]	2009	see Kim et al. [218] and Goldhaber-Fiebert et al. [159]	USA, HPV 16, 18, other high-risk, low-risk, CIN I, CIN II/III, cervical cancer, 100% vaccine coverage, 100% (70%) vaccine efficacy, vaccination of 35, 40 and 45 yo, lifelong (5, 10 years) protection, booster application, sexual activity and mixing according to [218], cervical screening, lifelong observation, vaccine price € 99.10, 3% discounting	€ 20,339.27 – € 331,871.57	—
Mennini et al. [257]	2009	see Myers et al. [263] and Kulasingam et al. [232]	Italy, no HPV type distinction, CIN I-III, cervical cancer, genital warts, 80% vaccine coverage, 100% vaccine efficacy, vaccination at the age of 12, lifelong (20 years) protection, booster application, cervical screening, lifetime observation horizon, vaccine price € 106, discounting 3% (costs) and 1.5% (effects) (0–5%)	€ 9,569 (€ 2,781 – € 48,122)	63.3% cervical cancer reduction
Oddsson et al. [274]	2009	Markov with fixed parameter values	Iceland, no HPV type distinction, CIN I, CIN II/III, cervical cancer, 90% coverage, 95% efficacy, vaccination at the age of 12, lifelong immunity, no booster, cervical screening, lifelong observation, vaccine price € 107, discounting at 3% (6%)	€ 18,547 (€ 14,000 – € 86,000)	50% reduction of cervical cancer deaths

Reynales-Shigematsu et al. [300]	2009	see Myers et al. [263] and Kulasingam et al. [232]	Mexico, no distinction between HPV types, CIN I-III, cervical cancer, 100% (30%) vaccine coverage, 95% vaccine efficacy, vaccination of 12 (12-25) year old females, duration of immunity not reported, no booster, cervical screening, observation time 73 years, vaccine price € 11.09 (incl. admin. cost, € 33.28 – € 184.88), 3% (6%) discounting	€ 11,778.40 per LYG (€ 50.26 – € 12,817.65)	13.49% – 77.27% reduction in cervical cancer
Rogoza et al. [304]	2009	see Rogoza et al. [303] and Kohli et al. [225]	The Netherlands, HPV 16, 18, 31, 45, 52, other high-risk, low-risk, CIN I-III, cervical cancer, 100% vaccine coverage, vaccine efficacy 50-100%, lifelong (20 years) duration of immunity, cervical screening, lifelong observation, vaccine price € 100 (€ 80 – € 120), discounting 4% costs and 1.5% benefits (0–5%)	€ 18,500 (€ 5,800 – € 103,800)	74% cervical cancer reduction
Sinanovic et al. [321]	2009	Markov with fixed parameter values	South Africa, no distinction between HPV types, CIN I, CIN II/III, cervical cancer, 80% coverage, 90% efficacy, vaccination of 12 year olds, lifelong (10 years) duration of immunity, booster application, cervical screening, observation time period of 85 years, vaccine price € 88.74 (€ 35.50, 4 doses necessary), 3% (6%) discounting	€ 796.81 – € 1,079.16	—
Thiry et al. [345]	2009	Probabilistic Markov	Belgium, no distinction between HPV types, CIN II/III, cervical cancer, 84% coverage, 60% (31-80%) efficacy, vaccination of 12 (16) year olds, 10 year (lifelong) immunity, booster application, cervical screening, lifelong observation, vaccine price € 114.5, discounting 3% costs, 1.5% effects (0–5%)	€ 32,665 (€ 14,382 – € 100,406)	50% reduction of cervical cancer
Accetta et al. [7]	2010	Static deterministic microsimulation	Italy, HPV 16/18, other high-risk, low-risk, CIN I, CIN II/III, cervical cancer, 100% vaccine coverage, 75.9% vaccine efficacy (85%, 95%), vaccination age of 11 years, lifelong immunity, waning after 10 or 20 years, booster application, cervical screening, lifelong observation period, vaccine price € 90 (€ 30, € 50, € 70), 3% discounting	Vaccination dominated by screening+DNA test, € 2,537 – € 270,943	76% (43.1% – 79.7%) cervical cancer risk reduction

Bergeron et al. [30]	2010	see Myers et al. [263] and Kulasingam et al. [232]	France, no distinction between HPV types, CIN I-III, cervical cancer, genital warts, 80% coverage, 80% (80-100%) efficacy, vaccination of 14 year olds, lifetime protection (10 years-lifetime), booster application, cervical screening, observation time period of 71 years, vaccine price € 135.60, discounting 3.5% (costs) and 1.5% (effects) (0–5%)	€ 8,408 (€ 2,019 – € 37,228)	64.79% cervical cancer reduction
Bogaards et al. [38]	2010	Deterministic PDE-based including Bayesian approach	The Netherlands, HPV 16, 18, 31, 33, 35, 39, 45, 51, 52, 56, 58, 59, 66, 68, CIN 0-III, 3 sexual activity levels, assortative mixing, cervical screening	—	—
Dasbach et al. [103]	2010	see Elbasha et al. [132]	Hungary, HPV 6, 11, 16, 18, CIN I, CIN II/III, cervical cancer, genital warts, 50% and 70% coverage, 95.2% efficacy against CIN, 98.9% efficacy against genital warts, vaccination of 12 year olds with catch-up in 12-24 year olds, duration of immunity 10 years to lifelong, no booster, sexual activity and mixing according to [132], cervical screening, observation time period of 100 years, vaccine price € 93 (incl. admin. cost), 5% (0%) discounting	€ 9,577 (€ 7,356 – € 16,880) for 12 yo vaccination and € 10,646 (€ 2,435 – € 40,083) for catch-up	90% reduction of cervical cancer
Demarteau et al. [114]	2010	see Debicki et al. [109], Suárez et al. [333], Anonychuk et al. [16], Colantonio et al. [87]	Italy, France, Ireland, bivalent vs. quadrivalent vaccine, low-risk HPV, high-risk HPV, CIN I, CIN II/III, cervical cancer, genital warts, 100% coverage, 95% (90%, 100%) efficacy, lifetime and 10 year duration of protection according to HPV type, booster application, cervical screening, lifetime observation period, vaccine price € 90 (France, Italy) and € 115 (Ireland), discounting 3%/1.5% (France), 3.5% (Ireland) and 3%/3% (France)	Quadrivalent dominates bivalent vaccine	—
Diaz et al. [119]	2010	see Goldie et al. [163], Goldhaber-Fiebert et al. [159], Kim et al. [220]: dynamic probabilistic microsimulation	Spain, HPV 16, 18, other high-risk, low-risk, CIN I, CIN II/III, cervical cancer, 90% (50-100%) coverage, 70-100% efficacy, vaccination of 11 year olds, 10 years to lifelong immunity, no booster, sexual activity and mixing according to Goldie [163], cervical screening, lifelong observation time, vaccine price € 104, discounting at 3%	€ 24,350 per LYG (screen + HPV test+vaccine vs. no intervention) (€ 16,060 – € 4,803,795)	61–98% reduction in cervical cancer

Konno et al. [228]	2010	see Debicki et al. [109]	Japan, no distinction between HPV types, CIN I, CIN II/III, cervical cancer, 50% coverage, 61% to 81% efficacy, vaccination of 12 (10-45) year olds, duration of immunity not reported, no booster, cervical screening, observation time horizon of 95 years, vaccine price € 266.50, discounting 3% (0–5%)	€ 13,585.54 (12 yo), € 20,239.41 (10–45yo)	73% cervical cancer reduction
La Torre et al. [234]	2010	see Goldie et al. [164]	Italy, HPV 16/18, other HPV, CIN I-III, cervical cancer, 100% vaccine coverage, 95.9% (HPV 16/18) or 27% (other HPV) efficacy, vaccination of 12 (11-55) year olds, cervical screening, lifelong observation, vaccine price € 106, 3% discounting	€ 22,055 (€ 3,566 – € 91,397)	67% cervical cancer reduction
Liu et al. [245]	2010	Probabilistic Markov	Taiwan, high-risk HPV, low-risk HPV, CIN I, CIN II/III, cervical cancer, 100% (30-100%) coverage, 75% efficacy (30-100%), vaccination of 12 (12-36) year olds, lifelong (10 years to lifelong) duration of immunity, booster application, cervical screening, lifelong observation period, vaccine price € 89.69 (€ 67.27 – € 112.11), discounting 3% (0–5%)	€ 10,124.39 (€ 1,475.91 – € 27,304.26)	73.3% reduction of cervical cancer
Obradovic et al. [273]	2010	see Myers et al. [263]	Slovenia, CIN I-III, cervical cancer, 80% (50-100%) coverage, 98% (86–100%) efficacy, vaccination of 12 year olds, lifelong (10 years to lifelong) duration of protection, booster application, cervical screening, observation time horizon of 73 years, vaccine price € 100 (€ 80 – € 120), 5% (0–5%) discounting	€ 23,178 (€ 1,708 – € 58,690)	89.69% (92.62%) cervical cancer reduction
Torvinen et al. [348]	2010	see Suárez et al. [333]	Finland, no distinction of HPV types, CIN I, CIN II/III, cervical cancer, 90% vaccine coverage, 52%-77% efficacy depending on HPV-induced disease, vaccination of 11 year olds, lifelong protection, no booster, cervical screening, observation time period of 96 years, vaccine price € 77.24, discounting at 0% or 3%	€ 17,294 (€ 2,592)	71% cervical cancer reduction

Vanagas et al. [365]	2010	Markov with fixed parameter values, indirect consideration of herd immunity	Lithuania, no distinction of HPV types, CIN I-III, cervical cancer, 10-90% coverage, 90-100% efficacy, vaccination of 12 (15) year olds, lifelong (15, 20 years) duration of immunity, booster application, cervical screening, lifelong observation time horizon, vaccine price not reported, 3% discounting	€ 2,999.74 per LYG (€ 237.20 – € 395,801.38)	76.9% cervical cancer reduction
Bogaards et al. [37]	2011	Hybrid: Deterministic PDE-based [38], static probabilistic microsimulation	The Netherlands, 14 HPV types, CIN I, CIN II/III, cervical cancer, 90% and 50% (0-100%) coverage, efficacy not reported, vaccination of 12 (13-16) year olds, lifelong protection, waning immunity after 10 years, no booster application, sexual activity and mixing according to [38], cervical screening, lifelong observation, vaccine price and discounting not reported	—	69% (60–74%) cervical cancer reduction
Bogaards et al. [36]	2011	see Bogaards et al. [37]	The Netherlands, cost-effectiveness analysis, 14 HPV types, CIN I, CIN II/III, cervical cancer, 50% coverage, efficacy 52-100% depending on HPV type, vaccination of 17-25 (12-16) year olds, lifelong immunity, waning immunity, no booster, sexual activity levels according to [38], assortative mixing, cervical screening, 100 years observation period, vaccine price € 125, € 65 or € 35, discounting at 4% (costs) and 1.5% (effects) (0%, 3%)	€ 22,526 (€ 4,149 – € 107,796)	53.85% (15.09%)
Campos et al. [70]	2011	see Goldie et al. [163] and Kim et al. [220]	East Africa (Kenya, Mozambique, Tanzania, Uganda, and Zimbabwe), HPV 16, 18, other high-risk, possible high-risk, low-risk, CIN, cervical cancer, 70% (25%, 50%, 75%) coverage, 100% efficacy, vaccination before the age of 12, lifelong immunity, no booster, cervical screening, lifelong observation, vaccine price € 1.23 – € 49.28 (incl. admin. cost), discounting not reported	Cost-saving – € 10,751.98 per LYG	7.5–47% cervical cancer reduction

Canfell et al. [72]	2011	see Barnabas et al. [26], Smith et al. [324], Canfell [71] et al.	China, no distinction between HPV types, CIN I-III, cervical cancer, 70% (40%) coverage, 100% (70%) efficacy, vaccination of 15 (12-20) year olds, lifelong protection, waning immunity after 10 years, no booster, cervical screening, lifelong observation, vaccine price € 2.46 – € 14.78, 3% discounting	€ 656.78 – € 4,400.41 per LYG	9.3–81.7% reduction in cervical cancer incidence
Capri et al. [75]	2011	Static deterministic prevalence- and population-based model	Italy, comparison of 2- and 4-valent, HPV 16/18, other high-risk, HPV 6/11, CIN I, CIN II/III, cervical cancer, genital warts (vaginal, vulvar cancer and the corresponding precancerous lesions), 100% coverage, 48.5%–86.5% efficacy depending on lesion and vaccine type, lifelong (10–50 years) duration of immunity, booster application, cervical screening, 1 year of follow-up, vaccine price not reported, no discounting	—	86.54% (bivalent) and 76.46% (quadrivalent) cervical cancer incidence reduction
Chen et al. [81]	2011	Bayesian Markov	Taiwan, HPV 16, 18, CIN I, CIN II/III, cervical cancer, 100% coverage, efficacy not reported, vaccination age not reported, lifetime duration of protection, no booster, cervical screening, lifetime observation period, vaccine price € 89.94 (incl. admin. cost), 3% discounting	€ 23,391.63 – € 32,977.64	—
Demarteau et al. [113]	2011	see Debicki [109] et al.	France, no distinction between HPV types, CIN I, CIN II/III, cervical cancer, coverage not reported, efficacy between 33.5% and 98.0%, vaccination of 12 (12-56) year olds with catch-up till 25 years, lifelong (15, 20 years) immunity, booster application, cervical screening, observation time horizon of 96 years, vaccine price € 133.82 (€ 107.06 – € 160.58), 3% (costs) and 1.5% (effects) discounting (0–5%)	€ 9,706 (€ 309)	85.5% cervical cancer reduction

Jit et al. [203]	2011	see Jit et al. [204], comparison of bivalent and quadrivalent vaccine	UK, HPV 6, 11, 16, 18, other type, bivalent vaccine: cervical cancer, quadrivalent vaccine: cervical cancer, genital warts, RRP, sensitivity analysis: in addition cervical, vaginal, anal and vulvar cancer, 80% coverage (30%–65% in the catch-up), 23.4-100% vaccine efficacy depending on vaccine and HPV type, duration of immunity for 10 or 20 years, no booster, sexual activity and mixing according to [204], cervical screening, observation time period of 100 years, vaccine price € 100.88, 3.5% (1.5% for benefits) discounting	bivalent: € 17,863.86 – € 47,636.96, quadrivalent: € 14,291.09 – € 26,200.33	bivalent prevents more cervical cancers, quadrivalent more non-cervical cancers and genital warts
Korostil et al. [229]	2011	Bayesian ODE-based, probabilistic sexual mixing, other model parameters deterministic	Australia, HPV 6, 11, genital warts, 80% coverage, 90% efficacy, vaccination at the age of 15-19 years, duration of immunity for 10-15, 20-25 and 40-45 years, no booster, 4 sexual activity levels, assortative mixing, no cervical screening, 120 years follow-up, vaccine price and discounting do not play a role	—	91.67% (males) and 95.24% (females) decrease in genital warts incidence
Lee et al. [241]	2011	Probabilistic Markov	Singapore, comparison of 2- and 4-valent vaccine, no distinction between HPV types, CIN I, CIN II/III, cervical cancer, genital warts, 100% (20-80%) coverage, efficacy: 88.3% for the bivalent, 79.4% for the quadrivalent, (70%, 90%), vaccination of 12 year olds, lifelong (5, 10, 20 years) immunity, booster application, cervical screening, lifelong observation, vaccine price € 79.24, 3% (0%) discounting	bivalent: € 6,125.14 (€ 490.98 – € 41,545.67), quadrivalent: € 5,346.53 (€ 1,635.61 – € 39,979.61)	86.03% (bivalent) and 76.86% (quadrivalent) cervical cancer reduction
Praditsitthikorn et al. [294]	2011	Probabilistic semi-Markov (time of leaving state depends on time spent)	Thailand, no distinction between HPV types, CIN I, CIN II/III, cervical cancer, 100% coverage, 79% efficacy, vaccination of 15 (16-25, 30, 40, 50, 60), lifelong (5, 10 years) duration of immunity, booster application, cervical screening, lifetime observation period, vaccine price € 116.66 (incl. admin. cost), 3% (0%, 5%, 10%) discounting	€ 499.97 – € 7,293.47	—

Sopina et al. [328]	2011	Probabilistic Markov	New Zealand, no distinction between HPV types, CIN I, CIN II/III, cervical cancer, 90% (30%, 50%, 70%) coverage, 99% efficacy, vaccination of 12 year olds, lifelong (10, 20 years) duration of protection, booster application, cervical screening, observation time horizon 73 years, vaccine price € 92.23, 3% (1–5%) discounting	€ 2,152.34 – € 6,144.62	54.05–85.14% cervical cancer reduction
Tay et al. [342]	2011	Markov with fixed parameter values	Singapore, no distinction between HPV types, CIN, cervical cancer, coverage not reported, 100% efficacy, vaccination of 12 (12–64) year olds, lifelong duration of protection, no booster, cervical screening, lifelong observation, vaccine price and discounting do not play a role	—	6.5–76.5% cervical cancer reduction
Westra et al. [382]	2011	see Rogoza et al. [303, 304], Kohli et al. [225] (static stochastic population-based Markov model)	The Netherlands, HPV 16, 18, 31, 33, 45, other high-risk, low-risk, CIN, cervical cancer, 100% coverage, 95% efficacy against HPV 16/18, 0% (0-78.7%) efficacy against other types, vaccination at the age of 12 (12–50), lifelong (20 years) duration of immunity, booster application, cervical screening, observation time period 100 years, vaccine price € 105 (€ 45 – € 125), discounting 4% (costs) and 1.5% (effects)	€ 19,900 – € 52,000	50% reduction in cervical cancer incidence
Demarteau et al. [115]	2012	see Debicki et al. [109] and Suárez et al. [333] (static, probabilistic, population-based Markov model), bivalent vs. quadrivalent vaccine	Taiwan, no distinction between HPV types, genital warts, CIN I, CIN II/III, cervical cancer, 100% coverage, 98% efficacy against HPV 16/18, bivalent: 79%, quadrivalent: 69.9% effectiveness against cervical cancer, vaccination of 12 year olds, lifelong (10 years for quadrivalent, 20 years for bivalent) duration of immunity, booster application, cervical screening, lifetime observation, vaccine price € 100.31, discounting 3% (costs), 1.5% (effects) (0–5%)	Bivalent vaccine dominates quadrivalent	29% less cervical cancer cases for bivalent vs. quadrivalent vaccine

El Hasnaoui et al. [130]	2012	see Debicki et al. [109]	France, no distinction between HPV types, CIN I, CIN II/III, cervical cancer, 100% coverage, 98% and 89% vaccine efficacy depending on previous exposure, vaccination of 11-13, 14-16 or 15-17 year olds (11–55 year olds), lifelong immunity, no booster, cervical screening, 90 (20, 30, 60) years follow-up, vaccine price and discounting do not play a role	—	63–86% cervical cancer reduction
Favato et al. [136]	2012	Bayesian Markov	Italy, no distinction between HPV types, CIN I-III, cervical cancer, genital warts, 84.7% coverage, 78.3% efficacy, vaccination of 12 and 15 (12,15,18 or 12,15,18,25) year olds, lifelong duration of immunity, no booster, cervical screening, observation time period of 90 years, vaccine price € 69.13 (€ 60.16 – € 79.58), discounting 3% (costs) and 1.5% (benefits)	€ 12,013 – € 15,890	55.79–67.54%
Goldie et al. [166]	2012	see Goldie et al. [161, 163, 168], Kim et al. [215, 217, 220], Goldhaber et al. [160] and Diaz et al. [120] for dynamic stochastic individual-based HPV transmission and natural history model	Peru, HPV 16, 18, other high-risk, low-risk, CIN I, CIN II/III, cervical cancer, 82% (61–98%) coverage, 100% (70%) efficacy, vaccination of 11 year olds, lifelong immunity, no booster, sexual activity levels and mixing strategies according to Goldie [163], cervical screening, lifelong observation, vaccine price € 5.17 (€ 3.69 – € 14.78), discounting 3%	Cost-saving – € 957.43 per LYG	11.9–67.5% reduction in cervical cancer
Kawai et al. [211]	2012	see Elbasha et al. [131]	Brazil, HPV 6, 11, 16, 18, CIN I, CIN II/III, cervical cancer, genital warts, 85% (50%) coverage in 12 year olds increasing to 95% (60%) in 26 year olds, 90% efficacy, lifelong (20 years) immunity, no booster, three sexual activity levels, age- and sexual activity specific mixing, cervical screening, 100 years follow-up, vaccine price € 11.19, 3% (0%, 5%) discounting	€ 161.29 and € 331.42 (catch-up) (cost-saving – € 884.52)	94–98% incidence reduction of cervical cancer

Kohli et al. [226]	2012	see Debicki et al. [109] and Anonychuk et al. [16]	Canada, bivalent vs. quadrivalent vaccine, no distinction between HPV types, CIN I, CIN II/III, cervical cancer, genital warts, 100% coverage, 98% efficacy, higher cross-protection with bivalent vaccine (68.4% vs. 32.5% or lower), vaccination of 12 year olds, lifelong immunity, no booster, cervical screening, observation time period 100 years, vaccine price € 73.88 (€ 71.67, € 72.40 for quadrivalent), 3% (0%) discounting	Bivalent dominates quadrivalent (€ 2,554.13 – € 107,359.63)	29.81% less cervical cancer with bivalent vaccine
Lee et al. [240]	2012	Static deterministic ODE-based	USA, no vaccination, cervical screening or sexual mixing, calculation of R_0 for treated and untreated individuals to estimate the number of infected individuals, vaccine price and discounting do not play a role	—	—
Schobert et al. [314]	2012	see Elbasha et al. [133]	Germany, HPV 6, 11, 16, 18, genital warts, CIN, cervical cancer, 6-38% coverage, 90-100% efficacy, vaccination age 12-17 years, lifelong (20 years) duration of immunity, no booster, sexual activity and mixing not reported, cervical screening, lifetime follow-up, vaccine price € 451.20, 3% (0-5%) discounting	€ 5525	65% reduction in cervical cancer incidence
Sharma et al. [316]	2012	see Goldie et al. [163] and Kim et al. [220]	Thailand, HPV 16, 18, other high-risk, low-risk, CIN I, CIN II/III, cervical cancer, 80% coverage, 100% (75%) efficacy, vaccination before the age of 12, lifelong duration of immunity, no booster, sexual activity and mixing according to [163], cervical screening, lifelong observation, vaccine price € 2.46 – € 123.14 (incl. admin. cost), 3% discounting	Cost-saving – € 14,670.78	4.7–70.1% reduction in cervical cancer
Termrungruanglert et al. [344]	2012	Markov with fixed parameter values	Thailand, no distinction between HPV types, CIN I, CIN II/III, cervical cancer, genital warts, 100% (80–100%) coverage, 97% (90–99.9%) efficacy, vaccination at age 12, lifelong immunity, no booster, no cervical screening, follow-up of 88 years, vaccine price € 48.13 (€ 48.13 – € 96.26), discounting 3% (2–6%)	€ 3,818.82 (no inter- vention vs. HPV vaccination), (€ 1,183.10 – € 23,020.45)	55.1% reduction of cervical cancer incidence

Tully et al. [349]	2012	Deterministic ODE-based	Canada, HPV 16/18, other HPV, CIN I, CIN II/III, cervical cancer, 80%, 60% and 40% coverage, 90–100% efficacy against HPV 16/18, 5–19% against other HPV, vaccination of 12 year olds, catch-up in 18 (12-26) year olds, lifelong (3% yearly waning) immunity, booster application, no distinction of sexual activity levels, cervical screening, follow-up of 80 years, vaccine price € 63.60, 3% discounting	€ 7,360.28 (€ 4,436.54 – € 7,035.27)	
Vanagas et al. [364]	2012	see Vanagas et al. [365] for multi-cohort model	Lithuania, HPV 16, 18, CIN I, CIN II/III, cervical cancer, 90% coverage, 90–100% efficacy, vaccination of 12 year olds, duration of protection not reported, no booster, cervical screening, observation for 90 years, vaccine price not reported, 3% discounting	€ 2,932.58 (€ 3,468.20 – € 607,095.40)	77% reduction of cervical cancer
van de Velde et al. [359]	2012	see van de Velde et al. [360]	Canada, bivalent vs. quadrivalent vs. nonavalent vaccine, 18 HPV types, CIN I-III, cervical, anal, vulvar, vaginal, head and neck cancer, genital warts, 70% coverage, 100% efficacy against vaccine types, 0–79% efficacy against non-vaccine types, vaccination of 12 year olds, lifelong (9, 15, 20 years) duration of immunity, no booster, four levels of sexual activity, age-dependent mixing, cervical screening, 70 (30, 50) years of follow-up, vaccine price and discounting do not play a role	—	Switching bivalent (quadrivalent) to nonavalent: 4.8% (6.6%) additional reduction of cervical cancer
Vanni et al. [367]	2012	Dynamic probabilistic microsimulation	Brazil, HPV 16, 18, 6/11, genital warts, CIN I-III, cervical cancer, 50%, 70% and 90% coverage, efficacy not reported, vaccination at 12 years, lifelong (10 years) immunity, booster application, four sexual activity levels, age- and sexual activity specific mixing (see [26] [215]), cervical screening, lifelong observation, vaccine price € 6.16 – € 136.93, discounting 5% (0%)	€ 83.09 – € 4 375.32	Prevalence of vaccine specific types reaches zero 30 years after vaccine introduction

Vokó et al. [370]	2012	Markov with fixed parameter values	Hungary, HPV 16, 18, CIN I, CIN II/III, cervical cancer, 80% coverage, 45.1%–94.3% efficacy, vaccination of 12 year olds, lifelong (20 years) immunity, booster application, cervical screening, observation period 88 years, vaccine price € 56.89, 3.7% (5%) discounting	€ 20,592.68 (€ 18,523.42 – € 40,897.85)	—
Yamamoto et al. [388]	2012	Markov with fixed parameter values	Japan, HPV 16, 18, other high-risk, low-risk, CIN I, CIN II/III, cervical cancer, 100% coverage, 88% efficacy against HPV 16/18, 50% efficacy against other HPV, vaccination of 11 year olds, lifelong immunity, no booster, cervical screening, lifelong observation, vaccine price € 142.99 (incl. admin. cost), 3% discounting	Screening + vaccination dominates screening only (€ 4.75 – € 61,878.30)	66.1–86.8% cervical cancer reduction
Aponte-Gonzales et al. [17]	2013	Markov with fixed parameter values	Colombia, HPV 6, 11, 16, 18, 31, 45, 52, 58, genital warts, CIN I, CIN II/III, cervical cancer, 80% (50-100%) vaccine coverage, 90% (5-100%) efficacy, vaccination age 12 years, lifelong (30 or 70 years) protection, no booster, no distinction between sexual activity, sexual mixing not reported, cervical screening, lifelong follow-up, vaccine price € 168.02 and € 191.26 for quadrivalent and bivalent vaccine, 3% (0-6%) discounting	€ 21665.03 (quadrivalent) and € 25708.29 (bivalent)	—
Berkhof et al. [31]	2013	see Bogaards et al. [37]	Central, Eastern Europe and central Asia, HPV type 16, 18, 31, 33, 35, 39, 45, 51, 52, 56, 58, 59, 66 and 68, cervical cancer, CIN II/III, 70% vaccine coverage, 100% vaccine efficacy, vaccination age 12 years, lifelong duration of protection, no booster, sexual activity levels and sexual mixing not reported, cervical screening, lifetime follow-up, bivalent vaccine price € 44.69 – € 178.75, 3% (0-5%) discounting	€ 1475.56 – € 2865.31	75% reduction in lifetime risk of cervical cancer

Brisson et al. [54]	2013	see van de Velde et al. [360]	Canada, bivalent vs. quadrivalent, 18 HPV types, cervical, vulvar, vaginal, anal, penile and oropharyngial cancer, genital warts, 80% coverage, 95% efficacy, vaccination of 10 yo with last shot in 14 yo, catch-up in 14 yo, duration of immunity 20 years (lifetime), duration of cross-protection 10 years, no booster, 4 levels of sexual activity, assortative, proportionate and disassortative mixing, cervical screening, observation time period 70 (30) years, vaccine price € 67.34, 3% (0%, 5%) discounting	Quadrivalent: € 10,812.49 (€ 3,627.42 – € 29,856.42), bivalent: € 14,091.12 (€ 2,581.05 – € 52,388.26)	Quadrivalent: 41%, bivalent: 43% reduction of cervical cancer
Brisson et al. [56]	2013	see van de Velde et al. [360]	Canada, bivalent vs. quadrivalent, 18 HPV types, CIN, genital warts, cervical, vulvar, vaginal, anal, penile and oropharyngial cancer, 80% (50-70%) coverage, 0-95% efficacy, vaccination of 10yo with last shot in 14 yo, catch-up in 14 yo, duration of immunity 20 years (lifetime), duration of cross-protection 10 years, no booster, sexual activity and mixing not reported, cervical screening, observation time period 70 (30) years, vaccine price € 67.34, 3% (0%, 5%) discounting	—	quadrivalent: 67% reduction in genital warts, 40% in CIN II/III, 35% in cervical cancer. bivalent: 0% reduction in genital warts, 42% in CIN II/III, 36% in cervical cancer
da Fonseca et al. [99]	2013	Markov with fixed parameter values	Brazilian Amazon region, CIN I, CIN II/III, cervical cancer, 100% (50%, 70%) coverage, 25–70% efficacy, vaccination age 12 years, lifelong (10 years) immunity, booster application, cervical screening, lifelong observation, vaccine price € 37.21 (incl. admin. cost) (€ 9.92 – € 124.02), 5% (0–10%) discounting	Vaccination dominates no vaccination (€ 606.66 – € 937.57)	20–71% reduction in cervical cancer
Demarteau et al. [116]	2013	see Debicki et al. [109]	Belgium, HPV 16/18, HPV 31/ 33/ 35/ 39/ 45/ 51/ 52/ 56/ 58/ 59, CIN I, CIN II/III, cervical cancer, 80% coverage, 98% efficacy, vaccination of 12–40 year olds, lifelong (10, 12 years) immunity, no booster, cervical screening, 95 years of follow-up, vaccine price € 143.67 (€ 115 – €172.67) (incl. admin. cost), 3% discounting (costs) and 1.5% (benefits) (0%, 5%)	€ 9,171 (€ 9,164 – € 49,028)	—

Drolet et al. [125]	2013	see van de Velde et al. [360]	Canada, comparison 4- to 9-valent vaccine, 18 HPV types, AGW, cervical, vulvar, vaginal, anal, penile, oropharyngeal cancer, 80% coverage, 95% efficacy (85% 9-valent in sensitivity analysis), vaccination age of 10 years, lifelong (20 year) protection, no booster, 4 levels of sexual activity, assortative and disassortative mixing, cervical screening, lifelong follow-up, vaccine price € 61.71, 3% discounting	4-valent: 10087.22, 9-valent: 7927.25	—
Kim et al. [222]	2013	MS Excel-based model [168]	Middle East, North Africa, HPV 16, 18, high-risk types, low-risk types, CIN, cervical cancer, 70% coverage, 100% efficacy, vaccination age 12 years, lifelong immunity, booster, sexual activity and mixing not reported, cervical screening, lifetime follow-up, vaccine price € 4.48 - € 448.37, 3% (0-6%) discounting	cost-saving – € 103752.86	68-75.3% reduction in lifetime risk of cervical cancer
Kim et al. [216]	2013	MS Excel-based model [161]	Sub-Saharan Africa, HPV 16, 18, high-risk types, low-risk types, CIN, cervical cancer, 70% coverage, 100% efficacy, vaccination age 12 years, lifelong immunity, booster, sexual activity and mixing not reported, cervical screening, lifetime follow-up, vaccine price € 4.48 - € 89.67, 3% (0-6%) discounting	€ 269.02 – € 7532.62	59.7-63.7% reduction in lifetime risk of cervical cancer
Luttjeboer et al. [248]	2013	Probabilistic Markov	The Netherlands, HPV 16, 18, 31, 33, 45, 51, cervical, vulvar, vaginal, anal, oropharyngeal cancer, 100% coverage, 44.8–92.9% efficacy, vaccination of 12 year olds, lifelong immunity, no booster, cervical screening, lifelong observation horizon, vaccine price € 120 (€ 30, 60, 90), 4% cost discount, 1.5% QALY discount	€ 5,815 (€ 6,471 – € 11,431)	—

Turner et al. [350]	2013	see Jit et al. [204]	Cost-effectiveness of bivalent vaccine application in older females, UK, HPV 16, 18, other high-risk with cross-protection, other high-risk without cross-protection, CIN I-III, cervical cancer, coverage 38.9% – 84.3%, 100% efficacy (0–100% in females with previous HPV exposure), vaccination of 12–34 year old females, lifelong (10, 20 years) duration of protection, no booster, 3 sexual activity levels, assortative mixing, cervical screening, observation time 100 years, vaccine price € 23.82 or € 47.64, 3.5% discounting	€ 1,946.75 (€ 2,154.95 – € 673,676.30)	—
Uusküla et al. [357]	2013	see Elbasha et al. [131]	Estonia, HPV 6, 11, 16, 18, CIN I-III, cervical cancer, genital warts, 85% (70%, 95%) coverage, 76% – 96.3% efficacy, vaccination of 12 year olds, lifelong (20 years) immunity, booster application, 3 sexual activity levels, mixing strategies not reported, cervical screening, follow-up 100 years, vaccine price € 59, discounting at 3%	€ 4,889 (€ 1,517 – € 11,148)	2–52% cervical cancer reduction
Westra et al. [383]	2013	see Kohli et al. [225]	Netherlands, comparison of 2- to 4-valent vaccine, HPV 16, 18, 31, 33, 45, other high-risk, other low-risk, genital warts, CIN, cervical cancer, 90% (30-70%) coverage, 0-95% efficacy, vaccination of 12 year olds, lifelong (20 years) duration of immunity, no booster, sexual activity and mixing not reported, cervical screening, lifetime follow-up, vaccine price per dose € 45 - € 105, 3% (0-4%) discounting	2-valent: € 17600, 4-valent: € 18900	—
Yamabe et al. [387]	2013	see Elbasha et al. [132]	Japan, HPV 6, 11, 16, 18, CIN I-III, cervical cancer, genital warts, 80% coverage, 50% catch-up coverage, 90% efficacy, vaccination in 12 year olds, catch-up in 12–24 year olds, lifelong (10 years) duration of protection, no booster, sexual activity levels and mixing according to [132], cervical screening, observation time period 100 years, vaccine price € 89, 3% discounting	€ 8,711.54 (€ 3,811.75 – € 53,727.93)	90.9% cervical cancer reduction

Blakely et al. [34]	2014	Static Markov model in MS Excel, partly probabilistic model parameters	New Zealand, HPV 6, 11, 16, 18, genital warts, CIN, cervical, vulvar, oropharyngeal, anal cancer, vaccine coverage 45-93%, 99% vaccine efficacy, vaccination of 12 year olds, duration of immunity of 20 years, no booster, sexual activity and mixing not reported, cervical screening, follow-up of 98 years, vaccine price not reported, 3% (0-6%) discounting	€ 10805.31 – € 17888.79	32-89% HPV prevalence reduction
Gomez et al. [169]	2014	see Debicki et al. [109]	Chile, HPV 6, 11, 16, 18, genital warts, CIN, cervical cancer, 95% (80%) coverage, 98% efficacy, 23.4-68.8% efficacy against non-oncogenic types, vaccination of 11 year olds, lifelong duration of protection, waning immunity, booster, sexual activit and mixing not reported, cervical screening, vaccine price € 12.03 (2-valent) and € 17.85 (12.71) (4-valent), lifetime follow-up, 6% (3%) discounting	4-valent: € 647.78, 2-valent: € 131.16	14.4% and 21.9% cervical cancer cases avoided (2-valent and 4-valent)
Han et al. [180]	2014	Simulation study	Korea, no distinction between HPV types, CIN, cervical cancer, vaccine coverage not reported, vaccine efficacy 88.04% or 83.99%, vaccination between 11 and 18 years, duration of immunity not reported, no booster, 2 sexual activity levels, mixing not reported, no cervical screening, duration of follow-up not reported, vaccine price € 123.06, 3% discounting	ICUR € 38991.68 (low-risk group) and € 7120.74 (high-risk group)	—
Jit et al. [202]	2014	Static deterministic model in MS Excel	179 countries, HPV 16, 18, CIN, cervical cancer, country-specific data on coverage, efficacy, vaccination age, duration of protection, vaccine price, discount rate (0-6%), sexual activity and mixing not reported, cervical screening, lifelong follow-up (in most cases)	€ 0.9 – € 89823.06	690000 cancer cases prevented
Khatibi et al. [213]	2014	Static deterministic model	Iran, HPV types not distinguished, genital warts, CIN, cervical cancer, 70% coverage, 100% efficacy, vaccination of 15 year olds, lifelong (10 years) protection, booster, sexual activity and mixing not reported, no cervical screening, follow-up of 59 (85) years	€ 13057.3 (€ 7476.9 – € 25056.04)	—

Kiatpongsan et al. [214]	2014	see Kim et al. [220]	Kenya, Uganda, HPV 6, 11, 16, 18, 31, 33, 45, 52, 58, CIN I, CIN II/III, cervical cancer, 100% coverage, 100% efficacy, vaccination of 12 year olds, duration of immunity not reported, no booster, sexual activity and mixing not reported, no cervical screening, lifetime follow-up, vaccine price € 4.04 (4-valent), € 4.13 (2-valent), 9-valent around € 3 more	9-valent very cost-effective when compared to 2- and 4-valent	—
Aguilar et al. [9]	2015	Markov model in MS Excel (CERVIVAC) [79]	Honduras, HPV 16 and 18, cervical cancer, 95% (80-100%) coverage, 94.3% (91.7-96.8%) efficacy, vaccination in 11 year old females, lifelong (20 or 30 years) duration of protection, booster in sensitivity analysis, no distinction between sexual activity levels, sexual mixing not reported, no cervical screening included, lifetime follow-up, vaccine price € 12.02, 3% discounting	€ 827.6 (governmental perspective)/DALY	62% cervical cancer reduction
Burger et al. [68]	2015	see Kim et al. [217, 218]	Norway, HPV 6, 11, 16, 18, genital warts, RRP, cervical, vaginal, vulvar, anal, oropharyngeal, penile cancer, 71% coverage in 12yo, 50% (30%) coverage in 18-26yo, 100% efficacy, vaccination of 12yo, catch-up in 18-26 yo, lifelong immunity, no booster, 4 levels of sexual activity, mixing not reported, cervical screening, lifelong follow-up, vaccine price € 44.68 – € 134.05, 4% (0-3%) discounting	€ 51923.68 – € 173376.83 including catch-up of 18-26yo	75% reduction in HPV 16/18 prevalence
Georgalis et al. [153]	2015	Probabilistic Markov	Spain, HPV 16 and 18, CIN, cervical cancer, 70% (20-100%) coverage, 100% efficacy, vaccination of 11 year olds, lifelong immunity, no booster, sexual activity and mixing not reported, cervical screening, follow-up of 74 years, vaccine price € 31, 3% discounting	€ 12214– € 70002	40% reduction in cervical cancer incidence
Graham et al. [172]	2015	see Praditsitthikorn et al. [294]	Phillipines, HPV 16, 18, CIN, cervical cancer, 20-80% coverage, 74% (59-84%) efficacy, vaccination at age 11 (13, 20 and 25), lifelong (waning) immunity, booster, sexual activity and mixing not reported, cervical screening, lifetime follow-up, vaccine price € 51.55, 3.5% discounting	dominant – € 1150.52	—

Jit et al. [201]	2015	see Jit et al. [204]	UK, comparison of two- to three-dose regimens, HPV 6, 11, 16, 18, genital warts, RRP, cervical, vulvar, vaginal, anal, penile, oropharyngeal cancer, 80% coverage, efficacy estimated through meta-analysis, vaccination of 12 year olds, catch-up in 18 year olds, lifelong or 10, 20, 30 years protection (3- vs. 2-dose regimen), no booster, sexual activity and mixing not reported, cervical screening, follow-up of 100 years, vaccine price € 104.76 (2-valent) and € 112.56 (4-valent), 3.5% (1.5%) discounting	3 doses: € 22104.19, compared to HPV-advise output (see van de Velde et al. [360]) of € 12612.39	73.08% cervical cancer case reduction
Levin et al. [243]	2015	see Goldhaber-Fiebert et al. [159]	China, HPV 16, 18, CIN, cervical cancer, 70% coverage, efficacy not reported, vaccination before 12 years of age, lifelong immunity, no booster, sexual activity and mixing not reported, cervical screening, lifetime follow-up, vaccine price € 8.97 - € 179.35, discounting not reported	€ 4045.2 – € 12796.48	51.90% reduction in lifetime cervical cancer risk
Novaes et al. [270]	2015	Markov model in MS Excel	Brazil, HPV 16, 18, cervical cancer, 50% (40-60%) coverage, 94.3% (91.7-96.8%) efficacy, vaccination age 11 years, lifelong (waning) immunity, booster, sexual activity and mixing not reported, cervical screening, lifetime follow-up, vaccine price € 11.83 (€ 10.64 - € 13.01) per dose, 5% discounting	€ 6544.41 – € 6871.72 per DALY	43% lifetime risk reduction of cervical cancer
Walwyn et al. [373]	2015	Markov model in MS Excel (CERVIVAC [79])	Belize, HPV 16, 18, cervical cancer, 95% coverage, 94.5% (91.7-96.8%) efficacy, vaccination of 10 year olds, lifelong (20 years) duration of protection, booster, sexual activity and mixing irrelevant due to static methodology, no cervical screening, lifetime follow-up, vaccine price per dose € 12.39 (€ 11.75 - € 12.80), 3% (0%) discounting	€ 385.07	—

B.2 Ordinary differential equation models

The ODE-based models on human papillomavirus in the literature are described in further detail in the following.

Deterministic models

The most widely applied ODE-based model in context of CEA of HPV vaccination strategies is presented by Elbasha et al. [132, 133]. The model is developed in an US setting, distinguishes between HPV 6/11 and 16/18, and includes genital warts, CIN-stages and cervical cancer. A stratification by sex, 17 age groups and three sexual activity groups is incorporated. Over the observation time period, individuals transfer between the age groups according to population-specific rates. Sexual mixing varies between fully assortative (like with like individuals) to proportionate (random). The vaccine is given to twelve year old individuals with a catch-up in twelve-24 year olds. In addition, the model is applied to identify cost-effective female catch-up strategies [134], to evaluate the inclusion of an extensive amount of HPV-induced diseases [131], and in a variety of international settings [49, 100–103, 188, 211, 314, 357, 387], incorporating country-specific information. In the original setting, the model results in dominating female-only over universal vaccination. However, once all HPV-induced diseases are considered [131], universal HPV vaccination is deemed to be cost-effective.

In contrast to Elbasha et al. [132], Jit et al. [204] apply their dynamic transmission model exclusively in an UK setting. The corresponding equations are not displayed; therefore, we are unable to evaluate whether the methodology is based on ODEs or PDEs. The model is sex-, age- and behavioural-specific and accounts for HPV types 16, 18, other high-risk types, and types 6 and 11. Details on behaviour groups and sexual mixing are not reported. As for HPV-induced diseases, CIN-stages, cervical

cancer, non-cervical cancers and genital warts in females are accounted for. Female-only and universal vaccination strategies are evaluated for the ages of twelve to 25 years; waning vaccine-induced immunity is accounted for. PSA is conducted in retrospect through LHS. The model results in cost-effective and non-cost-effective results for female-only and universal vaccination, respectively. The model is used by Choi et al. [85] to estimate HPV-induced disease outcome and is extended to compare the bi- to the quadrivalent vaccine [203], to evaluate vaccination up to 34 years of age [350], and to compare two to three dose regimens [201].

Barnabas et al. [26] present an innovative sexual mixing algorithm which is applied by [72, 143, 215, 316, 324, 366]. The PDE-based model is developed in a Finnish context. Females can acquire a CIN stage or cervical cancer. The population is stratified into age cohorts of five years, and four sexual activity levels are considered. The probability of HPV transmission per partnership is estimated by calibrating the HPV prevalence prediction of the model to HPV 16 seroprevalence data. The HPV vaccine is given to 15 year old individuals, and vaccine-specific immunity is assumed to remain lifelong.

Hughes et al. [187] modify an ODE-based HPV transmission model adapted from Anderson and May [13] and link it to a disease progression model accounting for cervical cancer in an US context. The authors account for HPV 16 transmission and assume 90% vaccine coverage and 75% efficacy. The vaccination age is not reported. The duration of immunity lasts for 10 years; however, no booster is applied. Three levels of sexual activity are accounted for. The model predicts a 44% and 30% reduction in HPV prevalence for universal and female-only vaccination, respectively.

Tully et al. [349] present an ODE-based model in a Canadian context. The model is stratified by age, sex and HPV type; seven age groups are considered, and HPV types are categorized into HPV 16/18 and other types. The model accounts for CIN and four stages of cervical cancer. The pro-

gression between the cancer stages is modelled through a submodel in MS Excel. Sexual mixing depends on age, with males tending to select younger female partners. The bivalent vaccine is given to twelve year old females. The model results in a cost-effective outcome.

Lee et al. [240] present the only exception of a static ODE-based model to investigate HPV infection and progression to cervical cancer in African American females in the US. The model exclusively includes females and does not incorporate HPV transmission dynamics between the sexes; the force of infection accounts for female HPV infection prevalence. The model is neither age- nor behavioural-specific, and predictions on prevalence or incidence are not conducted.

Bayesian models

Bogaards et al. [38] present a deterministic PDE-based model for the Netherlands; however, Bayesian methods are used to estimate the transmission probabilities, rates of waning resistance and progression of 14 high-risk HPV types. The endemic equilibrium is estimated through priors which are informed by data on HPV prevalence before initial vaccine introduction. The posterior distributions are updated through clinical trial data on newly acquired, persistent or cleared HPV infections at six and 18 months of follow-up. The results indicate that per partnership transmission probability is highest for HPV 66 (94%) and lowest for HPV 68 (43%). Waning resistance per year is slowest for HPV 68 and fastest for HPV 56. As for HPV-induced diseases, only CIN-stages are considered. The model parameters on sexual behaviour are informed by point estimates. Three sexual activity levels are considered, and individuals are allowed to switch between adjacent levels. Sexual mixing varies between proportionate and assortative. The model predicts that female-only vaccination results in a faster HPV prevalence reduction than universal vaccination [39]. The transmission model is linked to

a microsimulation model to result in a hybrid model [37] (see Section 4.4.4).

Another Bayesian ODE-based model is presented by Korostil et al. [229]; the impact of female-only HPV vaccination on genital warts prevalence in both sexes in Australia is investigated. Other HPV-induced diseases are not accounted for. Females and males divided into nine age groups populate the model. Four sexual activity levels are considered; switching between levels is not possible, however, sexual activity declines with age. Age-, sex- and behavioural-specific partner acquisition rates remain fixed values, whereas degrees of assortativity in the sexual mixing matrix, duration of infection, treatment and natural immunity as well transition probabilities are assigned distributions.

Vänskä et al. [368] present a PDE-based model in a Bayesian context for Finland. The model accounts for age, sex, and the age- and sex-specific numbers of partners. HPV-induced diseases are not considered, and sexual mixing is exclusively proportionate. Partner acquisition rates, HPV transmission probability, clearance rates and waning of natural immunity are assigned distributions, whereas all other model parameters are assigned fixed values. Multiple high-risk HPV infections can affect one individual independently at the same time. The model considers HPV infections originating from new partners and those acquired within persisting partnerships due to sexual intercourse with a third individual.

B.3 Markov models

In the following, Markov models in the literature on HPV transmission and induced disease progression modelling are described.

Models with fixed parameter values

Four publications [17, 248, 345, 370] conduct PSA in Markov models with fixed parameter values in retrospect once the model output is available and present CEACs and/or scatterplots obtained through MC sampling procedures.

To conduct PSA, Voko et al. [370], Aponte-Gonzales et al. [17] and Thiry et al. [345] assign suitable probability distributions to key model parameters. Luttjeboer et al. [248] inform the parameter distributions through data on the corresponding ranges. If no data are available, ranges are estimated to amount to 50%-150% of the base case values.

Probabilistic models

Three authors [81, 136, 358] present Markov models in a Bayesian framework. Chen et al. [81] develop a Bayesian Markov model to estimate the cost-effectiveness of female-only HPV vaccination in Taiwan, considering CIN stages and cervical cancer. Cost-effective results are presented, and PSA is conducted straightforwardly through cost-effectiveness scatterplots and CEACs.

Van de Velde et al. [358] introduce a static Bayesian Markov model and calculate the vaccine-induced decrease in the lifetime risk of cervical cancer in a Canadian setting by accounting for HPV 16 and 18 separately. The calibration approach is Bayesian; model parameters are fitted to data by updating the prior distributions into suitable posteriors. Females receive the vaccine at ages twelve, 15, 20 or 30 years.

The third Bayesian Markov model is introduced in the BEST I[1] study by Favato et al. [136] in an Italian setting and provides the basis for our research; we extend this static model by a dynamic approach for HPV trans-

[1] **B**ayesian modelling assessing the **E**ffectiveness of a vaccination **S**trategy **T**o prevent HPV-related diseases

mission (see Section 5.7) and include a greater variety of HPV-induced diseases (see Section 5.4) as well as cohorts of males and females (see Section 5.2 and Table 5.1). Furthermore, we vaccinate both sexes in different intervention scenarios (see Section 5.3). In its original version, the model does not distinguish between different HPV types and accounts for the HPV-induced diseases genital warts, CIN-stages and cervical cancer. Several cohorts of females are vaccinated in parallel, such as twelve and 15 year olds, twelve, 15 and 18 year olds or twelve, 15, 18 and 25 year olds. The authors report cost-effective results, including extensive PSA.

Praditsitthikorn et al. [294] present a probabilistic semi-Markov model in MS Excel for Thailand. A semi-Markov model implies that a transition to a future state does not only depend on the current state; in addition, the time spent in the state is considered in the transition probabilities. This model is not based on Bayesian statistics; however, forward simulation in terms of Monte Carlo sampling is incorporated in order to account for parameter uncertainty. One female cohort is observed from age 15 throughout their lifetime. The model accounts for CIN-stages and four stages of cervical cancer. The vaccine coverage rate is 100% on average, whereas mean vaccine efficacy is assumed to be 79%. In the base-case, vaccination takes place in 15 year old females, with catch-up opportunities at the ages of 16-25, 30, 40, 50, and 60 years, respectively. The authors assume a lifelong duration of vaccine-induced immunity and account for waning immunity after five and ten years in sensitivity analyses, involving booster application.

Blakely et al. [34] present a Markov model in MS Excel for New Zealand including probability distributions on model parameters; details on distributions are only reported for vaccination coverage. Forward sampling is conducted through 2,000 Monte Carlo simulations. The model accounts for genital warts, CIN, cervical, vulvar, oropharyngeal and anal cancer. The vaccine coverage rates vary between 45% and 93%, whereas vaccine efficacy is assumed to be as high as 99%. Vaccination is given to twelve year

old females, and they are observed for a follow-up of 98 years. Duration of immunity is assumed to last for 20 years. The effects of herd immunity in unvaccinated females and males are accounted for in an indirect way through a meta-regression on the output of the model described by Brisson et al. [59]. Firstly, the HPV prevalence reduction is estimated; afterwards, the estimate is multiplied by the incidence on HPV-induced diseases, resulting in reduced incidence due to indirect consideration of herd immunity. PSA is conducted in terms of the cost-effectiveness plane and the cost-effectiveness acceptability curve. The model results in a cost-effective outcome.

Georgalis et al. [153] present a stochastic Markov model; however, the authors do not report details on their methodology of incorporating parameter uncertainty, and only the mean values of model parameters are displayed. The vaccine is given to eleven year old girls at a 70% coverage rate in the base case, and vaccine efficacy of 100%, inducing lifelong immunity, is assumed. PSA is not conducted, and the model results in a cost-effective outcome and predicts a 40% reduction in cervical cancer cases.

B.4 Individual-based models

Accetta et al. [7] present a microsimulation model for Italy. The model is exclusively populated by females; therefore, sexual mixing does not take place, and herd immunity cannot be accounted for. Several cervical screening strategies including the HPV DNA-test are compared to vaccination. The model includes HPV 16/18, other high-risk and low-risk types. As for HPV-induced diseases, CIN- stages and cervical cancer are accounted for. The vaccine is given to eleven year old females at 100% coverage, and 75.9% vaccine efficacy is assumed. Vaccine-induced immunity lasts for a lifetime in the base-case; scenarios with booster application are evaluated in addition. HPV vaccination is cost-effective, and reduces lifetime risk of cervical cancer by 54%.

In accordance to Accetta et al. [7], Goldhaber-Fiebert et al. [159] and Kim et al. [220] present microsimulation models which only include females and account for the same HPV types and HPV-induced diseases in an US and Brazilian context, respectively. Acquisition of HPV infection is modelled in an age-dependent way, not incorporating the effects of herd immunity. In [159], the transition probabilities to the states of HPV infection can be modified through the integration of the output of a dynamic transmission model [215], resulting in a hybrid model. Both vaccine coverage and efficacy are assumed to be 100%, and females are vaccinated before the age of twelve. Observation time horizon and duration of immunity are assumed to be lifelong. The model predicts a reduction in cervical cancer of 55%-90%, depending on the screening strategy. The purpose of [220] is the calibration of the model output to Brazilian data, and HPV vaccination does not take place.

De Kok et al. [108] modify the MISCAN microsimulation model [177] to specifically account for HPV. The model structure is similar to [7, 159, 220]; however, no distinction according to HPV type is made. The model only incorporates females and is therefore static. The vaccine is given to twelve year old females; scenarios with one or multiple booster doses are evaluated in addition. In the base case, 85% vaccine coverage with lifelong protection, 70% vaccine efficacy against cervical cancer and 35% vaccine efficacy against CIN-stages are assumed. The model is the only one reviewed which results in non-cost-effective outcome of female-only HPV vaccination.

Vanni et al. [367] present a microsimulation model in a Brazilian context. Sexual mixing is based on the algorithm presented by Garnett et al. [150] and Barnabas et al. [26]; yet, difference equations rather than differential equations are used. The model population consists of 200,000 individuals which are stratified by sex, four sexual activity groups and 14 age groups. HPV 16, 18 and 6/11 infections are accounted for. In females, CIN-stages, cervical cancer and genital warts are accounted for, whereas males are only

vectors in virus transmission and do not develop genital warts. The vaccine is given to twelve year old females at coverage rates of 50%, 70% and 90%. Vaccine efficacy is not reported. Duration of follow-up and vaccine-induced immunity are lifelong. The model results in cost-effective outcome, and predicts vaccine-specific HPV type prevalence to be zero 30 years after vaccine introduction.

Van de Velde and Brisson et al. [58, 360] present by far the most extensive microsimulation model on HPV transmission and disease progression. In a Canadian setting, 18 HPV types are considered separately. In [58], the model extension to CIN-stages, cervical cancer, genital warts, and indirect prevalence reduction of HPV-induced cancers of vulva, vagina, anus, penis, and head/neck is described. The age-specific sexual mixing algorithm accounts for four levels of sexual activity, proportionate and assortative mixing, casual and stable relationships and the frequency of sex acts. Individuals are vaccinated at age twelve with a possible catch-up until age 18 in different scenarios. An economic evaluation is not conducted in [58, 360]; however, [54–57, 59, 122, 125, 236, 359] investigate the cost-effectiveness of different vaccination strategies. Laprise et al. [236] compare two- and three-dose vaccination schedules. In addition, Brisson et al. [55, 57] compare the quadrivalent to the bi- and nonavalent HPV vaccines, respectively.

Only one network model [140] is presented in the literature, which is modified by Olsen et al. [277] and adapted to an Irish context by Usher et al. [356]. In a Danish setting, vaccination is given to twelve year old females with a catch-up in twelve-26 year olds. Sexual mixing takes place with partners in an age range of ten years, and frequency of sexual intercourse as well as duration of partnerships is accounted for. Olsen et al. [277] account for HPV 6 and 11 in addition to HPV 16 and 18. As a consequence, individuals can develop genital warts in addition to a CIN-stage or cervical cancer. Furthermore, an universal vaccination scenario of twelve year old individuals is included. The model predicts cost-effective results for both universal and

female-only vaccination. The model is further modified by including anal, penile, vaginal, vulvar, head/neck cancer and comparing two- and three-dose vaccination scenarios, resulting in cost-effective results for two-dose regimens [278]. Usher et al. [356] process the output of the dynamic network model into a CEA in MS Excel. The HPV 16/18 incidence in twelve year old females predicted by the network model is adjusted in retrospect in MS Excel, depending on the vaccination scenario under investigation. The model predicts cost-effective female-only vaccination.

B.5 Hybrid models

Taira et al. [339] combine a probabilistic Markov model [311] estimating the natural history of HPV infection with a dynamic deterministic transmission model based on difference equations in an US context.

The hybrid model presented by Horn et al. [185] differs from Taira et al.'s model by the way HPV transmission is accounted for. Horn et al. apply a continuous-time ODE-based transmission model [132], whereas Taira et al. present a discrete-time model. Horn et al. use the output of the ODE-based transmission model as an input into a Markov model [313] in a German setting. Horn et al. do not conduct a health economic evaluation.

Kim et al. [218] adapt the sexual mixing algorithm from Barnabas et al. [26] (see Section B.2), and estimate disease progression through a probabilistic microsimulation model [215] in an US context. In addition to CIN-stages and cervical cancer, anal and oral cancers as well as recurrent respiratory papillomatosis are considered.

Bogaards et al. [37] combine a deterministic ODE-based transmission model [38] (described in Appendix B.2) to a static, probabilistic microsimulation model for disease progression in a Dutch setting. The authors do not analyse the cost-effectiveness of female-only vaccination.

Another hybrid approach in publications focussing on female-only vacci-

nation is given by the combination of the microsimulation model presented by Kim et al. [220] to the PDE-based HPV transmission model presented by Barnabas et al. [26], modified by Goldie et al. [163], and described in Appendix B.2. This methodology is used by Goldie et al. [161, 166–168], Kim et al. [217] and Sharma et al. [316]. Furthermore, Kim et al. [219] combine the same HPV transmission model to the microsimulation model presented by Goldhaber-Siebert et al. [159]. The microsimulation models are described in Appendix 4.4.3 and are used to simulate the natural history of HPV infection, whereas the output of the dynamic HPV transmission model is integrated into the microsimulation models in order to estimate transitions to the state of HPV infection. The methodology in [161, 166–168, 217, 316] is the same; however, the model assumptions and the country-specific input data differ. Goldie et al. conduct CEAs for the US, 72 developing countries, Latin America and the Carribbean as well as Vietnam, Kim et al. for the US, and Sharma et al. for a setting in Thailand. In most models, only HPV-induced diseases affecting the cervix are considered; however, Kim et al. [217] include a great variety of HPV-induced diseases.

B.6 Results of the cost-effectiveness analyses

The following section includes further details on the results of the health economic evaluations for female-only vaccination.

Female-only vaccination

Out of the 110 publications, 44 [7, 9, 16, 17, 34, 37, 75, 81, 83, 96, 99, 108, 109, 111, 136, 153, 159, 162, 168, 180, 202, 213, 220, 225, 229, 241, 245, 248, 263, 270, 274, 294, 311, 321, 328, 342, 344, 345, 349, 358, 365, 367, 370, 388] introduce newly developed models, whereas 46 [30, 31, 68, 70, 72, 87, 100–103, 113–116, 119, 120, 130, 161, 164, 166, 167, 169, 172, 183, 211, 214, 216,

219, 222, 226, 228, 231, 234, 243, 257, 273, 300, 314, 316, 333, 337, 348, 356, 357, 373, 387] adjust previously developed methodology to different country-specific settings, and 20 [36, 54, 56, 57, 125, 134, 160, 163, 201, 203, 217, 221, 232, 303, 304, 350, 359, 364, 382, 383] evaluate an extended aim of research.

The vast majority of newly developed models, altogether 31 [9, 17, 34, 81, 83, 96, 99, 109, 111, 136, 153, 162, 202, 225, 241, 245, 248, 263, 270, 274, 294, 311, 321, 328, 342, 344, 345, 358, 365, 370, 388], are static Markov models. These are not ideal since the effects of herd immunity are either not considered or only indirectly adjusted for [16, 34, 83, 365, 370]. As for universal vaccination, ignoring the effects of herd immunity is prone to induce an incorrect model outcome in female-only vaccination scenarios. In models incorporating exclusively female cohorts, additional reasons for falsified model outcome are given by ignoring the role of males as vectors in HPV transmission and the impact of HPV-induced diseases in males.

In addition to the Markov models, two newly developed ODE-based models [229, 349], five microsimulation models [7, 108, 159, 220, 367] and two hybrid models [37, 168] are presented in context of female-only vaccination. The ODE-based models are dynamic by definition and thus account for the effects of herd immunity; however, apart from [367], the microsimulation models exclusively observe female individuals and are therefore static. The hybrid models [37, 168] estimate disease transmission through ODE-based models [26, 38], and incorporate the predictions on HPV prevalence into microsimulation models [37, 220] which consist of female populations.

For the different interventions compared (cervical screening, vaccination strategies including catch-up, bivalent, quadrivalent, and nonavalent vaccine), the results range from cost-saving in nine publications [70, 120, 161, 166, 167, 211, 219, 222, 316] to not cost-effective in de Kok et al. [108]. Possible explanations for the outcome in [108] are the static methodology, the relatively low vaccine efficacy of only 70% against cervical cancer and 35% against CIN stages, and the high unit cost of vaccination of € 118 per dose.

Appendix C

Explanatory diagrams of HPV-induced cancer boxes

Appendix C shows the contents of the boxes of the HPV-induced diseases, including precancerous stages and possible transitions to the body areas affected.

We include the states of infection, clearance and reinfection into each explanatory diagram since transitions to and from precancerous stages to the mentioned states are possible. Furthermore, cancer survivors move to the state of clearance four years after initial cancer diagnosis. All intraepithelial neoplasiae, the corresponding cancer and the three states of survival post cancer diagnosis affecting the same body part are displayed in the same colour. We use different shades to distinguish disease severity, where darker tones represent more severe conditions.

Figure C.1 displays the contents of the box head/neck cancer. After HPV infection, individuals move directly to the state of head/neck cancer. The survivors enter the three tunnel states post cancer diagnosis. With each passing year, they reduce their probability of dying, potentially moving to clearance. Having been cured, they can be re-infected and develop a second HPV-induced disease.

In addition to head/neck cancer, anal cancer can affect both sexes. We

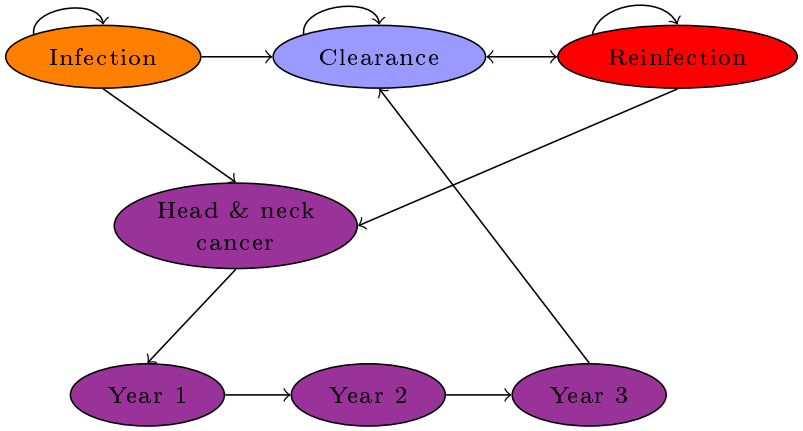

Figure C.1: Head/neck cancer can affect both sexes. This figure represents the contents of the box *Head&neck cancer* in the overview Figure 5.1 showing the model structure. We assume no precancerous stages for this HPV-induced cancer. Having been diagnosed with head/neck cancer, surviving individuals move to the tunnel states post cancer diagnosis. Once affected by head/neck cancer, the probability of dying increases. Those who have survived for four years after diagnosis move to the state of clearance. A reinfection, resulting in a second HPV-induced disease, might occur.

include the two precancerous stages LSIL and HSIL, as Figure C.2 shows. Those infected with HPV can develop a disease or clear their infection. Similarly to those suffering from head/neck cancer, we assume that anal cancer patients either die or enter the three states of cancer survival, possibly resulting in cancer clearance.

The HPV-induced diseases vaginal and vulvar cancer can only affect females. We display the process of infection, disease progression and regression in Figures C.3 and C.4. We include three precancerous stages in the vaginal cancer box, and assume only one for vulvar cancer. Comparable to the HPV-induced cancers described previously, individuals can either die from the disease or become cured.

HPV can also infect the penis. Penile cancer is the only male-specific HPV-induced cancer included in our model and the process of disease development and clearance is displayed in Figure C.5. Similarly to vulvar cancer, we only assume one precancerous stage.

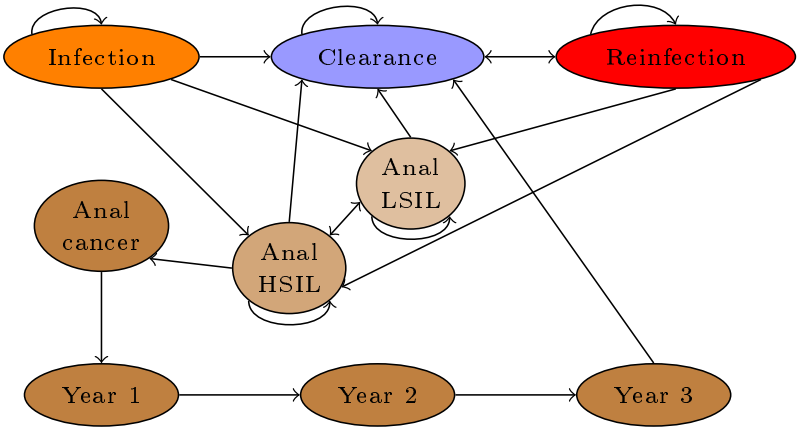

Figure C.2: Anal cancer is not a sex-specific disease; however, females are under a higher disease risk than heterosexual males. This figure shows the contents of the box *Anal cancer*. We assume the two precancerous stages anal LSIL and HSIL to be part of the disease progression process. Once infected with HPV, individuals can either move to anal LSIL or anal HSIL. A direct transition to anal cancer is impossible. After cancer diagnosis, surviving individuals enter the three stages of post cancer diagnosis. Those who have not died will move to the state of clearance. Individuals can possibly be reinfected, initiating a second disease development in the anus or another organ.

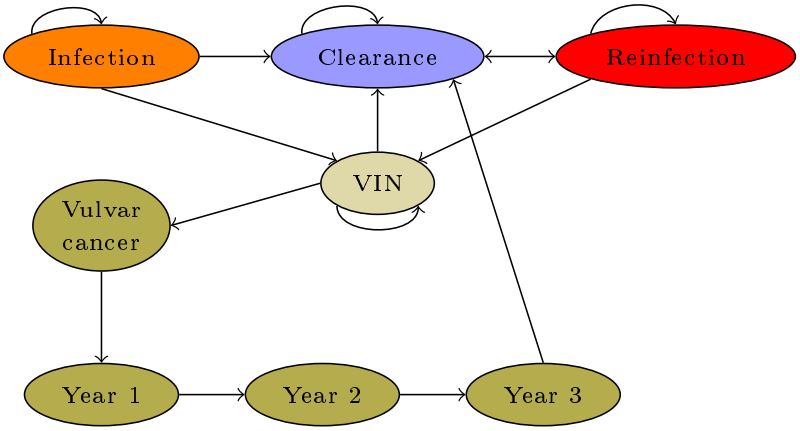

Figure C.4: In context of vulvar cancer, we only include the precancerous stage VIN. After acquiring the HPV infection and being affected by VIN, females can progress to vulvar cancer. In survivors, we assume vulvar cancer to be cured four years after diagnosis. A reinfection could initiate the same or another disease progression process.

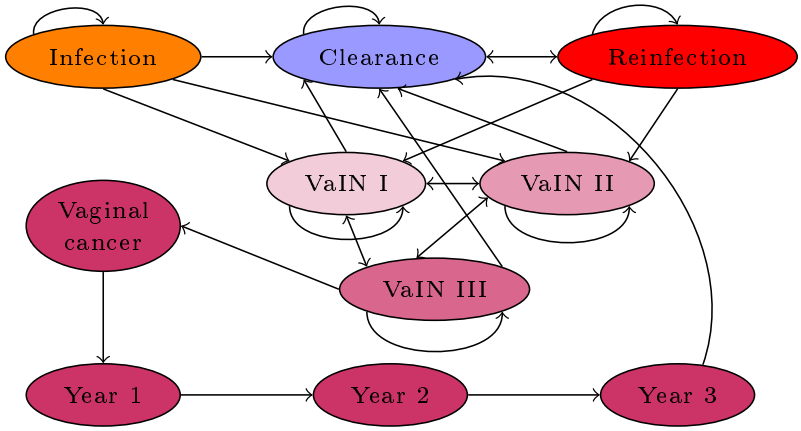

Figure C.3: The contents of the box *Vaginal cancer* are similar to those of *Cervical cancer* as shown in Figure 5.2. For this female-specific disease, we assume females infected with HPV to move in between the three precancerous stages VaIN I-III and to either clear their infection or progress to vaginal cancer during the process. Having survived vaginal cancer for four years, we assume females to be cured. A reinfection and repetition of disease development or the acquisition of another HPV-induced disease is possible.

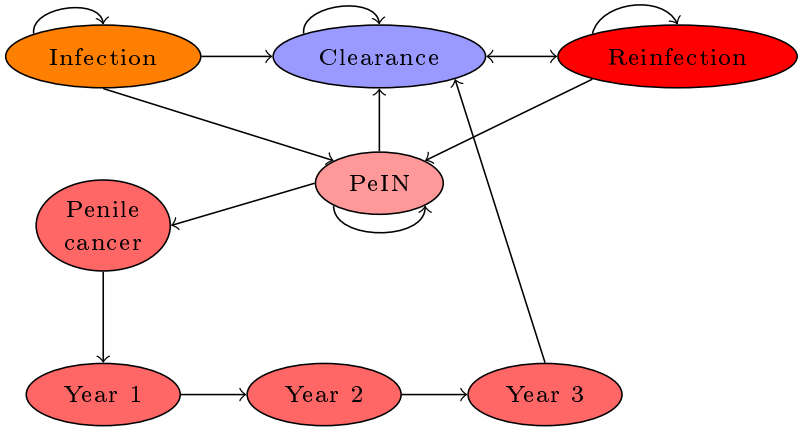

Figure C.5: Penile cancer is the only male-specific HPV-induced disease in our model. Similarly to vulvar cancer, we assume only one precancerous stage, PeIN. Having moved to PeIN, those who have not cleared their infection will progress to penile cancer. Having passed the three tunnel states without dying, we assume males to be cured. From the state of clearance, they can move to the state of reinfection.

Appendix D

Continuation of transition probabilities in females

In Section 5.8, the general approach of constructing the transition probabilities of the HPV model is shown for the states *Healthy* and *Exposure*. In this appendix, we present the remaining transition probabilities which are not described in the main part of this PhD thesis. In addition, this appendix includes an overview table (Table D.1) on the numbering of the 36 states of the female model compartment. This table is essential for an understanding of the corresponding transition probabilities.

Table D.1: This table gives an overview of the 36 states included in the female compartment of the dynamic HPV model with the corresponding numbering. This numbering will be considered in the equations of the transition probabilities.

No.	State	No.	State
1	Healthy	19	Post anal cancer (year two)
2	Exposure	20	Post anal cancer (year three)
3	Infection	21	Head/neck cancer
4	CIN I	22	Post head/neck cancer (year one)
5	CIN II	23	Post head/neck cancer (year two)
6	CIN III	24	Post head/neck cancer (year three)
7	Genital warts	25	VIN
8	Cervical cancer	26	Vulvar cancer
9	Death (for all causes)	27	Post vulvar cancer (year one)
10	Post cervical cancer (year one)	28	Post vulvar cancer (year two)
11	Post cervical cancer (year two)	29	Post vulvar cancer (year three)
12	Post cervical cancer (year three)	30	VAIN I
13	Clearance	31	VAIN II
14	Reinfection	32	VAIN III
15	Anal LSIL	33	Vaginal cancer
16	Anal HSIL	34	Post vaginal cancer (year one)
17	Anal cancer	35	Post vaginal cancer (year two)
18	Post anal cancer (year one)	36	Post vaginal cancer (year three)

From the state *Infection*

Figure 5.1 indicates that people infected by HPV can either clear the infection naturally ($s = 2$) or progress towards mild or moderate cervical neoplastic lesions (CIN I, $s = 4$, or CIN II, $s = 5$), genital warts ($s = 7$), anal LSIL ($s = 15$), anal HSIL ($s = 16$), head/neck cancer ($s = 21$), vulvar intraepithelial neoplasm (VIN, $s = 25$) or vaginal intraepithelial neoplasms (VaIN I, $s = 30$ or VaIN II, $s = 31$). Using the parameters specified in Section 5.5, we can define the transition probabilities.

For intervention $i = 1$

In intervention $i = 1$, screening-only, the probabilities of moving towards the target states are defined according to Equation D.1. We define $\mathcal{S} = \{2,$

$3, 4, 5, 7, 9, 15, 16, 21, 25, 30, 31\}$ to be a set of target states. All transitions to states different from $\mathcal{S}$ are impossible and as a consequence set to zero. The transition probabilities are defined as

$$
\begin{aligned}
\pi^{F}_{1,a,3,s} &= 0 \,\forall\, s \notin \{\mathcal{S}\} \\
\pi^{F}_{1,a,3,2} &= \delta_{Fa} \\
\pi^{F}_{1,a,3,4} &= \delta_1 \\
\pi^{F}_{1,a,3,5} &= \delta_2 \\
\pi^{F}_{1,a,3,7} &= \psi^{(gw)}_{a,F} \\
\pi^{F}_{1,a,3,9} &= d_{a,F} \\
\pi^{F}_{1,a,3,15} &= \delta_3 \rho_2^{\bigstar} \frac{1}{\rho_3^{\bigstar}} \\
\pi^{F}_{1,a,3,16} &= \delta_4 \rho_2^{\bigstar} \frac{1}{\rho_3^{\bigstar}} \\
\pi^{F}_{1,a,3,21} &= \psi^{(hn)}_{a,F} \\
\pi^{F}_{1,a,3,25} &= \delta_5 \\
\pi^{F}_{1,a,3,30} &= \delta_5 \\
\pi^{F}_{1,a,3,31} &= \delta_5 \\
\pi^{F}_{1,a,3,3} &= 1 - \sum_{s \neq 3} \pi^{F}_{1,a,3,s}.
\end{aligned}
\tag{D.1}
$$

The parameter δ_{Fa} represents age-dependent regression from infection, δ_1 and δ_2 progression to CIN I and CIN II, respectively, $\psi^{(gw)}_{a,F}$ is the observable variable of the age- and sex-specific acquisition of genital warts and δ_3 and δ_4 are the progression probabilities to anal LSIL and HSIL. Since δ_3 and δ_4 are taken from publications on anal LSIL and HSIL prevalence in homosexual males and HIV positive females [97, 98], these probabilities have to be adjusted by the correction factors $\rho_2^{\bigstar}$ and $\rho_3^{\bigstar}$, based on [145, 351] (see Section 5.5 and Appendix G.1).

The age- and sex-specific probability of the acquisition of head/neck can-

cer is represented by the observable variable $\psi_{a,F}^{(hn)}$. The parameter δ_5 represents a transition from the state of infection to VIN as well as VaIN I and II. The constraint implies that all transition probabilities sum up to one.

For intervention $i = 2$ and $i = 3$

Similarly to intervention $i = 1$, people who receive HPV vaccination in one of the interventions $i = 2$ or $i = 3$ can move to the states $\mathcal{S}$, as Equation D.1 shows. All other transition probabilities are set to zero. Equation D.2 is based on the indices $i = 2$; however, these are equivalent to the indices of $i = 3$ and can therefore be used equivalently.

The transition probability to the state $s = 2$ is not affected by vaccination because HPV-induced diseases do not regress more quickly following vaccination. The probability of acquiring a HPV-induced disease following infection is reduced considerably in vaccinated individuals, in accordance to Equation 5.2 depending on the levels of vaccine coverage and compliance. In other words, patients who take up the vaccination have a reduced chance of progressing towards one of the more advanced states, with the reduction being a function of their compliance level. Those who do not take up vaccination at all have the same risk as those under intervention $i = 1$.

In the HPV-induced diseases CIN I and CIN II, in addition to vaccine efficacy γ_1, we assume a cross-protection effect $\chi_\star$ against HPV genotypes different from HPV 16 and 18. At the current stage of research, we can only consider these protective effects in the two precancerous stages of the cervix. The corresponding transition probabilities are given as

$$
\begin{aligned}
\pi^{F}_{2,a,3,s} &= 0 \,\forall\, s \notin \{\mathcal{S}\} \\
\pi^{F}_{2,a,3,2} &= \delta_{0a} \\
\pi^{F}_{2,a,3,4} &= \alpha[\nu_3(1-\gamma_1-\chi_\star)\delta_1 + (1-\nu_3)(1-\zeta\gamma_1)\delta_1] + (1-\alpha)\delta_1 \\
\pi^{F}_{2,a,3,5} &= \alpha[\nu_3(1-\gamma_1-\chi_\star)\delta_2 + (1-\nu_3)(1-\zeta\gamma_1)\delta_2] + (1-\alpha)\delta_2 \\
\pi^{F}_{2,a,3,7} &= \alpha[\nu_3(1-\gamma_1)\psi^{(gw)}_{a,F} + (1-\nu_3)(1-\zeta\gamma_1)\psi^{(gw)}_{a,F}] + (1-\alpha)\psi^{(gw)}_{a,F} \\
\pi^{F}_{2,a,3,9} &= d_{a,F} \\
\pi^{F}_{2,a,3,15} &= \alpha[\nu_3(1-\gamma_2)\delta_3\rho_2^\star\frac{1}{\rho_3^\star} + (1-\nu_3)(1-\zeta\gamma_2)\delta_3\rho_2^\star\frac{1}{\rho_3^\star}] + (1-\alpha)\delta_3\rho_2^\star\frac{1}{\rho_3^\star} \\
\pi^{F}_{2/3/4,a,3,16} &= \alpha[\nu_3(1-\gamma_2)\delta_4\rho_2^\star\frac{1}{\rho_3^\star} + (1-\nu_3)(1-\zeta\gamma_2)\delta_4\rho_2^\star\frac{1}{\rho_3^\star}] + (1-\alpha)\delta_4\rho_2^\star\frac{1}{\rho_3^\star} \\
\pi^{F}_{2,a,3,21} &= \alpha[\nu_3(1-\gamma_3)\psi^{(hn)}_{a,F} + (1-\nu_3)(1-\zeta\gamma_3)\psi^{(hn)}_{a,F}] + (1-\alpha)\psi^{(hn)}_{a,F} \\
\pi^{F}_{2,a,3,25} &= \alpha[\nu_3(1-\gamma_1)\delta_5 + (1-\nu_3)(1-\zeta\gamma_1)\delta_5] + (1-\alpha)\delta_5 \\
\pi^{F}_{2,a,3,30} &= \alpha[\nu_3(1-\gamma_1)\delta_5 + (1-\nu_3)(1-\zeta\gamma_1)\delta_5] + (1-\alpha)\delta_5 \\
\pi^{F}_{2,a,3,31} &= \alpha[\nu_3(1-\gamma_1)\delta_5 + (1-\nu_3)(1-\zeta\gamma_1)\delta_5] + (1-\alpha)\delta_5 \\
\pi^{F}_{2,a,3,3} &= 1 - \sum_{s\neq 3}\pi^{F}_{2,a,3,s}.
\end{aligned}
\tag{D.2}
$$

From the state *Clearance*

People who previously experienced a HPV-induced precancerous stage, cancer or genital warts and cleared the disease (either naturally or through intervention) can remain in the state of clearance, be newly exposed to HPV, or die.

The transition towards the state of reinfection (indicated by $s = 14$) is affected at least partially by a set of social and demographic risk factors (such as age at first sexual intercourse and smoking). A proportion $1 - \zeta$ of the individuals in the state of clearance after neoplasia do not present risk factors and thus their chance of becoming reinfected by HPV is the

same as that of individuals moving from the state of exposure to that of infection. Conversely, the remaining proportion ζ of subjects, who are at increased risk, experience a higher chance of becoming reinfected by HPV, as described by the parameter $\rho_1^{\bigstar}$. These assumptions are encoded in

$$\begin{aligned}
\pi^{F}_{i,a,13,s} &= 0 \,\forall\, s \notin \{9, 13, 14\} \\
\pi^{F}_{i,a,13,9} &= d_{a,F} \\
\pi^{F}_{i,a,13,14} &= (1-\zeta)\pi^{F}_{i,a,2,3} + \zeta\pi^{F}_{i,a,2,3}\rho_1^{\bigstar} \\
\pi^{F}_{i,a,13,13} &= 1 - \sum_{s \neq 13} \pi^{F}_{i,a,13,s}.
\end{aligned}$$

From the state *Reinfection*

People who become re-exposed to HPV after a previous occurence of a HPV-induced disease are essentially in the same position as people who are infected for the first time, except for the effect of the risk factors that are assumed to be present at this stage. We define a set of target states $\mathcal{K} = \{4, 5, 9, 13, 14, 15, 16, 21, 25, 30, 31\}$. Consequently, the transition probabilities are

$$
\begin{aligned}
\pi^{F}_{i,a,14,s} &= 0 \,\forall\, s \notin \{\mathcal{K}\} \\
\pi^{F}_{i,a,14,4} &= (1-\zeta)\pi^{F}_{i,a,3,4} + \zeta\pi^{F}_{i,a,3,4}\rho_1^{\bigstar} \\
\pi^{F}_{i,a,14,5} &= (1-\zeta)\pi^{F}_{i,a,3,5} + \zeta\pi^{F}_{i,a,3,5}\rho_1^{\bigstar} \\
\pi^{F}_{i,a,14,9} &= d_{a,F} \\
\pi^{F}_{i,a,14,13} &= \pi^{F}_{i,a,3,2} \\
\pi^{F}_{i,a,14,15} &= (1-\zeta)\pi^{F}_{i,a,3,15} + \zeta\pi^{F}_{i,a,3,15}\rho_1^{\bigstar} \\
\pi^{F}_{i,a,14,16} &= (1-\zeta)\pi^{F}_{i,a,3,16} + \zeta\pi^{F}_{i,a,3,16}\rho_1^{\bigstar} \\
\pi^{F}_{i,a,14,21} &= (1-\zeta)\pi^{F}_{i,a,3,21} + \zeta\pi^{F}_{i,a,3,21}\rho_1^{\bigstar} \\
\pi^{F}_{i,a,14,25} &= (1-\zeta)\pi^{F}_{i,a,3,25} + \zeta\pi^{F}_{i,a,3,25}\rho_1^{\bigstar} \\
\pi^{F}_{i,a,14,30} &= (1-\zeta)\pi^{F}_{i,a,3,30} + \zeta\pi^{F}_{i,a,3,30}\rho_1^{\bigstar} \\
\pi^{F}_{i,a,14,31} &= (1-\zeta)\pi^{F}_{i,a,3,31} + \zeta\pi^{F}_{i,a,3,31}\rho_1^{\bigstar} \\
\pi^{F}_{i,a,14,14} &= 1 - \sum_{s \neq 14} \pi^{F}_{i,a,14,s}.
\end{aligned}
\tag{D.3}
$$

Equation D.3 assumes that the regression towards clearance is not affected by the risk factors and thus that the parameters ζ and $\rho_1^{\bigstar}$ are not present.

From the state *Genital warts*

Females affected by genital warts can move to the state of clearance ($s = 13$), die ($s = 9$) or persist in that condition ($s = 7$), indicated by the parameter υ_F. Remaining in the state of genital warts is age-specific; we assume that younger people have a considerably higher chance to recover in a shorter period of time when compared to older people [69]. The adjustment to age dependency is obtained through model calibration, as described in Section 6.3, and indicated by $\lambda_{v,a,r,s}$ with indices v, a, r, s representing sex, age cohort, original state and target state, respectively. Consequently, we model the possible transition probabilities as

$$\pi^{F}_{i,a,7,s} = 0 \,\forall\, s \notin \{7, 13, 9\}$$
$$\pi^{F}_{i,a,7,7} = \lambda_{F,a,7,7}\upsilon_F$$
$$\pi^{F}_{i,a,7,9} = d_{a,F}$$
$$\pi^{F}_{i,a,7,13} = 1 - \sum_{s \neq 7} \pi^{F}_{i,a,7,s}.$$

From the state *CIN I*

Once females have reached the state CIN I, screening becomes an important factor in all three interventions ($i = 1, 2, 3$). A proportion σ_a of people will participate in the screening programme, which makes their diagnosis earlier and thus increases their chance of clearing the infection (e.g. moving to the state of *clearance*, represented by the index $s = 13$).

Of all females screened, a proportion τ_1 will undergo an immediate intervention, conization, which will improve their chance of moving back to clearance, estimated by the parameter $\xi^{(cerv,1)}_{1,0}$. A different proportion τ_2 will undergo conization only after a follow-up period; nevertheless, once the intervention was performed, their chance of regressing to clearance is again $\xi^{(cerv,1)}_{1,0}$. Finally, those who do not undergo conization (a proportion of $1 - \tau_1 - \tau_2$) will have a lower chance of regression, represented by $\xi^{(cerv,2)}_{1,0}$.

The remaining individuals (in a proportion $1 - \sigma_a$) will not be screened and thus are less likely to move towards the state of clearance. In fact, their chance of transition is assumed to be the same as that of subjects who have not undergone conization $\xi^{(cerv,2)}_{1,0}$. We encode these assumptions in

$$
\begin{aligned}
\pi^{F}_{i,a,4,s} &= 0 \,\forall\, s \notin \{4,5,6,9,13\} \\
\pi^{F}_{i,a,4,5} &= \sigma_a[(\tau_1+\tau_2)\xi^{(cerv,1)}_{1,2} + (1-\tau_1-\tau_2)\xi^{(cerv,2)}_{1,2}] + (1-\sigma_a)\xi^{(cerv,2)}_{1,2} \\
\pi^{F}_{i,a,4,6} &= \sigma_a[(\tau_1+\tau_2)\xi^{(cerv,1)}_{1,3} + (1-\tau_1-\tau_2)\xi^{(cerv,2)}_{1,3}] + (1-\sigma_a)\xi^{(cerv,2)}_{1,3} \\
\pi^{F}_{i,a,4,9} &= d_{a,F} \\
\pi^{F}_{i,a,4,13} &= \sigma_a[(\tau_1+\tau_2)\xi^{(cerv,1)}_{1,0} + (1-\tau_1-\tau_2)\xi^{(cerv,2)}_{1,0}] + (1-\sigma_a)\xi^{(cerv,2)}_{1,0} \\
\pi^{F}_{i,a,4,4} &= 1 - \sum_{s \neq 4} \pi^{F}_{i,a,4,s}.
\end{aligned}
$$

From the state CIN I, females can only move to the states CIN II ($s = 5$), CIN III ($s = 6$), death ($s = 9$) and clearance ($s = 13$). All other transition probabilities are set to zero. The constraint of probabilities to sum up to one is represented by the last row of the system of transition probabilities, which results in the probability to remain in CIN I.

From the state *CIN II*

Following the scheme presented for the transitions from the state CIN I, we model the probabilities for the transitions from the state CIN II as

$$
\begin{aligned}
\pi^{F}_{i,a,5,s} &= 0 \,\forall\, s \notin \{4,5,6,9,13\} \\
\pi^{F}_{i,a,5,4} &= \sigma_a[(\tau_1+\tau_2)\xi^{(cerv,1)}_{2,1} + (1-\tau_1-\tau_2)\xi^{(cerv,2)}_{2,1}] + (1-\sigma_a)\xi^{(cerv,2)}_{2,1} \\
\pi^{F}_{i,a,5,6} &= \sigma_a[(\tau_1+\tau_2)\xi^{(cerv,1)}_{2,3} + (1-\tau_1-\tau_2)\xi^{(cerv,2)}_{2,3}] + (1-\sigma_a)\xi^{(cerv,2)}_{2,3} \\
\pi^{F}_{i,a,5,9} &= d_{a,F} \\
\pi^{F}_{i,a,5,13} &= \sigma_a[(\tau_1+\tau_2)\xi^{(cerv,1)}_{2,0} + (1-\tau_1-\tau_2)\xi^{(cerv,2)}_{2,0}] + (1-\sigma_a)\xi^{(cerv,2)}_{2,0} \\
\pi^{F}_{i,a,5,5} &= 1 - \sum_{h \neq 5} \pi^{F}_{i,a,5,s}.
\end{aligned}
$$

Similar interpretations to those in the previous case are applied.

From the state *CIN III*

Transitions from the state CIN III are age-specific. The older the female, the less likely she is to regress to a less severe precancerous stage or to move to clearance. Furthermore, females in CIN III can progress to cervical cancer. We assume that older females are more likely to develop cervical cancer [72, 263]. The age-specific transition probabilities are adjusted by comparing these to Brazilian data on CIN III prevalence, assuming Italian CIN III prevalence follows similar age trends as described in Section 6.3. The age-specific adjustment factor is indicated through the variable $\lambda_{v,a,r,s}$ and multiplied with the transition probabilities under the assumption of no conization ($\xi_{3,y}^{(cerv,2)}$). The system of equations is defined as

$$
\begin{aligned}
\pi_{i,a,6,s}^{F} &= 0 \,\forall\, s \notin \{4,5,6,8,9,13\} \\
\pi_{i,a,6,4}^{F} &= \lambda_{F,a,6,4}\xi_{3,1}^{(cerv,2)} \\
\pi_{i,a,6,5}^{F} &= \lambda_{F,a,6,5}\xi_{3,2}^{(cerv,2)} \\
\pi_{i,a,6,8}^{F} &= \lambda_{F,a,6,8}\xi_{3,4}^{(cerv,2)} \\
\pi_{i,a,6,9}^{F} &= d_{a,F} \\
\pi_{i,a,6,13}^{F} &= \lambda_{F,a,6,13}\xi_{3,0}^{(cerv,2)} \\
\pi_{i,a,6,6}^{F} &= 1 - \sum_{s \neq 4} \pi_{i,a,4,s}^{F}.
\end{aligned}
$$

From the state *Cervical cancer*

According to our model, patients who have entered the state of cervical cancer only have two possible options. They either die (which occurs at an increased rate as compared to individuals without cancer), or progress to the state of first year after diagnosis (indicated by $s = 10$). The probabilities of these transitions vary according to the stage at which the individuals are diagnosed: subjects who enter the state of cervical cancer at a more ad-

vanced stage have lower survival rates. The assumptions are encoded by

$$\begin{aligned}
\pi^{F}_{i,a,8,s} &= 0 \,\forall\, s \notin \{9, 10\} \\
\pi^{F}_{i,a,8,9} &= 1 - \sum_{s \neq 8} \pi^{F}_{i,a,8,s} \\
\pi^{F}_{i,a,8,10} &= \sum_{j=1}^{4} \mu_j^{(cerv)} \phi_{1,j}^{\diamondsuit(cerv)},
\end{aligned}$$

with $\mu_j^{(cerv)}$ indicating the probability that a patient is diagnosed with cervical cancer at stage j, whereas the parameter $\phi_{1,j}^{\diamondsuit(cerv)}$ represents the probability of one-year survival in stage j.

From the states *Post cervical cancer (year one, year two, year three)*

For each HPV-induced cancer, we define three tunnel states of one, two and three years post cancer diagnosis. We assume that cervical cancer patients in the first tunnel state post cancer diagnosis can either survive, with an increased probability compared to the state of cervical cancer (progressing to two years post cancer diagnosis), or die. Again, the progression to the next year depends on the disease stage. The transition probabilities from the state one year post cervical cancer diagnosis are defined as

$$\begin{aligned}
\pi^{F}_{i,a,10,s} &= 0 \,\forall\, s \notin \{9, 11\} \\
\pi^{F}_{i,a,10,11} &= \sum_{j=1}^{4} \mu_j^{(cerv)} \phi_{2,j}^{\diamondsuit(cerv)} \\
\pi^{F}_{i,a,10,9} &= 1 - \pi^{F}_{i,a,10,11},
\end{aligned} \tag{D.4}$$

where the index $s = 11$ designates the state two years after the diagnosis of cervical cancer. Those females who do not survive move to the state of

death ($s = 9$).

Having moved to $s = 11$, individuals can either die or move to the next year post cancer diagnosis (indicated by $s = 12$), which is not shown in Equation D.4; however, the principle is equivalent. The transition probabilities to the cancer survival states $s = 10$, $s = 11$ and $s = 12$ are a combination of the probabilities of diagnosis $\mu_j^{(cerv)}$ and the one-to four year survival probability $\phi_{q,j}^{\diamondsuit(cerv)}$, where q represents the year of survival and j the cancer stage, respectively. Moving to the state of death is in each case calculated by means of the statistical constraint of probabilities to sum up to one. Those females who survive for four years are assumed to be cured and move to the state of clearance ($s = 13$).

From the state *Anal LSIL*

In contrast to CIN, we assume only two pre-cancerous stages of anal cancer. The mildest is anal LSIL, from which a transition to anal HSIL ($s = 16$) or anal cancer ($s = 17$) is possible. Furthermore, patients can clear their infection, die or remain in the state of LSIL. The chance of clearance ($s = 13$) is higher in younger patients, whereas the risk of progressing to anal HSIL ($s = 16$) is higher in older patients.

The transitions to clearance, HSIL and anal cancer are indicated by the parameter $\xi_{1,y}^{(an)}$, representing the transition to states less severe ($y = 0$) or more severe ($y = 2, 3$) than anal LSIL. The exponent (an) shows that the anal area is infected by HPV. The transitions to $s = 13$ and $s = 16$ are adjusted according to age through variables $\lambda_{v,a,r,s}$, which are estimated through model calibration as described in Section 6.3. The transition probabilities are given by

$$\pi^{F}_{i,a,15,s} = 0 \,\forall\, s \notin \{9, 13, 15, 16, 17\}$$
$$\pi^{F}_{i,a,15,9} = d_{a,F}$$
$$\pi^{F}_{i,a,15,13} = \lambda_{F,a,15,13}\xi^{(an)}_{1,0}$$
$$\pi^{F}_{i,a,15,16} = \lambda_{F,a,15,16}\xi^{(an)}_{1,2}$$
$$\pi^{F}_{i,a,15,17} = \xi^{(an)}_{1,3}$$
$$\pi^{F}_{i,a,15,15} = 1 - \sum_{s \neq 15} \pi^{F}_{i,a,15,s}.$$

From the state *Anal HSIL*

The transition probabilities from the state anal HSIL are similar to those from the state LSIL. People can either clear their intraepithelial neoplasiae, move to the less severe stage LSIL ($s = 15$), develop anal cancer ($s = 16$), remain in anal HSIL, or die. We assume the transition probabilities to clearance and anal cancer to be age- and sex-specific, with younger people being more likely to move to clearance, and older people more likely to develop anal cancer. Dependency on age is again indicated by the variables $\lambda_{v,a,r,s}$, obtained through model calibration. The corresponding equations are presented as

$$\pi^{F}_{i,a,16,s} = 0 \,\forall\, s \notin \{9, 13, 15, 16, 17\}$$
$$\pi^{F}_{i,a,16,9} = d_{a,F}$$
$$\pi^{F}_{i,a,16,13} = \lambda_{F,a,16,13}\xi^{(an)}_{2,0}$$
$$\pi^{F}_{i,a,16,15} = \lambda_{F,a,16,15}\xi^{(an)}_{2,1}$$
$$\pi^{F}_{i,a,16,17} = \xi^{(an)}_{2,3}$$
$$\pi^{F}_{i,a,16,16} = 1 - \sum_{s \neq 16} \pi^{F}_{i,a,16,s}.$$

From the state *Anal cancer*

Similarly to all other HPV-induced cancers, the transitions from the state of anal cancer lead into so-called tunnel states. Once affected by cancer, people either die ($s = 9$) or initially survive for one year ($s = 18$). The probability of survival depends on whether anal cancer is diagnosed, indicated by the parameter $\mu_j^{(an)}$, with j representing the respective cancer stage. We assume that the probabilities of diagnosis affect the cancer outcome since only a recognized cancer can be treated properly and is therefore more likely to result in prolonged survival. In contrast to the transition probabilities for stages different from cancer, the probability of dying is no longer the age- and sex-specific observable variable $d_{a,F}$, but calculated with the constraint that all probabilities have to sum up to 1. Obviously, the probability of dying is increased in individuals who suffer from cancer. The transition probabilities are defined as

$$\begin{aligned}
\pi^{F}_{i,a,17,s} &= 0 \,\forall\, s \notin \{9, 18\} \\
\pi^{F}_{i,a,17,9} &= 1 - \pi^{F}_{i,a,17,18} \\
\pi^{F}_{i,a,17,18} &= \sum_{j=1}^{4} \mu_j^{(an)} \phi_{1,j}^{\diamondsuit(an)}.
\end{aligned}$$

From the states *Post anal cancer (year one, year two, year three)*

Having been diagnosed with anal cancer, people enter a sequence of three tunnel states. People who survived anal cancer for one year can either survive for another year, indicated by the probability of diagnosing anal cancer ($\mu_j^{(an)}$) and the probability of two-year survival ($\phi_{2,j}^{\diamondsuit(an)}$), or they can die from the disease. The corresponding transition probabilities are defined as

$$\pi^{F}_{i,a,18,s} = 0 \,\forall\, s \notin \{9, 19\}$$
$$\pi^{F}_{i,a,18,9} = 1 - \pi^{F}_{i,a,18,19}$$
$$\pi^{F}_{i,a,18,19} = \sum_{j=1}^{4} \mu_j^{(an)} \phi_{2,j}^{\diamondsuit(an)}.$$

Transitions to the states of two and three years after anal cancer ($s = 20$ and $s = 21$, respectively) are calculated in a similar way; however, the states r and s as well as the index q in $\phi^{\diamondsuit}_{q,j}$ have to be adjusted. The year after cancer diagnosis is represented by q. Having survived anal cancer for two years, individuals can either die from the disease or survive for another year, resulting in a survival of altogether three years.

We assume individuals who are still alive four years after diagnosis and treatment of cancer to be cured and therefore move to the state of clearance, indicated by $s = 13$.

From the state *Head/neck cancer*

In contrast to the other HPV-induced cancers, we assume no precancerous stages for head/neck cancer. Therefore, following HPV infection, people can directly move to the state of head/neck cancer. Similarly to the cancer states previously described, patients diagnosed with head/neck cancer can either survive for one year, indicated by the parameters $\mu_j^{(hn)}$ and $\phi_{1,j}^{\diamondsuit(hn)}$, or die from the disease, which is calculated through the constraint to ensure probabilities sum up to one. The parameter $\mu_j^{(hn)}$ represents the probability of diagnosis in stage $j = 1, 2, 3, 4$, and $\phi_{1,j}^{\diamondsuit(hn)}$ is the vector of one-year survival probabilities according to stage j. The transition probabilities are given as

$$\begin{aligned}
\pi^{F}_{i,a,21,s} &= 0 \,\forall\, s \notin \{9, 22\} \\
\pi^{F}_{i,a,21,9} &= 1 - \pi^{F}_{i,a,21,22} \\
\pi^{F}_{i,a,21,22} &= \sum_{j=1}^{4} \mu_j^{(hn)} \phi_{1,j}^{\diamondsuit(hn)}.
\end{aligned}$$

From the states *Post head/neck cancer (year one, year two, year three)*

Having survived head/neck cancer for one year, patients enter the first tunnel state post head/neck cancer diagnosis ($s = 22$) and can either survive for another year ($s = 23$), indicated by the parameters $\mu_j^{(hn)}$ and $\phi_{2,j}^{\diamondsuit(hn)}$, or die ($j = 9$). The transition probability to death is calculated by means of the constraint of probabilities, and the whole process is given as

$$\begin{aligned}
\pi^{F}_{i,a,22,s} &= 0 \,\forall\, s \notin \{9, 23\} \\
\pi^{F}_{i,a,22,9} &= 1 - \pi^{F}_{i,a,22,23} \\
\pi^{F}_{i,a,22,23} &= \sum_{j=1}^{4} \mu_j^{(hn)} \phi_{2,j}^{\diamondsuit(hn)}.
\end{aligned} \tag{D.5}$$

Similarly, patients in the state two years after diagnosis of head/neck cancer ($r = 23$) can either move to the state of three-year survival ($s = 24$) or die. Having survived head/neck cancer for three years ($r = 24$), patients can either move to the state of clearance, indicated by $s = 13$, or die. The corresponding transition probabilities are calculated as shown in Equation D.5; however, the states r and s as well as indices q of the cancer survival probabilities $\phi_{q,j}^{\diamondsuit(hn)}$ have to be adjusted accordingly.

From the state *VIN*

We assume one precancerous stage in context of vulvar cancer, the so-called vulvar intraepithelial neoplasia (VIN). Females can either clear their HPV infection and move to the state of clearance ($s = 13$), progress to the state of vulvar cancer ($s = 26$), die ($s = 9$) or remain in the state of vulvar cancer ($s = 25$). Probabilities of progression and regression are indicated by the parameter $\xi_{1,y}^{(vin)}$, where $y = 0, 2$ represent regression and vulvar cancer, respectively. Younger females have a higher chance of clearance, indicated by the variable $\lambda_{v,a,r,s}$, whereas older females have a higher risk to progress to vulvar cancer. The probability of remaining in VIN is calculated through the constraint of probabilities summing up to one. The system of equations is given as

$$
\begin{aligned}
\pi_{i,a,25,s}^{F} &= 0 \, \forall \, s \notin \{9, 13, 25, 26\} \\
\pi_{i,a,25,9}^{F} &= d_{a,F} \\
\pi_{i,a,25,13}^{F} &= \xi_{1,0}^{(vin)} \\
\pi_{i,a,25,26}^{F} &= \lambda_{F,a,25,26} \xi_{1,2}^{(vin)} \\
\pi_{i,a,25,25}^{F} &= 1 - \sum_{s \neq 25} \pi_{i,a,25,s}^{F}.
\end{aligned}
$$

From the state *Vulvar cancer*

Once affected by vulvar cancer, females can either survive for one year and move to the state of one year post vulvar cancer ($s = 27$), depending on the probability of diagnosis of vulvar cancer in the respective stage j, represented by the parameter $\mu_j^{(vulv)}$, and the stage-dependent one-year survival probability $\phi_{1,j}^{\diamondsuit(vulv)}$. Those who do not survive move to the state of death, calculated by means of the constraint for probabilities which must sum up to one. The corresponding transition probabilities are defined as

$$\begin{aligned}
\pi^{F}_{i,a,26,s} &= 0 \,\forall\, s \notin \{9, 27\} \\
\pi^{F}_{i,a,26,9} &= 1 - \pi^{F}_{i,a,26,27} \\
\pi^{F}_{i,a,26,27} &= \sum_{j=1}^{4} \mu_j^{(vulv)} \phi_{1,j}^{\diamondsuit(vulv)}.
\end{aligned}$$

From the states *Post vulvar cancer (year one, year two, year three)*

Females who have survived vulvar cancer for one year after diagnosis can either move to the state of two years post vulvar cancer ($s = 28$), or die, indicated by

$$\begin{aligned}
\pi^{F}_{i,a,27,s} &= 0 \,\forall\, s \notin \{9, 28\} \\
\pi^{F}_{i,a,27,9} &= 1 - \pi^{F}_{i,a,27,28} \\
\pi^{F}_{i,a,27,28} &= \sum_{s=1}^{4} \mu_j^{(vulv)} \phi_{2,j}^{\diamondsuit(vulv)}.
\end{aligned} \tag{D.6}$$

Similarly to the transition probabilities shown in Equation D.6, females who have survived vulvar cancer for two years ($r = 28$) can survive for another year and move to the state of three years post vulvar cancer ($s = 29$). Those who do not survive move to the state of death ($s = 9$). We assume females who survive vulvar cancer for four years ($r = 30$) to be cured and therefore to move to the state of clearance ($s = 13$). Those who do not survive for four years die, calculated through the constraint for probabilities. In contrast to Equation D.6, in order to move to the more advanced survival states, we have to adjust the numberings of the states r and s as well as the index q, representing the yearly survival probabilities in $\phi_{q,j}^{\diamondsuit(vulv)}$.

From the state *VaIN I*

Equivalent to the precancerous stages of cervical cancer, we assume three precancerous stages for vaginal cancer: vaginal intraepithelial neoplasms (VaIN) stage I, II and III. Females who are in the stage of VaIN I can either clear their infection and move to the state of clearance ($s = 13$), die ($s = 9$), remain in VaIN I ($s = 30$) or move to the more severe states of VaIN II ($s = 31$) or VaIN III ($s = 32$). The probabilities to move within the VaIN stages or to clear the infection are represented by the parameter $\xi_{1,y}^{(vag)}$, where $y = 0, 2, 3$ indicate states less or more severe than VaIN I. To remain in VaIN I is calculated through the constraint of probabilities. The transition probabilities are presented as

$$
\begin{aligned}
\pi_{i,a,30,s}^{F} &= 0 \, \forall \, s \notin \{9, 13, 30, 31, 32\} \\
\pi_{i,a,30,9}^{F} &= d_{a,F} \\
\pi_{i,a,30,13}^{F} &= \xi_{1,0}^{(vag)} \\
\pi_{i,a,30,31}^{F} &= \xi_{1,2}^{(vag)} \\
\pi_{i,a,30,32}^{F} &= \xi_{1,3}^{(vag)} \\
\pi_{i,a,30,30}^{F} &= 1 - \sum_{s \neq 30} \pi_{i,a,30,s}^{F}.
\end{aligned}
$$

From the state *VaIN II*

Having progressed to VaIN II, females can still clear their infection and move to the state of clearance ($s = 13$), regress to VaIN I ($s = 30$) or progress to the state of VaIN III ($s = 32$). These transition probabilities are indicated by the parameter $\xi_{2,y}^{(vag)}$, where $y = 0, 1, 3$ represent states less or more severe than VaIN II ($x = 2$). The progression to VaIN III is age-specific, indicated through the variable $\lambda_{F,a,31,32}$, with a higher risk in older females. Furthermore, females can die or remain in VaIN II. The corresponding equations are given as

$$\pi^{F}_{i,a,31,s} = 0 \,\forall\, s \notin \{9, 13, 30, 31, 32\}$$
$$\pi^{F}_{i,a,31,9} = d_{a,F}$$
$$\pi^{F}_{i,a,31,13} = \xi^{(vag)}_{2,0}$$
$$\pi^{F}_{i,a,31,30} = \xi^{(vag)}_{2,1}$$
$$\pi^{F}_{i,a,31,32} = \lambda_{F,a,31,32}\xi^{(vag)}_{2,3}$$
$$\pi^{F}_{i,a,31,31} = 1 - \sum_{s \neq 31} \pi^{F}_{i,a,31,s}.$$

From the state *VaIN III*

Affected by VaIN III, females can still clear their infection and move to the state of clearance ($s = 13$) or regress to VaIN I ($s = 30$) or VaIN II ($s = 31$). Furthermore, their disease can progress to vaginal cancer ($s = 33$), they can remain in VaIN III ($s = 32$), or die ($s = 9$). Moving between the pre-cancerous lesions and vaginal cancer is indicated by $\xi^{(vag)}_{3,y}$ with $y = 0, 1, 2, 3$, ranging from clearance to vaginal cancer. The risk of developing vaginal cancer is age-specific, indicated by $\lambda_{F,a,32,33}$. The transition probabilities are defined as

$$\pi^{F}_{i,a,32,s} = 0 \,\forall\, s \notin \{9, 13, 30, 31, 32, 33\}$$
$$\pi^{F}_{i,a,32,9} = d_{a,F}$$
$$\pi^{F}_{i,a,32,13} = \xi^{(vag)}_{3,0}$$
$$\pi^{F}_{i,a,32,30} = \xi^{(vag)}_{3,1}$$
$$\pi^{F}_{i,a,32,31} = \xi^{(vag)}_{3,2}$$
$$\pi^{F}_{i,a,32,33} = \lambda_{F,a,32,33}\xi^{(vag)}_{3,3}$$
$$\pi^{F}_{i,a,32,32} = 1 - \sum_{s \neq 32} \pi^{F}_{i,a,32,s}.$$

From the state *Vaginal cancer*

Once affected by vaginal cancer, females can either survive and move to the state of one year post vaginal cancer diagnosis ($s = 34$) or die. Those who do not survive obviously die, which is calculated by means of the constraint of probabilities to sum up to one. The transition probability of one-year survival is indicated by the parameter $\mu_j^{(vag)}$, the probability of diagnosis of vaginal cancer in stage $j = 1, 2, 3, 4$, and the one-year survival probability according to stage j, $\phi_{1,j}^{\diamondsuit(vag)}$, as shown in

$$\begin{aligned}
\pi^{F}_{i,a,33,s} &= 0 \,\forall\, s \notin \{9, 34\} \\
\pi^{F}_{i,a,33,9} &= 1 - \pi^{F}_{i,a,33,34} \\
\pi^{F}_{i,a,33,34} &= \sum_{r=1}^{4} \mu_j^{(vag)} \phi_{1,j}^{\diamondsuit(vag)}.
\end{aligned}$$

From the states *Post vaginal cancer (year one, year two, year three)*

Females who have survived vaginal cancer for one year can either move to the state of two-year survival post vaginal cancer ($s = 35$), or die ($s = 9$). As for the states post cancer diagnosis, the probability of dying is calculated through the constraint of probabilities which must sum up to one. The corresponding transition probabilities are defined as

$$\begin{aligned}
\pi^{F}_{i,a,34,s} &= 0 \,\forall\, s \notin \{9, 35\} \\
\pi^{F}_{i,a,34,9} &= 1 - \pi^{F}_{i,a,34,35} \\
\pi^{F}_{i,a,34,35} &= \sum_{r=1}^{4} \mu_j^{(vag)} \phi_{2,j}^{\diamondsuit(vag)}.
\end{aligned} \tag{D.7}$$

Having survived vaginal cancer for two years, females can either survive for

another year and move to the state three years post vaginal cancer ($s = 36$), or die ($s = 9$). We assume vaginal cancer to be cured four years after diagnosis. Therefore, females who are in the state of three years post vaginal cancer can either move to the state of clearance ($s = 13$), or die ($s = 9$). These transition probabilities are calculated similarly to Equation D.7; however, the numberings of the states r and s as well as indices q of the survival probabilities $\phi_{q,j}^{\diamondsuit(vag)}$ have to be adjusted. The index $q = 1, 2, 3, 4$ represents the yearly cancer survival.

From the state *Death*

As is obvious, all people who end up in the state of death cannot move to another state (death is said to be an *absorbing* state). Therefore, we set all transition probabilities to states apart from $s = 9$ to zero, and remaining in the state of death to one, resulting in

$$\pi_{i,a,9,s}^{F} = 0 \,\forall\, s \neq 9$$
$$\pi_{i,a,9,9}^{F} = 1.$$

Appendix E

The male model compartment

Appendix E focusses on the male compartment of the model, reporting each state in males with its corresponding numbering. Afterwards, the transition probabilities in males are explained, including a detailed description of all equations. The corresponding transition probabilities in females are given in Section 5.8 and Appendix D.

Several aspects of the male model compartment have already been presented in Section 5.4. The exact numbering of the states in males which is essential for an understanding of the transition probabilities is given in the following. As for the transition probabilities, we report those for males in Appendix E.2.

E.1 Numbering of states in males

In contrast to 36 states in females, there are only 22 states in males since a smaller number of organs can be affected by HPV. The states are given in Table E.1. The corresponding numbering is of importance for the transition probabilities which are described in Appendix E.2.

Table E.1: Overview of the 22 states included in the male model compartment

No.	State	No.	State
1	Healthy	12	Post anal cancer (year two)
2	Exposure	13	Post anal cancer (year three)
3	Infection	14	Head/neck cancer
4	Genital warts	15	Post head/neck cancer (year one)
5	Death (for all causes)	16	Post head/neck cancer (year two)
6	Clearance	17	Post head/neck cancer (year three)
7	Reinfection	18	PeIN
8	Anal LSIL	19	Penile cancer
9	Anal HSIL	20	Post penile cancer (year one)
10	Anal cancer	21	Post penile cancer (year two)
11	Post anal cancer (year one)	22	Post penile cancer (year three)

E.2 Transition probabilities in males

In this appendix, the transition probabilities in males between the 22 states included are described in detail. We distinguish between the original states r and the target states s. We set transition probabilities to states where movements are not enabled to zero. Furthermore, we use the mathematical constraint for probabilities to sum up to one to make sure that the sum of transition probabilities from the same state r cannot take values outside of the interval [0;1]. From the states *Exposure* and *Infection*, the application of different interventions i plays a role; in these cases, transition probabilities for the interventions $i = 1, 2, 3$ are described separately.

The notation of transition probabilities in males, $\pi^{M}_{i,a,r,s}$, is similar to $\pi^{F}_{i,a,r,s}$ in females (see Section 5.8), where

- i represents the intervention (see Section 5.3);
- a represents the age cohort of the male (see Table 5.1 in Section 5.3);
- r represents the original state;
- s represents the target state.

In sex-specific model parameters, v indexes the population member's sex, where $v = F$ represents females and $v = M$ males. We have to consider the different numbering of states r, s in males compared to those in females, reported in Tables E.1 and D.1, respectively.

From the state *Healthy*

Equivalent to females, the transition probabilities from the state *Healthy* in males enable moving to the state of exposure ($s = 2$) or death ($s = 5$). Furthermore, for people who have not had a sexual relationship yet ($1 - w_a$), it is possible to remain in perfect health ($s = 1$). We assume the probability of first intercourse, w_a, to be age-dependent. Death probabilities $d_{a,M}$ in males are different from those in females ($d_{a,F}$), since death is not only age-, but also sex-specific, indicating a longer life expectancy in females. The corresponding set of equations is defined as

$$\begin{aligned}
\pi^{M}_{i,a,1,s} &= 0 \,\forall\, s \notin \{1, 2, 5\} \\
\pi^{M}_{i,a,1,2} &= w_a \\
\pi^{M}_{i,a,1,5} &= d_{a,M} \\
\pi^{M}_{i,a,1,1} &= 1 - \sum_{s \neq 1} \pi^{M}_{i,a,1,s}.
\end{aligned}$$

From the state *Exposure*

Vaccination in males takes place in intervention $i = 3$. Interventions $i = 1, 2$ do not include vaccination in males and therefore do not result in lower transition probabilities to the state of infection.

For intervention $i = 1$ and $i = 2$

We assume males in interventions $i = 1, 2$ not to receive the HPV vaccine. As for females, males move to the state of HPV infection $s = 3$ through a dynamic process of sexual mixing, represented by the force of infection $\pi^{\bigstar}_{M,b,a}(\mathcal{I}_t)$, which is described in detail in Section 5.7.5. This parameter depends on sex, sexual behaviour, age and time interval of observation. Furthermore, people can either die ($s = 5$) or remain in the state of exposure which is calculated through the constraint of probabilities which have to sum up to one. The transition probabilities for intervention $i = 1$ are given by

$$\begin{aligned}
\pi^{M}_{1,a,2,s} &= 0 \,\forall\, s \notin \{2, 3, 5\} \\
\pi^{M}_{1,a,2,3} &= \pi^{\bigstar}_{M,b,a}(\mathcal{I}_t) \text{ (see Section 5.7.5)} \\
\pi^{M}_{1,a,2,5} &= d_{a,M} \\
\pi^{M}_{1,a,2,2} &= 1 - \sum_{s \neq 2} \pi^{M}_{1,a,2,s};
\end{aligned}$$

however, those for $i = 2$ are equivalent.

For intervention $i = 3$

In contrast to the previous interventions, we assume males receive the HPV vaccine in intervention $i = 3$. Therefore, their transition probability to move to the state of infection ($s = 3$) is considerably reduced. The reduction depends on the vaccine coverage α, the vaccine compliance ν_3, the vaccine efficacy γ_1 and the decrease in vaccine efficacy due to incomplete compliance ζ. Furthermore, males can either die ($s = 5$) or remain in the state of exposure, calculated with the constraint of probabilities. We assume vaccine related parameters not to be sex-specific, and define the transition probabilities as

$$\pi^{M}_{3,a,2,s} = 0 \, \forall h \notin \{2,3,5\}$$

$$\pi^{M}_{3,a,2,5} = d_{a,M}$$

$$\pi^{M}_{3,a,2,3} = \alpha_1[\nu_3(1-\gamma_1)\pi^{\bigstar}_{M,b,a}(\mathcal{I}_t) + (1-\nu_3)(1-\zeta\gamma_1)\pi^{\bigstar}_{M,b,a}(\mathcal{I}_t)] + (1-\alpha)\pi^{\bigstar}_{M,b,a}(\mathcal{I}_t)$$

$$\pi^{M}_{3,a,2,2} = 1 - \sum_{s \neq 2} \pi^{M}_{3,a,2,s}.$$

From the state *Infection*

Once infected, males can move to a selection of HPV-induced disease states, remain in the state of infection, regress to the state of exposure or die. Obviously, these transition probabilities are also affected by vaccination which takes place in males in intervention $i = 3$.

For intervention $i = 1$ and $i = 2$

Males are not vaccinated in interventions $i = 1, 2$; therefore, the transition probabilities to HPV-induced disease states are not reduced. Once infected with HPV, males can either clear their infection and move back to the state of exposure ($s = 2$), indicated by δ_{0a}, develop genital warts ($s = 7$) with age- and sex-specific probability $\psi^{(gw)}_{a,M}$ or die ($s = 5$) with age- and sex-specific probability $d_{a,M}$. Furthermore, they can move to the states anal LSIL ($s = 8$), anal HSIL ($s = 9$), head/neck cancer ($s = 14$) or penile intraepithelial neoplasia (PeIN, $s = 18$).

Penile cancer and its precancerous stage penile intraepithelial neoplasm (PeIN) are the only HPV-induced diseases included in the model which can only affect males. Moving to PeIN is indicated by the parameter δ_6. The parameters δ_3 and δ_4 refer to transitions to anal LSIL and HSIL, respectively. Since the information found in the literature corresponds to homosexual males and HIV-positive females, these parameters are adjusted by $\rho^{\bigstar}_3$, the risk decrease for heterosexual males when compared to homosexual

males as described in Section 5.5 and Appendix G.1.

The transition to head/neck cancer is age- and sex-specific and represented by the variable $\psi_{a,M}^{(hn)}$. We define the set of states $\mathcal{D} = \{2, 3, 4, 5, 8, 9, 14, 18\}$. Transitions to states different from $\mathcal{D}$ are impossible and therefore set to zero. Remaining in the state of infection is calculated through the constraint of probabilities which have to sum up to one. The transition probabilites for screening-only are presented as

$$
\begin{aligned}
\pi_{1,a,3,s}^{M} &= 0 \, \forall \, s \notin \{\mathcal{D}\} \\
\pi_{1,a,3,2}^{M} &= \delta_{0a} \\
\pi_{1,a,3,4}^{M} &= \psi_{a,M}^{(gw)} \\
\pi_{1,a,3,5}^{M} &= d_{a,M} \\
\pi_{1,a,3,8}^{M} &= \delta_3 \frac{1}{\rho_3^{\bigstar}} \\
\pi_{1,a,3,9}^{M} &= \delta_4 \frac{1}{\rho_3^{\bigstar}} \\
\pi_{1,a,3,14}^{M} &= \psi_{a,M}^{(hn)} \\
\pi_{1,a,3,18}^{M} &= \delta_6 \\
\pi_{1,a,3,3}^{M} &= 1 - \sum_{s \neq 3} \pi_{1,a,3,s}^{M};
\end{aligned}
$$

those for intervention $i = 2$ are analogue.

For intervention $i = 3$

In intervention $i = 3$, males receive the vaccine. Therefore, the corresponding transition probabilities to HPV-induced diseases are functions of vaccine related parameters. The vaccine coverage rate is represented by α, whereas ν_3 is the vaccine compliance rate, γ_2 the vaccine efficacy against HPV-induced diseases of the anus, γ_3 against head/neck cancer and γ_1 against all other HPV-related infections. The parameter $\chi_{\bigstar}$ represents cross-

protection against HPV genotypes which are not included in the HPV vaccine and ζ is the reduction in effectiveness due to non-compliance. The transition probabilities are given by

$$
\begin{aligned}
\pi^{M}_{3,a,3,s} &= 0 \,\forall\, s \notin \{\mathcal{D}\} \\
\pi^{M}_{3,a,3,2} &= \delta_{0a} \\
\pi^{M}_{3,a,3,4} &= \alpha[\nu_3(1-\gamma_1-\chi_\bigstar)\psi^{(gw)}_{a,M} + (1-\nu_3)(1-\zeta\gamma_1)\psi^{(gw)}_{a,M}] + (1-\alpha)\psi^{(gw)}_{a,M} \\
\pi^{M}_{3,a,3,5} &= d_{a,M} \\
\pi^{M}_{3,a,3,8} &= \alpha[\nu_3(1-\gamma_2-\chi_\bigstar)\delta_3\frac{1}{\rho^{\bigstar}_3} + (1-\nu_3)(1-\zeta\gamma_2)\delta_3\frac{1}{\rho^{\bigstar}_3}] + (1-\alpha)\delta_3\frac{1}{\rho^{\bigstar}_3} \\
\pi^{M}_{3,a,3,9} &= \alpha[\nu_3(1-\gamma_2-\chi_\bigstar)\delta_4\frac{1}{\rho^{\bigstar}_3} + (1-\nu_3)(1-\zeta\gamma_2)\delta_4\frac{1}{\rho^{\bigstar}_3}] + (1-\alpha)\delta_4\frac{1}{\rho^{\bigstar}_3} \\
\pi^{M}_{3,a,3,14} &= \alpha[\nu_3(1-\gamma_3-\chi_\bigstar)\psi^{(hn)}_{a,M} + (1-\nu_3)(1-\zeta\gamma_3)\psi^{(hn)}_{a,M}] + (1-\alpha)\psi^{(hn)}_{a,M} \\
\pi^{M}_{3,a,3,18} &= \alpha[\nu_3(1-\gamma_1-\chi_\bigstar)\delta_6 + (1-\nu_3)(1-\zeta\gamma_1)\delta_6] + (1-\alpha)\delta_6 \\
\pi^{M}_{3,a,3,3} &= 1 - \sum_{s\neq 3}\pi^{M}_{1,a,3,s}.
\end{aligned}
$$

From the state *Clearance*

Having cleared their HPV infection or recovered from a HPV-induced disease, people either die ($s = 5$), move to the state of reinfection ($s = 7$) or remain in the state of clearance. Remaining in clearance is again calculated by means of the constraint of probabilities. Moving to reinfection is similar to the transition from exposure to infection; however, if certain risk factors are present with a probability of ζ, the risk of reinfection is increased by the factor $\rho^{\bigstar}_1$. The corresponding set of equations is defined as

$$\pi^{M}_{i,a,6,s} = 0 \, \forall \, s \notin \{5,6,7\}$$
$$\pi^{M}_{i,a,6,5} = d_{a,M}$$
$$\pi^{M}_{i,a,6,7} = (1-\zeta)\pi^{M}_{i,a,2,3} + \zeta\pi^{M}_{i,a,2,3}\rho_1^{\bigstar}$$
$$\pi^{M}_{i,a,6,6} = 1 - \sum_{s \neq 13} \pi^{M}_{i,a,6,s}.$$

From the state *Reinfection*

Once reinfected, males can progress to all disease states equivalent to those from the state of infection; however, the transition probabilities are higher in case of the presence of risk factors. Furthermore, people can either die ($s = 5$) or remain in the state of reinfection ($s = 7$), depending on the constraint of probabilities. We define a set of states $\mathcal{Q} = \{4, 5, 6, 7, 8, 9, 14, 18\}$. As previously described, ζ represents the probability of risk factors and $\rho_1^{\bigstar}$ the risk increase which occurs as a consequence of their presence as shown in

$$\pi^{M}_{i,a,7,s} = 0 \, \forall \, s \notin \mathcal{Q}$$
$$\pi^{M}_{i,a,7,4} = (1-\zeta)\pi^{M}_{i,a,3,4} + \zeta\pi^{M}_{i,a,3,4}\rho_1^{\bigstar}$$
$$\pi^{M}_{i,a,7,5} = d_{a,M}$$
$$\pi^{M}_{i,a,7,6} = \pi^{M}_{i,a,3,2}$$
$$\pi^{M}_{i,a,7,8} = (1-\zeta)\pi^{M}_{i,a,3,8} + \zeta\pi^{M}_{i,a,3,8}\rho_1^{\bigstar}$$
$$\pi^{M}_{i,a,7,9} = (1-\zeta)\pi^{M}_{i,a,3,9} + \zeta\pi^{M}_{i,a,3,9}\rho_1^{\bigstar}$$
$$\pi^{M}_{i,a,7,14} = (1-\zeta)\pi^{M}_{i,a,3,14} + \zeta\pi^{M}_{i,a,3,14}\rho_1^{\bigstar}$$
$$\pi^{M}_{i,a,7,18} = (1-\zeta)\pi^{M}_{i,a,3,18} + \zeta\pi^{M}_{i,a,3,18}\rho_1^{\bigstar}$$
$$\pi^{M}_{i,a,7,7} = 1 - \sum_{s \neq 7} \pi^{M}_{i,a,7,s}.$$

From the state *Genital warts*

Males who are affected by genital warts can either remain in the corresponding state ($s = 4$), indicated by the parameter υ_M, die ($s = 5$), or move to the state of clearance ($s = 6$). As described for females, remaining in the state of genital warts is age-specific. The adjustment to age dependency is obtained through model calibration, as described in Section 6.3 and Appendix G.1, and indicated by $\lambda_{v,a,r,s}$ with indices v, a, r, s representing sex, age cohort, original state and target state, respectively. According to our assumptions, dying is age- and sex-specific, and clearing the condition depends on the other transition probabilities from the state genital warts, calculated through the constraint of probabilities. The transition probabilities are given by

$$\begin{aligned}
\pi^{M}_{i,a,4,s} &= 0 \,\forall\, s \notin \{4,5,6\} \\
\pi^{M}_{i,a,4,4} &= \lambda_{M,a,4,4}\upsilon_M \\
\pi^{M}_{i,a,4,5} &= d_{a,M} \\
\pi^{M}_{i,a,4,6} &= 1 - \sum_{s \neq 4} \pi^{M}_{i,a,4,s}.
\end{aligned}$$

From the state *Anal LSIL*

Males who are affected by anal LSIL can either die ($s = 5$), clear their infection ($s = 6$), progress to anal HSIL ($s = 9$), anal cancer ($s = 10$) or remain in the state of LSIL ($s = 8$). The chance of clearance is higher in younger people, whereas the risk of progressing to anal HSIL is higher in older people.

The probabilities of moving to more advanced stages of anal neoplasia, or to clear the precancerous lesion, are represented by the parameter $\xi^{(an)}_{1,y}$, where $y = 0, 2, 3$ represent clearance, HSIL and anal cancer, respectively. The transitions to $s = 6$ and $s = 9$ are adjusted according to age through the variable $\lambda_{v,a,r,s}$, which is estimated through model calibration as described in Section 6.3. Remaining in anal LSIL is calculated through the constraint

of probabilities to sum up to one. The system of equations is given as

$$\begin{aligned}
\pi^{M}_{i,a,8,s} &= 0 \,\forall\, s \notin \{5,6,8,9,10\} \\
\pi^{M}_{i,a,8,5} &= d_{a,M} \\
\pi^{M}_{i,a,8,6} &= \lambda_{M,a,8,6}\xi^{(an)}_{1,0} \\
\pi^{M}_{i,a,8,9} &= \lambda_{M,a,8,9}\xi^{(an)}_{1,2} \\
\pi^{M}_{i,a,8,10} &= \xi^{(an)}_{1,3} \\
\pi^{M}_{i,a,8,8} &= 1 - \sum_{s \neq 8} \pi^{M}_{i,a,8,s}.
\end{aligned}$$

From the state *Anal HSIL*

Males who are affected by anal HSIL, the more severe precancerous lesion, can still clear their infection ($s = 6$), progress to anal cancer ($s = 10$), die ($s = 5$) or remain in anal HSIL. We assume the transition probabilities to clearance and anal cancer to be age- and sex-specific, with younger people being more likely to move to clearance, and older males more likely to develop anal cancer. Dependency on age is again indicated by the variable $\lambda_{v,a,r,s}$, obtained through model calibration. The probabilities of progressing or regressing are indicated by the parameter $\xi^{(an)}_{2,y}$, where $y = 0, 1, 3$ represents states less or more severe than $x = 2$, anal HSIL. If males remain in HSIL, we calculate the corresponding probability by applying the statistical constraint that probabilites have to sum up to one. We present the corresponding equations as

$$\pi^{M}_{i,a,9,s} = 0 \,\forall\, s \notin \{5,6,8,9,10\}$$
$$\pi^{M}_{i,a,9,5} = d_{a,M}$$
$$\pi^{M}_{i,a,9,6} = \lambda_{M,a,9,6}\xi^{(an)}_{2,0}$$
$$\pi^{M}_{i,a,9,8} = \xi^{(an)}_{2,1}$$
$$\pi^{M}_{i,a,9,10} = \lambda_{M,a,9,10}\xi^{(an)}_{2,3}$$
$$\pi^{M}_{i,a,9,9} = 1 - \sum_{s \neq 9} \pi^{M}_{i,a,9,s}.$$

From the state *Anal cancer*

Having been diagnosed with anal cancer, males can either move to the state one year post anal cancer ($s = 11$) or die ($s = 5$). The probability of one-year survival depends on the probability of diagnosis $\mu^{(an)}_{j}$ in stage $j = 1, 2, 3, 4$, and the probability of surviving for one year, $\phi^{\diamondsuit(an)}_{1,j}$, depending on stage j. Once affected by anal cancer, males who do not die enter the tunnel states of one to three years post anal cancer. The transition probabilities are defined as

$$\pi^{M}_{i,a,10,s} = 0 \,\forall\, s \notin \{5,11\}$$
$$\pi^{M}_{i,a,10,5} = 1 - \pi^{M}_{i,a,10,11}$$
$$\pi^{M}_{i,a,10,11} = \sum_{j=1}^{4} \mu^{(an)}_{j}\phi^{\diamondsuit(an)}_{1,j}.$$

From the states *Post anal cancer (year one, year two, year three)*

Individuals who have survived anal cancer for one year after diagnosis can either die ($s = 5$) or move to two years post anal cancer ($s = 12$), which is calculated through the constraint of probabilities, necessarily summing up

to one. Two years after the diagnosis of anal cancer, patients who are still alive can either die ($s = 5$) or move to the state of three years post anal cancer ($s = 13$). We assume that patients who have survived anal cancer for three years finally move to the state of clearance ($s = 6$), or die ($s = 5$). The system of equations is given as

$$\begin{aligned} \pi^{M}_{i,a,11,s} &= 0 \,\forall\, s \notin \{5, 12\} \\ \pi^{M}_{i,a,11,5} &= 1 - \pi^{M}_{i,a,11,12} \\ \pi^{M}_{i,a,11,12} &= \sum_{j=1}^{4} \mu_j^{(an)} \phi_{2,j}^{\diamondsuit(an)}. \end{aligned} \tag{E.1}$$

Equation E.1 shows the transition probabilities of moving from the state $r = 11$; however, transitions from the states $r = 12$ and $r = 13$ are similar. The only changes are the indices of the original and target states r and s as well as the index q in the anal cancer survival probabilities $\phi_{q,j}^{\diamondsuit(an)}$, with $q = 1, 2, 3, 4$ representing one to four year survival.

From the state *Head/neck cancer*

In contrast to all other HPV-induced cancers included in the model, we assume that there are no precancerous stages for head/neck cancer. Suffering from head/neck cancer, patients can either survive and move to the state one year post head/neck cancer ($s = 15$), indicated by the stage-dependent probabilities of diagnosis $\mu_j^{(hn)}$ and one-year survival $\phi_{1,j}^{\diamondsuit(hn)}$, or die ($s = 5$). As usual, the probability of dying is calculated with the constraint of probabilities which must sum up to one. The transition probabilities are defined as

$$\begin{aligned}
\pi^{M}_{i,a,14,s} &= 0 \,\forall\, s \notin \{5, 15\} \\
\pi^{M}_{i,a,14,5} &= 1 - \pi^{M}_{i,a,14,15} \\
\pi^{M}_{i,a,14,15} &= \sum_{j=1}^{4} \mu_j^{(hn)} \phi_{1,j}^{\diamondsuit(hn)}.
\end{aligned}$$

From the states *Post head/neck cancer (year one, year two, year three)*

Having survived head/neck cancer for one year, patients can either move to the state of two years post head/neck cancer ($s = 16$), or die ($s = 5$). Males who are still alive two years after diagnosis of head/neck cancer can either survive for another year and move to the state of three years post head/neck cancer ($s = 17$), or die ($s = 5$). We assume that patients who survived head/neck cancer for four years are cured. Therefore, they move to the state of clearance ($s = 6$). Those who do not survive for four years move to the state of death ($s = 5$). Equation E.2 shows the transition probabilities of moving from the state one year post head/neck cancer diagnosis ($r = 15$). The transition probabilities of moving from the states $r = 16$ and $r = 17$ are similar, only the indices r and s for original and target states as well as the index q in the parameter $\phi_{q,j}^{\diamondsuit(an)}$ change. The yearly survival probabilities are represented by the index $q = 1, 2, 3, 4$. The transition probabilities are given by

$$\begin{aligned}
\pi^{M}_{i,a,15,s} &= 0 \,\forall\, s \notin \{5, 16\} \\
\pi^{M}_{i,a,15,5} &= 1 - \pi^{M}_{i,a,15,16} \\
\pi^{M}_{i,a,15,16} &= \sum_{j=1}^{4} \mu_j^{(hn)} \phi_{2,j}^{\diamondsuit(hn)}.
\end{aligned} \tag{E.2}$$

From the state *PeIN*

After HPV infection, males can move to penile intraepithelial neoplasia (PeIN, $s = 18$). We assume that penile cancer only has one precancerous stage in contrast to most other HPV-induced cancers. Once affected by PeIN, males can either clear their lesions ($s = 6$), progress to penile cancer ($s = 19$), or die ($s = 5$). Younger males have a higher chance of clearing their infection, whereas older males have a higher risk of progressing to penile cancer. This is indicated by the variable $\lambda_{v,a,r,s}$. Those who do not move to another state remain in PeIN, which is calculated through the constraint of probabilities. The corresponding equations are defined as

$$
\begin{aligned}
\pi^{M}_{i,a,18,s} &= 0 \, \forall \, s \notin \{5, 6, 18, 19\} \\
\pi^{M}_{i,a,18,5} &= d_{a,M} \\
\pi^{M}_{i,a,18,6} &= \lambda_{M,a,18,6} \xi^{(pen)}_{1,0} \\
\pi^{M}_{i,a,18,19} &= \lambda_{M,a,18,19} \xi^{(pen)}_{1,2} \\
\pi^{M}_{i,a,18,18} &= 1 - \sum_{h \neq 8} \pi^{M}_{i,a,18,s}.
\end{aligned}
$$

From the state *Penile cancer*

Individuals affected by penile cancer can either survive and move to the state of one year post penile cancer ($s = 20$), or die ($s = 5$). The probability of one-year survival depends on the probability of diagnosis $\mu^{(pen)}_{j}$, where j represents the respective cancer stage. The probability of dying is calculated through the constraint of probabilities. The transition probabilities are given by

$$\begin{aligned}
\pi^{M}_{i,a,19,s} &= 0 \,\forall\, s \notin \{5, 20\} \\
\pi^{M}_{i,a,19,5} &= 1 - \pi^{M}_{i,a,19,20} \\
\pi^{M}_{i,a,19,20} &= \sum_{j=1}^{4} \mu_j^{(pen)} \phi_{1,j}^{\diamondsuit(pen)}.
\end{aligned}$$

From the states *Post penile cancer (year one, year two, year three)*

Having survived penile cancer for one year, males can either survive for another year and move to the state of two years post penile cancer ($s = 21$), or die ($s = 5$). Individuals who are still alive two years after they received their diagnosis of penile cancer can either move to the state of three years post penile cancer ($s = 22$), or die. Our assumptions imply that males who survived for four years after having been diagnosed with penile cancer are cured from their disease and move to the state of clearance ($s = 6$). Those who are not cured are assumed to die ($s = 5$). The corresponding transition probabilities are defined as

$$\begin{aligned}
\pi^{M}_{i,a,20,s} &= 0 \,\forall\, s \notin \{5, 21\} \\
\pi^{M}_{i,a,20,5} &= 1 - \pi^{M}_{i,a,20,21} \\
\pi^{M}_{i,a,20,21} &= \sum_{j=1}^{4} \beta_j^{(pen)} \phi_{2,j}^{\diamondsuit(pen)}.
\end{aligned} \tag{E.3}$$

Equation E.3 displays the transition probabilities of moving from the state one year post penile cancer diagnosis; the transitions from the states post two and three years are similar, however, the numberings of the states r and s as well as the indices q of the survival probabilities $\phi_{q,j}^{\diamondsuit(pen)}$ change.

From the state *Death*

Equivalent to the corresponding transition probability in females, males who are in the state of death can only remain there; movements to other states are no longer possible. Thus, the transition probabilities are defined as

$$\pi^{M}_{i,a,5,s} = 0 \,\forall\, s \neq 5$$
$$\pi^{M}_{i,a,5,5} = 1.$$

Appendix F

Posterior result tables

In this appendix, we present tables including summary statistics of the posterior distributions, distributional assumptions of each model parameter as well as the corresponding literature sources of prior information. The acronym *EO* represents the term *Expert Opinion*, meaning the assumptions were based on discussions with medical experts in the field of HPV-induced diseases. The result tables are structured according to the underlying clinical background.

The assumptions and results of the parameters introduced in

- Table F.1 are related to screening;
- Table F.2 are related to vaccination;
- Table F.3 are related to infection;
- Table F.4 are transition probabilities;
- Table F.5 are diagnostic probabilities;
- Table F.6 are cancer survival probabilities;
- Table F.7 are related to costs;
- Table F.8 are related to utilities.

F.1 Screening-related model parameters

Table F.1 shows the defined age groups for cervical screening, as well as the corresponding distributional assumptions, posterior mean values, 95% credible intervals and the sources of prior information. The three-yearly cervical screening rates increase until the age of 45–54 years, and constantly decrease afterwards.

Table F.1: Distributional assumptions and estimated values for the annual screening coverage used in the model. For each age group, the table presents the mean values and an interval estimation of the expected coverage.

Var.	Description	Distribution	Mean and 95%-CI	Source
σ_a	Screening at $12-24$ yrs	Informative Beta	0.0500 [0.0500;0.0500]	EO
σ_a	Screening at $25-29$ yrs	Informative Beta	0.1530 [0.1480;0.1590]	EO
σ_a	Screening at $30-34$ yrs	Informative Beta	0.2150 [0.2100;0.2190]	EO
σ_a	Screening at $35-44$ yrs	Informative Beta	0.2460 [0.2440;0.2470]	EO
σ_a	Screening at $45-54$ yrs	Informative Beta	0.2600 [0.2540;0.2660]	[157, 194, 195, 244, 307]
σ_a	Screening at $55-64$ yrs	Informative Beta	0.2420 [0.2320;0.2520]	[157, 194, 195, 244, 307]
σ_a	Screening at $65-74$ yrs	Informative Beta	0.1840 [0.1640;0.2020]	[157, 194, 195, 244, 307]
σ_a	Screening at ≥ 75 yrs	Informative Beta	0.1080 [0.0920;0.1250]	[157, 194, 195, 244, 307]

F.2 Vaccine-related model parameters

Table F.2 shows the distributional assumptions, posterior results and sources of prior information of vaccine-related parameters. Vaccine efficacies depend on the corresponding body part, where all organs apart from the *anus* and the *head and neck* are summarized into the category *cervix*. According to expert opinion, we can only assume cross-protection effects for *cervical* diseases and not in the context of *anal* and *head/neck* cancers. We assume people who receive three shots of the vaccine to be fully compliant and fully protected; this is a conservative estimate, accounting for the fact that new research results indicate that two shots of the vaccine are already sufficient for protection [236]. All prior distributions in Table F.2 are informative.

Table F.2: Distributional values, means, corresponding 95% credible intervals and sources of prior information of vaccine-related parameters used in the model

Var.	Description	Distribution	Mean and 95%-CI	Source
γ_1	Vaccine efficacy cervix	Informative LogNorm	0.7816 [0.6847;0.8888]	[19, 148, 233]
γ_2	Vaccine efficacy anus	Informative LogNorm	0.7019 [0.6055;0.7981]	EO
γ_3	Vaccine efficacy head/neck	Informative LogNorm	0.5008 [0.4563;0.5497]	EO
α	Vaccine coverage rate (VCR)	Informative Beta	0.9048 [0.6597;0.9992]	[63, 82, 215, 339], EO
$\chi_\star$	Cross-protection effect cervix	Informative LogNorm	0.0701 [0.0395;0.1076]	[62, 384]
ξ	Efficacy decrease non-compliance	Informative Beta	0.4993 [0.3301;0.7002]	[19]
ν_1	Probability of receiving 1 shot	Informative Beta	0.0241 [0.0062; 0.0526]	[193]
ν_2	Probability of receiving 2 shots	Informative Beta	0.0410 [0.0104; 0.0929]	[193]
ν_3	Probability of receiving 3 shots	Informative Beta	0.9350 [0.8718; 0.9725]	[193]

F.3 Infection-related model parameters

Table F.3 focusses on infection-related parameters. All prior distributions are informative and the corresponding sources are given. The three compartments of the vector $\boldsymbol{\rho}^\star$ represent risk increases and decrease, respectively. Risk increases are given by $\rho_1^\star$ and $\rho_2^\star$, and $\rho_3^\star$ is a risk decrease. The relative risk $\rho_1^\star$ represents the risk increase of HPV reinfection in patients who smoke, had early sexual debut, show a history of five years or longer of exposure to hormonal contraception, previously acquired another sexually transmitted infection such as chlamydia trachomatis, herpes genitalis or syphillis, or are multipara. The proportion of people under increased risk, ζ, has a $\rho_1^\star$ times higher probability to move to the state of reinfection. For a detailed description of these parameters, the reader is referred to Section 5.5 and Appendix G.1.

We assume different HPV transmission probabilites for people with frequent partner change in contrast to those in longer, stable relationships, indicated by the parameters β_1 and β_2, respectively. We explain the underlying assumptions in Section 5.7.1.

Table F.3: Distributional values, means, corresponding 95% credible intervals and sources of prior information of infection-related variables used in the model

Var.	Description	Distribution	Mean and 95%-CI	Source
$\rho_1^\star$	Risk increase (relative risk)	Informative LogNorm	3.2262 [1.1408;5.4778]	[256]
$\rho_2^\star$	Risk increase anal cancer females	Informative Gamma	1.6975 [1.5055; 1.9026]	[351]
$\rho_3^\star$	Risk decrease anal cancer males	Informative Gamma	17.1880 [0.8714; 53.5615]	[145]
ζ	Population at increased risk	Informative Beta	0.3139 [0.2140;0.4054]	[319]
τ_1	Conization in CIN I (immediate)	Informative Beta	0.3029 [0.2101;0.4180]	[158]
τ_2	Conization in CIN I (delayed)	Informative Beta	0.1701 [0.1525;0.1909]	EO
β_1	HPV transmission (average risk)	Informative Normal	0.2532[0.1707; 0.3607]	EO
β_2	HPV transmission (high risk)	Informative Normal	0.5220 [0.2915; 0.7439]	EO

F.4 Model parameters related to transition probabilities

In Table F.4, we display all the information on parameters necessary to estimate the transition probabilities between the 36 states in females (see Section 5.8 and Appendix D) and 22 in males (see Appendix E.2). For transitions from infection back to exposure, the so-called disease regression, as well as for all transitions between states affecting the cervix, anus, vulva and penis, we assume informative prior distributions. The same approach is conducted in genital warts. In contrast, we assume minimally informative prior distributions for most transitions in HPV-induced diseases affecting the vagina and update these by means of data we extract from the literature.

According to Watson et al. [375], a transition from the state anal LSIL to anal cancer is not possible; only those affected by anal HSIL can develop cancer. Therefore, we set the parameter $\xi_{1,3}^{(an)}$ to zero and do not make any distributional assumptions. Accordingly, based on expert opinion, patients who underwent conization after diagnosis of a CIN stage cannot regress to less severe precancerous lesions because we assume the infection to be cleared after this treatment.

In addition to posterior results, transition probabilities adjusted through

model calibration as described in Section 6.3 are reported. Rather than the posterior results of the respective model parameters, the values of the transition probabilities after calibration (or comparison of age-specific trends as for CIN III) are reported directly, indicated by $\pi^{F}_{i,a,r,s}$ and $\pi^{M}_{i,a,r,s}$ for females and males, respectively. As described in Section 5.8, the indices i, a, r and s represent intervention, age cohort, original and target states, respectively. If transition probabilities in females and males are identical, only those in females are reported.

Table F.4: Distributional values, means, corresponding 95% credible intervals and sources of prior information of epidemiological and clinical parameters used in the model

Var.	Description	Distribution	Mean and 95%-CI	Source
Regression				
δ_{0a}	Infection → Exposure (12−24 yrs)	Inform. Beta	0.7188 [0.6463;0.7830]	[71,78,305,306], EO
δ_{0a}	Infection → Exposure (25−29 yrs)	Inform. Beta	0.6984 [0.5898;0.7952]	[71,78,305,306], EO
δ_{0a}	Infection → Exposure (30−39 yrs)	Inform. Beta	0.3503 [0.2860; 0.4188]	[71,78,305,306], EO
δ_{0a}	Infection → Exposure (40−49 yrs)	Inform. Beta	0.2048 [0.1118;0.3022]	[71,78,305,306], EO
δ_{0a}	Infection → Exposure ($\geq$ 50 yrs)	Inform. Beta	0.1004 [0.0546; 0.1567]	[71,78,305,306], EO
Cervix				
δ_1	Infection → CIN I	Inform. Beta	0.0450 [0.0279; 0.0661]	[71,78,263,305]
δ_2	Infection → CIN II	Inform. Beta	0.0115 [0.0034; 0.0234]	[71,263,305,306]
$\xi^{(cerv,1)}_{1,3}$	CIN I → CIN III	Inform. Beta	0.0464 [0.0098; 0.1297]	[71,78,158,263,305, 306], EO
$\xi^{(cerv,1)}_{2,3}$	CIN II → CIN III	Inform. Beta	0.3498 [0.0904;0.8654]	[71,78,105,158,263, 305,306], EO
Subject to conization				
$\xi^{(cerv,1)}_{1,2}$	CIN I → CIN II	Inform. Beta	0.1212 [0.0434; 0.2418]	[71,305,306], EO
$\xi^{(cerv,1)}_{2,1}$	CIN II → CIN I	—	0 [0;0]	EO
$\xi^{(cerv,1)}_{1,0}$	CIN I → Clearance	Inform. Beta	0.9003[0.8382; 0.9498]	[71,78,158,263,305, 306], EO
$\xi^{(cerv,1)}_{2,0}$	CIN II → Clearance	Inform. Beta	0.8588 [0.8153; 0.8965]	[71,78,105,158,263, 305,306], EO
$\pi^{F}_{i,a,6,4}$	CIN III → CIN I	Inform. Beta	0.0392 [0.0077; 0.1148]	[71,263], EO
$\pi^{F}_{i,a,6,5}$	CIN III → CIN II	Inform. Beta	0.0579 [0.0132; 0.1555]	[71,263], EO
$\pi^{F}_{i,a,6,8}$	CIN III → Cancer	Inform. Beta	0.1019 [0.0189; 0.2906]	[71,263], EO
$\pi^{F}_{i,a,6,13}$	CIN III → Clearance	Inform. Beta	0.1576 [0.0017; 0.8977]	[71,263], EO

Not subject to conization				
$\xi_{1,2}^{(cerv,2)}$	CIN I → CIN II	Inform. Beta	0.2240 [0.1608;0.2972]	[71, 305, 306], EO
$\xi_{2,1}^{(cerv,2)}$	CIN II → CIN I	Inform. Beta	0.2494[0.1994; 0.2992]	[71, 263], EO
$\xi_{1,0}^{(cerv,2)}$	CIN I → Clearance	Inform. Beta	0.7008 [0.6077;0.7933]	[71, 78, 105, 158, 263, 305, 306], EO
$\xi_{2,0}^{(cerv,2)}$	CIN II → Clearance	Inform. Beta	0.3490 [0.2101;0.5026]	[71, 78, 105, 158, 263, 305, 306], EO

Genital warts

$\psi_{a,F}^{(gw)}$	Infection → Genital warts in females	Inform. Beta	0.0104 [0.0003; 0.0495]	[252], EO
$\psi_{a,M}^{(gw)}$	Infection → Genital warts in males	Inform. Beta	0.0114 [0;0.0467]	[252], EO
$\pi_{i,a,7,7}^{F}$	Recurrence females	Inform. Beta	0.3104 [0; 0.9244]	[69, 144], EO
$\pi_{i,a,4,4}^{M}$	Recurrence males	Inform. Beta	0.2847 [0;0.9098]	[69, 144], EO

Anus

δ_3	Infection → LSIL	Inform. Beta	0.0286 [0.1003;0.1387]	[98, 145, 351]
δ_4	Infection → HSIL	Inform. Beta	0.0104 [0.0008;0.0496]	[97, 98, 145, 351]
$\pi_{i,a,15,13}^{F}$	LSIL → Clearance	Inform. Beta	0.1475 [0.0190; 0.4771]	[98, 285, 375]
$\pi_{i,a,15,16}^{F}$	LSIL → HSIL	Inform. Beta	0.0588 [0.0077; 0.1884]	[98]
$\xi_{1,3}^{(an)}$	LSIL → Anal cancer	—	0 [0;0]	[375]
$\pi_{i,a,16,13}^{F}$	HSIL → Clearance females	Inform. Beta	0.1576 [0.0017; 0.8977]	[145, 165]
$\pi_{i,a,9,6}^{M}$	HSIL → Clearance males	Inform. Beta	0.1667 [0.0093; 0.8977]	[145, 165]
$\pi_{i,a,16,15}^{F}$	HSIL → LSIL	Inform. Beta	0.0997 [0.0810; 0.1209]	[98]
$\pi_{i,a,16,17}^{F}$	HSIL → Anal cancer females	Inform. Beta	0.0026 [0; 0.0059]	[145, 250, 375]
$\pi_{i,a,9,10}^{M}$	HSIL → Anal cancer males	Inform. Beta	0.0020 [0; 0.0053]	[145, 250, 375]

Vagina

δ_5	Infection → VaIN I/II	Inform. Beta	0.0073 [0.0053; 0.0096]	[147]
$\xi_{1,2}^{(vag)}$	VaIN I → VaIN II/VaIN III	Min. inf. Beta	0.0270 [0.0021; 0.0782]	[10]
$\xi_{1,0}^{(vag)}$	VaIN I → Clearance	Min. inf. Beta	0.2528 [0.1813; 0.3062]	[10]
$\xi_{2,1}^{(vag)}$	VaIN II → VaIN I	Min. inf. Beta	0.2528 [0.1813; 0.3062]	[10]
$\xi_{2,0}^{(vag)}$	VaIN II → Clearance	Min. inf. Beta	0.2528 [0.1813; 0.3062]	[10]
$\xi_{2,1}^{(vag)}$	VaIN II → VaIN I	Min. inf. Beta	0.2502 [0.1787;0.3075]	[10]
$\pi_{i,a,31,32}^{F}$	VaIN II → VaIN III	Min. inf. Beta	0.2656 [0.0066;1]	[10], EO
$\xi_{3,1}^{(vag)}$	VaIN III → VaIN I	Min. inf. Beta	0.2502 [0.1218; 0.3265]	[10]
$\xi_{3,2}^{(vag)}$	VaIN III → VaIN II	Min. inf. Beta	0.2502 [0.1218; 0.3265]	[10]
$\xi_{3,0}^{(vag)}$	VaIN III → Clearance	Inform. Beta	0.2174 [0.0107;0.9229]	EO
$\pi_{i,a,32,33}^{F}$	VaIN III → Vaginal cancer	Inform. Beta	0.1576 [0.0017;0.9091]	[10]

Vulva

$\xi_{1,0}^{(vulv)}$	VIN → Clearance	Inform. Beta	0.1579 [0.0017; 0.9091]	[207], EO
$\pi_{i,a,25,26}^{F}$	VIN → Vulvar cancer	Inform. Beta	0.0815 [0.0269;0.3538]	[207], EO

Penis

δ_6	Infection → PeIN	Inform. Beta	0.0002 [0;0.0014]	[261], EO
$\pi^M_{i,a,18,6}$	PeIN → Clearance	Inform. Beta	0.1577 [0.0017; 0.8977]	[318], EO
$\pi^M_{i,a,18,19}$	PeIN → Penile cancer	Inform. Beta	0.1539 [0.0076; 0.6465]	[25], EO

F.5 Model parameters related to diagnostic probabilities

Precancerous stages and cancer can only result in costs and reduced values in the corresponding utilities after diagnosis. Beforehand, people may possibly experience symptoms which they might not link to a severe health condition such as cancer. Many states, for example the cervical lesions CIN I-III do not cause any symptoms; however, these are serious health threats. If undiscovered and left untreated, they can progress to cancer and possibly lead to death.

Table F.5: Distributional values, mean, corresponding 95% credible intervals and sources of prior information of probabilities of diagnosis used in the model

Var.	Description	Distribution	Mean and 95%-CI	Source
Cervix				
η_1	Diagnosis CIN II (without screening)	Inform. Beta	0.0265 [0.0001;0.1229]	EO
η_2	Diagnosis CIN III (without screening)	Inform. Beta	0.0750 [0.0562; 0.0955]	EO
$\mu_1^{(cerv)}$	Diagnosis FIGO I	Min. inf. Dirichlet	0.5498 [0.5333;0.5654]	[29, 138, 142, 275], EO
$\mu_2^{(cerv)}$	Diagnosis FIGO II	Min. inf. Dirichlet	0.1505 [0.1387;0.1626]	[29, 138, 142, 275], EO
$\mu_3^{(cerv)}$	Diagnosis FIGO III	Min. inf. Dirichlet	0.1200 [0.1089;0.1310]	[29, 138, 142, 275], EO
$\mu_4^{(cerv)}$	Diagnosis FIGO III	Min. inf. Dirichlet	0.1797 [0.1668;0.1926]	[29, 138, 142, 275], EO

Anus

η_3	Diagnosis LSIL	Informative Beta	0.0500 [0.0404;0.0607]	EO
η_4	Diagnosis HSIL	Informative Beta	0.1000 [0.0904; 0.1096]	EO
$\mu_1^{(an)}$	Diagnosis anal cancer stage I	Min. inf. Dirichlet	0.2432 [0.1953;0.2934]	[347]
$\mu_2^{(an)}$	Diagnosis anal cancer stage II	Min. inf. Dirichlet	0.4815 [0.4254;0.5371]	[347]
$\mu_3^{(an)}$	Diagnosis anal cancer stage III	Min. inf. Dirichlet	0.1235 [0.0887;0.1650]	[347]
$\mu_4^{(an)}$	Diagnosis anal cancer stage IV	Min. inf. Dirichlet	0.1521 [0.1113;0.1937]	[347]

Head and neck

$\mu_1^{(hn)}$	Diagnosis head/neck cancer stage I	Min. inf. Dirichlet	0.2222 [0.0960;0.4034]	[61, 184, 310, 334]
$\mu_2^{(hn)}$	Diagnosis head/neck cancer stage II	Min. inf. Dirichlet	0.2316 [0.1055;0.4239]	[61, 184, 310, 334]
$\mu_3^{(hn)}$	Diagnosis head/neck cancer stage III	Min. inf. Dirichlet	0.2748 [0.0880;0.5826]	[61, 184, 310, 334]
$\mu_4^{(hn)}$	Diagnosis head/neck cancer stage IV	Min. inf. Dirichlet	0.2878 [0.0937; 0.5925]	[61, 184, 310, 334]

Vagina

η_5	Diagnosis VaIN I/II	Informative Beta	0.1996 [0.1798;0.2204]	EO
$\mu_1^{(vag)}$	Diagnosis vaginal cancer stage I	Min. inf. Dirichlet	0.2586 [0.0007;0.9966]	[11, 197]
$\mu_2^{(vag)}$	Diagnosis vaginal cancer stage II	Min. inf. Dirichlet	0.3431 [0.0009;0.9974]	[11, 197]
$\mu_3^{(vag)}$	Diagnosis vaginal cancer stage III	Min. inf. Dirichlet	0.2147 [0;1]	[11, 197]
$\mu_4^{(vag)}$	Diagnosis vaginal cancer stage IV	Min. inf. Dirichlet	0.1836 [0.0010; 0.9893]	[11, 197]

Vulva

$\mu_1^{(vulv)}$	Diagnosis vulvar cancer stage I	Min. inf. Dirichlet	0.2385 [0.0023;0.9841]	[297, 361]
$\mu_2^{(vulv)}$	Diagnosis vulvar cancer stage II	Min. inf. Dirichlet	0.3311 [0.0027; 0.9888]	[297, 361]
$\mu_3^{(vulv)}$	Diagnosis vulvar cancer stage III	Min. inf. Dirichlet	0.2366 [0;1]	[297, 361]
$\mu_4^{(vulv)}$	Diagnosis vulvar cancer stage IV	Min. inf. Dirichlet	0.1938 [0.0001; 0.9911]	[297, 361]

Penis

$\mu_1^{(pen)}$	Diagnosis penile cancer stage I	Min. inf. Dirichlet	0.5878 [0.5229;0.6488]	[265]
$\mu_2^{(pen)}$	Diagnosis penile cancer stage II	Min. inf. Dirichlet	0.1222 [0.0748;0.1569]	[265]
$\mu_3^{(pen)}$	Diagnosis penile cancer stage III	Min. inf. Dirichlet	0.2852 [0.2171;0.3336]	[265]
$\mu_4^{(pen)}$	Diagnosis penile cancer stage IV	Min. inf. Dirichlet	0.0048 [0;0.01065]	[265]

We assume informative Beta distributions for the diagnostic probabilities of all precancerous stages. Since we have not found information to inform the diagnostic probability of penile intraepithelial neoplasiae, PeIN, we assume the same value as for VaIN I/II, indicated by the parameter η_5. According to expert opinion, the probabilities of diagnosis for VaIN I/II and VIN are equivalent. For all cancer stages in all organs possibly affected by HPV, we

define minimally informative Dirichlet prior distributions which are informed by eligible data from the literature. We account for cancer survival by linking the probabilities of diagnosis in the respective stage to the survival probabilities since only a detected cancer can be treated properly. Therefore, the information presented in Table F.5 is of greatest importance.

F.6 Model parameters related to cancer survival probabilities

Table F.6 provides information on one- to four-year cancer survival, depending on the affected organ and the respective cancer stage $j = 1, 2, 3, 4$. We assume informative Beta distributions for the survival probabilities of cervical cancer. In contrast, for all other HPV-induced cancers, we assume minimally informative distributions which are informed by eligible data taken from the literature. We define both Normal and Beta distributions, corresponding to the data given. In some cases of minimally informative Normal distributions, the credible intervals result in extremely wide ranges between [0;1]. This is a consequence of the definition of the minimally informative priors, assuming a very large variance in order to avoid convergence problems.

Table F.6: Distributional values, means, corresponding 95% credible intervals and sources of prior information of cancer survival probabilities used in the model

Var.	Description	Distribution	Mean and 95%-CI	Source
Cervix				
$\phi_{1,1}^{\diamond(cerv)}$	1 year surv. cervical cancer stage I	Inform. Beta	0.9782 [0.8931;0.9999]	[46, 89, 260], EO
$\phi_{1,2}^{\diamond(cerv)}$	1 year surv. cervical cancer stage II	Inform. Beta	0.8275 [0.7648;0.8789]	[46, 89, 260], EO
$\phi_{1,3}^{\diamond(cerv)}$	1 year surv. cervical cancer stage III	Inform. Beta	0.5908 [0.5348;0.6504]	[46, 89, 260], EO
$\phi_{1,4}^{\diamond(cerv)}$	1 year surv. cervical cancer stage IV	Inform. Beta	0.5025 [0.4490;0.5584]	[46, 89, 260], EO
$\phi_{2,1}^{\diamond(cerv)}$	2 year surv. cervical cancer stage I	Inform. Beta	0.9736 [0.8659;1.0000]	[46, 89, 260], EO
$\phi_{2,2}^{\diamond(cerv)}$	2 year surv. cervical cancer stage II	Inform. Beta	0.8341 [0.7699;0.8827]	[46, 89, 260], EO
$\phi_{2,3}^{\diamond(cerv)}$	2 year surv. cervical cancer stage III	Inform. Beta	0.6918 [0.6405;0.7515]	[46, 89, 260], EO

$\phi_{2,4}^{\diamond(cerv)}$	2 year surv. cervical cancer stage IV	Inform. Beta	0.7819 [0.7296;0.8342]	[46, 89, 260], EO
$\phi_{3,1}^{\diamond(cerv)}$	3 year surv. cervical cancer stage I	Inform. Beta	0.9632 [0.8959;0.9974]	[46, 89, 260], EO
$\phi_{3,2}^{\diamond(cerv)}$	3 year surv. cervical cancer stage II	Inform. Beta	0.7565 [0.6985;0.8079]	[46, 89, 260], EO
$\phi_{3,3}^{\diamond(cerv)}$	3 year surv. cervical cancer stage III	Inform. Beta	0.7780 [0.7161;0.8319]	[46, 89, 260], EO
$\phi_{3,4}^{\diamond(cerv)}$	3 year surv. cervical cancer stage IV	Inform. Beta	0.7209 [0.6623;0.7797]	[46, 89, 260], EO
$\phi_{4,1}^{\diamond(cerv)}$	4 year surv. cervical cancer stage I	Inform. Beta	0.9873 [0.8924;1.0000]	[46, 89, 260], EO
$\phi_{4,2}^{\diamond(cerv)}$	4 year surv. cervical cancer stage II	Inform. Beta	0.8700 [0.8094;0.9224]	[46, 89, 260], EO
$\phi_{4,3}^{\diamond(cerv)}$	4 year surv. cervical cancer stage III	Inform. Beta	0.9293 [0.8502;0.9784]	[46, 89, 260], EO
$\phi_{4,4}^{\diamond(cerv)}$	4 year surv. cervical cancer stage IV	Inform. Beta	0.9267 [0.8626;0.9692]	[46, 89, 260], EO

Anus

$\phi_{1,1}^{\diamond(an)}$	1 year surv. anal cancer stage I/II	Min. inf. Normal	0.9900 [0.9800;1.0000]	[391, 393]
$\phi_{1,3}^{\diamond(an)}$	1 year surv. anal cancer stage III	Min. inf. Beta	0.9629 [0.9209;0.9892]	[312]
$\phi_{1,4}^{\diamond(an)}$	1 year surv. anal cancer stage IV	Min. inf. Beta	0.9179 [0.8374;0.9751]	[312]
$\phi_{2,1}^{\diamond(an)}$	2 year surv. anal cancer stage I/II	Min. inf. Normal	0.7554 [0.0003;1]	[312, 393]
$\phi_{2,3}^{\diamond(an)}$	2 year surv. anal cancer stage III	Min. inf. Beta	0.8902 [0.8317;0.9418]	[312]
$\phi_{2,4}^{\diamond(an)}$	2 year surv. anal cancer stage IV	Min. inf. Beta	0.7691 [0.6507;0.8692]	[312]
$\phi_{3,1}^{\diamond(an)}$	3 year surv. anal cancer stage I/II	Min. inf. Normal	0.5979 [0;1]	[393]
$\phi_{3,3}^{\diamond(an)}$	3 year surv. anal cancer stage III/IV	Min. inf. Beta	0.5438 [0.4269;0.6527]	[347]
$\phi_{4,1}^{\diamond(an)}$	4 year surv. anal cancer stage I/II	Min. inf. Normal	0.6493 [0.0503;0.9732]	[390, 393]
$\phi_{4,3}^{\diamond(an)}$	4 year surv. anal cancer stage III/IV	Min. inf. Beta	0.4351 [0.2231;0.6783]	[390]

Head/neck

$\phi_{1,1}^{\diamond(hn)}$	1 year surv. head/neck cancer stage I	Min. inf. Beta	0.9839 [0.9334;1]	[126]
$\phi_{1,2}^{\diamond(hn)}$	1 year surv. head/neck cancer stage II	Min. inf. Beta	0.9522 [0.8829;0.9929]	[126]
$\phi_{1,3}^{\diamond(hn)}$	1 year surv. head/neck cancer stage III/IV	Min. inf. Normal	0.8587 [0.6212;0.9757]	[126, 235]
$\phi_{2,1}^{\diamond(hn)}$	2 year surv. head/neck cancer stage I	Min. inf. Normal	0.8424 [0.0078;1]	[86, 126, 310]
$\phi_{2,2}^{\diamond(hn)}$	2 year surv. head/neck cancer stage II	Min. inf. Normal	0.7995 [0.0053;1]	[86, 126, 310]
$\phi_{2,3}^{\diamond(hn)}$	2 year surv. head/neck cancer stage III	Min. inf. Normal	0.6624 [0.2273;0.9365]	[126, 235, 310]
$\phi_{2,4}^{\diamond(hn)}$	2 year surv. head/neck cancer stage IV	Min. inf. Normal	0.6129 [0.4496;0.7600]	[126, 235, 310]
$\phi_{3,1}^{\diamond(hn)}$	3 year surv. head/neck cancer stage I	Min. inf. Beta	0.9040 [0.7645;0.9846]	[126]
$\phi_{3,2}^{\diamond(hn)}$	3 year surv. head/neck cancer stage II	Min. inf. Beta	0.6812 [0.5429;0.8031]	[126]
$\phi_{3,3}^{\diamond(hn)}$	3 year surv. head/neck cancer stage III/IV	Min. inf. Normal	0.4528 [0.0028;0.9988]	[235, 290]
$\phi_{4,1}^{\diamond(hn)}$	4 year surv. head/neck cancer stage I	Min. inf. Beta	0.9057 [0.7747;0.9833]	[126]
$\phi_{4,2}^{\diamond(hn)}$	4 year surv. head/neck cancer stage II	Min. inf. Beta	0.6642[0.5269;0.7775]	[126]
$\phi_{4,3}^{\diamond(hn)}$	4 year surv. head/neck cancer stage III/IV	Min. inf. Normal	0.5060 [0;1]	[235]

Vagina

$\phi_{1,1}^{\diamond(vag)}$	1 year surv. vaginal cancer stage I	Min. inf. Beta	0.9531 [0.8014;0.9999]	[11]
$\phi_{1,2}^{\diamond(vag)}$	1 year surv. vaginal cancer stage II	Min. inf. Beta	0.8882 [0.7601;0.9695]	[11]
$\phi_{1,3}^{\diamond(vag)}$	1 year surv. vaginal cancer stage III	Min. inf. Beta	0.6859 [0.3856;0.9167]	[11]

$\phi_{1,4}^{\diamond(vag)}$	1 year surv. vaginal cancer stage IV	Min. inf. Beta	0.3150 [0.0674;0.6392]	[11]
$\phi_{2,1}^{\diamond(vag)}$	2 year surv. vaginal cancer stage I	Min. inf. Beta	0.9542 [0.7809;1]	[11]
$\phi_{2,2}^{\diamond(vag)}$	2 year surv. vaginal cancer stage II	Min. inf. Beta	0.7263 [0.5488;0.8634]	[11]
$\phi_{2,3}^{\diamond(vag)}$	2 year surv. vaginal cancer stage III	Min. inf. Beta	0.6797 [0.3821;0.9011]	[11]
$\phi_{2,4}^{\diamond(vag)}$	2 year surv. vaginal cancer stage IV	Min. inf. Beta	0.1885 [0.0152;0.4877]	[11]
$\phi_{3,1}^{\diamond(vag)}$	3 year surv. vaginal cancer stage I	Min. inf. Beta	0.7685 [0.4827;0.9569]	[11]
$\phi_{3,2}^{\diamond(vag)}$	3 year surv. vaginal cancer stage II	Min. inf. Beta	0.6946 [0.5313;0.8399]	[11]
$\phi_{3,3}^{\diamond(vag)}$	3 year surv. vaginal cancer stage III	Min. inf. Beta	0.4945 [0.2322;0.7459]	[11]
$\phi_{3,4}^{\diamond(vag)}$	3 year surv. vaginal cancer stage IV	Min. inf. Beta	0.1856 [0.0157;0.4972]	[11]
$\phi_{4,1}^{\diamond(vag)}$	4 year surv. vaginal cancer stage I	Min. inf. Beta	0.7736 [0.5058;0.9594]	[11]
$\phi_{4,2}^{\diamond(vag)}$	4 year surv. vaginal cancer stage II	Min. inf. Beta	0.7914 [0.6321;0.9122]	[11]
$\phi_{4,3}^{\diamond(vag)}$	4 year surv. vaginal cancer stage III	Min. inf. Beta	0.4965 [0.2067;0.7576]	[11]
$\phi_{4,4}^{\diamond(vag)}$	4 year surv. vaginal cancer stage IV	Min. inf. Beta	0.1862 [0.0138;0.4925]	[11]

Vulva

$\phi_{1,1}^{\diamond(vulv)}$	1 year surv. vulvar cancer stage I	Min. inf. Normal	0.7808 [0;1]	[338]
$\phi_{1,2}^{\diamond(vulv)}$	1 year surv. vulvar cancer stage II	Min. inf. Normal	0.7251 [0;1]	[338]
$\phi_{1,3}^{\diamond(vulv)}$	1 year surv. vulvar cancer stage III	Min. inf. Normal	0.6406 [0;1]	[338]
$\phi_{1,4}^{\diamond(vulv)}$	1 year surv. vulvar cancer stage IV	Min. inf. Normal	0.4909 [0;1]	[338]
$\phi_{2,1}^{\diamond(vulv)}$	2 year surv. vulvar cancer stage I	Min. inf. Normal	0.7264 [0;1]	[338]
$\phi_{2,2}^{\diamond(vulv)}$	2 year surv. vulvar cancer stage II	Min. inf. Normal	0.7106 [0;1]	[338]
$\phi_{2,3}^{\diamond(vulv)}$	2 year surv. vulvar cancer stage III	Min. inf. Normal	0.5853 [0;1]	[338]
$\phi_{2,4}^{\diamond(vulv)}$	2 year surv. vulvar cancer stage IV	Min. inf. Normal	0.4317 [0;1]	[338]
$\phi_{3,1}^{\diamond(vulv)}$	3 year surv. vulvar cancer stage I	Min. inf. Normal	0.7639 [0;1]	[338]
$\phi_{3,2}^{\diamond(vulv)}$	3 year surv. vulvar cancer stage II	Min. inf. Normal	0.7001[0;1]	[338]
$\phi_{3,3}^{\diamond(vulv)}$	3 year surv. vulvar cancer stage III	Min. inf. Normal	0.5946 [0;1]	[338]
$\phi_{3,4}^{\diamond(vulv)}$	3 year surv. vulvar cancer stage IV	Min. inf. Normal	0.4081 [0;1]	[338]
$\phi_{4,1}^{\diamond(vulv)}$	4 year surv. vulvar cancer stage I	Min. inf. Normal	0.7396 [0;1]	[338]
$\phi_{4,2}^{\diamond(vulv)}$	4 year surv. vulvar cancer stage II	Min. inf. Normal	0.6903 [0;1]	[338]
$\phi_{4,3}^{\diamond(vulv)}$	4 year surv. vulvar cancer stage III	Min. inf. Normal	0.5625 [0;1]	[338]
$\phi_{4,4}^{\diamond(vulv)}$	4 year surv. vulvar cancer stage IV	Min. inf. Normal	0.4018 [0;1]	[338]

Penis

$\phi_{1,1}^{\diamond(pen)}$	1 year surv. penile cancer stage I	Min. inf. Beta	0.8933 [0.7584;0.9822]	[32]
$\phi_{1,2}^{\diamond(pen)}$	1 year surv. penile cancer stage II/III	Min. inf. Beta	0.8196 [0.6391;0.9538]	[32]
$\phi_{1,4}^{\diamond(pen)}$	1 year surv. penile cancer stage IV	Min. inf. Beta	0.4244 [0.2770;0.5845]	[171]
$\phi_{2,1}^{\diamond(pen)}$	2 year surv. penile cancer stage I	Min. inf. Beta	0.8594 [0.6984;0.9623]	[32]
$\phi_{2,2}^{\diamond(pen)}$	2 year surv. penile cancer stage II/III	Min. inf. Beta	0.6291 [0.4154;0.8170]	[32]
$\phi_{2,4}^{\diamond(pen)}$	2 year surv. penile cancer stage IV	Min. inf. Beta	0.2030 [0.0926;0.3495]	[171]
$\phi_{3,1}^{\diamond(pen)}$	3 year surv. penile cancer stage I	Min. inf. Beta	0.7820 [0.6008;0.9227]	[32]

$\phi_{3,2}^{\diamond(pen)}$	3 year surv. penile cancer stage II/III	Min. inf. Beta	0.4751[0.2711;0.6867]	[32]
$\phi_{3,4}^{\diamond(pen)}$	3 year surv. penile cancer stage IV	Min. inf. Beta	0.2003 [0.0880;0.3395]	[171]
$\phi_{4,1}^{\diamond(pen)}$	4 year surv. penile cancer stage I	Min. inf. Beta	0.7422 [0.5611;0.8858]	[32]
$\phi_{4,2}^{\diamond(pen)}$	4 year surv. penile cancer stage II/III	Min. inf. Beta	0.4284 [0.2284;0.6388]	[32]
$\phi_{4,4}^{\diamond(pen)}$	4 year surv. penile cancer stage IV	Min. inf. Beta	0.2033 [0.0929; 0.3405]	[171]

F.7 Model parameters related to costs

In order to conduct the cost-effectiveness analysis, estimating the costs and utilities presented in Tables F.7 and F.8 is essential. All unit costs are defined in € and all assumptions on costs are based on Log-Normal distributions. For the costs of most diagnostic procedures and disease states related to the cervix, we assume informative prior distributions; similarly for genital warts and anal LSIL. In contrast, all other cost parameters are based on minimally informative priors.

Table F.7: Distributional values, means, corresponding 95% credible intervals and sources of prior information of cost variables used in the model (unit cost in €)

Var.	Description	Distribution	Mean and 95%-CI	Source
Vaccination and diagnostic procedures				
c^{adm}	Administration cost	Inform. LogNorm	6.64 [5.05;8.65]	[21, 95, 258]
c^{acq}	Cost per dose	Inform. LogNorm	56.10 [36.48;77.43]	EO
c^{pap}	Pap test	Inform. LogNorm	17.07 [14.05;20.83]	[112]
c^{col}	Colposcopy	Inform. LogNorm	54.27 [49.63;59.49]	[112]
c^{cyt}	Anal cytology	Min. inf. LogNorm	43.03 [23.59;83.06]	[238]
c^{anbiop}	Anoscopy/biopsy	Min. inf. LogNorm	348.33 [234.58;487.13]	[98, 238]
c^{dna}	HPV DNA test	Inform. LogNorm	79.10 [76.98;81.13]	[6, 369]
Cervix				
c_1^{cin}	CIN I	Inform. LogNorm	309.33 [225.36;405.64]	[94, 158]
c_2^{cin}	CIN II	Inform. LogNorm	1,342.30 [1,032.51;1,701.10]	[158]
c_3^{cin}	CIN III	Inform. LogNorm	1,750.03 [1,381.00;2,193.80]	[158]
c_1^{cerv}	FIGO I	Inform. LogNorm	14,782.17 [2,459.13;44,084.05]	[139]
c_2^{cerv}	FIGO II	Inform. LogNorm	24,924.69 [8,620.06; 54,870.83]	[139]

c_3^{cerv}	FIGO III	Inform. LogNorm	35,270.93 [6,132.54; 130,201.47]	[139]
c_4^{cerv}	FIGO IV	Inform. LogNorm	34,517.86 [2,396.80; 173,662.38]	[139]

Genital warts

c^{gw}	Genital warts	Inform. LogNorm	283.48 [242.04;328.56]	[94, 259]

Anus

c^{lsil}	LSIL	Inform. LogNorm	115.46 [76.56;166.75]	[165]
c^{hsil}	HSIL	Min. inf. LogNorm	2,389.34 [1,165.65;4,360.13]	[98, 238]
c_1^{an}	Anal cancer stage I	Min. inf. LogNorm	7,618.94 [3,885.66;12,058.58]	[23, 340]
c_2^{an}	Anal cancer stage II	Min. inf. LogNorm	11,548.85 [5,984.78; 20,078.67]	[23, 340]
c_3^{an}	Anal cancer stage III	Min. inf. LogNorm	17,966.93 [9,369.01;31,605.76]	[23, 340]
c_4^{an}	Anal cancer stage IV	Min. inf. LogNorm	11,767.32 [6,247.62; 20,102.68]	[23, 340]

Head/neck

c_1^{hn}	Cancer stage I/II	Min. inf. LogNorm	10,081.71 [5,457.09;18,036.06]	[23, 110, 385]
c_3^{hn}	Cancer stage III/IV	Min. inf. LogNorm	28,437.01 [14,792.75; 48,955.00]	[23, 110, 308, 385]

Vagina

c^{vain}	VaIN I/II/III	Min. inf. LogNorm	3,236.98 [1,686.22;5,376.87]	[179]
c_1^{vag}	Vaginal cancer stage I	Min. inf. LogNorm	2,939.32 [1,684.02;5,029.46]	[23, 149]
c_2^{vag}	Vaginal cancer stage II	Min. inf. LogNorm	12,274.97 [6,126.71;20,723.95]	[23, 189]
c_3^{vag}	Vaginal cancer stage III	Min. inf. LogNorm	20,973.04 [10,751.42;39,290.42]	[23, 91]
c_4^{vag}	Vaginal cancer stage IV	Min. inf. LogNorm	29,617.99 [19,467.22;43,391.43]	[23, 261]

Vulva

c^{vin}	VIN	Min. inf. LogNorm	3,158.80 [1,920.52;5,405.63]	[179]
c_1^{vulv}	Vulvar cancer stage I	Min. inf. LogNorm	8,304.24 [4,650.56;14,302.42]	[149]
c_2^{vulv}	Vulvar cancer stage II	Min. inf. LogNorm	11,691.60 [5,822.31;20,301.77]	[149]
c_3^{vulv}	Vulvar cancer stage III	Min. inf. LogNorm	15,770.82 [7,903.39;28,129.61]	[149]
c_4^{vulv}	Vulvar cancer stage IV	Min. inf. LogNorm	20,003.88 [10,306.98;34,978.37]	[149]

Penis

c^{pein}	PeIN	Min. inf. LogNorm	437.13 [63.13;811.13]	[126]
c^{pen}	Penile cancer	Min. inf. LogNorm	5,807.15 [3,472.35;9,233.68]	[126, 315]

Vaccine costs are a combination of administration (c^{adm}) and acquisition costs (c^{acq}), respectively. The actual value of c^{acq} is crucial since it largely influences the outcome of the cost-effectiveness analysis. We assume a mean unit cost per dose of €56.10 with corresponding 95% credible interval of [€36.48;€77.43], estimated according to expert opinion. Individuals

need three vaccine shots to be fully protected; therefore, these costs as well as the administration costs have to be multiplied by three.

HPV-induced diseases related to the cervix produce costs which are a combination of the expenses for two Pap-tests (c^{pap}) and two colposcopies (c^{colp}) in females affected by a CIN stage or cervical cancer. Moreover, the costs of a HPV-DNA test (c^{dna}) in those suffering from CIN III or cervical cancer have to be considered, in addition to the costs caused by the disease.

Neoplasiae in the anus lead to costs induced by the diagnostic procedures of anal cytology (c^{cyt}) in addition to anoscopy and biopsy (c^{anbiop}). Furthermore, obviously, the treatment costs of the disease have to be considered. For all other HPV-induced diseases, we assume that the information we found in the literature does not only include treatment costs, but additionally those of all diagnostic procedures involved.

F.8 Model parameters related to utilities

Table F.8 shows the utilities we assume for the different states in the model. We define informative Beta distributions for all parameters. Since we have not found information on utilities for all HPV-induced diseases considered, we assume the utilities of the precancerous stages of vaginal and vulvar cancers to be equivalent to those of anal LSIL and HSIL, and those of vaginal and vulvar cancers equivalent to cervical cancer. In penile cancer and its precancerous stage, we assume the same utility for all cancer stages, estimating an average value. For more information about the sources to inform costs and utilities, see Section 5.5.1.

Table F.8: Distributional values, means, corresponding 95% credible intervals and sources of prior information of utilities used in the model

Var.	Description	Distribution	Mean and 95%-CI	Source
Cervix				
u^{ascus}	ASCUS	Inform. Beta	0.8302 [0.5725;0.9767]	[256]
u_1^{cin}	CIN I	Inform. Beta	0.8396 [0.2058;0.9999]	[256]
u_2^{cin}	CIN II	Inform. Beta	0.7967 [0.0469;0.9999]	[256]
u_3^{cin}	CIN III	Inform. Beta	0.8396 [0.1845;0.9999]	[256]
u_1^{cerv}	FIGO I	Inform. Beta	0.5769 [0.2766;0.8641]	[256]
u_2^{cerv}	FIGO II	Inform. Beta	0.5228 [0.2254;0.8085]	[256]
u_3^{cerv}	FIGO III	Inform. Beta	0.5656 [0.3915;0.7413]	[256]
u_4^{cerv}	FIGO IV	Inform. Beta	0.4472 [0.1562;0.7456]	[256]
Genital warts				
u_M^{gw}	Genital warts in males	Inform. Beta	0.6961 [0.1172;0.9999]	[256]
u_F^{gw}	Genital warts in females	Inform. Beta	0.7761 [0.0520;0.9999]	[256]
Anus				
u^{lsil}	LSIL	Inform. Beta	0.9793 [0.9517;0.9955]	[210]
u^{hsil}	HSIL	Inform. Beta	0.9793 [0.9480;0.9959]	[210]
$u_{1,M}^{an}$	Cancer stage I in males	Inform. Beta	0.6654 [0.1847;0.9850]	[256, 341]
$u_{2,M}^{an}$	Cancer stage II in males	Inform. Beta	0.6145 [0.1207;0.9783]	[256, 341]
$u_{3,M}^{an}$	Cancer stage III in males	Inform. Beta	0.4540 [0.0486;0.9157]	[256, 341]
$u_{4,M}^{an}$	Cancer stage IV in males	Inform. Beta	0.2165 [0;0.8309]	[256, 341]
$u_{1,F}^{an}$	Cancer stage I in females	Inform. Beta	0.7275 [0.0669;0.9999]	[256, 341]
$u_{2,F}^{an}$	Cancer stage II females	Inform. Beta	0.6776 [0.0268;1]	[256, 341]
$u_{3,F}^{an}$	Cancer stage III females	Inform. Beta	0.4917 [0.0105;0.9929]	[256, 341]
$u_{4,F}^{an}$	Cancer stage IV females	Inform. Beta	0.2739 [0;0.9796]	[256, 341]
Head/neck				
$u_{1,M}^{hn}$	Cancer stage I/II males	Inform. Beta	0.8171 [0.0135;1]	[110, 256]
$u_{3,M}^{hn}$	Cancer stage III/IV males	Inform. Beta	0.5937 [0.0160;0.9979]	[110, 137, 256, 308]
$u_{1,F}^{hn}$	Cancer stage I/II females	Inform. Beta	0.7413 [0.2500;0.9911]	[110, 256]
$u_{3,F}^{hn}$	Cancer stage III/IV females	Inform. Beta	0.5377 [0.1450;0.9021]	[110, 137, 256, 308]
Vagina				
u_1^{vain}	VaIN I	see anal LSIL	—	EO
u_2^{vain}	VaIN II	see anal HSIL	—	EO
u_3^{vain}	VaIN III	see anal HSIL	—	EO
u_1^{vag}	Cancer stage I	see cervical cancer stage I	—	EO
u_2^{vag}	Cancer stage II	see cervical cancer stage II	—	EO
u_3^{vag}	Cancer stage III	see cervical cancer stage III	—	EO

u_4^{vag}	Cancer stage IV	see cervical cancer stage IV	—	EO

Vulva

u^{vin}	VIN	see anal HSIL	—	EO
u_1^{vulv}	Cancer stage I	see cervical cancer stage I	—	EO
u_2^{vulv}	Cancer stage II	see cervical cancer stage II	—	EO
u_3^{vulv}	Cancer stage III	see cervical cancer stage III	—	EO
u_4^{vulv}	Cancer stage IV	see cervical cancer stage IV	—	EO

Penis

u^{pen}	PeIN, cancer all stages	Inform. Beta	0.7922 [0.7489;0.8455]	[91]

Appendix G

Continuation of calibration results

In Section 6.3, the visual calibration approach of the BMM applied to human papillomavirus is described in detail. The terms “incidence” and “prevalence” are explained; in addition, calibration results of the model outcome on HPV prevalence to data are presented. Furthermore, the calibration results for cervical cancer are shown. This appendix includes the calibration results of genital warts as well as HPV-induced diseases of the anus, head/neck, vagina, vulva and penis. As explained in Section 6.3, the results are displayed separately for the two sexes and the three interventions screening-only, female-only vaccination and universal vaccination.

G.1 Anal cancer and genital warts

Anal cancer incidence data for the general population are given by Cancer Research UK [351]. The age- and sex-specific yearly incidence rates are reported in age groups of five years. To the best of our knowledge, research on the development of precursors of anal cancer is solely conducted for homosexual males. Thus, we use prevalence data on LSIL and HSIL from the US on this subpopulation [84]. These are adjusted by the relative risk of on

average 17.2 of homosexual males to develop anal cancer when compared to the general population, informed by Danish data [145] and indicated by the parameter $\rho_3^\bigstar$ in Section 5.5. In females, we assume an on average 1.7 times higher risk of acquiring anal precancerous lesions when compared to heterosexual males; we estimate this by comparing the UK data on female and male anal cancer incidence [351]. The corresponding adjustment factor is indicated by $\rho_2^\bigstar$.

The transition probabilities from the state *LSIL* to *Clearance*, *LSIL* to *HSIL*, *HSIL* to *Clearance* and *HSIL* to *LSIL* are modified in an age- and sex-specific way, multiplied by $\lambda_{F,a,15,13}$, $\lambda_{F,a,15,16}$, $\lambda_{F,a,16,13}$, $\lambda_{F,a,16,15}$ in females and $\lambda_{M,a,8,6}$, $\lambda_{M,a,8,9}$, $\lambda_{M,a,9,6}$, $\lambda_{M,a,9,8}$ in males, respectively.

Due to non-existing Italian data, we calibrate the age- and sex-specific model output on genital warts prevalence by means of Canadian prevalence data reported by Marra et al. [253]. These are displayed in age groups of five years from the ages of 15 to 85, and we interpolate these to a starting age of twelve years. In the model, genital warts prevalence includes individuals who newly acquire the condition, and those who suffer from a relapse. In accordance to a literature source from the US [69], we assume genital warts recurrence to be age-specific with an around five to twelve times higher probability in older individuals when compared to the younger, indicated by $\lambda_{F,a,7,7}$ in females and $\lambda_{M,a,4,4}$ in males.

Until the age of 52 years, we estimate the age- and sex-specific transition probabilities of moving to the state of *Genital warts* in age groups of five years; as a consequence, the model output does not look like a smooth curve, but saw-toothed.

Our calibration results in Figure G.1 show that our model estimates both female and male LSIL and HSIL prevalence reasonably well, whereas anal cancer and genital warts in males are under- and overestimated in older people, respectively. Since the overall anal cancer incidence is extremely small and the effects of discounting are considerably high in the older, we

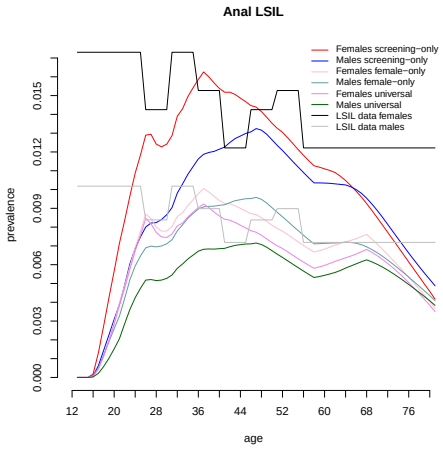

(a) The calibration result of anal LSIL shows that the model outcome fits the data reasonably well; female prevalence is higher than male prevalence as a result of different sexual behaviour.

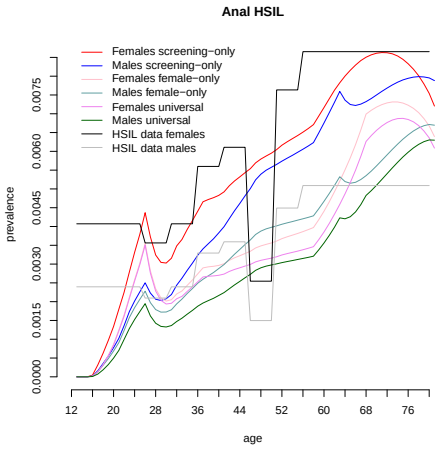

(b) The model outcome on anal HSIL shows a good approximation to the data, peak prevalence in older people is realistically estimated.

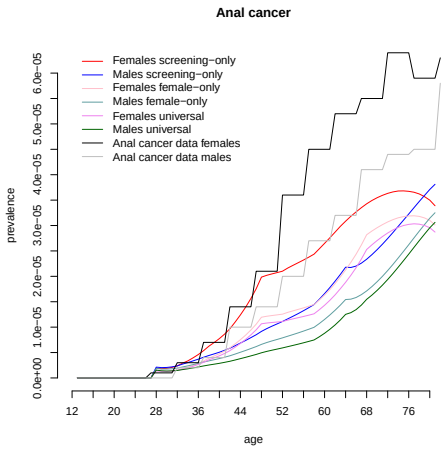

(c) The model outcome fits the trend of increasing anal cancer incidence by age; however, the data show a steeper increase, especially in older people.

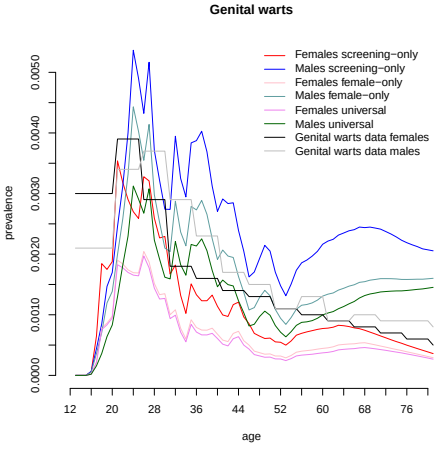

(d) Genital warts prevalence in females is well estimated by our model, whereas it is overestimated especially in older males. However, both due to the small number of old age cohorts in our model and discounting, these effects are not relevant.

Figure G.1: Calibration results for anus-related, HPV-induced diseases and genital warts. The prevalence of the precancerous stages anal LSIL and anal HSIL is realistically estimated, whereas anal cancer incidence and male genital warts prevalence are under- and overestimated in older individuals, respectively.

assume that this underestimation does not have an impact on the results of the health economic evaluation. As for genital warts prevalence, the overestimation in older males does not falsify the results (following the same

reasoning as for anal cancer).

G.2 Other HPV-induced cancers

The calibration of the model outcome on head/neck cancer is relatively straightforward since we do not account for a precancerous stage. The expression “head/neck cancer” summarizes cancers located in the nasal cavity, pharynx, tongue, lips, larynx, esophagus and trachea; however, only 20-25% of all head/neck cancers seem to be HPV-associated, with a higher percentage of 60-70% in oropharyngeal cancers. Cancers in other parts of the head and neck are mainly attributed to excessive smoking and drinking [284]. As a consequence, we use age- and sex-specific data on oral cancer incidence in the UK, reported by Cancer Research UK [352]. In order to avoid an underestimation of head/neck cancer incidence, especially in older ages, we incorporate the incidence rates reported into the lower bounds of the corresponding prior distributions, assuming high variance. As a consequence, we result in wide distributions, incorporating a large amount of parameter uncertainty.

UK penile cancer incidence data are reported by the National Cancer Date Repository of the Office for National Statistics [267]. These data summarise penile cancer incidence over three years and therefore have to be adjusted. As for anal and oral cancer, age-specific incidence rates on vulvar as well as vaginal cancer are reported by Cancer Research UK [353, 354]. Despite an extensive literature review, we neither found prevalence data on penile intraepithelial neoplasm (PeIN) nor on the precancerous stage of vulvar cancer (VIN) or the three precancerous stages of vaginal cancer (VaIN I-III); yet, incidence data on PeIN [266], VaIN and VIN [271] were found. However, incidence data on these precancerous stages cannot be used for model calibration since the corresponding model outcome does not refer to those who newly acquire the condition as described in Section 6.3.1.

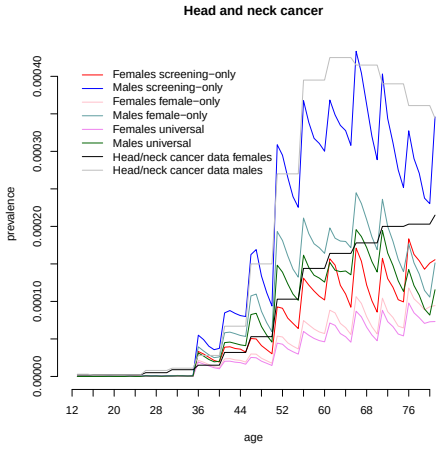

(a) The calibration result of head/neck cancer incidence shows a good fit to the data in both sexes.

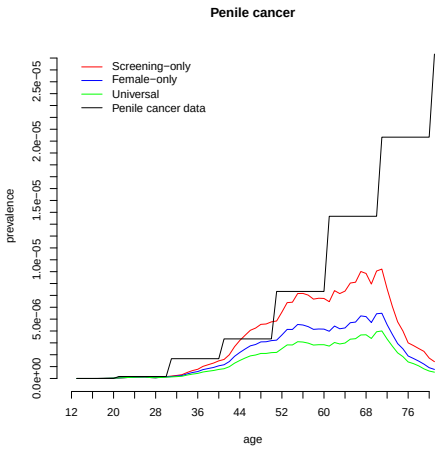

(b) Penile cancer incidence is sufficiently well estimated in younger ages and underestimated in older ages.

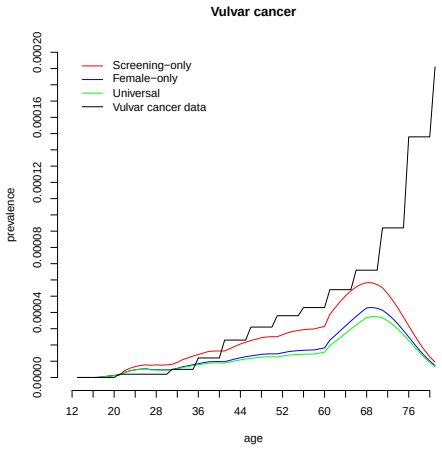

(c) The calibration results of vulvar cancer incidence are comparable to those of penile cancer.

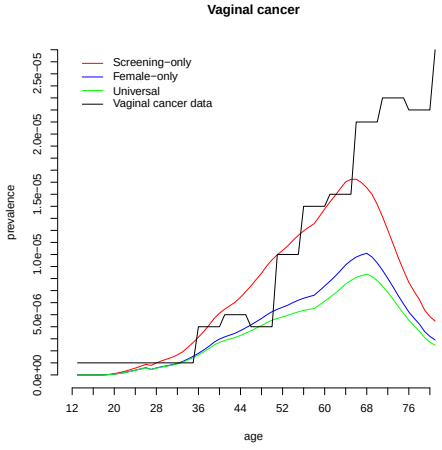

(d) As for penile and vulvar cancer incidence, vaginal cancer incidence is estimated well in younger individuals, and the fit to the data becomes less optimal in older ages.

Figure G.2: The model outcome on incidence of the rare HPV-induced cancers in the head/neck, penis, vulva and vagina is displayed and compared to data. We account for sex-specific incidence in head/neck cancer with males under higher risk; the other cancers presented are sex-specific. Incidence in the sex-specific cancers in the older ages is underestimated. However, due to discounting and the relatively low number of old age cohorts in the model, this does not falsify the results of the cost-effectiveness analysis.

As a consequence, we estimate the prevalence of these precancerous stages in a way to result in realistic outcomes of the corresponding can-

cers. We assume that young individuals clear a precancerous stage more easily and are as a result less likely to progress to cancer. In contrast, the probability of developing cancer considerably increases in older individuals affected by PeIN or VIN. In the vaginal cancer compartment, we adjust the transition probabilities to clear VaIN III and to move to vaginal cancer in an age-specific way to increase vaginal cancer incidence in the older.

All assumptions are supported by the data on incidence, indicating considerably higher incidence of the precancerous lesions in the older. Given these data, we can assume that if incidence in older individuals is higher, prevalence must be as well. For the age- and sex-specific variables $\lambda_{v,a,r,s}$, see Section 5.8 and Appendices D and E.2.

We show the calibration results of the rare HPV-induced diseases head/neck, penile, vulvar and vaginal cancer in Figure G.2. As for genital warts, we estimate the transition probabilities to the state head/neck cancer in age groups of five years, resulting in saw-toothed curves. For both sexes, the output fits the data well. In penile cancer, the model estimates the age-specific trend of a peak incidence in the oldest fairly well; however, the increase in incidence is steeper in the data. Similar effects can be seen in vulvar and vaginal cancer.

Bibliography

[1] SAVI - Sheffield Accelerated Value of Information. Available from *http://savi.shef.ac.uk/SAVI/*, last accessed 18/03/2017.

[2] Centers for Disease Control and Prevention. Human Papillomavirus (HPV). HPV and men (fact sheet), 2015. Available from *http://www.cdc.gov/std/hpv/stdfact-hpv-and-men.htm*, last accessed 18/03/2017.

[3] Package BCEA. Bayesian cost-effectiveness analysis, 2015. Available from *http://cran.r-project.org/web/packages/BCEA/BCEA.pdf*, last accessed 18/03/2017.

[4] Stan: A C++ Library for Probability and Sampling, Version 2.8.0, 2015. Available from *http://mc-stan.org/*, last accessed 18/03/2017.

[5] Stan Modeling Language. User's Guide and Reference Manual, Version 2.14.0, 2016. Available from *http://mc-stan.org/*, last accessed 01/02/2017.

[6] Nomenclatore Tariffario Regionale 2006. Regione Lazio. Aggiornamento del Nomenclatore Tariffario Regionale delle Prestazioni Specialistiche Ambulatoriali. Modificazioni ed Integrazioni alla DGR no. 439 del 21/07/2006. Available from *http://www.asplazio.it/asp_online/att_territoriale/files/sias/normativa/DGR562_5_09_06.pdf*, last accessed 18/03/2017.

[7] G. Accetta, A. Biggeri, G. Carreras, G. Lippi, F.M. Carozzi, M. Confortini, M. Zappa, and E. Paci. Is Human Papillomavirus Screening Preferable to Current Policies in Vaccinated and Unvaccinated Women? A Cost-Effectiveness Analysis. *Journal of Medical Screening*, 17(4):181–189, 2010.

[8] H. Afzali and J. Karnon. Exploring Structural Uncertainty in Model-Based Economic Evaluations. *PharmacoEconomics*, 33(5):435–443, 2015.

[9] I. Aguilar, L. Mendoza, L. Garcia, I. Diaz, J. Figueroa, R. Duarte, G. Perdomo, A. Garcia, and C. Janusz. Cost-effectiveness analysis of the introduction of the human papillomavirus vaccine in Honduras. *Vaccine*, 33(Suppl 1):A167–A173, 2015.

[10] M. Aho, E. Vesterinen, B. Meyer, E. Purola, and J. Paavonen. Natural History of Vaginal Intraepithelial Neoplasia. *Cancer*, 68(1):195–197, 1991.

[11] I. Alonso, A. Felix, A. Torné, V. Vusté, M. del Pino, P. Castillo, J. Balasch, J. Pahisa, J. Rios, and J. Ordi. Human Papillomavirus as a Favorable Prognostic Biomarker in Squamous Cell Carcinomas of the Vagina. *Gynecologic Oncology*, 125(1):194–199, 2012.

[12] R. Anderson and R. May. Vaccination and herd immunity to infectious diseases. *Nature*, 318(6044):323–329, 1985.

[13] R. Anderson and R. May. *Infectious Diseases of Humans Dynamics and Control.* Oxford University Press, Oxford, United Kingdom, 1991.

[14] W. J. Anderson. *Continuous-Time Markov Chains: An Applications-Oriented Approach.* Springer, New York, USA, 1991.

[15] L. Andronis, P. Barton, and S. Bryan. Sensitivity analysis in economic evaluation: an audit of NICE current practice and a review of its

use and value in decision-making. *Health Technology Assessment*, 13(29), 2009.

[16] A. Anonychuk, C. Bauch, M.F. Merid, G. van Kriekinge, and N. Demarteau. A Cost-Utility Analysis of Cervical Cancer Vaccination in Preadolescent Canadian Females. *BioMed Central Public Health*, 9(401), 2009.

[17] J. Aponte-Gonzales, L. Fajardo-Bernal, J. Diaz, J. Eslava-Schmalbach, O. Gamboa, and J. Hay. Cost-Effectiveness Analysis of the Bivalent and Quadrivalent Human Papillomavirus Vaccines from a Societal Perspective in Colombia. *PLoS One*, 8(11), 2013.

[18] A. Attema, Y. Edelaar-Peeters, M. Versteegh, and E. Stolk. Time trade-off: one methodology, different methods. *The European Journal Of Health Economics*, 14(Suppl 1):53–64, 2003.

[19] K. Ault and The Future II Study Group. Effect of Prophylactic Human Papillomavirus L1 Virus-like-particle Vaccine on Risk of Cervical Intraepithelial Neoplasia Grade 2, Grade 3, and Adenocarcinoma in Situ: a Combined Analysis of Four Randomised Clinical Trials. *The Lancet*, 369(9576), 2007.

[20] K. Auranen, M. Eichner, H. Käyhty, A. Takala, and E. Arjas. A Hierarchical Bayesian Model to Predict the Duration of Immunity to Haemophilus influenzae Type b. *Biometrics*, 55(4):1306–1313, 1999.

[21] C. Azzari, C. Massai, C. Poggiolesi, G. Indolfi, G. Spagnolo, and M. De Luca. Cost of Varicella-Related Hospitalizations in an Italian Paediatric Hospital: Comparison with Possible Vaccination Expenses. *Current Medical Research and Opinion*, 23(12):2945–2954, 2007.

[22] G. Baio. *Bayesian Methods in Health Economics*. Chapman& Hall, CRC Biostatistics Series, 2013.

[23] G. Baio, A. Capone, A. Marcellusi, FS. Mennini, and G. Favato. Economic Burden of Human Papillomavirus-Related Diseases in Italy. *PLoS ONE*, 7(11), 2012.

[24] G. Baio and AP. Dawid. Probabilistic Sensitivity Analysis in Health Economics. *Statistical Methods in Medical Research*, 2011.

[25] G. Barbagli, E. Palminteri, F. Mirri, G. Guazzoni, D. Turini, and M. Lazzeri. Penile Carcinoma in Patients With Genital Lichen Sclerosus: A Multicenter Survey. *The Journal of Urology*, 175(4):1359–1363, 2006.

[26] RV. Barnabas, P. Laukkanen, and P. Koskela. Epidemiology of HPV 16 and Cervical Cancer in Finland and the Potential Impact of Vaccination: Mathematical Modelling Analyses. *PLoS Medicine*, 3(5), 2006.

[27] C. Bauch, A. Anonychuk, T. van Effelterre, B. Pham, and M. Merid. Incorporating Herd Immunity Effects into Cohort Models of Vaccine Cost-Effectiveness. *Medical Decision Making*, 29(5):557–569, 2009.

[28] I. Baussano, S. Franceschi, A. Gillio-Tos, F. Carozzi, M. Confortini, P. Dalla Palma, M. De Lillo, A. Del Mistro, L. De Marco, C. Naldoni, P. Pierotti, P. Schincaglia, N. Segnan, M. Zorzi, P. Giorgi-Rossi, and G. Ronco. Difference in overall and age-specific prevalence of high-risk human papillomavirus infection in Italy: evidence from NTCC trial. *BioMed Central Infectious Diseases*, 13(238), 2013.

[29] J. Benedet, H. Bender, I. Jones, H. Ngan, and S. Pecorelli. International Federation of Gynecology and Obstetrics (FIGO). Committee on Gynecologic Oncology. FIGO Staging Classifications and Clinical Practice Guidelines in the Management of Gynecologic Cancers. *International Journal of Gynecology & Obstetrics*, 70(2):221–229, 2000.

[30] C. Bergeron, N. Largeron, R. McAllister, P. Mathevet, and V. Remy. Cost-Effectiveness Analysis of the Introduction of a Quadrivalent Human Papillomavirus Vaccine in France. *International Journal of Technology Assessment in Health Care*, 24(1):10–19, 2008.

[31] J. Berkhof, J. Bogaards, E. Demirel, M. Diaz, M. Sharma, and J. Kim. Cost-Effectiveness of Cervical Cancer Prevention in Central and Eastern Europe and Central Asia. *Vaccine*, 31(Suppl 7):H71–H79, 2013.

[32] G. Bethune, J. Campbell, A. Rocker, D. Bell, R. Rendon, and J. Merrimen. Clinical and Pathologic Factors of Prognostic Significance in Penile Squamous Cell Carcinoma in a North American Population. *Urology*, 79(5):1092–1097, 2012.

[33] J. Bilcke, R. Chapman, C. Atchison, D. Cromer, H. Johnson, L. Willem, M. Cox, W. Edmunds, and M. Jit. Quantifying Parameter and Structural Uncertainty of Dynamic Disease Transmission Models Using MCMC: An Application to Rotavirus Vaccination in England and Wales. *Medical Decision Making*, 35(5):633–647, 2015.

[34] T. Blakely, G. Kvizhinadze, T. Karvonen, A. Pearson, M. Smith, and N. Wilson. Cost-effectiveness and equity impacts of three HPV vaccination programmes for school-aged girls in New Zealand. *Vaccine*, 32(22):2645–2656, 2014.

[35] S. Blower and H. Dowlatabadi. Sensitivity and Uncertainty Analysis of Complex Models of Disease Transmission: An HIV Model, as an Example. *International Statistical Review*, 62(2):229–243, 1994.

[36] J. Bogaards, V. Coupé, C. Meijer, and J. Berkhof. The Clinical Benefit and Cost-Effectiveness of Human Papillomavirus Vaccination for Adult Women in the Netherlands. *Vaccine*, 29(48):8929–8936, 2011.

[37] JA. Bogaards, VMH. Coupe, M. Xiridou, CJLM. Meijer, J. Wallinga, and J. Berkhof. Long-term Impact of Human Papillomavirus Vaccination on Infection Rates, Cervical Abnormalities, and Cancer Incidence. *Epidemiology*, 22(4):505–515, 2011.

[38] JA. Bogaards, M. Kretzschmar, M. Xiridou, CJLM. Meijer, J. Berkhof, and J. Wallinga. Model-Based Estimation of Viral Transmissibility and Infection-Induced Resistance From the Age-Dependent Prevalence of Infection for 14 High-Risk Types of Human Papillomavirus. *American Journal of Epidemiology*, 171(7):817–825, 2010.

[39] JA. Bogaards, M. Kretzschmar, M. Xiridou, CJLM. Meijer, J. Berkhof, and J. Wallinga. Sex-Specific Immunization for Sexually Transmitted Infections Such as Human Papillomavirus: Insights from Mathematical Models. *PLoS Medicine*, 8(12), 2011.

[40] L. Bojke, K. Claxton, S. Palmer, and M. Sculpher. *Defining and characterising structural uncertainty in decision analytic models.* Centre for Health Economics, University of York, UK, 2006.

[41] L. Bojke, K. Claxton, M. Sculpher, and S. Palmer. Characterizing Structural Uncertainty in Decision Analytic Models: A Review and Application of Methods. *Value in Health*, 12(5):739–749, 2008.

[42] L. Bonneux and E. Birnie. The Discount Rate in the Economic Evaluation of Prevention: a Thought Experiment. *Journal of Epidemiology and Community Health*, 55(2):123–125, 2001.

[43] M. Borenstein, L. Hedges, J. Higgins, and H. Rothstein. *Introduction to Meta-Analysis*. John Wiley & Sons, Chichester, West Sussex, United Kingdom, 2009.

[44] FX. Bosch, A. Lorincz, and N. Munoz. The Causal Relation between Human Papillomavirus and Cervical Cancer. *Journal of Clinical Pathology*, 55(4):244–265, 2002.

[45] HC. Boshuizen and PHM. van Baal. Probabilistic Sensitivity Analysis: Be a Bayesian. *Value in Health*, 12(8):1210–1214, 2009.

[46] P. Boyle and B. Levin. World Cancer Report 2008. World Health Organization and International Agency for Research on Cancer, 2008. Published by the International Agency for Research on Cancer, Lyon, France, pages 418–423. Available from *http://www.iarc.fr/en/publications/pdfs-online/wcr/2008/*, last accessed 18/03/2017.

[47] G. Bratton Lazenby, E. Ramsey Unal, A. Lintzenich Andrews, and K. Simpson. A Cost-Effectiveness Analysis of Anal Cancer Screening in HIV-Positive Women. *Journal of Lower Genital Tract Disease*, 16(3):275–280, 2012.

[48] P. Breheny. MCMC Methods: Gibbs and Metropolis, 2013. Available from *http://web.as.uky.edu/statistics/users/pbreheny/701/S13/notes/2-28.pdf*, last accessed 18/03/2017.

[49] X. Bresse, C. Goergen, B. Prager, and E. Joura. Universal vaccination with the quadrivalent HPV vaccine in Austria: impact on virus circulation, public health and cost-effectiveness analysis. *Expert Review of Pharmacoeconomics & Outcomes Research*, 14(2):269–281, 2014.

[50] C. Breto, D. He, E. Ionides, and A. King. Time series analysis via mechanistic models. *The Annals of Applied Statistics*, 3(1):319–348, 2009.

[51] A. Briggs, M. Sculpher, and K. Claxton. *Decision Modelling for Health Economic Evaluation*. Oxford University Press, Oxford, UK, 2006.

[52] A. Briggs, M. Weinstein, E. Fenwick, J. Karnon, M. Sculpher, and D. Paltiel. Model Parameter Estimation and Uncertainty: A Report of the ISPOR-SMDM Modeling Good Research Practices Task Force-6. *Value in Health*, 15(6):835–842, 2012.

[53] M. Brisson and W. Edmunds. Economic Evaluation of Vaccination Programs: The Impact of Herd-Immunity. *Medical Decision Making*, 23(1):76–82, 2003.

[54] M. Brisson and W. Edmunds. Impact of Model, Methodological, and Parameter Uncertainty in the Economic Analysis of Vaccination Programs. *Medical Decision Making*, 26(5):434–446, 2006.

[55] M. Brisson, J. Laprise, H. Chesson, M. Drolet, T. Malagon, M.C. Boily, and L. Markowitz. Health and Economic Impact of Switching From a 4-Valent to a 9-Valent HPV Vaccination Program in the United States. *Journal of the National Cancer Institute*, 108(1), 2016.

[56] M. Brisson, J. Laprise, M. Drolet, N. van de Velde, E. Franco, E. Kliewer, G. Ogilvie, S. Deeks, and M.C. Boily. Comparative cost-effectiveness of the quadrivalent and bivalent human papillomavirus vaccines: A transmission-dynamic modeling study. *Vaccine*, 31(37):3863–3871, 2013.

[57] M. Brisson, N. van de Velde, P. de Wals, and M.C. Boily. The Potential Cost-Effectiveness of Prophylactic Human Papillomavirus Vaccines in Canada. *Vaccine*, 25(29):5399–5408, 2007.

[58] M. Brisson, N. van de Velde, M. Drolet, M.-C. Boily, E. Franco, and M. Mayrand. HPV Advise. Technical Appendix., 2012. Available from *http://www.marc-brisson.net/HPVadvise.pdf*, last accessed 18/03/2017.

[59] M. Brisson, N. van de Velde, EL. Franco, M. Drolet, and MC. Boily. Incremental Impact of Adding Boys to Current Human Papillomavirus Vaccination Programs: Role of Herd Immunity. *The Journal of Infectious Diseases*, 204(3):372–376, 2011.

[60] T. Britton. Stochastic epidemic models: A survey. *Mathematical Biosciences*, 225(1):24–35, 2010.

[61] X. Brouha, D. Tromp, G.-J. Hordijk, J. Winnubst, and R.J. de Leeuw. Oral And Pharyngeal Cancer: Analysis Of Patient Delay At Different Tumor Stages. *Head Neck*, 27(11):939–945, 2005.

[62] DR. Brown, SK. Kjaer, K. Sigurdsson, OE. Iversen, M. Hernandez-Avila, CM. Wheeler, G. Perez, LA. Koutsky, EH. Tay, P. Garcia, KA. Ault, SM. Garland, S. Leodolter, SE. Olsson, GW. Tang, DG. Ferris, J. Paavonen, M. Steben, FX. Bosch, J. Dillner, EA. Joura, RJ. Kurman, S. Majewski, N. Munoz, ER. Myers, LL. Villa, FJ. Taddeo, C. Roberts, A. Tadesse, J. Bryan, LC. Lupinacci, KE. Giacoletti, HL. Sings, M. James, TM. Hesley, and E. Barr. The Impact of Quadrivalent Human Papillomavirus (HPV; Types 6, 11, 16, and 18) L1 Virus-Like Particle Vaccine on Infection and Disease due to Oncogenic Nonvaccine HPV Types in Generally HPV-naive Women Aged 16-26 Years. *Journal of Infectious Diseases*, 199:926–935, 2009.

[63] VL. Brown and KAJ. White. The Role of Optimal Control in Assessing the Most Cost-Effective Implementation of a Vaccination Programme: HPV as a Case Study. *Mathematical Biosciences*, 231(2):126–134, 2011.

[64] A. Burchell, F. Coutlee, P.-P. Tellier, J. Hanley, and E. Franco. Genital Transmission of Human Papillomavirus in Recently Formed Heterosexual Couples. *The Journal of Infectious Diseases*, 204(11):1723–1729, 2011.

[65] A. Burchell, P. Pellier, J. Hanley, F. Coutlée, and E. Franco. Human papillomavirus infections among couples in new sexual relationships. *Epidemiology*, 21(1):31–37, 2010.

[66] A. Burchell, H. Richardson, S.M. Mahmud, H. Trottier, P. Tellier, J. Hanley, F. Coutlée, and E. Franco. Modeling the Sexual Transmissibility of Human Papillomavirus Infection using Stochastic Computer Simulation and Empirical Data from a Cohort Study of Young Women in Montreal, Canada. *American Journal of Epidemiology*, 163(6):534–543, 2006.

[67] E. Burger, S. Sy, M. Nygard, S. Kristiansen, and J. Kim. Prevention of HPV-Related Cancers in Norway: Cost-Effectiveness of Expanding the HPV Vaccination Program to Include Pre-Adolescent Boys. *PLoS One*, 9(3), 2014.

[68] E. Burger, S. Sy, M. Nygard, S. Kristiansen, and J. Kim. Too Late to Vaccinate? The Incremental Benefits and Cost-effectiveness of a Delayed Catch-up Program Using the 4-Valent Human Papillomavirus Vaccine in Norway. *The Journal of Infectious Diseases*, 211(2):206–215, 2015.

[69] DR. Camenga, EF. Dunne, MM. Desai, J. Gee, LE. Markowitz, A. Desiliva, and NP. Klein. Incidence of genital warts in adolescents and young adults in an integrated health care delivery system in the United States before human papillomavirus vaccine recommendations. *Sexually Transmitted Diseases*, 40(7):534–538, 2013.

[70] N. Campos, J. Kim, P. Castle, J. Ortendahl, M. O'Shea, M. Diaz, and S. Goldie. Health and Economic Impact of HPV 16/18 Vaccination and Cervical cancer screening in Eastern Africa. *International Journal of Cancer*, 130(11):2672–2684, 2011.

[71] K. Canfell, R. Barnabas, J. Patnick, and V. Beral. The Predicted Effect of Changes in Cervical Screening Practice in the UK: Results from a Modelling Study. *British Journal of Cancer*, 91(3):530–536, 2004.

[72] K. Canfell, J.-F. Shi, J.-B. Lew, R. Walker, F.-H. Zhao, L. Simonella, J.-F. Chen, R. Legood, M.A. Smith, C. Nickson, and Y.-L. Qiao. Prevention of Cervical Cancer in Rural China: Evaluation of HPV Vaccination and Primary HPV Screening Strategies. *Vaccine*, 29(13):2487–2494, 2011.

[73] Q. Cao, E. Buskens, T. Feenstra, T. Jaarsma, H. Hillege, and D. Postmus. Continuous-Time Semi-Markov Models in Health Economic Decision Making: An Illustrative Example in Heart Failure Disease Management. *Medical Decision Making*, 36(1):59–71, 2016.

[74] S. Capri, A. Ceci, L. Terranova, F. Merlo, and L. Mantovani. Guidelines for economic evaluations in Italy: recommendations from the Italian group of pharmacoeconomic studies. *Drug Information Journal*, 35:189–201, 2001.

[75] S. Capri, R. Gasparini, D. Panatto, and N. Demarteau. Cost-Consequences Evaluation between Bivalent and Quadrivalent HPV Vaccines in Italy: The Potential Impact of Different Cross-Protection Profiles. *Gynecologic Oncology*, 121(3):514–521, 2011.

[76] X. Castellsague and N. Munoz. Chapter 3: Cofactors in Human Papillomavirus Carcinogenesis - Role of Parity, Oral Contraceptives, and Tobacco Smoking. *Journal of the National Cancer Institute*, 31:20–28, 2003.

[77] S. Cauchemez and N. Ferguson. Likelihood-based estimation of continuous-time epidemic models from time-series data: application to measles transmission in London. *Journal of the Royal Society Interface*, 5(25):885–897, 2008.

[78] MG. Centurioni, A. Puppo, DF. Merlo, G. Pasciucco, ER. Cusimano, R. Sirito, and CA. Gustavino. Prevalence of Human Papillomavirus Cervical Infection in an Italian Asymptomatic Population. *BioMed Central Infectious Diseases*, 5:77, 2005.

[79] CERVIVAC. CERVIVAC. Models and tools. Pan American Health Organization., 2014. Available from *http://www.paho.org/provac/index.php?option=com_content&view=article&id=1640%3Amodels-and-tools&Itemid=1614&lang=en*, last accessed 18/03/2017.

[80] A. Chatterjee. The Next Generation of HPV Vaccines: Nonavalent Vaccine V503 on the Horizon. *Expert Review of Vaccines*, 13(11):1279–1290, 2014.

[81] M.-K. Chen, H.-F. Hung, S. Duffy, A M.-F. Yen, and H.-H. Chen. Cost-Effectiveness Analysis for Pap Smear Screening and Human Papillomavirus DNA Testing and Vaccination. *Journal of Evaluation in Clinical Practice*, 17(6):1050–1058, 2011.

[82] HW. Chesson, DU. Ekwueme, M. Saraiya, EF. Dunne, and LE. Markowitz. The Cost-Effectiveness of Male HPV Vaccination in the United States. *Vaccine*, 29(46):8443–8450, 2011.

[83] H.W. Chesson, DU. Ekwueme, M. Saraiya, and LE. Markowitz. Cost-Effectiveness of Human Papillomavirus Vaccination in the United States. *Emerging Infectious Diseases*, 14(2):244–251, 2008.

[84] PV. Chin-Hong, E. Vittinghoff, RD. Cranston, L. Browne, S. Buchbinder, G. Colfax, M. Da Costa, T. Darragh, D. Jones Benet, F. Judson, B. Koblin, KH. Mayer, and JM. Palefsky. Age-Related Prevalence of Anal Cancer Precursors in Homosexual Men: The EXPLORE Study. *Journal of the National Cancer Institute*, 97(12):896–905, 2005.

[85] YH. Choi, M. Jit, N. Gay, A. Cox, GP. Garnett, and WJ. Edmunds. Transmission Dynamic Modelling of the Impact of Human Papillomavirus Vaccination in the United Kingdom. *Vaccine*, 28(24):4091–4102, 2010.

[86] MK. Chung, Y.-I. Son, JK. Cho, YK. So, SH. Woo, H.-S. Jeong, and C.-H. Baek. Therapeutic Options in Patients with Early T Stage and Advanced N Stage of Tonsillar Squamous Cell Carcinomas. *Otolaryngology-Head and Neck Surgery*, 143(6):808–814, 2010.

[87] L. Colantonio, J.A. Gómez, N. Demarteau, B. Standaert, A. Pichón-Rivière, and F. Augustovski. Cost-Effectiveness Analysis of a Cervical Cancer Vaccine in Five Latin American Countries. *Vaccine*, 27(40):5519–5529, 2009.

[88] D. Coleman, N. Day, G. Douglas, E. Farmery, E. Lynge, J. Philip, and N. Segnan. European Guidelines for Quality Assurance in Cervical Cancer Screening. *European Journal of Cancer*, 29A(Suppl. 4):S1–S38, 1993.

[89] MP. Coleman, G. Gatta, A. Verdecchia, J. Estève, M. Sant, and H. Storm. EUROCARE Working Group. EUROCARE-3 Summary: Cancer Survival in Europe at the End of the 20th Century. *Annals of Oncology (Suppl. 5)*, 14:v128–v149, 2003.

[90] The Cochrane Collaboration. Cochrane Handbook for Systematic Reviews of Interventions. Version 5.1.0., 2011. Available from *http://handbook.cochrane.org/*, last accessed 18/03/2017.

[91] E. Conway, K. Farmer, W. Lynch, G. Rees, G. Wain, and J. Adams. Quality of Life Valuations of HPV-Associated Cancer Health States by the General Population. *Sexually Transmitted Infections*, 88(7):517–521, 2012.

[92] B. Cooper and M. Lipsitch. The analysis of hospital infection data using hidden Markov models. *Biostatistics*, 5(2):223–237, 2004.

[93] N Cooper, K Abrams, A Sutton, D Turner, and P Lambert. A Bayesian approach to Markov modelling in cost-effectiveness analyses: application to taxane use in advanced breast cancer. *Journal of the Royal Statistical Society, Series A*, 166(3):389–405, 2003.

[94] S. Costa and G. Favato. Evaluation of the Economic Impact Produced by the Prevention of Events Induced by the HPV 6-11 Virus Types Contained in the Quadrivalent Vaccine, 2008. Available from the Social Science Research Network (SSRN) website: *http://www.ssrn.com/abstract=1080113*, last accessed 18/03/2017.

[95] L. Coudeville, A. Brunot, C. Giaquinto, C. Lucioni, and B. Dervaux. Varicella Vaccination in Italy: An Economic Evaluation of Different Scenarios. *Pharmacoeconomics*, 22(13):839–855, 2004.

[96] V. Coupé, J. van Ginkel, H.E. de Melker, P.J.F. Snijders, C.J.L.M. Meijer, and J. Berkhof. HPV 16/18 Vaccination to Prevent Cervical Cancer in The Netherlands: Model-Based Cost-Effectiveness. *International Journal of Cancer*, 124(4):970–978, 2009.

[97] C.W. Critchlow, C.M. Surawicz, K.K. Holmes, J. Kuypers, J.R. Daling, S.E. Hawes, G.M. Goldbaum, J. Sayer, C. Hurt, and C. Dunphy. Prospective Study of High Grade Anal Squamous Intraepithelial Neoplasia in a Cohort of Homosexual Men: Influence of HIV Infection, Immunosuppression and Human Papillomavirus Infection. *AIDS*, 9(11):1255–1262, 1995.

[98] C. Czoski-Murray, J. Karnon, R. Jones, K. Smith, and G. Kinghorn. Cost-Effectiveness of Screening High Risk HIV-Positive Men Who Have Sex With Men (MSM) and HIV-Positive Women for Anal Cancer. *Health Technology Assessment*, 14(53):iii–iv, ix–x, 2010.

[99] A.J. da Fonseca, L.C. de Lima Ferreira, and G.B. Neto. Cost-Effectiveness of the Vaccine against Human Papillomavirus in the Brazilian Amazon Region. *Revista Da Associacao Medica Brasileira*, 59(5):442–451, 2013.

[100] E.J. Dasbach, R.P. Insinga, Y. Cheng Yang, R.-F. Pwu, C. Lac, and E.H. Elbasha. The Cost-Effectiveness of a Quadrivalent Human Papillomavirus Vaccine in Taiwan. *Asian Pacific Journal of Cancer Prevention*, 9(3):459–466, 2008.

[101] E.J. Dasbach, R.P. Insinga, and E.H. Elbasha. The Epidemiological and Economic Impact of a Quadrivalent Human Papillomavirus Vaccine (6/11/16/18) in the UK. *British Journal of Obstetrics and Gynaecology*, 115(8):947–956, 2008.

[102] E.J. Dasbach, N. Largeron, and E.H. Elbasha. Assessment of the Cost-Effectiveness of a Quadrivalent HPV Vaccine in Norway Using a Dynamic Transmission Model. *Expert Reviews*, 8(5):491–500, 2008.

[103] E.J. Dasbach, L. Nagy, A. Brandtmüller, and E.H. Elbasha. The Cost-Effectiveness of a Quadrivalent Human Papillomavirus Vaccine (6/11/16/18) in Hungary. *Journal of Medical Economics*, 13(1):110–118, 2010.

[104] D. Davey, M. Neal, D. Wilbur, T. Colgan, P. Styer, and D. Mody. Bethesda 2001 implementation and reporting rates: 2003 practices of participants in the College of American Pathologists Interlaboratory Comparison Program in Cervicovaginal Cytology. *Archives of Pathology & Laboratory Medicine*, 128(11):1224–1229, 2004.

[105] D. De Aloysio, L. Miliffi, T. Iannicelli, P. Penacchioni, and F. Bottiglioni. Intramuscular Interferon-Beta Treatment of Cervical Intraepithelial Neoplasia II Associated with Human Papillomavirus Infection. *Acta Obstetricia et Gynecologica Scandinavica*, 73(5):420–424, 1994.

[106] D. de Angelis, M. Sweeting, AE. Ades, M. Hickman, V. Hope, and M. Ramsay. An evidence synthesis approach to estimating Hepatitis C Prevalence in England and Wales. *Statistical Methods in Medical Research*, 19(4):361–379, 2009.

[107] I. de Kok, J. Habbema, J. van Rosmalen, and M. van Ballegooijen. Would the Effect of HPV Vaccination on Non-Cervical HPV-Positive Cancers Make the Difference for its Cost-Effectiveness? *European Journal of Cancer*, 47(6):428–435, 2011.

[108] I. de Kok, M. van Ballegooijen, and J. Habbema. Cost-Effectiveness Analysis of Human Papillomavirus Vaccination in the Netherlands. *Journal of the National Cancer Institute*, 101(15):1083–1092, 2009.

[109] D. Debicki, N. Ferko, N. Demarteau, S. Gallivan, C. Bauch, A. Anonychuk, L. Mantovani, S. Capri, C.-Y. Chou, B. Standaert, and L. Annemans. Comparison of Detailed and Succinct Cohort Modelling Approaches in a Multi-Regional Evaluation of Cervical Cancer Vaccination. *Vaccine*, 26S(Suppl 5):F16–F28, 2008.

[110] R. Dedhia, K. Smith, J. Johnson, and M. Roberts. The Cost-Effectiveness of Community-Based Screening for Oral Cancer in High-Risk Males in the United States: A Markov Decision Analysis Approach. *The Laryngoscope*, 121(5):952–960, 2011.

[111] A. Dee and F. Howell. A Cost-Utility Analysis of Adding a Bivalent or Quadrivalent HPV Vaccine to the Irish Cervical Screening Programme. *European Journal of Public Health*, 20(2):213–219, 2009.

[112] Ministero della Salute. Nomenclatore Tariffario. Prestazioni di Assistenza Specialistica Ambulatoriale. Available from *http://www.ministerosalute.it/imgs/C_17_bacheca_6_listaelencodocumenti_elenco0_listadocumenti_documento0_listafile_file0_linkfile.xls*, last accessed: 18/03/2017.

[113] N. Demarteau, B. Detournay, B. Tehard, A. El Hasnaoui, and B. Standaert. A Generally Applicable Cost-Effectiveness Model for the Evaluation of Vaccines Against Cervical Cancer. *International Journal of Public Health*, 56(2):153–162, 2011.

[114] N. Demarteau and B. Standaert. Modelling the Economic Value of Cross- and Sustained-Protection in Vaccines against Cervical Cancer. *Journal of Medical Economics*, 13(2):324–338, 2010.

[115] N. Demarteau, C.-H. Tang, H.-C. Chen, C.-J. Chen, and G. van Kriekinge. Cost-Effectiveness Analysis of the Bivalent Compared with the Quadrivalent Human Papillomavirus Vaccines in Taiwan. *Value in Health*, 15(5):622–631, 2012.

[116] N. Demarteau, G. van Kriekinge, and P. Simon. Incremental Cost-Effectiveness Evaluation of Vaccinating Girls against Cervical Cancer Pre- and Post- Sexual Debut in Belgium. *Vaccine*, 31(37):3962–3971, 2013.

[117] S. Dias, N. Welton, A. Sutton, and A. Ades. NICE DSU Technical Support Document 1: Introduction To Evidence Synthesis For Decision Making, 2011. Available from *http://www.nicedsu.org.uk/TSD1%20Introduction.final.08.05.12.pdf*, last accessed 18/03/2017.

[118] S. Dias, N. Welton, A. Sutton, and A.E. Ades. Evidence Synthesis Technical Support Document Series, 2011. Available from *http://www.nicedsu.org.uk/evidence-synthesis-tsd-series(2391675).htm*, last accessed 18/03/2017.

[119] M. Diaz, S. de Sanjosé, J. Orthendahl, M. O'Shea, S. Goldie, F. Bosch, and J. Kim. Cost-effectiveness of Human Papillomavirus Vaccination and Screening in Spain. *European Journal of Cancer*, 46(16):2973–2985, 2010.

[120] M. Diaz, J. Kim, G. Albero, S. de Sanjosé, G. Clifford, F. Bosch, and S. Goldie. Health and Economic Impact of HPV 16 and 18 Vaccination and Cervical Cancer Screening in India. *British Journal of Cancer*, 99(2):230–238, 2008.

[121] MGL. d'Ottaviano Morelli, L. Zeferino, GJ. Cecatti, DR. Terrabuio, and EZ. Martinez. Prevalence of cervical intraepithelial neoplasia and invasive carcinoma based on cytological screening in the region of Campinas, Sao Paulo, Brazil. *Cadernos de Saúde Pública*, 20(1):153–159, 2004.

[122] M. Drolet, M.-C. Boily, N. van de Velde, E. Franco, and M. Brisson. Vaccinating Girls and Boys with Different Human Papillomavirus Vaccines: Can It Optimise Population-Level Effectiveness? *PLoS ONE*, 8(6), 2013.

[123] M. Drolet, M. Brisson, E. Maunsell, E.L. Franco, F. Coutlée, A. Ferenczy, W. Fisher, and J.A. Mansi. The psychosocial impact of an abnormal cervical smear result. *Psycho-Oncology*, 21(10):1071–1081, 2012.

[124] M. Drolet, M. Brisson, E. Maunsell, E.L. Franco, F. Coutlée, A. Ferenczy, S. Ratnam, W. Fisher, and J.A. Mansi. The Impact of Anogenital Warts on Health-Related Quality of Life: A 6-Month Prospective Study. *Sexually Transmitted Diseases*, 38(10):949–956, 2011.

[125] M. Drolet, J.-F. Laprise, M.-C. Boily, E. Franco, and M. Brisson. Potential cost-effectiveness of the nonavalent human papillomavirus (HPV) vaccine. *International Journal of Cancer*, 134(9):2264–2268, 2013.

[126] P. Dulguerov, M. Jacobsen, A. Allal, W. Lehmann, and T. Calcaterra. Nasal and Paranasal Sinus Carcinoma: Are We Making Progress? A Series of 220 Patients and a Systematic Review. *Cancer*, 92(12):3012–29, 2001.

[127] E. Dunne and L. Markowitz. Genital Human Papillomavirus Infection. *Clinical Infectious Disease*, 43(5):624–629, 2006.

[128] R. Durrett. *Essentials of stochastic processes*. Springer, New York, USA, 2004.

[129] J. Edmunds, G. Medley, and D. Nokes. Evaluating The Cost-Effectiveness Of Vaccination Programmes: A Dynamic Perspective. *Statistics in Medicine*, 18(23):3263–3282, 1999.

[130] A. El Hasnaoui, N. Demarteau, D. Granados, B. Standaert, and B. Detournay. Public Health Impact of Human Papillomavirus Vaccination on Prevention of Cervical Cancer in France. *International Journal of Public Health*, 57(1):149–158, 2012.

[131] EH. Elbasha and EJ. Dasbach. Impact of Vaccinating Boys and Men against HPV in the United States. *Vaccine*, 28(42):6858–6867, 2010.

[132] EH. Elbasha, EJ. Dasbach, and RP. Insinga. Model for Assessing Human Papillomavirus Vaccination Strategies. *Emerging Infectious Diseases*, 13(1):28–41, 2007.

[133] EH. Elbasha, EJ. Dasbach, and RP. Insinga. A Multi-Type HPV Transmission Model. *Bulletin of Mathematical Biology*, 70(8):2126–2176, 2008.

[134] E.H. Elbasha, E.J. Dasbach, R.P. Insinga, R.M. Haupt, and E. Barr. Age-Based Programs for Vaccination against HPV. *Value in Health*, 12(5):697–707, 2009.

[135] G. Fattore, G. Aguzzi, and G. Baio. AIES (Associazione Italiana di Economia Sanitaria) Proposta di Linee-Guida per la valutazione economica degli interventi sanitari, 2009.

[136] G. Favato, G. Baio, A. Capone, A. Marcellusi, S. Costa, G. Garganese, M. Picardo, M. Drummond, B. Jonsson, G. Scambia, P. Zweifel, and F. Mennini. Novel Health Economic Evaluation of a Vaccination Strategy to Prevent HPV-related Diseases: The BEST Study. *Medical Care*, 50(12):1076–1085, 2012.

[137] M. Ferguson. Optimal Management when Unsuspected N2 Nodal Disease is Identified during Thoracotomy for Lung Cancer: Cost-Effectiveness Analysis. *The Journal of Thoracic and Cardiovascular Surgery*, 126(6):1935–1942, 2003.

[138] J. Ferlay, F. Bray, P. Pisani, and DM. Parkin. Globocan 2002: Cancer Incidence, Mortality and Prevalence Worldwide. Descriptive Epidemiology Group of International Agency for Research on Cancer (IARC). Release September 16, 2005. Website of the IARC: *http://www-dep.iarc.fr*, last accessed: 18/03/2017.

[139] G. Ferrandina, A. Marcellusi, FS. Mennini, M. Petrillo, C. Di Falco, and G. Scambia. Hospital Costs Incurred by the Italian National Health Service for Invasive Cervical Cancer. *Gynecological Oncology*, 119(2):243–249, 2010.

[140] Danish Centre for Health Technology Assessment (DACEHTA). Reduction in the Risk of Cervical Cancer by Vaccination against Human Papillomavirus (HPV) - a Health Technology Assessment. Health Technology Assessment, 2007. Available at: *http://www.sst.dk/publ/Publ2007/MTV/HPV/HPV_vaccination_en.pdf*, last accessed: 18/03/2017.

[141] M. Forrester and A. Pettitt. Use of Stochastic Epidemic Modeling to Quantify Transmission Rates of Colonization With Methicillin-Resistant Staphylococcus aureus in an Intensive Care Unit. *Infection Control and Hospital Epidemiology*, 26(7):598–606, 2005.

[142] S. Franceschi. HPV e Prevenzione. Gruppo Italiano Screening del Cervicocarcinoma, National Congress; Rome, April 20-21, 2006. Available from *http://www.gisci.it/documenti/convegni/roma2006/franceschi_roma.pdf*, last accessed: 18/03/2017.

[143] KM. French, RV. Barnabas, M. Lehtinen, O. Kontula, E. Pukkala, J. Dillner, and GP. Garnett. Strategies for the Introduction of Human Papillomavirus Vaccination: Modelling the Optimum Age- and Sex-Specific Pattern of Vaccination in Finland. *British Journal of Cancer*, 96(3):514–518, 2007.

[144] L. French and J. Nashelsky. Clinical Inquiries. What is the Most Effective Treatment for External Genital Warts? *The Journal of Family Practice*, 51(4):313, 2002.

[145] M. Frisch, E. Smith, A. Grulich, and C. Johansen. Cancer in a Population-based Cohort of Men and Women in Registered Homosexual Partnerships. *American Journal of Epidemiology*, 157(11):966–972, 2003.

[146] A. Gafni. The standard gamble method: what is being measured and how it is interpreted. *Health Services Research*, 29(2):207–224, 1994.

[147] S. Garland, M. Hernandez-Avila, C. Wheeler, G. Perez, D. Harper, S. Leodolter, G. Tang, D. Ferris, M. Steben, J. Bryan, F. Taddeo, R. Railkar, M. Esser, H. Sings, M. Nelson, J. Boslego, C. Sattler, E. Barr, and L. Koutsky. Quadrivalent Vaccine against Human Papillomavirus to Prevent Anogenital Diseases. *The New England Journal of Medicine*, 356(19):1928–1943, 2007.

[148] S. Garland, M. Hernandez-Avila, C. Wheeler, G. Perez, D. Harper, S. Leodolter, G. Tang, D. Ferris, M. Steben, J. Bryan, F. Taddeo,

R. Railkar, M. Esser, H. Sings, M. Nelson, J. Boslego, C. Sattler, E. Barr, L. Koutsky, and The Future I Study Group. Quadrivalent Vaccine against Human Papillomavirus to Prevent Anogenital Diseases. *The New England Journal of Medicine*, 356(19), 2007.

[149] S. Garland, R. Insinga, H. Sings, F. Palazzo, G. Furnari, S. Valle, N. Largeron, and A. Federici. Human Papillomavirus Infections and Vulvar Disease Development. *Cancer Epidemiology, Biomarkers & Prevention*, 18(6):1777–1784, 2009.

[150] GP. Garnett, JJ. Kim, K. French, and SJ. Goldie. Chapter 21: Modelling the Impact of HPV Vaccines on Cervical Cancer and Screening Programmes. *Vaccine*, 24(S3):178–186, 2006.

[151] A. Gelman, JB. Carlin, HS. Stern, and DB. Rubin. *Bayesian Data Analysis.* Chapman&Hall/CRC, London, UK, 2004.

[152] S. Geman and D. Geman. Stochastic Relaxation, Gibbs Distributions, and the Bayesian Restoration of Images. *IEEE Transactions on Pattern Analysis and Machine Intelligence*, 6(6):721–741, 1984.

[153] Georgalis. Present and future of cervical cancer prevention in Spain: a cost-effectiveness analysis. *European Journal of Cancer Prevention*, 25(5):430–439, 2015.

[154] E. George. Lecture I. A Gentle Introduction to Markov Chain Monte Carlo (MCMC), 2005. Available from *http://statwww.epfl.ch/teaching/3eCycleRomand/printemps-2005/EG.lectures.villars05.pdf*, last accessed 18/03/2017.

[155] G.J. Gibson and E.J. Austin. Fitting and testing spatio-temporal stochastic models with application in plant epidemiology. *Plant Pathology*, 45(2):172–184, 1996.

[156] G.J. Gibson and E. Renshaw. Likelihood estimation for stochastic compartmental models using Markov chain methods. *Statistics and Computing*, 11(4):347–358, 2001.

[157] P. Giorgi Rossi, G. Esposito, S. Brezzi, A. Brachini, P. Raggi, and A. Federici. Estimation of Pap-Test Coverage in an Area with an Organised Screening Program: Challenges for Survey Methods. *BioMed Central Health Services Research*, pages 6–36, 2006.

[158] P. Giorgi Rossi, A. Ricciardi, C. Cohet, F. Palazzo, G. Furnari, S. Valle, N. Largeron, and A. Federici. Epidemiology and Costs of Cervical Cancer Screening and Cervical Dysplasia in Italy. *BioMed Central Public Health*, 9, 2009.

[159] J. Goldhaber-Fiebert, N. Stout, J. Ortendahl, K. Kuntz, S. Goldie, and J. Salomon. Modeling Human Papillomavirus and Cervical Cancer in the United States for Analyses of Screening and Vaccination. *Population Health Metrics*, 5:11, 2007.

[160] J. Goldhaber-Fiebert, N. Stout, J. Salomon, K. Kuntz, and S. Goldie. Cost-Effectiveness of Cervical Cancer Screening With Human Papillomavirus DNA Testing and HPV-16,18 Vaccination. *Journal of the National Cancer Institute*, 100(5):308–320, 2008.

[161] S. Goldie, M. Diaz, D. Constenla, N. Alvis, J.K. Andrus, and S.-Y. Kim. Mathematical Models of Cervical Cancer Prevention in Latin America and the Caribbean. *Vaccine*, 26(Suppl 11):L59–L72, 2008.

[162] S. Goldie, D. Grima, M. Kohli, T. Wright, M. Weinstein, and E. Franco. A Comprehensive Natural History Model of HPV Infection and Cervical Cancer to Estimate the Clinical Impact of a Prophylactic HPV-16/18 Vaccine. *International Journal of Cancer*, 106(6):896–904, 2003.

[163] S. Goldie, J. Kim, K. Kobus, J. Goldhaber-Fiebert, J. Salomon, M. O'Shea, F. Bosch, S. de Sanjosé, and E. Franco. Cost-Effectiveness of HPV 16, 18 Vaccination in Brazil. *Vaccine*, 25(33):6257–6270, 2007.

[164] S. Goldie, M. Kohli, D. Grima, M. Weinstein, T. Wright, F. Bosch, and E. Franco. Projected Clinical Benefits and Cost-Effectiveness of a Human Papillomavirus 16/18 Vaccine. *Journal of the National Cancer Institute*, 96(8):604–615, 2004.

[165] S. Goldie, K. Kuntz, M. Weinstein, K. Freedberg, and J. Palefsky. Cost-Effectiveness of Screening for Anal Squamous Intraepithelial Lesions and Anal Cancer in Human Immunodeficiency Virusnegative Homosexual and Bisexual Men. *American Journal of Medicine*, 108(8):634–641, 2000.

[166] S. Goldie, C. Levin, N.R. Mosqueira-Lovón, J. Ortendahl, J. Kim, M. O'Shea, M.D. Sanchez, and M.A. Mendoza Araujo. Health and Economic Impact of Human Papillomavirus 16 and 18 Vaccination of Preadolescent Girls and Cervical Cancer Screening of Adult Women in Peru. *Revista Panamericana de Salud Pública*, 32(6):426–434, 2012.

[167] S. Goldie, M. O'Shea, M. Diaz, and S.-Y. Kim. Benefits, Cost Requirements and Cost-Effectiveness of the HPV 16,18 Vaccine for Cervical Cancer Prevention in Developing Countries: Policy Implications. *Reproductive Health Matters*, 16(32):86–96, 2008.

[168] S. Goldie, M. O'Shea, N. Gastineau Campos, M. Diaz, S. Sweet, and S.-Y. Kim. Health and Economic Outcomes of HPV 16,18 Vaccination in 72 GAVI-Eligible Countries. *Vaccine*, 26(32):4080–4093, 2008.

[169] J. Gomez, A. Lepetic, and N. Demarteau. Health economic analysis of human papillomavirus vaccines in women of Chile: perspective of

the health care payer using a Markov model. *BioMed Central Public Health*, 14:1222, 2014.

[170] A. Goubar and AE. Ades. Estimates of human immunodeficiency virus prevalence and proportion diagnosed based on Bayesian multiparameter synthesis of surveillance data. *Journal of the Royal Statistical Society*, 171(3):541–580, 2008.

[171] NM. Graafland, RHA. Verhoeven, J.-W. Coebergh, and S. Horenblas. Incidence Trends and Survival of Penile Squamous Cell Carcinoma in The Netherlands. *International Journal of Cancer*, 128(2):426–432, 2011.

[172] D. Graham, W. Isaranuwatchai, M. Habbous, C. de Oliveira, G. Liu, L. Siu, and J. Hoch. A Cost-Effectiveness Analysis of Human Papillomavirus Vaccination of Boys for the Prevention of Oropharyngeal Cancer. *Cancer*, 121(11):1785–1792, 2015.

[173] D. Graham, W. Isaranuwatchai, S. Habbous, C. de Oliveira, G. Liu, L. Siu, and J. Hoch. A Cost-Effectiveness Analysis of Human Papillomavirus Vaccination of Boys for the Prevention of Oropharyngeal Cancer. *Cancer*, 121(11):1785–1792, 2015.

[174] J. Green, A. Berrington de Gonzalez, S. Sweetland, V. Beral, C. Chilvers, B. Crossley, J. Deacon, C. Hermon, P. Jha, D. Mant, J. Peto, M. Pike, and M.P. Vessey. Risk factors for adenocarcinoma and squamous cell carcinoma of the cervix in women aged 20–44 years: the UK National Case – Control Study of Cervical Cancer. *British Journal of Cancer*, 89(11):2078–2086, 2003.

[175] G. Grimmett and D. Stirzaker. *Probability and Random Processes*. Oxford University Press, Oxford, United Kingdom, 2001.

[176] L. Gustafsson and M. Sternad. When can a deterministic model of a population system reveal what will happen on average? *Mathematical Biosciences*, 243(1):28–45, 2013.

[177] J. Habbema, G. van Oortmarssen, J. Lubbe, and P. van der Maas. The MISCAN Simulation Program for the Evaluation of Screening for Disease. *Computer Methods and Programs in Biomedicine*, 20(1):79–93, 1985.

[178] K. Haeussler, A. Marcellusi, FS. Mennini, G. Favato, M. Picardo, G. Garganese, M. Bononi, S. Costa, G. Scambia, P. Zweifel, A. Capone, and G. Baio. Cost-Effectiveness Analysis of Universal Human Papillomavirus Vaccination Using a Dynamic Bayesian Methodology: The BEST II Study. *Value in Health*, 18(8):956–968, 2015.

[179] M. Hampl, E. Huppertz, O. Schulz-Holstege, P. Kok, and S. Schmitter. Economic Burden of Vulvar and Vaginal Intraepithelial Neoplasia: Retrospective Cost Study at a German Dysplasia Centre. *BioMed Central Infectious Diseases*, 11:73, 2011.

[180] K.-T. Han, S. Kim, S. Lee, and E.-C. Park. Cost-Effectiveness Analysis of HPV Vaccination: Comparing the General Population with Socially Vulnerable Individuals. *Asian Pacific Journal of Cancer Prevention*, 15(19):8503–8508, 2014.

[181] W.K. Hastings. Monte Carlo Sampling Methods Using Markov Chains and Their Applications. *Biometrika*, 57(1):97–109, 1970.

[182] D. He, E. Ionides, and A. King. Plug-and-play inference for disease dynamics: measles in large and small populations as a case study. *Journal of The Royal Society Interface*, 7(43):271–283, 2010.

[183] P. Hillemanns, K.U. Petry, N. Largeron, R. McAllister, K. Tolley, and K. Büsch. Cost-Effectiveness of a Tetravalent Human Papillomavirus Vaccine in Germany. *Journal of Public Health*, 17:77, 2009.

[184] J. Holmes, E. Dierks, L. Homer, and B. Potter. Is Detection of Oral and Oropharyngeal Squamous Cancer by a Dental Health Care Provider Associated With a Lower Stage at Diagnosis? *Journal of Oral and Maxillofacial Surgery*, 61(3):285–291, 2003.

[185] J. Horn, O. Damm, M.E.E. Kretzschmar, Y. Delere, O. Wichmann, A.M. Kaufmann, E. Garbe, A. Krämer, W. Greiner, and R.T. Mikolajczyk. Estimating the Long-term Effects of HPV Vaccination in Germany. *Vaccine*, 31(19):2372–2380, 2013.

[186] HSCIC. Cervical Screening Programme, England 2012–2013. Available from *http://www.hscic.gov.uk/searchcatalogue?productid=12601*, last accessed 18/03/2017.

[187] JP. Hughes, GP. Garnett, and L. Koutsky. The Theoretical Population-Level Impact of a Prophylactic Human Papilloma Virus Vaccine. *Epidemiology*, 13(6):631–639, 2002.

[188] R. Insinga, E. Dasbach, E. Elbasha, A. Puig, and L. Reynales-Shigematsu. Cost-Effectiveness of Quadrivalent Human Papillomavirus (HPV) Vaccination in Mexico: A Transmission Dynamic Model-Based Evaluation. *Vaccine*, 26(1):128–139, 2007.

[189] RP. Insinga, X. Ye, PK. Singhal, and GW. Carides. Healthcare Resource Use and Costs Associated with Cervical, Vaginal and Vulvar Cancers in a Large U.S. Health Plan. *Gynecologic Oncology*, 111(2):188–196, 2008.

[190] E. Ionides, C. Bretó, and A. King. Inference for non-linear dynamical systems. *Proceedings of the National Academy of Sciences of the United States of America*, 103(49):18438–18443, 2006.

[191] V. Isham. Assessing the Variability of Stochastic Epidemics. *Mathematical Biosciences*, 107(2):209–224, 1991.

[192] ISPOR. ISPOR Pharmacoeconomics guidelines, 2012. Available from *http://www.ispor.org/peguidelines/index.asp*, last accessed 18/03/2017.

[193] ISS. Stato di Avanzamento della Campagna Vaccinale per HPV Dati di Copertura, 2012. Full text available from the ISS website: *http://www.epicentro.iss.it/problemi/hpv/pdf/Aggiornamento_HPV_30062012_validato.pdf*, last accessed 18/03/2017.

[194] ISTAT. I Determinanti del Ricorso Allo Screening dei Tumori Femminili. Informazione Statistica e Politiche per la Promozione Della Salute - Atti del Convegno di Roma, 2002. Available from *http://www.istat.it/dati/catalogo/20041201_01/Atti_del_convegno_salute.pdf*, last accessed 18/03/2017.

[195] ISTAT. La Prevenzione dei Tumori Femminili in Italia; il Ricorso a Pap Test e Mammografia: anni 2004-2005, 2006. Available from *http://www.istat.it/salastampa/comunicati/non_calendario/20061204_00/testointegrale.pdf*, last accessed 18/03/2017.

[196] S. Jackman. *Bayesian Analysis for the Social Sciences*. John Wiley and Sons, New York, NY, 2009.

[197] WI. Jang, H.-G. Wu, SW. Ha, HJ. Kim, SB. Kang, YS. Song, N.-H. Park, and JW. Kim. Definitive Radiotherapy for Treatment of Primary Vaginal Cancer. Effectiveness and Prognostic Factors. *International Journal of Gynecological Cancer*, 22(3):521–527, 2012.

[198] JCVI. Joint Committee on Vaccination and Immunisation. Code of Practice, 2013. Available from *https://www.gov.uk/government/uploads/system/uploads/attachment_data/file/224864/JCVI_Code_of_Practice_revision_2013_-_final.pdf*, last accessed 18/03/2017.

[199] S. Jenness. Package `EpiModel`, 2015. Available from *https://cran.r-project.org/web/packages/EpiModel/EpiModel.pdf*, last accessed 18/03/2017.

[200] Y. Jiang, A. Gauthier, M. Postma, L. Ribassin-Majed, N. Largeron, and X. Bresse. A Critical Review of Cost-Effectiveness Analyses of Vaccinating Males against Human Papillomavirus. *Human Vaccines & Immunotherapeutics*, 9(11):2285–2295, 2013.

[201] M. Jit, M. Brisson, J.-F. Laprise, and Y. Choi. Comparison of two dose and three dose human papillomavirus vaccine schedules: cost effectiveness analysis based on transmission model. *British Medical Journal*, 350(g7584), 2015.

[202] M. Jit, M. Brisson, A. Portnoy, and R. Hutubessy. Cost-effectiveness of female human papillomavirus vaccination in 179 countries: a PRIME modelling study. *The Lancet Global Health*, 2(7):e406–414, 2014.

[203] M. Jit, R. Chapman, O. Hughes, and Y. Choi. Comparing Bivalent and Quadrivalent Human Papillomavirus Vaccines: Economic Evaluation Based on Transmission Model. *British Medical Journal*, 343:d5775, 2011.

[204] M. Jit, Y. Choi, and W. Edmunds. Economic Evaluation of Human Papillomavirus Vaccination in the United Kingdom. *British Medical Journal*, 337:a769, 2008.

[205] M. Jit, N. Gay, K. Soldan, YH. Choi, and W. Edmunds. Estimating Progression Rates for Human Papillomavirus Infection from Epidemiological Data. *Medical Decision Making*, 30(1):84–98, 2010.

[206] AM. Johnson, CH. Mercer, B. Erens, AJ. Copas, S. McManus, K. Wellings, KA. Fenton, C. Korovessis, W. Macdowall, K. Nanchahal, S. Purdon, and J. Field. Sexual Behaviour in Britain: Partnerships, Practices, and HIV Risk Behaviours. *The Lancet*, 358:1835–1842, 2001.

[207] R. Jones, D. Rowan, and A. Stewart. Vulvar Intraepithelial Neoplasia. Aspects of the Natural History and Outcome in 405 Women. *Obstetrics & Gynecology*, 106(6):1319–1326, 2005.

[208] L. Joseph, T. Gyorkos, and L. Coupal. Bayesian Estimation of Disease Prevalence and the Parameters of Diagnostic Tests in the Absence of a Gold Standard. *American Journal of Epidemiology*, 141(3):263–272, 1995.

[209] J. Karnon, C. Czoski-Murray, K. Smith, and C. Brand. A Hybrid Cohort Individual Sampling Natural History Model of Age-Related Macular Degeneration: Assessing the Cost-Effectiveness of Screening Using Probabilistic Calibration. *Medical Decision Making*, 29(3):304–316, 2009.

[210] J. Karnon, R. Jones, C. Czoski-Murray, and K. Smith. Cost-Utility Analysis of Screening High-Risk Groups for Anal Cancer. *Journal of Public Health*, 30(3):293–304, 2008.

[211] K. Kawai, T. Tannus Branco de Araujo, M. Fonseca, M. Pillsbury, and P. Singhal. Estimated Health and Economic Impact of Quadrivalent HPV (Types 6/11/16/18) Vaccination in Brazil Using a Transmission Dynamic Model. *BioMed Central Infectious Diseases*, 12(250), 2012.

[212] M. Keeling and J. Ross. On methods for studying stochastic disease dynamics. *Journal of the Royal Society Interface*, 5(19):171–181, 2008.

[213] M. Khatibi, H. Rasekh, Z. Shahverdi, and H. Jamshidi. Cost-Effectiveness Evaluation of Quadrivalent Human Papilloma Virus Vaccine for HPV-Related Disease in Iran. *Iranian Journal of Pharmaceutical Research*, 13(Suppl):225–234, 2014.

[214] S. Kiatpongsan and J. Kim. Costs and Cost-Effectiveness of 9-Valent Human Papillomavirus (HPV) Vaccination in Two East African Countries. *PLoS ONE*, 9(9), 2014.

[215] J. Kim, B. Andres-Beck, and S. Goldie. The Value of Including Boys in an HPV Vaccination Programme: a Cost-Effectiveness Analysis in a Low-Resource Setting. *British Medical Journal*, 97(9):1322–1328, 2007.

[216] J. Kim, N. Campos, M. O'Shea, M. Diaz, and I. Mutyaba. Model-Based Impact and Cost-Effectiveness of Cervical Cancer Prevention in Sub-Saharan Africa. *Vaccine*, 31(Suppl 5):F60–F72, 2013.

[217] J. Kim and S. Goldie. Health and Economic Implications of HPV Vaccination in the United States. *The New England Journal of Medicine*, 359(8):821–832, 2008.

[218] J. Kim and S. Goldie. Cost-Effectiveness Analysis of Including Boys in a Human Papillomavirus Vaccination Programme in the United States. *British Medical Journal*, 339:b3884, 2009.

[219] J. Kim, K. Kobus, M. Diaz, M. O'Shea, H. van Minh, and S. Goldie. Exploring the Cost-Effectiveness of HPV Vaccination in Vietnam: Insights for Evidence-Based Cervical Cancer Prevention Policy. *Vaccine*, 26(32):4015–4024, 2008.

[220] J. Kim, K. Kuntz, N. Stout, S. Mahmud, L. Villa, E. Franco, and S. Goldie. Multiparameter Calibration of a Natural History Model of Cervical Cancer. *American Journal of Epidemiology*, 166(2):137–150, 2007.

[221] J. Kim, J. Ortendahl, and S. Goldie. Cost-Effectiveness of Human Papillomavirus Vaccination and Cervical Cancer Screening in Women Older Than 30 Years in the United States. *Annals of Internal Medicine*, 151(8):538–545, 2009.

[222] J. Kim, M. Sharma, M. O'Shea, S. Sweet, M. Diaz, H. Sancho-Garnier, and M. Seoud. Model-Based Impact and Cost-Effectiveness of Cervical Cancer Prevention in the Extended Middle East and North Africa (EMENA). *Vaccine*, 31(Suppl 6):G65–G77, 2013.

[223] A. King, E. Ionides, M. Pascual, and M. Bouma. Inapparent infections and cholera dynamics. *Nature*, 454(7206):877–880, 2008.

[224] A. King, D. Nguyen, and E. Ionides. Statistical Inference for Partially Observed Markov Processes via the `R` Package `pomp`. *Journal of Statistical Software*, 69(12), 2016.

[225] M. Kohli, N. Ferko, A. Martin, E. Franco, D. Jenkins, S. Gallivan, C. Sherlaw-Johnson, and M. Drummond. Estimating the Long-term Impact of a Prophylactic Human Papillomavirus 16/18 Vaccine on the Burden of Cervical Cancer in the UK. *British Journal of Cancer*, 96:143–150, 2007.

[226] M. Kohli, D. Lawrence, J. Haig, A. Anonychuk, and N. Demarteau. Modeling the Impact of the Difference in Cross-Protection Data Between a Human Papillomavirus (HPV)-16/18 AS04-Adjuvanted Vaccine and a Human Papillomavirus (HPV)-6/11/16/18 Vaccine in Canada. *BioMed Central Public Health*, 12(1), 2012.

[227] R. König. Deterministic and stochastic parameters in inertial survey adjustment. *Bulletin géodésique*, 64(2):111–125, 1990.

[228] R. Konno, T. Sasagawa, T. Fukuda, G. van Kriekinge, and N. Demarteau. Cost-Effectiveness Analysis of Prophylactic Cervical Cancer Vaccination in Japanese Women. *International Journal of Gynecological Cancer*, 20(3):385–392, 2010.

[229] IA. Korostil, GW. Peters, J. Cornebise, and DG. Regan. Adaptive Markov Chain Monte Carlo Forward Projection for Statistical Analysis in Epidemic Modelling of Human Papillomavirus. *Statistics in Medicine*, 32(11):1917–1953, 2012.

[230] T. Koulis, J. Ramsay, and D. Levitin. From Zero to Sixty: Calibrating Real-Time Responses. *Psychometrika*, 73(2):321–339, 2008.

[231] S. Kulasingam, S. Benard, R. Barnabas, N. Largeron, and E. Myers. Adding a Quadrivalent Human Papillomavirus Vaccine to the UK Cervical Cancer Screening Programme: A Cost-Effectiveness Analysis. *Cost Effectiveness and Resource Allocation*, 6(4), 2008.

[232] S. Kulasingam and E. Myers. Potential Health and Economic Impact of Adding a Human Papillomavirus Vaccine to Screening Programs. *Journal of the American Medical Association*, 290(6):781–789, 2003.

[233] G. La Torre. Revisione Sistematica e Meta-Analisi dei Trial Clinici Sull'Efficacia del Vaccino Quadrivalente Anti-HPV. Report HTA del Vaccino Quadrivalente Anti-HPV Gardasil. *Italian Journal of Public Health*, 2(Suppl.2):S25–S32, 2009. Available from *http://www.ijph.it/pdf//22/25.pdf*, last accessed 08/04/2016.

[234] G. La Torre, C. de Waure, G. Chiaradia, A. Mannocci, S. Capri, and W. Ricciardi. The Health Technology Assessment of Bivalent HPV Vaccine Cervarix ® in Italy. *Vaccine*, 28(19):3379–3384, 2010.

[235] P. Lam, APW. Yuen, CM. Ho, WK. Ho, and WI. Wei. Prospective Randomized Study of Post-Operative Chemotherapy with Levamisole and UFT for Head and Neck Carcinoma. *European Journal of Surgical Oncology*, 27(8):750–753, 2001.

[236] J.-F. Laprise, M. Drolet, M.-C. Boily, M. Jit, C. Sauvageau, E. Franco, P. Lemieux-Mellouki, T. Malagon, and M. Brisson. Comparing the cost-effectiveness of two- and three-dose schedules of human papillomavirus vaccination: A transmission-dynamic modelling study. *Vaccine*, 32(44):5845–5853, 2014.

[237] P. Laramée, A. Millier, T.-H. Brodtkorb, N. Rahhali, O. Cristeau, S. Aballéa, S. Montgomery, S. Steeves, M. Toumi, and J. Rehm. A Comparison of Markov and Discrete-Time Microsimulation Approaches: Simulating the Avoidance of Alcohol-Attributable Harmful Events from Reduction of Alcohol Consumption Through Treatment of Alcohol Dependence. *Clinical Drug Investigation*, 36(11):945–956, 2016.

[238] G. Lazenby, E. Unal, A. Andrews, and K. Simpson. A Cost-Effectiveness Analysis of Anal Cancer Screening in HIV-Positive Women. *Journal of Lower Genital Tract Disease*, 16(3):275–280, 2012.

[239] Q. Le. Structural Uncertainty of Markov Models for Advanced Breast Cancer: A Simulation Study of Lapatinib. *Medical Decision Making*, 36(5):629–640, 2016.

[240] S. Lee and A. Tameru. A Mathematical Model of Human Papillomavirus (HPV) in the United States and its Impact on Cervical Cancer. *Journal of Cancer*, 3:262–268, 2012.

[241] V. Lee, S.K. Tay, Y.L. Teoh, and M.Y. Tok. Cost-Effectiveness of Different Human Papillomavirus Vaccines in Singapore. *BioMed Central Public Health*, 11:203, 2011.

[242] A. Lenzi, V. Mirone, V. Gentile, R. Bartoletti, V. Ficarra, C. Foresta, L. Mariani, S. Mazzoli, SG. Parisi, A. Perino, M. Picardo, and CM. Zotti. Rome Consensus Conference - Statement; Human Papilloma Virus Diseases in Males. *BioMed Central Public Health*, 13:117, 2013.

[243] C. Levin, M. Sharma, Z. Olson, S. Verguet, J.-F. Shi, S.-M. Wang, Y.-L. Qiao, D. Jamison, and J. Kim. An extended cost-effectiveness analysis of publicly financed HPV vaccination to prevent cervical cancer in China. *Vaccine*, 33(24):2830–2841, 2015.

[244] W.A. Leyden, M.M. Manos, A.M. Geiger, S. Weinmann, J. Mouchawar, K. Bischoff, M.U. Yood, J. Gilbert, and S.H. Taplin. Cervical Cancer in Women with Comprehensive Health Care Access: Attributable Factors in the Screening Process. *Journal of the National Cancer Institute*, 97(9):675–683, 2005.

[245] P.-H. Liu, F.-C. Hu, P.-I. Lee, S.-N. Chow, C.-W. Huang, and J.-D. Wang. Cost-Effectiveness of Human Papillomavirus Vaccination for Prevention of Cervical Cancer in Taiwan. *BioMed Central Health Services Research*, 10:11, 2010.

[246] J. Lord and MA. Asante. Estimating uncertainty ranges for costs by the bootstrap procedure combined with probabilistic sensitivity analysis. *Health Economics*, 8(4):323–333, 1999.

[247] D. Lunn. WinBUGS Differential Interface (WBDiff), 2004. Available from *http://winbugs-development.mrc-bsu.cam.ac.uk/wbdiff.html*, last accessed 18/03/2017.

[248] J. Luttjeboer, T. Westra, J. Wilschut, H. Nijman, T. Daemen, and M. Postma. Cost-Effectiveness of the Prophylactic HPV vaccine: An Application to The Netherlands Taking Non-Cervical Cancers and Cross-protection into Account. *Vaccine*, 31(37), 2013.

[249] A. Marcellusi, A. Capone, G. Favato, FS. Mennini, G. Baio, K. Haeussler, M. Bononi, A. Crocetti, A. De Cesare, M. Miccini, P. Sapienza, C. Da Mosto, C. Boscolo Rizzo, M. Stellin, R. Fuson, G. Palamara, M. Giuliani, M. Picardo, D. Panatto, P. Cristoforoni, R. De Vincenzo, E. Di Capua, G. Ferrandina, M. Petrillo, T. Sasso, C. Ricci, N. Trivellizzi, R. Gasparini, and G. Scambia. Health Utilities Loss with HPV-Induced Diseases in Men and Women: the HPV Italian Collaborative Study Group. *BioMed Central Infectious Diseases*, 37(1):156–167, 2013.

[250] T. Marfing, M. Abel, and D. Gallagher. Perianal Bowen's Disease and Associated Malignancies. Results of a Survey. *Diseases of the Colon & Rectum*, 30(10):782–785, 1987.

[251] M. Marks, P. Gravitt, S. Gupta, K.-L. Liaw, A. Tadesse, E. Kim, C. Phongnarisorn, V. Wootipoom, P. Yuenyao, C. Vipupinyo, S. Sriplienchan, and D. Celentano. Combined Oral Contraceptive Use Increases HPV Persistence but Not New HPV Detection in a Cohort of Women From Thailand. *The Journal of Infectious Diseases*, 204(10):1505–1513, 2011.

[252] F. Marra, K. Cloutier, B. Oteng, C. Marra, and G. Ogilvie. Effectiveness and Cost Effectiveness of Human Papillomavirus Vaccine: A Systematic Review. *Pharmacoeconomics*, 27(2):127–147, 1999.

[253] F. Marra, G. Ogilvie, L. Colley, E. Kliewer, and CA. Marra. Epidemiology and costs associated with genital warts in Canada. *Sexually Transmitted Infections*, 85(2):111–115, 2009.

[254] K. Marsh, R. Chapman, R. Baggaley, N. Largeron, and X. Bresse. Mind the Gap: What's Missing from Current Economic Evaluations of Universal HPV Vaccination? *Vaccine*, 32(30):3732–3739, 2014.

[255] MD. McKay, WJ. Conover, and RJ. Beckman. A Comparison of Three Methods for Selecting Values of Input Variables in the Analysis of Output from a Computer Code. *Technometrics*, 21(2):239–245, 1979.

[256] F. Mennini, S. Costa, G. Favato, and M. Picardo. Anti-HPV vaccination: a review of recent economic data for Italy. *Vaccine*, 27 (Suppl. 1):A54–A61, 2009.

[257] F. Mennini, P. Giorgi Rossi, F. Palazzo, and N. Largeron. Health and Economic Impact Associated with a Quadrivalent HPV Vaccine in Italy. *Gynecologic Oncology*, 112(2):370–376, 2009.

[258] FS. Mennini, G. Baio, G. Montagano, G. Cauzillo, F. Locuratolo, G. Becce, L. Gitto, A. Marcellusi, P. Zweifel, A. Capone, and G. Favato. Governance of Preventive Health Intervention and On Time Verification of Its Efficiency: the GIOVE Study. *British Medical Journal Open*, 2(2):e000736, 2012.

[259] M. Merito, N. Largeron, C. Cohet, L. Timelli, F. Boselli, A. Matteelli, L. Naldi, and G. Vittori. Treatment Patterns and Associated Costs for Genital Warts in Italy. *Current Medical Research and Opinion*, 24(11):3175–3183, 2008.

[260] L. Minelli, F. Stracci, S. Prandini, IF. Moffa, and F. La Rosa. Gynaecological Cancers in Umbria (Italy): Trends of Incidence, Mortality and Survival, 1978-1998. *European Journal of Obstetrics & Gynecology and Reproductive Biology*, 115(1):59–65, 2004.

[261] S. Minhas, A. Mansek, S. Watya, and P. Hegarty. Penile Cancer-Prevention and Premalignant Conditions. *Urology*, 76(Suppl 2):S24–S35, 2010.

[262] C. Moler. Stiff Differential Equations. Technical Articles and Newsletters. MathWorks, 2003. Available from *https://www.mathworks.com/company/newsletters/articles/stiff-differential-equations.html*, last accessed 18/03/2017.

[263] E. Myers, D. McCrory, K. Nanda, L. Bastian, and D. Matchar. Mathematical Model for the Natural History of Human Papillomavirus Infection and Cervical Carcinogenesis. *American Journal of Epidemiology*, 151(12):1158–1171, 2000.

[264] D. Naimark, M. Bott, and M. Krahn. The Half-Cycle Correction Explained: Two Alternative Pedagogical Approaches. *Medical Decision Making*, 28(5):706–712, 2008.

[265] AS. Narayana, LE. Olney, SA. Loening, GW. Weimar, and DA. Culp. Carcinoma of the Penis. Analysis of 219 Cases. *Cancer*, 49(10):2185–2191, 1982.

[266] National Cancer Intelligence Network. Penile Cancer Report: Malignant and In-Situ Tumours. Urology SSCRG. Available from *www.ncin.org.uk/view?rid=2268*, last accessed 18/03/2017.

[267] National Cancer Intelligence Network. Rare Urological Cancers. Urological Cancers SSCRG. Available from *http://www.ncin.org.uk/view?rid=1718*, last accessed 18/03/2017.

[268] NICE. National Institute for Clinical Excellence. Guide to the Methods of Technology Appraisal. London: NICE, 2013. Available from *https://www.nice.org.uk/article/pmg9/resources/non-guidance-guide-*

to-the-methods-of-technology-appraisal-2013-pdf, last accessed 18/03/2017.

[269] J.R. Norris. *Markov Chains*. Cambridge University Press, Cambridge, United Kingdom, 1997.

[270] H. Novaes, P. Soarez, G. Silva, A. Ayres, A. Itria, C. Rama, A. Sartori, A. Clark, and S. Resch. Cost-effectiveness analysis of introducing universal human papillomavirus vaccination of girls aged 11 years into the National Immunization Program in Brazil. *Vaccine*, 33(Suppl 1):A135–A142, 2015.

[271] M. Nygard, BT. Hansen, J. Dillner, C. Munk, K. Oddsson, L. Tryggvadottir, M. Hortlund, KL. Liaw, EJ. Dasbach, and SK. Kjaer. Targeting human papillomavirus to reduce the burden of cervical, vulvar and vaginal cancer and pre-invasive neoplasia: establishing the baseline for surveillance. *PLoS One*, 9(2), 2014.

[272] J. Oakley and A. O'Hagan. Probabilistic sensitivity analysis of complex models: a Bayesian approach. *Journal of the Royal Statistical Society*, 66(3):751–769, 2004.

[273] M. Obradovic, A. Mrhar, and M. Kos. Cost-Effectiveness Analysis of HPV Vaccination alongside Cervical Cancer Screening Programme in Slovenia. *European Journal of Public Health*, 20(4):415–421, 2010.

[274] K. Oddsson, J. Johannsson, T. Laufey Asgeirdottir, and T. Gudnason. Cost-Effectiveness of Human Papillomavirus Vaccination in Iceland. *Acta Obstetricia et Gynecologica*, 88(12):1411–1416, 2009.

[275] AIRum: Italian Network of Cancer Registries Work Group. Italian Cancer Figures - Report 2006. Incidence, Mortality and Estimates. I Dati di Incidenza e Mortalità dei Registri Tumori Generali, 1998-2002. Epi-

demiol Prev, Suppl 2: 1-148, 2006. Available from *http://www.registri-tumori.it/cms/?q=Indice2006*, last accessed 18/03/2017.

[276] A. O'Hagan, J. Stevens, and J. Montmartin. Bayesian cost-effectiveness analysis from clinical trial data. *Statistics in Medicine*, 20(5):733–753, 2001.

[277] J. Olsen and MR. Jepsen. Human Papillomavirus Transmission and Cost-Effectiveness of Introducing Quadrivalent HPV Vaccination in Denmark. *International Journal of Technology Assesment in Health Care*, 26(2):183–191, 2010.

[278] J. Olsen and T. Jorgensen. Revisiting the cost-effectiveness of universal HPV-vaccination in Denmark accounting for all potentially vaccine preventable HPV-related diseases in males and females. *Cost Effectiveness and Resource Allocation*, 13:4, 2015.

[279] WA. Orenstein. Eradicating polio: how the world's pediatricians can help stop this crippling illness forever. *Pediatrics*, 135(1):196–202, 2015.

[280] World Health Organization. Cost effectiveness and strategic planning (WHO-CHOICE). Table: Threshold values for intervention cost-effectiveness by Region. Available from *http://www.who.int/choice/costs/CER_levels/en/*, last accessed 18/03/2017.

[281] World Health Organization. Making Choices in Health: WHO Guide to Cost-Effectiveness Analysis, 2003. Available from *http://www.who.int/choice/publications/p_2003_generalised_cea.pdf*, last accessed 18/03/2017.

[282] World Health Organization. Immunization, Vaccines and Biologicals, 2013. Available from *http://www.who.int/immunization/monitoring_surveillance/en/*, last accessed 18/03/2017.

[283] A. Oxman and G. Guyatt. A Consumer's Guide to Subgroup Analyses. *Annals of Internal Medicine*, 116(78–84):1, 1992.

[284] SI. Pai and WH. Westra. Molecular Pathology of Head and Neck Cancer: Implications for Diagnosis, Prognosis, and Treatment. *Annual Review of Pathology*, 4:49–70, 2009.

[285] JM. Palefsky, EA. Holly, CJ. Hogeboom, ML. Ralston, MM. DaCosta, R. Botts, JM. Berry, N. Jay, and TM. Darragh. Virologic, Immunologic, and Clinical Parameters in the Incidence and Progression of Anal Squamous Intraepithelial Lesions in HIV-Positive and HIV-Negative Homosexual Men. *Journal of Acquired Immune Deficiency Syndromes & Human Retrovirology*, 17(4):314–319, 1998.

[286] O. Papaspiliopoulos and A. Beskos. An introduction to modelling and likelihood inference with stochastic differential equations. Available from *http://84.89.132.1/õmiros/course_notes.pdf*, last accessed 18/03/2017.

[287] L. Pasquale, P. Giorgi-Rossi, F. Carozzi, C. Pedretti, C. Ruggeri, V. Scalvinoni, M. Cotti Cottini, A. Tosini, C. Morana, M. Chiaramonte, M.F. Sacristani, R. Cirelli, D. Chiudinelli, M. Piccolimini, R. Marchione, L. Romano, S. Domenighini, G. Pieragi, and M. Confortini. Cervical cancer screening with HPV testing in the Valcamonica (Italy) screening programme. *Journal of Medical Screening*, 22(1):38–48, 2015.

[288] DJ. Pasta, JL. Taylor, and JM. Henning. Probabilistic Sensitivity Analysis Incorporating the Bootstrap: An Example Comparing Treatments for the Eradication of Helicobacter pylori. *Medical Decision Making*, 19(3):353–363, 1999.

[289] A. Pearson, G. Kvizhinadze, N. Wilson, M. Smith, K. Canfell, and T. Blakely. Is expanding HPV vaccination programs to include school-aged boys likely to be value-for-money: a cost-utility analysis in a country with an existing school-girl program. *BioMed Central Infectious Diseases*, 14:351, 2014.

[290] L. Pinto, P. Canary, C. Araújo, S. Bacelar, and L. Souhami. Prospective Randomized Trial Comparing Hyperfractionated Versus Conventional Radiotherapy In Stages III And IV Oropharyngeal Carcinoma. *International Journal of Radiation Oncology Biology Physics*, 21(3):557–562, 1991.

[291] R. Pitman, D. Fisman, G. Zaric, M. Postma, M. Kretzschmar, J. Edmunds, and M. Brisson. Dynamic Transmission Modeling: A Report of the ISPOR-SMDM Modeling Good Research Practices Task Force-5. *Value in Health*, 15(6):828–834, 2012.

[292] A. Plavnick. The fundamental theorem of Markov Chains. Available from *http://www.math.uchicago.edu/ may/VIGRE/VIGRE2008/REUPapers/Plavnick.pdf*, last accessed 18/03/2017.

[293] M. Plummer. `JAGS` Version 4.0.0 user manual, 2015. Available from *http://sourceforge.net/projects/mcmc-jags/files/Manuals/4.x/jags_user_manual.pdf*, last accessed 18/03/2017.

[294] N. Praditsitthikorn, Y. Teerawattananon, S. Tantivess, S. Limwattananon, A. Riewpaiboon, S. Chichareon, N. Ieumwananonthachai, and V. Tangcharoensathien. Economic Evaluation of Policy Options for Prevention and Control of Cervical Cancer in Thailand. *Pharmacoeconomics*, 29(9):781–806, 2011.

[295] G. Prue. Human papillomavirus: a strong case for vaccinating boys. *Trends in Urology & Men's Health*, pages 7–11, 2016.

[296] V. Racaniello. Permissive vaccines and viral virulence. Virology blog. Available from *http://www.virology.ws/2015/07/30/permissive-vaccines-and-viral-virulence/*, last accessed: 18/03/2017.

[297] R. Ramanah, B. Lesieur, M. Ballester, E. Darai, and R. Rouzier. Trends in Treatment and Survival of Late-Stage Squamous Cell Vulvar Carcinomas Analysis of the Surveillance, Epidemiology, and End Results (SEER) Database. *International Journal of Gynecological Cancer*, 22(5):854–859, 2012.

[298] M. Rawlins and A. Culyer. National Institute for Clinical Excellence and its Value Judgements. *British Medical Journal*, 329(7459):224–227, 2004.

[299] A. Read, S. Baigent, C. Powers, L. Kgosana, L. Blackwell, L. Smith, D. Kennedy, S. Walkden-Brown, and V. Nair. Imperfect Vaccination Can Enhance the Transmission of Highly Virulent Pathogens. *PLoS Biology*, 13(7):e1002198, 2015.

[300] L. Reynales-Shigematsu, E. Rodrigues, and E. Lazcano-Ponce. Cost-Effectiveness Analysis of a Quadrivalent Human Papilloma Virus Vaccine in Mexico. *Archives of Medical Research*, 40(6):503–513, 2009.

[301] C. Robert. *The Bayesian Choice: From Decision-Theoretic Foundations to Computational Implementation*. Springer, New York, USA, 2007.

[302] M. Roberts, V. Andreasen, A. Lloyd, and L. Pellis. Nine challenges for deterministic epidemic models. *Epidemics*, 10:49–53, 2015.

[303] R. Rogoza, N. Ferko, J. Bentley, C. Meijer, J. Berkhof, K.-L. Wang, L. Downs, J. Smith, and E. Franco. Optimization of Primary and Secondary Cervical Cancer Prevention Strategies in an Era of Cervi-

cal Cancer Vaccination: A Multi-Regional Health Economic Analysis. *Vaccine*, 26(Suppl 5):F46–F58, 2008.

[304] R. Rogoza, T. Westra, N. Ferko, J. Tamminga, M. Drummond, T. Daemen, J. Wilschut, and M. Postma. Cost-Effectiveness of Prophylactic Vaccination against Human Papillomavirus 16/18 for the Prevention of Cervical Cancer: Adaptation of an Existing Cohort Model to the Situation in The Netherlands. *Vaccine*, 27(35):4776–4783, 2009.

[305] G. Ronco, V. Ghisetti, N. Segnan, PJ. Snijders, A. Gillio-Tos, and CJ. Meijer. Prevalence of Human Papillomavirus Infection in Women in Turin, Italy. *European Journal of Cancer*, 41(2):297–305, 2005.

[306] G. Ronco, P. Giorgi-Rossi, F. Carozzi, P. Dalla Palma, A. Del Mistro, and L. De Marco. New Technologies for Cervical Cancer Screening Working Group. Human papillomavirus Testing and Liquid-based Cytology in Primary Screening of Women Younger than 35 years: Results at Recruitment for a Randomised Controlled Trial. *The Lancet Oncology*, 7(7):547–555, 2006.

[307] G. Ronco, P. Giubilato, M. Naldoni, E. Zorzi, A. Anghinoni, P. Scalisi, L. Dalla Palma, A. Zanier, C. Barca, MD. Angeloni, R. Gaimo, E. Maglietta, R. Mancini, A. Pizzuti, N. Iossa, and M. Segnan. Activity Level and Process Indicators of Organised Programmes for Cervical Cancer Screening in Italy. *Osservatorio Nazionale Screening - Settimo Rapporto*, pages 56–73, 2008.

[308] V. Rètel, L. van der Molen, F. Hilgers, C. Rasch, A. L'Ortye, L. Steuten, and W. van Harten. A Cost-Effectiveness Analysis of a Preventive Exercise Program for Patients with Advanced Head and Neck Cancer Treated with Concomitant Chemo-Radiotherapy. *BioMed Central Cancer*, 11:475, 2011.

[309] Runge. Über die numerische Auflösung von Differentialgleichungen. *Mathematische Annalen*, 46:167–178, 1895.

[310] K. Rusthoven, D. Raben, J. Song, M. Kane, T. Altoos, and C. Chen. Survival and Patterns of Relapse in Patients With Oral Tongue Cancer. *Journal of Oral and Maxillofacial Surgery*, 68(3):584–589, 2010.

[311] G. Sanders and A. Taira. Cost-Effectiveness of a Potential Vaccine for Human papillomavirus. *Emerging Infectious Diseases*, 9(1):37–48, 2003.

[312] M. Schlienger, C. Krzisch, F. Pene, J.-L. Marin, B. Gindrey-Vie, S. Mauban, N. Barthelemy, J.-L. Habrand, G. Socie, R. Parc, D. Gallot, M. Malafosse, and A. Laugier. Epidermoid Carcinoma of the Anal Canal Treatment Results and Prognostic Variables in a Series of 242 Cases. *International Journal of Radiation Oncology * Biology * Physics*, 17(6):1141–1151, 1989.

[313] A. Schneider, T. Hammerschmidt, T.F. Schwarz, R.M. Rogoza, N. Ferko, and U. Siebert. Long-term Public Health Impact of Vaccination against Cervical Cancer in Germany. *Geburtshilfe Frauenheilkunde*, 67(8):850–858, 2007.

[314] D. Schobert, V. Remy, and O. Schoeffski. Cost-effectiveness of vaccination with a quadrivalent HPV vaccine in Germany using a dynamic transmission model. *Health Economics Review*, 2(1):19, 2012.

[315] E. Schoen, C. Colby, and T. To. Cost-Analysis of Neonatal Circumcision in a Large Health Maintenance Organization. *The Journal of Urology*, 175(3 Pt 1):1111–1115, 2006.

[316] M. Sharma, J. Ortendahl, E. van der Ham, S. Sy, and J. Kim. Cost-Effectiveness of Human Papillomavirus Vaccination and Cervical Can-

cer Screening in Thailand. *British Journal of Obstetrics and Gynaecology*, 119(2):166–176, 2012.

[317] M. Sharma, S. Sy, and J. Kim. The value of male human papillomavirus vaccination in preventing cervical cancer and genital warts in a low-resource setting. *British Journal of Obstetrics and Gynaecology*, 123(6):917–926, 2015.

[318] R. Silva, J. Casseb, M. Andreoli, and L. Villa. Persistence and Clearance of HPV From the Penis of Men Infected and Non-Infected With HIV. *Journal of Medical Virology*, 83(1):127–131, 2011.

[319] C. Silvestri, F. Voller, C. Cipriani, A. Berti, C. Orsini, J. Pasquini, and E. Buiatti. Adolescenti e Stili di Vita: Quando il Sesso Puo Diventare un Rischio, 2006. Agenzia Regionale di Sanita della Toscana. 30 Congresso dell'Associazione Italiana di Epidemiologia. Abstract 210, page 118. Available from *http://www.doesicilia.it/media/Atti_AIE_2006.pdf*, last accessed 18/03/2017.

[320] H. Simpson, E. Petkova, J. Cheng, J. Huppert, E. Foa, and M. Liebowitz. Statistical choices can affect inferences about treatment efficacy: A case study from obsessive compulsive disorder research. *Journal of Psychiatric Research*, 42(8):631–638, 2008.

[321] E. Sinanovic, J. Moodley, M. Barone, S. Mall, S. Cleary, and J. Harries. The Potential Cost-Effectiveness of Adding a Human Papillomavirus Vaccine to the Cervical Cancer Screening Programme in South Africa. *Vaccine*, 27(44):6196–6202, 2009.

[322] EM. Smith, JM. Ritchie, KF. Summersgill, HT. Hoffman, DH. Wang, TH. Haugen, and LP. Turek. Human Papillomavirus in Oral Exfoliated Cells and Risk of Head and Neck Cancer. *Journal of the National Cancer Institute*, 96(6):449–455, 2004.

[323] JS. Smith, C. Bosetti, and N. Munoz. Chlamydia Trachomatis and Invasive Cervical Cancer: a Pooled Analysis of the IARC Multicentric Case-control Study. *International Journal of Cancer*, 111(3):431–439, 2004.

[324] JS. Smith, R. Herrero, and C. Bosetti. Herpes Simplex Virus 2 as a Human Papillomavirus Cofactor in the Etiology of Invasive Cervical Cancer. *Journal of the National Cancer Institute*, 94(21):1604–1613, 2002.

[325] J.S. Smith, L. Lindsay, B. Hoots, J. Keys, S. Franceschi, R. Winer, and G.M. Clifford. Human papillomavirus type distribution in invasive cervical cancer and high-grade cervical lesions: a meta-analysis update. *International Journal of Cancer*, 121(3):621–632, 2007.

[326] K. Soetaert, T. Petzoldt, and R. Woodrow Setzer. Package `deSolve`: Solving Initial Value Differential Equations in `R`, 2015. Available from *https://cran.r-project.org/web/packages/deSolve/vignettes/deSolve.pdf*, last accessed 18/03/2017.

[327] F. Sonnenberg and J. Beck. Markov models in medical decision making: a practical guide. *Medical Decision Making*, 13(4):322–338, 1993.

[328] E. Sopina and T. Ashton. Cost-Effectiveness of a Cervical Screening Program with Human Papillomavirus Vaccine. *International Journal of Technology Assessment in Health Care*, 27(4):290–297, 2011.

[329] D. Spiegelhalter and N. Best. Bayesian Approaches to Multiple Sources of Evidence and Uncertainty in Complex Cost-Effectiveness Modelling. *Statistics in Medicine*, 22(23):3687–3709, 2003.

[330] KR. Stratton, JS. Durch, and RS. Lawrence. Vaccines for the 21st Century: A Tool for Decisionmaking. *National Academies Press, Washington, DC*, 2000.

[331] M. Strong, JE. Oakley, and A. Brennan. Estimating Multiparameter Partial Expected Value of Perfect Information from a Probabilistic Sensitivity Analysis Sample: A Nonparametric Regression Approach. *Medical Decision Making*, 34(311):311–326, 2014.

[332] M. Strong, H. Pilgrim, JE. Oakley, and J. Chilcott. Structural Uncertainty in Health Economic Decision Models, 2009. ScHARR Occasional Paper. Available from *https://www.researchgate.net/publication/267547298_Structural_Uncertainty_in_Health_Economic_Decision_Models*, last accessed: 18/03/2017.

[333] E. Suárez, J. Smith, F. Bosch, P. Nieminen, C.-J. Chen, S. Torvinen, N. Demarteau, and B. Standaert. Cost-Effectiveness of Vaccination against Cervical Cancer: A Multi-regional Analysis Assessing the Impact of Vaccine Characteristics and Alternative Vaccination Scenarios. *Vaccine*, 26(Suppl 5):F29–F45, 2008.

[334] S. Subramanian, R. Sankaranarayanan, B. Bapat, T. Somanathan, G. Thomas, B. Mathew, J. Vinodae, and K. Ramadasb. Cost-Effectiveness of Oral Cancer Screening: Results from a Cluster Randomized Controlled Trial in India. *Bull World Health Organ*, 87(3):200–206, 2009.

[335] R. Sur and P. Dahm. History of evidence-based medicine. *Indian Journal of Urology*, 27(4):487–489, 2011.

[336] A. Sutton and K. Abrams. Bayesian methods in meta-analysis and evidence synthesis. *Statistical Methods in Medical Research*, 10(4):277–303, 2001.

[337] T. Szucs, N. Largeron, K. Dedes, R. Rafia, and S. Bénard. Cost-Effectiveness Analysis of Adding a Quadrivalent HPV Vaccine to the Cervical Cancer Screening Programme in Switzerland. *Current Medical Research and Opinion*, 24(5):1473–1483, 2008.

[338] ZM. Tabbaa, J. Gonzalez, JJ. Sznurkowski, AL. Weaver, A. Mariani, and WA. Cliby. Impact of the New FIGO 2009 Staging Classification for Vulvar Cancer on Prognosis and Stage Distribution. *Gynecologic Oncology*, 127(1):147–152, 2012.

[339] A. Taira, C. Neukermans, and G. Sanders. Evaluating Human Papillomavirus Vaccination Programs. *Emerging Infectious Diseases*, 10(11):1915–1923, 2004.

[340] P. Tappenden, J. Chilcott, S. Eggington, J. Patnick, H. Sakai, and J. Karnon. Option Appraisal of Population-based Colorectal Cancer Screening Programmes in England. *Gut*, 56(5):677–684, 2007.

[341] P. Tappenden, S. Eggington, R. Nixon, J. Chilcott, H. Sakai, and J. Karnon. Colorectal Cancer Screening Options Appraisal Cost-Effectiveness, Cost-Utility and Resource Impact of Alternative Screening Options for Colorectal Cancer, 2004. Report to the English Bowel Cancer Screening Working Group. Available from *https://pdfs.semanticscholar.org/09a0/8003b99c2abaf7d49308229a72ddfe54f677.pdf*, last accessed 18/03/2017.

[342] K. Tay and S.K. Tay. The Impact of Cytology Screening and HPV Vaccination on the Burden of Cervical Cancer. *Asian Pacific Journal of Clinical Oncology*, 7(2):154–159, 2011.

[343] H. Taylor and S. Karlin. *An introduction to stochastic modelling*. Academic Press, San Diego, USA, 1998.

[344] W. Termrungruanglert, P. Havanond, N. Khemapech, S. Lertmaharit, S. Pongpanich, C. Khorprasert, and S. Taneepanichskul. Cost and Effectiveness Evaluation of Prophylactic HPV Vaccine in Developing Countries. *Value in Health*, 15(1 Suppl):S29–S34, 2012.

[345] N. Thiry, C. De Laet, F. Hulstaert, M. Neyt, M. Huybrechts, and I. Cleemput. Cost-Effectiveness of Human Papillomavirus Vaccination in Belgium: Do not Forget about Cervical Cancer Screening. *International Journal of Technology Assessment in Health Care*, 25(2):161–170, 2009.

[346] S. Thompson and J. Higgins. How should meta-regression analyses be undertaken and interpreted? *Statistics in Medicine*, 21:1559–1573, 2002.

[347] J. Tomaszewski, E. Link, T. Leong, A. Heriot, M. Vazquez, S. Chander, J. Chu, M. Foo, M. Lee, AC. Lynch, J. Mackay, M. Michael, P. Tran, and S. Ngan. Twenty-Five-Year Experience with Radical Chemoradiation for Anal Cancer. *International Journal of Radiation Oncology * Biology * Physics*, 83(2):552–558, 2011.

[348] S. Torvinen, P. Nieminen, M. Lehtinen, J. Paavonen, N. Demarteau, and J. Hahl. Cost-Effectiveness of Prophylactic HPV 16/18 Vaccination in Finland: Results from a Modelling Exercise. *Journal of Medical Economics*, 13(2):284–294, 2010.

[349] S. Tully, A. Anonychuk, D. Sanchez, A. Galvani, and C. Bauch. Time for Change? An Economic Evaluation of Integrated Cervical Screening and HPV Immunization Programs in Canada. *Vaccine*, 30(2):425–435, 2012.

[350] H. Turner, I. Baussano, and G. Garnett. Vaccinating Women Previously Exposed to Human Papillomavirus: A Cost-Effectiveness Analysis of the Bivalent Vaccine. *PLoS One*, 8(9):e75552, 2013.

[351] Cancer Research UK. Anal Cancer 2009–2011. Average Number of New Cases Per Year and Age-Specific Incidence Rates per 100,000 Population, UK. Available from *http://www.cancerresearchuk.org/cancer-info/cancerstats/types/anal-cancer/Incidence/anal-incidence*, last accessed: 18/03/2017.

[352] Cancer Research UK. Oral Cancer 2008–2010. Average Number of New Cases Per Year and Age-Specific Incidence Rates per 100,000 Population, UK. Available from *http://www.cancerresearchuk.org/cancer-info/cancerstats/types/oral/incidence/#By2*, last accessed: 18/03/2017.

[353] Cancer Research UK. Vaginal Cancer 2009–2011. Average Number of New Cases Per Year and Age-Specific Incidence Rates per 100,000 Population, Females, UK. Available from *http://www.cancerresearchuk.org/cancer-info/cancerstats/types/vagina/incidence/#By2*, last accessed: 18/03/2017.

[354] Cancer Research UK. Vulvar Cancer 2009–2011. Average Number of New Cases Per Year and Age-Specific Incidence Rates per 100,000 Population, Females, UK. Available from *http://www.cancerresearchuk.org/cancer-info/cancerstats/types/vulva/incidence/uk-vulva-cancer-incidence-statistics#By2*, last accessed: 18/03/2017.

[355] MRC Biostatistics Unit. WinBUGS 14, 2016. Available from *http://www.mrc-bsu.cam.ac.uk/software/bugs/the-bugs-project-winbugs/*, last accessed 18/03/2017.

[356] C. Usher, L. Tilson, J. Olsen, M. Jepsen, C. Walsh, and M. Barry. Cost-Effectiveness of Human Papillomavirus Vaccine in Reducing the Risk of Cervical Cancer in Ireland due to HPV Types 16 and 18 using a Transmission Dynamic model. *Vaccine*, 26(44):5654–5661, 2008.

[357] A. Uusküla, A. Müürsepp, K. Kawai, M. Raag, M. Jürisson, and M. Pillsbury. The Epidemiological and Economic Impact of a Quadrivalent Human Papillomavirus (HPV) Vaccine in Estonia. *BioMed Central Infectious Diseases*, 13:304, 2013.

[358] N. Van de Velde. Modeling Human Papillomavirus Vaccine Effectiveness: Quantifying the Impact of Parameter Uncertainty. *American Journal of Epidemiology*, 165(7):762–775, 2007.

[359] N. Van de Velde, M.-C. Boily, M. Drolet, E. Franco, M.-H. Mayrand, E. Kliewer, F. Coutlée, J.-F. Laprise, T. Malagón, and M. Brisson. Population-Level Impact of the Bivalent, Quadrivalent, and Nonavalent Human Papillomavirus Vaccines: A Model-Based Analysis. *Journal of the National Cancer Institute*, 104(22):1712–1723, 2012.

[360] N. Van de Velde, M. Brisson, and M.-C. Boily. Understanding Differences in Predictions of HPV Vaccine Effectiveness: A Comparative Model-based Analysis. *Vaccine*, 28(33):5473–5484, 2010.

[361] L. van den Einden, K. Aben, L. Massuger, DJ. van Spronsen, and JA. de Hullu. Successful Centralisation of Patients with Vulvar Carcinoma: A Population-based Study in The Netherlands. *European Journal of Cancer*, 48(13):1997–2003, 2012.

[362] R. van Howe. A Cost-Utility Analysis of Neonatal Circumcision. *Medical Decision Making*, 24(6):584–601, 2004.

[363] J. van Rosmalen, M. Toy, and JF. O'Mahony. A Mathematical Approach for Evaluating Markov Models in Continuous Time without Discrete-Event Simulation. *Medical Decision Making*, 33(6):767–779, 2013.

[364] G. Vanagas and Z. Padaiga. Healthcare Spending in the Case of a HPV16/18 Population-wide Vaccination Programme. *Scandinavian Journal of Public Health*, 40(5):406–411, 2012.

[365] G. Vanagas, Z. Padaiga, J. Kurtinaitis, and Z. Logminiene. Cost-Effectiveness of 12- and 15-year-old Girls' Human Papillomavirus 16/18 Population-based Vaccination Programmes in Lithuania. *Scandinavian Journal of Public Health*, 38(6):639–647, 2010.

[366] T. Vanni, J. Karnon, J. Madan, R. White, W. Edmunds, A. Foss, and R. Legood. Calibrating models in economic evaluation: a seven-step approach. *Pharmacoeconomics*, 29(1):35–49, 2011.

[367] T. Vanni, P. Mendes Luz, A. Foss, M. Mesa-Frias, and R. Legood. Economic Modelling Assessment of the HPV Quadrivalent Vaccine in Brazil: A Dynamic Individual-based Approach. *Vaccine*, 30(32):4866–4871, 2012.

[368] S. Vänskä, K. Auranen, T. Leino, H. Salo, P. Nieminen, T. Kilpi, P. Tiihonen, D. Apter, and M. Lehtinen. Impact of Vaccination on 14 High-Risk HPV Type Infections: A Mathematical Modelling Approach. *PLoS ONE*, 8(8):e72008, 2013.

[369] Nomenclatore Tariffario Regionale 2006 (versione secondo la classificazione ICD-IX). Regione Emilia-Romagna. Available from *http://www.saluter.it/wcm/saluter/sanitaer/ssr/assistenza_territoriale/Dipartimento_cure_primarie/specialistica/linkallegati/nomenclatore/allegati_2/nomencla_ICDIX_nov07.pdf.*, last accessed 18/03/2017.

[370] Z. Vokó, L. Nagyjánosi, and Z. Kaló. Cost-Effectiveness of Adding Vaccination with the AS04-adjuvanted Human Papillomavirus 16/18 Vaccine to Cervical Cancer Screening in Hungary. *BioMed Central Public Health*, 12:924, 2012.

[371] E. Vynnycky and R. White. *An Introduction to Infectious Disease Modelling*. Oxford University Press, New York, NY, 2010.

[372] E. Waddingham, S. Mt-Isa, R. Nixon, and D. Ashby. A Bayesian approach to probabilistic sensitivity analysis in structured benefit-risk assessment. *Biometrical Journal*, 58(1):28–42, 2015.

[373] L. Walwyn, C. Janusz, A. Clark, E. Prieto, E. Waight, and N. Largaespada. Cost-effectiveness of HPV vaccination in Belize. *Vaccine*, 33(Suppl 1):A174–A181, 2015.

[374] P. Wang, E. Bradlow, and E. George. Meta-analyses using information reweighting: An application to online advertising. *Quantitative Marketing and Economics*, 12:209–233, 2014.

[375] A. Watson, B. Smith, M. Whitehead, P. Sykes, and F. Frizelle. Malignant Progression of Anal Intraepithelial Neoplasia. *ANZ Journal of Surgery*, 76(8):715–717, 2006.

[376] M. Wayne and B. Bolker. *Infectious Disease. A Very Short Introduction.* Oxford University Press, Oxford, United Kingdom, 2015.

[377] F. Weidemann, M. Dehnert, J. Koch, O. Wichmann, and M. Hoehle. Bayesian parameter inference for dynamic infectious disease modelling: rotavirus in Germany. *Statistics in Medicine*, 33(9):1580–1599, 2014.

[378] RA. Weiss and J. Esparza. The prevention and eradication of smallpox: a commentary on Sloane (1755). An account of inoculation. *Philosophical Transactions of the Royal Society B*, 370(1666), 2014.

[379] N. Welton and AE. Ades. A model of toxoplasmosis incidence in the UK: evidence synthesis and consistency of evidence. *Journal of Applied Statistics*, 54(2):385–404, 2005.

[380] N. Welton, A. Sutton, N. Cooper, K. Abrams, and A. Ades. *Evidence Synthesis for Decision Making in Healthcare*. John Wiley & Sons, Ltd., Chichester, United Kingdom, 2012.

[381] T. Westra, M. Parouty, W. Brouwer, P. Beutels, R. Rogoza, M. Rozenbaum, T. Daemen, J. Wilschut, C. Boersma, and M. Postma. On Discounting of Health Gains from Human Papillomavirus Vaccination: Effects of Different Approaches. *Value in Health*, 15(3):562–567, 2012.

[382] T. Westra, M. Rozenbaum, R. Rogoza, H. Nijman, T. Daemen, M. Postma, and J. Wilschut. Until Which Age Should Women Be Vaccinated Against HPV Infection? Recommendation Based on Cost-effectiveness Analyses. *The Journal of Infectious Diseases*, 204(3):377–384, 2011.

[383] T. Westra, I. Stirbu-Wagner, S. Dorsman, E. Tutuhatunewa, E. de Vrij, H. Nijman, T. Daemen, J. Wilschut, and M. Postma. Inclusion of the benefits of enhanced crossprotection against cervical cancer and prevention of genital warts in the cost-effectiveness analysis of human papillomavirus vaccination in the Netherlands. *BioMed Central Infectious Diseases*, 13:75, 2013.

[384] CM. Wheeler, SK. Kjaer, K. Sigurdsson, OE. Iversen, M. Hernandez-Avila, G. Perez, DR. Brown, LA. Koutsky, EH. Tay, P. Garcia, KA. Ault, SM. Garland, S. Leodolter, SE. Olsson, GW. Tang, DG. Ferris, J. Paavonen, M. Steben, FX. Bosch, J. Dillner, EA. Joura, RJ. Kurman, S. Majewski, N. Munoz, ER. Myers, LL. Villa, FJ. Taddeo, C. Roberts, A. Tadesse, J. Bryan, LC. Lupinacci, KE. Giacoletti, M. James, S. Vuocolo, TM. Hesley, and E. Barr. The Impact of Quadrivalent Human Papillomavirus (HPV; types 6, 11, 16, and 18) L1 Virus-like Particle Vaccine on Infection and Disease due to Oncogenic Nonvaccine HPV

Types in Sexually Active Women Aged 16-26 years. *Journal of Infectious Diseases*, 199(7):936–944, 2009.

[385] A. Wineland and B. Stack. Modern Methods to Predict Costs for the Treatment and Management of Head and Neck Cancer Patients: Examples of Methods Used in the Current Literature. *Current Opinion in Otolaryngology & Head and Neck Surgery*, 16(2):113–116, 2008.

[386] CJM. Witty. Milroy Lecture: eradication of disease: hype, hope and reality. *Clinical Medicine*, 14(4):419–421, 2014.

[387] K. Yamabe, P. Singhal, M. Abe, E. Dasbach, and E. Elbasha. The Cost-Effectiveness Analysis of a Quadrivalent Human Papillomavirus Vaccine (6/11/16/18) for Females in Japan. *Value in Health Regional Issues*, 2(1):92–97, 2013.

[388] N. Yamamoto, R. Mori, P. Jacklin, Y. Osuga, K. Kawana, K. Shibuya, and Y. Taketani. Introducing HPV Vaccine and Scaling up Screening Procedures to Prevent Deaths from Cervical Cancer in Japan: a Cost-Effectiveness Analysis. *British Journal of Obstetrics and Gynaecology*, 119(2):177–186, 2012.

[389] R. Yang and J.O. Berger. A Catalog of Noninformative Priors. 1998, Available from *http://www.stats.org.uk/priors/noninformative/YangBerger1998.pdf*, last accessed 18/03/2017.

[390] H.-Y. Yhim, N.-R. Lee, E.-K. Song, J.-Y. Kwak, ST. Lee, JH. Kim, J.-S. Kim, HS. Park, I.-J. Chung, H.-J. Shim, J.-E. Hwang, HR. Kim, T.-K. Nam, M.-R. Park, H. Shim, HS. Park, HS. Kim, and C.-Y. Yim. The Prognostic Significance of Tumor Human Papillomavirus Status for Patients with Anal Squamous Cell Carcinoma Treated with Combined Chemoradiotherapy. *International Journal of Cancer*, 129(7):1752–1760, 2011.

[391] M. Zampino, E. Magni, MC. Leonardi, L. Santoro, E. Petazzi, C. Fodor, G. Petralia, C. Trovato, F. Nolè, and R. Orecchia. Concurrent Cisplatin, Continuous Infusion Fluorouracil and Radiotherapy Followed by Tailored Consolidation Treatment in Non-metastatic Anal Squamous Cell Carcinoma. *BioMed Central Cancer*, 11:55, 2011.

[392] I. Zechmeister, B. Freiesleben de Blasio, G. Garnett, AR. Neilson, and U. Siebert. Cost-Effectiveness Analysis of Human Papillomavirus Vaccination Programs to Prevent Cervical Cancer in Austria. *Vaccine*, 27(37):5133–5141, 2009.

[393] T. Zilli, U. Schick, M. Ozsahin, P. Gervaz, AD. Roth, and AS. Allal. Node-negative T1-T2 Anal Cancer: Radiotherapy Alone or Concomitant Chemoradiotherapy? *Radiotherapy and Oncology*, 102(1):62–67, 2012.